DOT/FAA/AR-05/19

Office of Aviation Research
Washington, D.C. 20591

A Study of Sampling Rate Requirements for Load Parameter Statistics

August 2005

Final Report

This document is available to the U.S. public through the National Technical Information Service (NTIS), Springfield, Virginia 22161.



U.S. Department of Transportation
Federal Aviation Administration

AUTHENTICATED
U.S. GOVERNMENT
INFORMATION
GPO

NOTICE

This document is disseminated under the sponsorship of the U.S. Department of Transportation in the interest of information exchange. The United States Government assumes no liability for the contents or use thereof. The United States Government does not endorse products or manufacturers. Trade or manufacturer's names appear herein solely because they are considered essential to the objective of this report. This document does not constitute FAA certification policy. Consult your local FAA aircraft certification office as to its use.

This report is available at the Federal Aviation Administration William J. Hughes Technical Center's Full-Text Technical Reports page: actlibrary.tc.faa.gov in Adobe Acrobat portable document format (PDF).

Technical Report Documentation Page

1. Report No.	2. Government Accession No.	3. Recipient's Catalog No.
DOT/FAA/AR-05/19		

4. Title and Subtitle	5. Report Date
A STUDY OF SAMPLING RATE REQUIREMENTS FOR LOAD PARAMETER STATISTICS	August 2005
	6. Performing Organization Code

7. Author(s)	8. Performing Organization Report No.
John Rustenburg*, Daniel O. Tipps*, Donald Skinn*, and Thomas DeFiore**	UDR-TR-2004-00146

9. Performing Organization Name and Address	10. Work Unit No. (TRAIS)
*University of Dayton Research Institute Structural Integrity Division 300 College Park Dayton, OH 45469-0120 **Federal Aviation Administration William J. Hughes Technical Center Airport And Aircraft Safety Research and Development Division Airworthiness Assurance Atlantic City International Airport, New Jersey 08405	RPD-510
	11. Contract or Grant No.
	01-G005

12. Sponsoring Agency Name and Address	13. Type of Report and Period Covered
U.S. Department of Transportation Federal Aviation Administration Office of Aviation Research Washington, DC 20591	Final Report
	14. Sponsoring Agency Code
	ANM-110

15. Supplementary Notes

16. Abstract

The objective of the operational loads monitoring research is to support the Federal Aviation Administration Operational Loads program by developing new and improved methods and criteria for processing and presenting large commercial transport airplane flight and ground loads usage data. This report presents the result of a study to determine the minimum sampling rates required for selected parameters to ensure the detection of peaks and peak amplitudes representative of the basic signal for use in deriving operational load statistics. The selected parameters included vertical, lateral, and longitudinal accelerations, and pitch and bank angle, as well as elevator, aileron, and rudder deflections recorded at higher than normal sampling rates obtained during 108 flights of an Airbus A319 used in normal commercial operations. The study included (1) the use of power spectral density analyses of some high-activity flights to evaluate the frequency content of the recorded data, (2) an investigation of sampling rates required to identify peaks and peak amplitudes based on the frequency content of the parameters, and (3) an evaluation of the impact of varying sampling rates on derived operational load statistics. Resulting sampling rates were compared to sampling rate requirements specified in Title 14 Code of Federal Regulations (CFR) Part 121, Appendices B and M. Although the data used in the study were recorded at higher than normal sampling rates, it was concluded that the sampling rates were not high enough to determine the minimum sampling rates for detection of peaks and associated peak amplitudes with any certainty. Although the sampling rates specified in 14 CFR Part 121 appear adequate to identify peaks, they are too low to identify the associated peak amplitude.

17. Key Words	18. Distribution Statement
Digital flight data recorder, Load parameter recording, Parameter sampling rates, Parameter statistics	This document is available to the public through the National Technical Information Service (NTIS), Springfield, Virginia 22161.

19. Security Classif. (of this report)	20. Security Classif. (of this page)	21. No. of Pages	22. Price
Unclassified	Unclassified	150	N/A

PREFACE

This report covers the results from a study to evaluate the effect of different sampling rates on some operational load parameter statistics. The objective of the study was to determine if existing sampling rates could provide reasonable estimates of accelerations, pitch and bank angles, and control surface deflection occurrences from measured flight loads data. The Flight Systems Integrity Group of the Structural Integrity Division of the University of Dayton Research Institute (UDRI) performed this study in support of the Federal Aviation Administration (FAA) Airborne Data Monitoring Systems Research Program. Mr. Daniel Tipps provided UDRI oversight direction for this study effort. Mr. John Rustenburg directed the data processing effort, performed the data analysis, and prepared the report. Mr. Donald Skinn established data reduction criteria, developed the data reduction algorithms, and provided the data. Mr. Thomas DeFiore of the FAA William J. Hughes Technical Center was the program manager for the FAA and also provided valuable insight to the accomplishment of the study objective.

As only 108 flights of A319 data were used in this study, it is recommended that the exceedance data contained herein not be used for certification or design studies. The 108 flights were used only to determine the effects of a variety of sample rates on the precision of selected parameters recorded on the Digital Flight Data Recorder.

TABLE OF CONTENTS

		Page
EXECUTIVE SUMMARY		xvii
1.	INTRODUCTION	1
2.	GENERAL DATA PROCESSING DISCUSSION	2
2.1	Data Digitization	2
2.2	Data Sampling Rate	2
2.3	Power Spectral Density	3
2.4	Parameter Peak Amplitude	4
2.5	Downsampling	4
2.6	Peak Counting	4
2.7	Effect of Bin Size on Cumulative Occurrences	5
2.8	Effect of Sampling Rate on Bin Counts	5
3.	SAMPLING RATE STUDY	6
3.1	Power Spectral Density Analysis	6
3.1.1	Vertical Load Factor PSDs	7
3.1.2	Lateral Load Factor PSDs	7
3.1.3	Longitudinal Load Factor PSDs	8
3.1.4	Pitch and Bank Angle PSDs	8
3.1.5	Control Surface Deflection Angle PSDs	9
3.2	Cumulative Occurrences Statistics	9
3.2.1	Incremental Vertical Load Factor Statistics	10
3.2.2	Lateral Load Factor Statistics	10
3.2.3	Longitudinal Load Factor Statistics	11
3.2.4	Pitch and Bank Angle Statistics	11
3.2.5	Control Surface Deflection Angle Statistics	11
3.3	Minimum Sampling Rates for Amplitude Detection	12
3.4	Comparison of Sampling Rate Requirements	12
3.5	Derivation of Flight Control Deflection Statistics	13
4.	CONCLUDING REMARKS	14
5.	REFERENCES	15

APPENDICES

A—Appendix B to 14 CFR Part 121, Airplane Flight Recorder Specification

B—Appendix M to 14 CFR Part 121, Airplane Flight Recorder Specifications

C—Derivation of Flight Control Deflection Statistics From Data Obtained at Low Sampling Rates

D—Comments on UDR-TR-2004-00146, R. Howes, Cessna Aircraft Company

LIST OF FIGURES

Figure		Page
1	Analog Signal to Digitized Binning	16
2	Digitized Aileron Signal	16
3	Peak Cropping due to Digitization	17
4	Sine Wave Sampled at Twice its Frequency	17
5	Analog Signal Sampled at Different Sampling Rates	18
6	Vertical Load Factor Time History Sampled at Different Sampling Rates	18
7	Vertical Load Factor PSD, Preflight	19
8	Variation of rms Vertical Load Factor With Frequency, Postflight	19
9	Calculation of Maximum Peak Amplitude Error	20
10	Downsampling Technique	20
11	Peak Between Mean Counting	21
12	Effect of Using Different Class Intervals on an Incremental Vertical Load Factor Distribution	21
13	Effect of Sampling Rate on Phase of Flight Bin Count	22
14	Incremental Vertical Load Factor Time History, Flight Sequence 3	22
15	Normalized PSD of Incremental Vertical Load Factor, Flight Sequence 3, Preflight	23
16	Percent of Total Incremental Vertical Load Factor rms vs Frequency, Flight Sequence 3, Preflight	23
17	Normalized PSD of Incremental Vertical Load Factor, Flight Sequence 3, in Flight	24
18	Percent of Total Incremental Vertical Load Factor rms vs Frequency, Flight Sequence 3, in Flight	24
19	Normalized PSD of Incremental Vertical Load Factor, Flight Sequence 3, Postflight	25

20	Percent of Total Incremental Vertical Load Factor rms vs Frequency, Flight Sequence 3, Postflight	25
21	Lateral Load Factor Time History, Flight Sequence 3	26
22	Normalized PSD of Lateral Load Factor, Flight Sequence 3, Preflight	26
23	Percent of Total Lateral Load Factor rms vs Frequency, Flight Sequence 3, Preflight	27
24	Normalized PSD of Lateral Load Factor, Flight Sequence 3, in Flight	27
25	Percent of Total Lateral Load Factor rms vs Frequency, Flight Sequence 3, in Flight	28
26	Normalized PSD of Lateral Load Factor, Flight Sequence 3, Postflight	28
27	Percent of Total Lateral Load Factor rms vs Frequency, Flight Sequence 3, Postflight	29
28	Longitudinal Load Factor Time History, Flight Sequence 3	29
29	Normalized PSD of Longitudinal Load Factor, Flight Sequence 3, Preflight	30
30	Percent of Total Longitudinal Load Factor rms vs Frequency, Flight Sequence 3, Preflight	30
31	Normalized PSD of Longitudinal Load Factor, Flight Sequence 3, in Flight	31
32	Percent of Total Longitudinal Load Factor rms vs Frequency, Flight Sequence 3, in Flight	31
33	Normalized PSD of Longitudinal Load Factor, Flight Sequence 3, Postflight	32
34	Percent of Total Longitudinal Load Factor rms vs Frequency, Flight Sequence 3, Postflight	32
35	Pitch Angle Time History, Flight Sequence 3	33
36	Normalized PSD of Pitch Angle, Flight Sequence 3, in Flight	33
37	Percent of Total Pitch Angle rms vs Frequency, Flight Sequence 3, in Flight	34
38	Bank Angle Time History, Flight Sequence 3	34
39	Normalized PSD of Bank Angle, Flight Sequence 3, in Flight	35
40	Percent of Total Bank Angle rms vs Frequency, Flight Sequence 3, in Flight	35

41	Aileron Angle Time History, Flight Sequence 3	36
42	Normalized PSD of Aileron Angle, Flight Sequence 3, in Flight	36
43	Percent of Total Aileron Angle rms vs Frequency, Flight Sequence 3, in Flight	37
44	Elevator Angle Time History, Flight Sequence 3	37
45	Normalized PSD of Elevator Angle, Flight Sequence 3, in Flight	38
46	Percent of Total Elevator Angle rms vs Frequency, Flight Sequence 3, in Flight	38
47	Rudder Angle Time History, Flight Sequence 3	39
48	Normalized PSD of Rudder Angle, Flight Sequence 3, in Flight	39
49	Percent of Total Rudder Angle rms vs Frequency, Flight Sequence 3, in Flight	40
50	Incremental Vertical Load Factor Time History, Flight Sequence 35	40
51	Normalized PSD of Incremental Vertical Load Factor, Flight Sequence 35, Preflight	41
52	Percent of Total Incremental Vertical Load Factor rms vs Frequency, Flight Sequence 35, Preflight	41
53	Normalized PSD of Incremental Vertical Load Factor, Flight Sequence 35, in Flight	42
54	Percent of Total Incremental Vertical Load Factor rms vs Frequency, Flight Sequence 35, in Flight	42
55	Normalized PSD of Incremental Vertical Load Factor, Flight Sequence 35, Postflight	43
56	Percent of Total Incremental Vertical Load Factor rms vs Frequency, Flight Sequence 35, Postflight	43
57	Lateral Load Factor Time History, Flight Sequence 35	44
58	Normalized PSD of Lateral Load Factor, Flight Sequence 35, Preflight	44
59	Percent of Total Lateral Load Factor rms vs Frequency, Flight Sequence 35, Preflight	45
60	Normalized PSD of Lateral Load Factor, Flight Sequence 35, in Flight	45
61	Percent of Total Lateral Load Factor rms vs Frequency, Flight Sequence 35, in Flight	46

62	Normalized PSD of Lateral Load Factor, Flight Sequence 35, Postflight	46
63	Percent of Total Lateral Load Factor rms vs Frequency, Flight Sequence 35, Postflight	47
64	Longitudinal Load Factor Time History, Flight Sequence 35	47
65	Normalized PSD of Longitudinal Load Factor, Flight Sequence 35, Preflight	48
66	Percent of Total Longitudinal Load Factor rms vs Frequency, Flight Sequence 35, Preflight	48
67	Normalized PSD of Longitudinal Load Factor, Flight Sequence 53, in Flight	49
68	Percent of Total Longitudinal Load Factor rms vs Frequency, Flight Sequence 35, in Flight	49
69	Normalized PSD of Longitudinal Load Factor, Flight Sequence 35, Postflight	50
70	Percent of Total Longitudinal Load Factor rms vs Frequency, Flight Sequence 35, Postflight	50
71	Pitch Angle Time History, Flight Sequence 35	51
72	Normalized PSD of Pitch Angle, Flight Sequence 35, in Flight	51
73	Percent of Total Pitch Angle rms vs Frequency, Flight Sequence 35, in Flight	52
74	Bank Angle Time History, Flight Sequence 35	52
75	Normalized PSD of Bank Angle, Flight Sequence 35, in Flight	53
76	Percent of Total Bank Angle rms vs Frequency, Flight Sequence 35, in Flight	53
77	Aileron Angle Time History, Flight Sequence 35	54
78	Normalized PSD of Aileron Angle, Flight Sequence 35, in Flight	54
79	Percent of Total Aileron Angle rms vs Frequency, Flight Sequence 35, in Flight	55
80	Elevator Angle Time History, Flight Sequence 35	55
81	Normalized PSD of Elevator Angle, Flight Sequence 35, in Flight	56
82	Percent of Total Elevator Angle rms vs Frequency, Flight Sequence 35, in Flight	56
83	Rudder Angle Time History, Flight Sequence 35	57
84	Normalized PSD of Rudder Angle, Flight Sequence 35, in Flight	57

85	Percent of Total Rudder Angle rms vs Frequency, Flight Sequence 35, in Flight	58
86	Incremental Vertical Load Factor Time History, Flight Sequence 62	58
87	Normalized PSD of Incremental Vertical Load Factor, Flight Sequence 62, Preflight	59
88	Percent of Total Incremental Vertical Load Factor rms vs Frequency, Flight Sequence 62, Preflight	59
89	Normalized PSD of Incremental Vertical Load Factor, Flight Sequence 62, in Flight	60
90	Percent of Total Incremental Vertical Load Factor rms vs Frequency, Flight Sequence 62, in Flight	60
91	Normalized PSD of Incremental Vertical Load Factor, Flight Sequence 62, Postflight	61
92	Percent of Total Incremental Vertical Load Factor rms vs Frequency, Flight Sequence 62, Postflight	61
93	Lateral Load Factor Time History, Flight Sequence 62	62
94	Normalized PSD of Lateral Load Factor, Flight Sequence 62, Preflight	62
95	Percent of Total Lateral Load Factor rms vs Frequency, Flight Sequence 62, Preflight	63
96	Normalized PSD of Lateral Load Factor, Flight Sequence 62, in Flight	63
97	Percent of Total Lateral Load Factor rms vs Frequency, Flight Sequence 62, in Flight	64
98	Normalized PSD of Lateral Load Factor, Flight Sequence 62, Postflight	64
99	Percent of Total Lateral Load Factor rms vs Frequency, Flight Sequence 62, Postflight	65
100	Longitudinal Load Factor Time History, Flight Sequence 62	65
101	Normalized PSD of Longitudinal Load Factor, Flight Sequence 62, Preflight	66
102	Percent of Total Longitudinal Load Factor rms vs Frequency, Flight Sequence 62, Preflight	66
103	Normalized PSD of Longitudinal Load Factor, Flight Sequence 62, in Flight	67

104	Percent of Total Longitudinal Load Factor rms vs Frequency, Flight Sequence 62, in Flight	67
105	Normalized PSD of Longitudinal Load Factor, Flight Sequence 62, Postflight	68
106	Percent of Total Longitudinal Load Factor rms vs Frequency, Flight Sequence 62, Postflight	68
107	Pitch Angle Time History, Flight Sequence 62	69
108	Normalized PSD of Pitch Angle, Flight Sequence 62, in Flight	69
109	Percent of Total Pitch Angle rms vs Frequency, Flight Sequence 62, in Flight	70
110	Bank Angle Time History, Flight Sequence 62	70
111	Normalized PSD of Bank Angle, Flight Sequence 62, in Flight	71
112	Percent of Total Bank Angle rms vs Frequency, Flight Sequence 62, in Flight	71
113	Aileron Angle Time History, Flight Sequence 62	72
114	Normalized PSD of Aileron Angle, Flight Sequence 62, in Flight	72
115	Percent of Total Aileron Angle rms vs Frequency, Flight Sequence 62, in Flight	73
116	Elevator Angle Time History, Flight Sequence 62	73
117	Normalized PSD of Elevator Angle, Flight Sequence 62, in Flight	74
118	Percent of Total Elevator Angle rms vs Frequency, Flight Sequence 62, in Flight	74
119	Rudder Angle Time History, Flight Sequence 62	75
120	Normalized PSD of Rudder Angle, Flight Sequence 62, in Flight	75
121	Percent of Total Rudder Angle rms vs Frequency, Flight Sequence 62, in Flight	76
122	Cumulative Occurrences of Incremental Vertical Load Factor, Preflight	76
123	Effect of Sampling Rate on Cumulative Occurrences of Incremental Vertical Load Factor, Preflight	77
124	Percent of Incremental Vertical Acceleration Peak Counts as a Function of Sampling Rate, Preflight	77
125	Cumulative Occurrences of Incremental Vertical Load Factor, in Flight	78

126 Effect of Sampling Rate on Cumulative Occurrences of Incremental Vertical Load Factor, in Flight 78

127 Percent of Incremental Vertical Acceleration Peak Counts as a Function of Sampling Rate, in Flight 79

128 Cumulative Occurrences of Incremental Vertical Load Factor, Postflight 79

129 Effect of Sampling Rate on Cumulative Occurrences of Incremental Vertical Load Factor, Postflight 80

130 Percent of Incremental Vertical Acceleration Peak Counts as a Function of Sampling Rate, Postflight 80

131 Cumulative Occurrences of Lateral Load Factor, Preflight 81

132 Effect of Sampling Rate on Cumulative Occurrences of Lateral Load Factor, Preflight 82

133 Percent of Lateral Load Peak Counts as a Function of Sampling Rate, Preflight 83

134 Cumulative Occurrences of Lateral Load Factor, in Flight 83

135 Effect of Sampling Rate on Cumulative Occurrences of Lateral Load Factor, in Flight 84

136 Percent of Lateral Load Factor Peak Counts as a Function of Sampling Rate, in Flight 85

137 Cumulative Occurrences of Lateral Load Factor, Postflight 85

138 Effect of Sampling Rate on Cumulative Occurrences of Lateral Load Factor, Postflight 86

139 Percent of Lateral Load Factor Peak Counts as a Function of Sampling Rate, Postflight 87

140 Cumulative Occurrences of Longitudinal Load Factor, Preflight 87

141 Effect of Sampling Rate on Cumulative Occurrences of Longitudinal Load Factor, Preflight 88

142 Percent of Longitudinal Load Factor Peak Counts as a Function of Sampling Rate, Preflight 89

143 Cumulative Occurrences of Longitudinal Load Factor, in Flight 89

144 Effect of Sampling Rate on Cumulative Occurrences of Longitudinal Load Factor, in Flight 90

145 Percent of Longitudinal Load Factor Peak Counts as a Function of Sampling Rate, in Flight 91

146 Cumulative Occurrences of Longitudinal Load Factor, Postflight 91

147 Effect of Sampling Rate on Cumulative Occurrences of Longitudinal Load Factor, Postflight 92

148 Percent of Longitudinal Load Factor Peak Counts as a Function of Sampling Rate, Postflight 93

149 Cumulative Occurrences of Pitch Angle 93

150 Effect of Sampling Rate on Cumulative Occurrences of Pitch Angle, in Flight 94

151 Percent of Pitch Angle Peak Counts as a Function of Sampling Rate, in Flight 95

152 Cumulative Occurrences of Bank Angle 95

153 Effect of Sampling Rate on Cumulative Occurrences of Bank Angle, in Flight 96

154 Percent Bank Angle Peak Counts as a Function of Sampling Rate, in Flight 97

155 Cumulative Occurrences of Aileron Deflection Angle 97

156 Effect of Sampling Rate on Cumulative Occurrences of Aileron Deflection Angle, in Flight 98

157 Percent Aileron Deflection Angle Peak Counts as a Function of Sampling Rate, in Flight 99

158 Cumulative Occurrences of Elevator Deflection Angle 99

159 Effect of Sampling Rate on Cumulative Occurrences of Elevator Deflection Angle, in Flight 100

160 Percent Elevator Deflection Angle Peak Counts as a Function of Sampling Rate, in Flight 101

161 Cumulative Occurrences of Rudder Deflection Angle 101

162 Effect of Sampling Rate on Cumulative Occurrences of Rudder Deflection Angle, in Flight 102

163 Percent Rudder Deflection Angle Peak Counts as a Function of Sampling Rate, in Flight 102

LIST OF TABLES

Table		Page
1	Parameter Sampling Rates	103
2	Figure Layout for Three Flights	104
3	Peak Counting Criteria	105
4	Figure Layout for Cumulative Occurrence Data	105
5	Sampling Rate Requirements	106

LIST OF ACRONYMS

CFR	Code of Federal Regulations
FAA	Federal Aviation Administration
FFT	Fast Fourier transform
Hz	Hertz
PSD	Power spectral density
rms	Root mean square
sps	Samples per second

EXECUTIVE SUMMARY

The University of Dayton is supporting Federal Aviation Administration (FAA) research on the structural integrity requirements for the U.S. commercial transport airplane fleet. The primary objective of this research is to support the FAA Airborne Data Monitoring Systems Program by developing new and improved methods and criteria for processing and presenting large commercial transport airplane flight and ground loads usage data. This report presents the result of a study to determine the minimum sampling rates required for selected parameters to ensure the detection of peaks and peak amplitudes representative of the basic signal for use in deriving operational load statistics. The selected parameters included vertical, lateral, and longitudinal accelerations, and pitch and bank angle, as well as elevator, aileron, and rudder deflections recorded at higher than normal sampling rates obtained during 108 flights of an Airbus A319 used in normal commercial operations. The study included (1) the use of power spectral density analyses of some high-activity flights to evaluate the frequency content of the recorded data, (2) an investigation of sampling rates required to identify peaks and peak amplitudes based on the frequency content of the parameters, and (3) an evaluation of the impact of varying sampling rates on derived operational load statistics. Resulting sampling rates were compared to sampling rate requirements specified in Title 14 Code of Federal Regulations Part 121, Appendices B and M. Although the data used in the study was recorded at higher than normal sampling rates, it was concluded that the sampling rates were not high enough to allow the selection of minimum sampling rates for detection of peaks and associated peak amplitudes with any certainty. Although the sampling rates specified in 14 CFR Part 121 appear adequate to identify peaks, they are too low to identify the associated peak amplitude.

1. INTRODUCTION.

The Federal Aviation Administration (FAA) Airborne Data Monitoring Systems Research Program collects and provides statistical loads data from transport aircraft used in normal commercial airline operations. The sampling rates used to record the various selected load parameter signals vary from parameter to parameter and are often the subject of questions regarding their adequacy in obtaining realistic estimates of the actual signal peaks. For instance, the relatively low sampling rates, from one to four samples per second, of flight control surface deflections measurements has been a particular concern. As a result, the loads data reduction and analysis community has been reluctant to use the flight control surface deflection measurements to derive usage spectra for design criteria or the evaluation of existing designs.

Sampling rates must be sufficiently high to be able to not only detect the existence of a parameter peak or valley, but also to describe the maximum amplitude of the peak or valley. This requires knowledge of (1) the frequency content of the parameter time history, (2) the relationship between parameter frequency content and sampling rate for identifying peaks and valleys, and (3) the relationship between the parameter's frequency bandwidth and the sampling rate needed to ensure that the maximum parameter peak and valley amplitudes are obtained with an acceptable accuracy when a peak or valley is identified. Thus, in its most basic form, the sampling rate requirements are determined by the frequency content of the original analog time histories. Unfortunately, the basic analog signals are not available, but their digitized or sampled representations are available. A sampled time history may provide a distorted picture of the basic analog time history that does not faithfully convey all the frequencies in the original analog time history. To get an accurate picture of the waveform, a sampling rate of 10 to 20 times the highest frequency in the analog signal is usually suggested. Such high sampling rates were not available for this study. For purposes of this study, one must assume that the maximum sampling rates available provided a representative description of the original continuous analog signal. One can then evaluate if lower sampling rates from those available for this study would significantly affect the derived statistical load spectra. Based on the assumption that the maximum available sampling rates provide a satisfactory definition of the original parameter activity, this study conducted power spectral density (PSD) analyses of each available parameter for three maximum activity flights (i.e., flights in moderate turbulence) to obtain a representative description of the frequency content of the measured parameter. Based on the frequency content of the parameter, the study selected the minimum sampling rates necessary to define the existence of peaks and valleys as well as to adequately determine the amplitude of the existing peak or valley. The study calculated and compared parameter peak count statistics for different sampling rates. The effect of sampling rate on the peak count statistics were analyzed with respect to the minimum sampling rates selected from the PSD analyses. The minimum sampling rates selected from this study were compared with the sampling rates specified in Title 14 Code of Federal Regulations Part 121, Appendices B and M. It is very important for the reader to keep in mind that the selected minimum sampling rates are based on an already sampled continuous parameter signal that does not reflect the exact or entire frequency content of the original signal.

2. GENERAL DATA PROCESSING DISCUSSION.

The objective of aircraft and systems loading or usage statistics is to provide usable information for the evaluation of durability and damage tolerance of existing operational aircraft as well as the establishment of design criteria for new aircraft designs. For this information to be useful, it is desirable that it reflects the real world experience as accurately as possible within realistic limits. For instance, usage statistics of limited accuracy, but derived from available measurements, are better than usage statistics based on guesses or anecdotal information. Also, the use of highly accurate and detailed operational statistics in analyses that use gross averages of such data as input does not improve the accuracy of the final results and some error in the input is acceptable. If the operational statistics for a specific aircraft model are used for comparison of the operational statistics on other operational aircraft of the same model, some error can be tolerated in the operational statistics. If the operational statistics represent an absolute environment to which all aircraft are subject, such as atmospheric turbulence, increased accuracy is desirable for use on a variety of different aircraft types. In the derivation of usage statistics, it is, therefore, important to keep in mind the ultimate use of the data.

In this study, a review of the general effects of real-world data digitization, signal frequency, and sampling rates will be reviewed first. The purpose of this review is to provide a basic understanding of the effect of data digitization of an analog signal and the effect of data binning during data processing on the final derived operational statistics.

2.1 DATA DIGITIZATION.

The time histories obtained from the flight loads data recorder represent binned digital measurements of an analog signal sampled at specific time intervals. Therefore, the digitally recorded time history provides only a representation of the analog signal. The resolution of this representation is dependent on the binning interval used for the digitized data. The digital binning interval is actually the digital resolution of the analog signal; it is normally quite small and is a function of the number of bits used to represent the digitized data point. Figure 1 shows an example of the binning of a simple sine wave. Figures 2 and 3 show the effect of this digital binning on two short segments of an aileron deflection time history. Figure 2 shows the steps resulting from the digitizing process from what was a smooth analog signal. Figure 3 shows the cropping of the true peaks in the time history due to the binning process. The two figures show digital binning intervals of 0.065 degrees. These values are quite small and are of no real concern. They are shown here to emphasize the point that a digitized time history is not an exact duplication of the original analog signal, regardless of the sampling rate used.

2.2 DATA SAMPLING RATE.

For digitally sampled data to be useful in any analysis, the sampling rate must be high enough to provide an accurate approximation of the basic signal. If the sampling rate is high enough, then the original signal can be approximated by joining the sampled points by small linear portions. If the sampling rate is too low, the digitized time history of the analog signal may not capture larger analog values if they occur within the sampling time increments. This is more a concern with rapidly changing data of a short cyclic nature. For slower changing parameters, a slower sampling rate may be quite acceptable. A generally accepted theory advanced by Nyquist is that

as a minimum, the sampling rate should be twice the maximum frequency exhibited in the original signal. Figure 4 presents an example of a simple sine wave of 2 hertz (Hz) sampled at four samples per second. As can be seen, the sampled data does not accurately depict the original signal but does identify the existence of peaks at the proper amplitude and frequency. Figure 5 presents a sine wave of 7 Hz sampled at 16, 8, and 4 samples per second. The deterioration in the sampled time history, in its ability to represent the original signal as the sampling rate is reduced, is quite obvious. In this case, peaks are identified at the proper frequency but do not provide the proper amplitude. It is clear that as the sampling rate deviates from an absolute ratio of the signal frequency peak amplitude, values may be missed even at high sampling rates. As can be seen, a sampling rate of four samples per second, which equates to a Nyquist frequency of 2 Hz, results in a sampled time history with a completely different frequency content from the original analog signal. This phenomenon is called aliasing and results in contributing parameter cycles to the digitized time history at a frequency that may not exist in the original analog signal or add cycles to the digitized time history at the same frequency that existed in the original analog signal. In either case, subsequent PSD analysis of such a digitized time history will include errors due to aliasing, resulting from an inadequate sampling rate. Figure 6 shows digitized time histories of vertical load factor for four different sampling rates. Upon close examination, the figure shows changes in peak values as well as in the loss of peaks. Thus, the higher the frequency of the components in the signal, the higher the sampling rate should be.

2.3 POWER SPECTRAL DENSITY.

Figures 5 and 6 have shown that knowledge of the frequency content of the original signal is important in deciding the sampling rate necessary to capture an acceptable digitized representation of the analog signal. A time history displays the magnitude of the data parameter as a function of time. A PSD provides an indication of the relative contribution of the data parameter frequencies to the total variance of the time history as a function of frequency. It thus provides insight into the frequencies that contribute the most to the total variance of the data parameter. Figure 7 presents a PSD of a sampled vertical load factor digitized time history for a ground operational segment. As can be seen, the low frequencies (below 2 Hz) are the predominant frequencies in the PSD. Some additional power is evident at the higher frequencies, between 6 and 8 Hz.

The square root of total area under the PSD curve is equal to the root mean square (rms) of the time history. Taking the square root of a continuous integration of the PSD over the entire frequency band provides an indication of the change in the standard deviation with increasing frequency. Figure 8 shows an example of the variation of the rms as a function of increasing frequency. The figure shows how the different frequencies in the power spectrum contribute to the overall rms level. Steep slopes indicate a strong contribution within a narrow frequency band. Shallow slopes indicate little contribution over a wide frequency bandwidth. The figure shows that for the data represented by this figure, the primary contributor to the total rms acceleration are the accelerations occurring at frequencies below 2 cycles per second. Accelerations occurring at frequencies between 2 and 8 cycles per second contribute significantly less to the total rms of the digitized signal. In this case, a sampling rate of four samples per second (2 Hz) would include most of the signal's overall standard deviation.

It must be kept in mind that the flight load time histories used are not true continuous functions but represent digitally sampled data that may include aliasing effects as discussed above. Thus, the PSD may show power reflected at frequencies below the Nyquist frequency for power at frequencies above the Nyquist frequency. The approach to limiting the aliasing effects is to filter the original signal to remove frequencies above the Nyquist frequency. It is not known if this is done in the airborne data monitoring system used for data recording. Aliasing effects cannot be removed from the PSD obtained from sampled data. If the original signal is competently sampled, the PSD will approach zero as the frequency nears the Nyquist frequency. If the PSD moves toward a finite value, aliasing effects most likely exist in the sampled time history.

2.4 PARAMETER PEAK AMPLITUDE.

Figure 5 showed that in accordance with the Nyquist theorem, the 16 samples per second sampling rate is able to identify the existence of peaks in the analog signal. However, it also shows that while the 16 samples per second sampling rate ensures the identification of important peaks over the bandwidth of interest, it is not necessarily high enough to sample the true peak magnitude. Reference 1 presents a study of the relationship between sampling rate and measurement accuracy and shows that the data accuracy is dependent on the ratio of the signal frequency to the sampling frequency. Figure 9 shows the signal frequency of 3.5 Hz shown earlier in figure 5, with a sampling rate of 16 samples per second offset to portray the maximum possible amplitude error. The equation in the figure, as derived in reference 1, shows how data accuracy is dependent on the ratio of the signal frequency to the sampling frequency. The figure also shows that the maximum error does not necessarily occur during each cycle, even for a signal of constant frequency. For a signal with varying frequencies, the relationship between the sample time and the time of the analog signal peak is random and the sample time may occur at any time during the signal cycle with equal probability. In other words, it is as likely that the sample time coincides with the true peak, i.e., 0% error, as it is that it coincides with a maximum error value.

2.5 DOWNSAMPLING.

The parameters used in this study were recorded at the fixed sampling rates shown in table 1. To obtain representative digitized time histories representative of slower sampling rates, a downsampling technique was employed. Downsampling in its basic form is the process of reducing the number of samples in a time history without the use of a low-pass filtering operation. This is accomplished through the application of a decimation factor M equal to the input sampling rate divided by the output sampling rate, thus, M = input rate/output rate. In practical terms, this means that for a sample rate reduction of M = 2, every other point in the time history would be retained while the intermediate point would be deleted, for a sample rate reduction of four, only every fourth point would be retained, etc. In this study, downsampling is used to change the primary time history based on a higher sampling rate to one or more based on lower sampling rates. Figure 10 illustrates the application of downsampling.

2.6 PEAK COUNTING.

A counting technique is used to interrogate the digitized time histories and place the selected points into fixed class intervals or bins. A variety of counting techniques are available, but

practically all available statistical data is obtained from peak between mean readings. UDRI has used this method of peak counting in deriving operational load statistics. In this method, a peak is defined as the maximum excursion of a mean time history trace between successive crossings of the mean level. Figure 11 illustrates the peak-between-mean criteria. This method counts upward events as positive and downward events as negative. Only one peak or one valley is counted between two successive crossings of the mean. A threshold zone or dead band is normally used in the data reduction to ignore irrelevant loads variations around the mean. Therefore, the peak between the mean counting method requires determination of the mean level for the peak-counted parameter time history. Most parameters exhibit a nearly constant mean level throughout the time history, and the peak counting technique was used for all parameters in this study.

2.7 EFFECT OF BIN SIZE ON CUMULATIVE OCCURRENCES.

Operational statistics are generally presented as cumulative probabilities or cumulative frequencies of a given parameter. For the purposes of obtaining cumulative occurrences, the point in the bins are accumulated from the points in the highest absolute bin size to the lowest. When the accumulated occurrences in each of the data bins are plotted to obtain cumulative distribution plots, it is common practice to draw straight lines between successive points of cumulative occurrences in each bin rather than by steps or in a histogram format. Since cumulative occurrences are viewed as exceedances, the cumulative occurrences or bin frequencies are plotted at the inner boundaries of the bin increments. As a consequence, accumulated points may be plotted at lower or higher bin boundaries, depending on the magnitude of the bin increment used. This becomes especially critical at the highest bin values. In theory, the greater the number of increments, the more accurately the distribution can be presented. Figures 12 shows the cumulative occurrences for an identical time history, but at varying bin increments. The most negative count was -0.183 g, while the most positive count was +0.134 g. Notice that the most negative load factor count of -0.183 g is plotted at -0.18 g when using a bin increment of 0.01 g. As the bin size becomes larger, this occurrence is plotted at lower and lower load factor levels so that for a bin size of 0.05 g, the -0.183 g peak is plotted at -0.15 g. For positive load factors, a similar situation occurs for the occurrence between 0.13 and 0.14 g. Thus, the bin size used influences the accuracy of the statistical curve. For a bin size of 0.01 g, the error for the -0.183 g reading was -0.003/-0.183 = 1.64%. For a bin size of 0.05 g, this error changes to -0.033/-0.183 = 18.03%. A fixed bin size results in a varying error as a function of the parameter value with the errors changing from high values at lower parameter values progressing to lower errors at the higher parameter values.

2.8 EFFECT OF SAMPLING RATE ON BIN COUNTS.

Sampling rate effects the magnitude of the counted peak as well as the flight phase into which the peak is placed. Figure 13 shows an analog data signal sampled at 16 and 8 samples per second divided into preflight, in-flight, and postflight phases. When sampling the analog signal at 16 samples per second, the first peak identified would be point A. This peak would be placed in a bin of 0.9 to 1.0 g for the preflight phase. When sampling at eight samples per second, the first peak identified would be point B. This point would be placed in a bin of 0.3 to 0.4 for the in-flight phase. Thus, in this particular case, the same analog peak would be binned in different bins as well as flight phases, depending on the sampling rate used. Similarly, for points C and D,

point C would be binned in -0.8 to -0.9 g and point D would be binned in -0.7 to -0.8 g, but both peaks would be counted in the in-flight phase. Points E and F identify the last analog peak based on 8 and 16 samples per second respectively. Point E would be binned in 0.3 to 0.4 g in the in-flight phase, while point F would be binned in 0.9 to 1.0 g for the postflight phase. The example discussed here is designed to provide insight into the peak count differences as a function of sampling rate, as presented in the following section.

3. SAMPLING RATE STUDY.

The database used for this study consisted of selected parameters that were recorded at higher than normal sampling rates on 108 flights of a single Airbus A319 aircraft while conducting normal flight operations. Table 1 presents a listing of the parameters and their sampling rates.

For this effort, the impact of changing sampling rates was studied for the vertical, lateral, and longitudinal accelerations, pitch and bank angles, and the elevator, aileron, and rudder deflection parameters. Because pressure altitude was not available, the time histories could not be broken down in the mission phases used in previous studies. However, since the squat switch parameter was available, the missions were broken down in preflight, flight, and postflight segments.

3.1 POWER SPECTRAL DENSITY ANALYSIS.

To conduct the PSD analysis, time histories were derived from the database for three flights (3, 35, and 62) that exhibited maximum load factor activity. For each of the flights, the time histories included the vertical, lateral, and longitudinal load factors, pitch and bank angles, and aileron, elevator, and rudder deflections. For each parameter, PSDs were calculated using the fast Fourier transform (FFT) technique. For the load factor parameter, PSDs were calculated for the preflight, in-flight, and postflight segments of the time histories. For the pitch angle, bank angle, and control surface deflection parameters, PSDs were calculated for the in-flight segment of the time histories only. The square root of total area under the PSD curve is equal to the rms of the time history segment on which the PSD is based. All PSDs were normalized to a unit rms by dividing the PSD by the square of its rms value. As was shown in figure 8, the square root of a continuous integration of the PSD demonstrates how the standard deviation or rms changes with increasing frequencies in the measured parameter and, thus, provided insight into the ability of increasing sampling rates to capture the higher magnitudes of the parameter. Dividing the continuously integrated rms by the total rms, as obtained from the area under the PSD curve, the rms can be plotted versus frequency as a percentage of the total rms. Applying the Nyquist theorem that a minimum of two samples per cycle is required, the percentage can be evaluated as a function of the sampling rate. The results are presented for each of the three flights independently. Within each flight, each parameter is presented in the form of the time history, the PSD, and the variation of the rms with frequency. Table 2 shows the layout of figures 14 through 121 for each of the three flights. Review of the PSDs will show that in all cases the power does not approach zero, but will maintain an almost constant value as it approaches the Nyquist frequency. As mentioned previously, this is an indication that the sampled data contains aliasing effects. This in turn suggests that frequencies higher than the Nyquist frequency existed in the original signal and the selected sampling rates were too low for the sampled signal to get an accurate picture of its power content. On the other hand, the change in the rms values as they

approach the Nyquist frequency will be seen to be quite small, indicating that the aliasing effects are correspondingly small.

3.1.1 Vertical Load Factor PSDs.

Figures 15, 51, and 87 present the PSDs for the vertical load factor for the preflight phase of the three flights. As can be seen, the normalized PSDs for the three flights are virtually identical. This is as would be expected. The PSD of the acceleration is shaped by the frequency response characteristics of the airplane to an external input. Because the flight profiles in terms of speed, altitude, and airplane weight distribution are expected to be similar from flight to flight, the frequency response characteristics of the airplane will also be similar from flight to flight. While the overall amplitudes of the inputs may vary, the frequency content of the inputs, such as runway roughness and atmospheric turbulence, will also be similar from flight to flight. As a consequence, when the calculated PSD of the response is normalized to account for amplitude differences of the input, they should be very much alike.

Figures 16, 52, and 88 show the cumulative changes in the relative rms values for the preflight segments of the three flights as a function of increased bandwidth of the 16 samples per second digitized time histories. As can be seen, most of the cumulative rms is contained in the spectrum between 0 and 3 Hz, after which the gain in the cumulative rms starts to level off. Approximately 95% of the total rms in the digitized time history is contained within a bandwidth from 0 to 4.0-5.0 Hz. The remaining 5% is accumulated as the sampled bandwidth is increased to 8 Hz. This suggests that there is little additional dispersion in the digitized data as a result of frequencies above approximately 4.5 cycles per second. Selecting a cutoff frequency of 5 Hz would require a minimum sampling rate of 10 samples per second to ensure adequate representation of peak counts.

As would be expected, the normalized PSDs for the in-flight cases, as presented in figures 17, 53, and 89, and the variation in rms, as presented in figures 19, 55, and 91, are also almost identical. However, in the case of in-flight operation, the primary frequency content of the digitized time history is found to be below 1 Hz. For peak count purposes, a minimum sampling rate of two samples per second would be indicated.

The postflight load factor PSDs of figures 19, 55, and 91 and the variation in rms, as shown in figures 20, 56, and 92, again show them to be virtually identical for the three flights. In addition, the PSDs and the associated rms variations with frequency for the postflight phase are very similar to those observed for the preflight phase and the same observations apply.

3.1.2 Lateral Load Factor PSDs.

Comparisons of the lateral acceleration PSD and rms variation plots in figures 22, 58, and 94 and 23, 59, and 95, respectively, for the preflight phase of the three flights show the same close agreement, as observed for the vertical acceleration. Review of the figures shows that 95% of the total lateral load factor rms is contained within a bandwidth of less than 1 Hz. A sampling rate of twice this bandwidth or two samples per second would identify practically all peaks.

Comparisons of the lateral acceleration PSD and rms variation plots in figures 24, 60, and 96 and 25, 61, and 97, respectively, for the in-flight phase of the three flights also show close agreement, as observed for the preflight case. Review of the figures shows that 95% of the total lateral load factor rms is contained within a bandwidth from 0 to slightly above 1 Hz. Again, a sampling rate of twice this bandwidth or two samples per second would identify practically all peaks.

Comparisons of the lateral acceleration PSD and rms variation plots in figures 26, 62, and 98 and 27, 63, and 99, respectively, for the postflight phase of the three flights also show close agreement, as observed for the preflight case. Review of the figures shows that 95% of the total lateral load factor rms is contained within a bandwidth from 0 to 0.5 Hz. In this case, a sampling rate of twice this bandwidth or one sample per second would be acceptable for peak counting.

3.1.3 Longitudinal Load Factor PSDs.

For the longitudinal acceleration, the PSDs of figures 29, 65, and 101 again show very close agreement for the preflight phase of the three flights. The same observation is made for the rms variation shown in figures 30, 66, and 102. The rms variation shown in the last three figures shows that the primary activity occurs at very low frequencies, less than 0.5 Hz. A sampling rate of one sample per second should, therefore, identify the majority of peaks.

For the in-flight phase of longitudinal acceleration, the PSDs of figures 31, 67, and 103 again show very close agreement for the three flights. The same observation is made for the rms variation shown in figures 32, 68, and 104. The rms variation shown in the last three figures shows that the primary activity occurs at very low frequencies less than 0.5 Hz. A sampling rate of one sample per second should, therefore, identify the majority of peaks.

The longitudinal acceleration PSDs of figures 33, 69, and 105 for the postflight phase of the three flights also show very close agreement. The rms variation as shown in figures 34, 70, and 106 are also in close agreement. The rms variation shown in the last three figures shows that the primary activity occurs at very low frequencies less than 0.5 Hz. A sampling rate of one sample per second should, therefore, identify the majority of peaks.

3.1.4 Pitch and Bank Angle PSDs.

The pitch angle information contained in figures 36, 72, 108, 37, 73, and 109 show the same close agreements observed for the accelerations with the major activity occurring below 0.25 Hz. Thus, a sampling rate equal to once per 2 seconds should be adequate to identify the important peaks.

Similarly based on the bank angle PSDs of figures 39, 75, and 111 and the rms variation shown in figures 40, 76, and 112, a sampling rate of once per 2 seconds should be more than adequate to detect the major peaks.

3.1.5 Control Surface Deflection Angle PSDs.

The aileron surface deflection PSDs of figures 42, 78, and 114 and the rms variation shown in figures 43, 79, and 115 again show close agreement for the three flights and indicate that a sampling rate of once per second is adequate.

The elevator deflection PSDs for the three flights shown in figures 45, 81, and 117 are not in as close an agreement as the agreements observed for all previously discussed parameters. As a consequence, the rms variation shown in figures 46, 82, and 118 also show less of an agreement. Overall, the important activity still is at very low frequencies, and a sampling rate of one sample per second would account for 95% of the total activity.

Finally, for the rudder deflections, the PSDs of figures 48, 84, and 120 and the rms variation plots in figures 49, 85, and 121 indicate a sampling rate of one sample per second to be sufficient to detect most peaks.

3.2 CUMULATIVE OCCURRENCES STATISTICS.

The effect of different sampling rates on peak counts was evaluated through comparison of the distributions of cumulative occurrence at different sampling rates. Table 3 presents an overview of the parameters studied and their respective sampling rates, dead band, and binning increments used.

As discussed previously, digitization of a continuous signal without prefiltering results in aliasing information at higher frequencies into lower frequencies. Time histories for the different sampling rates were obtained through down sampling of the digitized time histories available for the maximum sampling rates, as shown in table 1. Unfortunately without filtering this process, results in further aliasing frequency information above half the sampling rate into the lower frequencies. Nevertheless, cumulative occurrence statistics were obtained for different sampling rates using simple down sampling from a database containing digitized time histories for 108 flights.

The accelerations cumulative occurrence was obtained for preflight, in-flight, and postflight operations. For the pitch angle, bank angle, and control surface deflections, only in-flight cumulative occurrences were derived. Because this part of the study was oriented towards evaluating the effect of sampling rates on occurrence statistics, the gravitational effects on the transverse sensitivity of the accelerometers was not considered. For the vertical and lateral accelerometers, this effect is not great and has always been neglected. However, the errors introduced in the longitudinal accelerometer readings can be significant, especially during the departure and climb phases of flight. Fortunately, longitudinal acceleration statistics during flight have not been of interest and have not generally been published.

The cumulative occurrence statistics for each parameter is presented in three formats, as shown in table 4. For each parameter, the first figure presents a curve of the cumulative occurrences. The second figure contains a table containing a tabulation of the numerical occurrences behind the curves shown in the first figure. The table also shows the occurrences as a percent of the occurrences counted for the maximum sampling rate. The third figure is a graphical presentation

of the percentages shown in the table. In evaluating the effect of different sampling rates on peak counts, it is important to keep in mind that the effects are presented as a percentage of the maximum sampling rate used for the parameter. There is no assurance that the maximum sampling rate used in this study was adequate to define all the peaks in the original signal. In other words, the peak count statistics for the maximum sampling rates used may be in error.

3.2.1 Incremental Vertical Load Factor Statistics.

Figures 122, 123, and 124 present the vertical load factor statistics in three different formats for the preflight phase of 108 flights. The figures show that reducing the sampling rate from 16 to 8 samples per second has an unmistakable but not large impact on the overall load factor statistics. For the four, two, and one sample per second cases, the peak counts and the magnitudes show significant and unacceptable reductions.

Figures 125, 126, and 127 present the vertical load factor statistics in three different formats for the in-flight phase of 108 flights. The figures show that reducing the sampling rate from 16 to 8 samples per second has very little impact on the overall load factor statistics. For the preflight phase statistics, the peak counts and the magnitudes sampled at four, two, and one sample per second show significant and unacceptable reductions.

Figures 128, 129, and 130 present the vertical load factor statistics in three different formats for the postflight phase of 108 flights. In contrast to the preflight phase, these figures show that reducing the sampling rate from 16 to 8 samples per second has some impact on the overall load factor statistics. For the preflight phase statistics, the peak counts and the magnitudes sampled at four, two, and one sample per second show significant and unacceptable reductions.

In summation, for the purpose of peak counting, the minimum sampling rate for ground operations, a sampling rate greater than eight samples per second would be desirable, and for the flight phase, a sampling rate of eight samples per second is acceptable.

3.2.2 Lateral Load Factor Statistics.

Figures 131, 132, and 133 show the lateral load factor statistics for preflight operations. The figures show that, as with the vertical accelerations, reducing the sampling rate to eight samples per second has no large effect on the overall lateral load factor statistics in the preflight phase. Sampling at four samples per second has an unacceptable effect on the measurement of negative peaks, but the positive peaks are acceptably identified. Sampling rates lower than four samples per second, however, do not provide adequate sampling of peaks and valleys.

Figures 134, 135, and 136 show the lateral load factor statistics for in-flight operations. The figures show that, as with the lateral accelerations recorded during the preflight phase, sampling at less than eight samples per second will result in loss of peak counts.

Figures 137, 138, and 139 show the lateral load factor statistics for postflight operations. The figures show that sampling rates as low as four samples per second will provide results in generally equal peak counts.

3.2.3 Longitudinal Load Factor Statistics.

Figures 140, 141, and 142 present the longitudinal load factor statistics for the preflight operational phase. The figures show that the minimum acceptable sampling rate is eight samples per second. The higher magnitudes of positive load factor during the preflight phase are likely associated with the takeoff portion of the preflight phase.

Figures 143, 144, and 145 present the longitudinal load factor statistics for the in-flight operational phase. The figures show that the minimum acceptable sampling rate is four samples per second. Sampling rates at two or one sample per second result in large peak count losses. In the case of the in-flight phase, the higher magnitudes of the positive load factors are associated with the departure and climb phases. During these phases, the longitudinal accelerometer measures the gravitational forces caused by the pitch angle inclination of the accelerometer axis from the horizontal.

Figures 146, 147, and 148 present the longitudinal load factor statistics for the postflight operational phase. The figures show that the minimum acceptable sampling rate is four samples per second. Sampling rates at two or one sample per second result in large peak count losses. The more severe negative accelerations during the postflight phase are the result of braking forces during landing.

3.2.4 Pitch and Bank Angle Statistics.

Figures 149, 150, and 151 present the pitch angle cumulative peak counts. Sampling rates of four, two, and one sample per second have no significant effect on the peak count data. This is consistent with the fact that the frequency content of pitch angle changes is very low.

Figures 152, 153, and 154 present the bank angle cumulative peak counts. Similarly to the pitch angle changes, the frequency content of bank angle changes is also very low.

Therefore, sampling rates of four, two, and one sample per second have no significant effect on the peak count data. The large percent difference noted at the most negative bank angles result from the fact that very few peaks were counted. For instance, if sampling at two samples per second resulted in a single peak count while sampling at four samples per second resulted in a two-peak count, the resulting percent difference would be 50 percent.

3.2.5 Control Surface Deflection Angle Statistics.

Figures 155, 156, and 157 present the aileron deflection angle cumulative peak counts. Sampling rates of 16, 8, and 4 samples per second are seen to provide almost identical peak counts. Only at sampling rates of two and one sample per second do significant differences in peak counts occur. This is consistent with the fact that the frequency content of aileron deflection angle changes is very low.

Figures 158, 159, and 160 present the elevator deflection angle cumulative peak counts. The figures show a significant change in peak counts when the sampling rate is reduced from four samples per second.

Figures 161, 162, and 163 present the rudder deflection angle cumulative peak counts. The figures show no significant difference in peak counts between data recorded at 16 and 8 samples per second. However, at sampling rates below eight samples per second, significant peak count losses occur.

3.3 MINIMUM SAMPLING RATES FOR AMPLITUDE DETECTION.

In determining the minimum sampling rate requirements, two questions need to be answered (1) Does the selected sampling rate provide for identification of peaks occurring at different frequencies? (2) If a peak exists does the sampling rate provide an accurate description of the peak amplitude? While the selected sampling rates suggested as a result of the PSD analyses and the peak count statistics discussed previously assume the identification of important peaks over the bandwidth of interest, the same rate is not necessarily high enough to sample the true peak magnitude. Reference 1 presents a study of the relationship between sampling rate and measurement accuracy. This study showed that for a sinusoidal signal, a relationship between measurement accuracy and signal frequency could be established. This relationship takes the following form.

$$\%Error = 100 * (1 - \cos\frac{2\pi F}{2f})$$

Where: F = signal bandwidth frequency
f = sampling rate

The equation can be transformed to calculate the minimum sampling rate required for a specific error value and frequency bandwidth.

$$f = \frac{F\pi}{\cos^{-1}\left(1 - \frac{\%error}{100}\right)}$$

For a maximum allowable error of 10 percent in any amplitude measurement, a sampling rate of 7 times the data signal bandwidth is necessary. The relationship between the sample time and the time of the analog signal peak is random, thus, the sample time may occur at any time during the signal cycle with equal probability. In other words, it is as likely that the sample time coincides with the true peak, i.e., 0% error, as it coincides with a lower value that results in a 10% error. This means that the average error would be expected to be 5%. Using the sinusoid as a simplistic description of a ground or flight loads parameter, average errors in the recorded peak amplitudes can be calculated for different parameter frequencies and sampling rates.

3.4 COMPARISON OF SAMPLING RATE REQUIREMENTS.

The evaluation of the PSDs of the various parameters discussed in section 2 provided suggested minimum sampling rates for each of the studied parameters. Similarly, comparison of the peak counting results for different sampling rates suggested minimum sampling rates that would provide peak counts comparable to the counts obtained from the maximum sampling rates used. Unfortunately, there is no agreement between the minimum sampling rates gleaned from the

PSD analyses and the parameter peak count statistics. In addition, these suggested sampling rates are based on identifying peaks without consideration of the sampling rates needed to ensure identification of the peak amplitudes.

For the PSD analyses, the minimum sampling rates were selected based on the premise that the frequency bandwidth that contained 95% of the total time history rms of the parameter measurement would ensure the identification of peaks that are the most important contributors to the overall peak count statistics. The minimum sampling rates were selected so that they would result in a fixed number of even time increments in each second. From the peak count statistics, the minimum sampling rates were selected so that they encompassed at least 95% of the peak counts obtained from the maximum sampling rate available in this study. The minimum sampling rates to ensure acceptable estimates of peak amplitudes were based on not exceeding a maximum 10 percent error over the frequency bandwidth that encompassed at least 95% of the total rms of the parameter measurement. Airplane flight recorder specifications are contained in 14 CFR Part 121, Appendices B and M. Appendix A in this report contains Part 121 Appendix B and Appendix B in this report contains Part 121 Appendix M. Table 5 presents the selected sampling rates from this study and compares them to the 14 CFR requirements of Part 121 Appendices B and M.

Comparison of the selected sampling rates from the PSD analyses and the peak count statistics show considerable differences. The selected minimum sampling rates based on the PSD results are lower than those obtained from the peak count statistics. Agreement of the PSD-selected sampling rates with the sampling rates selected from the peak count, the results can be improved if instead of a 95% rms level, an rms level approaching 100% of the total rms is used in the selection of the PSD-based sampling rates. It is also worth noting that, except for the aileron deflections, slower sampling rates below the maximum sampling rates available for the study resulted in measurable changes in the peak count statistics. This raises the suspicion that the maximum sampling rates used in this study may also be too low to obtain realistic peak statistics. It is interesting to note that different sampling rates are indicated for ground and flight operations.

3.5 DERIVATION OF FLIGHT CONTROL DEFLECTION STATISTICS.

Figures 122 through 163 show the changes in parameter peak count statistics as a function of the sampling rate. These figures tend to be interpreted as indicating a loss in the number of peaks that are counted as the sampling rate is reduced. Column three in table 5 shows the minimum samples per second required to capture a peak as based on the rms frequency distribution of the PSDs. Column five shows the minimum sampling rate required to ensure that the recorded amplitude of the peak is within a maximum error of 10 percent. Since the sampling rate required to capture the correct amplitude is higher than needed to capture the existence of a peak, the differences seen in the peak count statistics is more likely due to the inability to record the correct peak amplitudes than it is to record the existence of a peak. Thus, assuming that the number of peaks counted is more likely correct, then cumulative occurrence spectra derived at low sampling rates could be corrected to account for the errors in peak amplitude using the approach developed in reference 1. Appendix C presents the results of a subsequent study to apply such a correction to the flight control surface statistics.

4. CONCLUDING REMARKS.

This study used digitized time histories based on relatively low sampling rates. Signal information at frequencies above half the sampling rates was placed at lower frequencies through aliasing, thus distorting the true signal information. It is conceivable that the original signal exhibited important activity at higher frequencies that were aliased into the digitized time histories used. For instance, the vertical load factor activity seen at the higher frequencies nearer to the Nyquist frequency may have been real or an alias. Intuitively, it might be argued that these higher frequencies would be expected to consist of lower peak values, however, without the analysis of digitized time histories sampled at much higher sampling rates, this must remain an open question. The desired sampling rates derived in this study were based on the evaluation of gains in parameter signal power with increased bandwidth and empirical comparisons of parameter statistics for different sampling rates using digitized time history inputs. Because the digitized time histories were based on low sampling rates, serious questions remain about the accuracy of the digitized time histories to reflect the true frequency content of the original signal. The fact that reduction of the sampling rates below the maximum available for this study had measurable effects on the peak count statistics would suggest that the maximum sampling rates used in the study may also have been too low to provide true peak count statistics. In that case, using the peak count statistics obtained from maximum sampling rates as a benchmark to evaluate the effects of lower sampling rates may result in drawing suspect conclusions regarding the minimum acceptable sampling rates.

Acceleration response during ground operations is spread over a much wider frequency range than it is during flight operations, where most of the activity occurs at frequencies below 3 Hz. As a result, the sampling rate requirements, as derived from peak count statistics, show differences for ground and flight operations. To obtain acceleration peak statistics during ground operations with accuracy, similar to those obtained for flight operations, a higher sampling rate for ground operations is required. These differences in sampling rate requirements based on ground or flight operations suggest a need to change the recorded sampling rate as a function of main landing gear squat switch position.

To be completely rigorous, any conclusions to be drawn from this study are applicable to the A319 aircraft only. The power spectral densities (PSDs) of the accelerations represent the of the aircraft response to an input. The in-flight response to the input is filtered through the dynamic response characteristics of the airplane, particularly the natural frequencies, modes, and associated damping as defined by the transfer function. By the same token, the PSDs for control surface deflections are representative of the A319 control system characteristics. For general application, it is reasonable to assume that the airframe system of other airplanes in the same category as the A319 will exhibit the same dynamic response characteristic and, thus, will respond in the same dynamic manner to a given external in-flight input. In that case, the acceleration sampling rate results from this study would be applicable to such other aircraft. Also, if the flight control system characteristics of other aircraft are generally identical to those of the A319, the control surface sampling rate results from this study can reasonably be applied to such other aircraft. The pre- and postflight acceleration responses, especially in the vertical direction, result from runway roughness and are affected by the landing gear damping characteristics. It seems reasonable to assume that the landing gear damping characteristics of the A319 landing gear are similar to those on other airplanes in its weight class that have landing

gears with nearly alike design configurations. Again, in that case, the acceleration sampling rate results from this study would be applicable to such other aircraft.

The maximum sampling rates used to form the database for this study were still too low to define minimum acceptable sampling rates with confidence. In any case, the minimum sampling rates derived in this study cannot be considered conservative estimates. Any specific sampling rate recommendation requires further study using digitized time histories obtained from much faster sampled signals and with proper filtering to prevent the appearance of aliasing in the digitized time history. However, while no specific minimum sampling rates can be recommended with any degree of confidence, it is clear that the sampling rates specified in Title 14 Code of Federal Regulations Part 121, Appendices B and M are low, and there is no doubt that they should be raised.

5. REFERENCES.

1. Anonymous, "Analysis of Relationship Between Sample Rate, Data Bandwidth and Accuracy for Flight Data Recorders with A/D Converters," Technical Note EER-912, Esprit Technology Inc., September 1991.

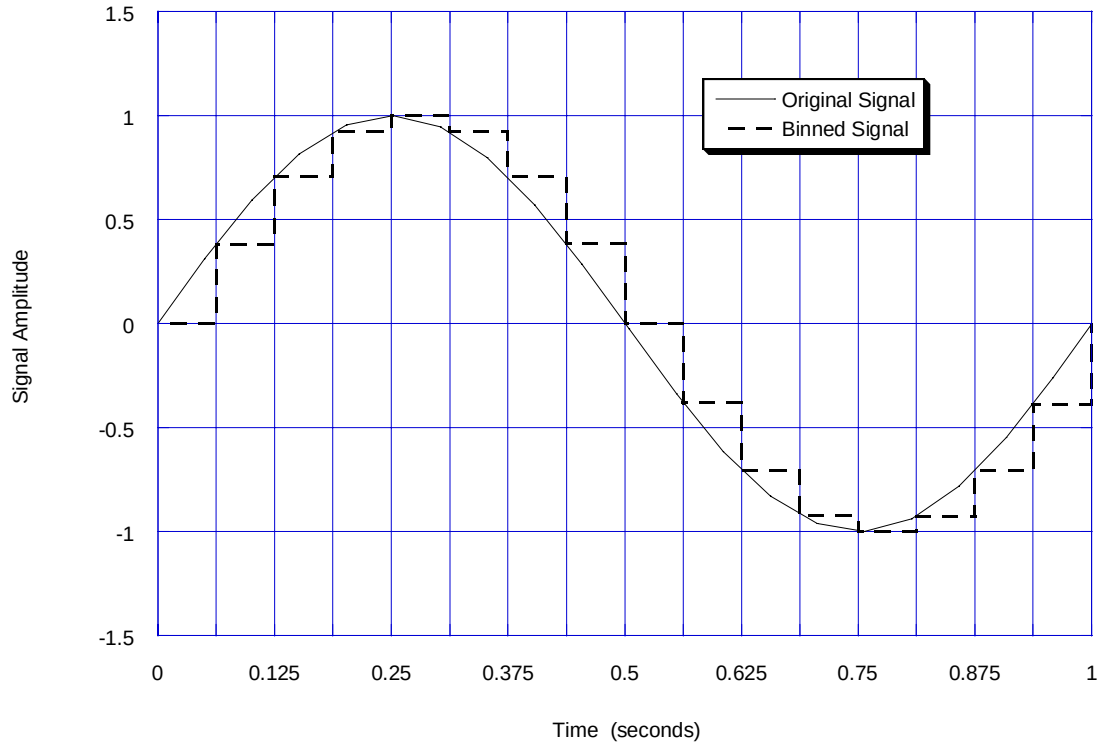

FIGURE 1. ANALOG SIGNAL TO DIGITIZED BINNING

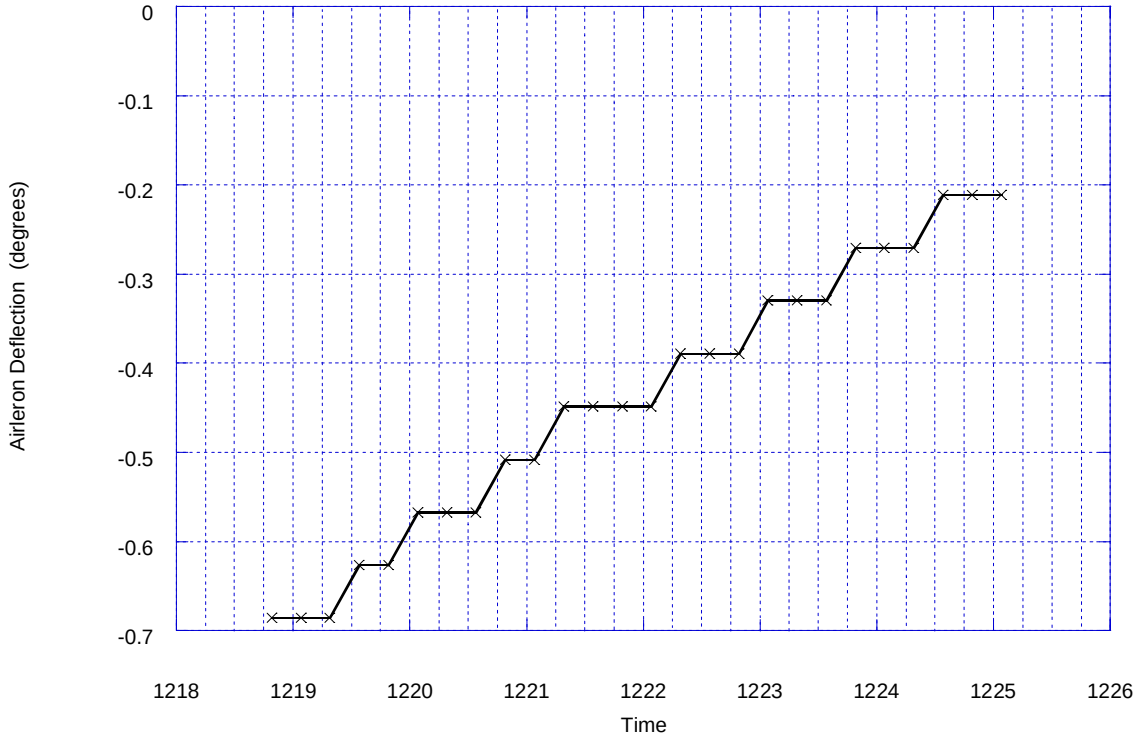

FIGURE 2. DIGITIZED AILERON SIGNAL

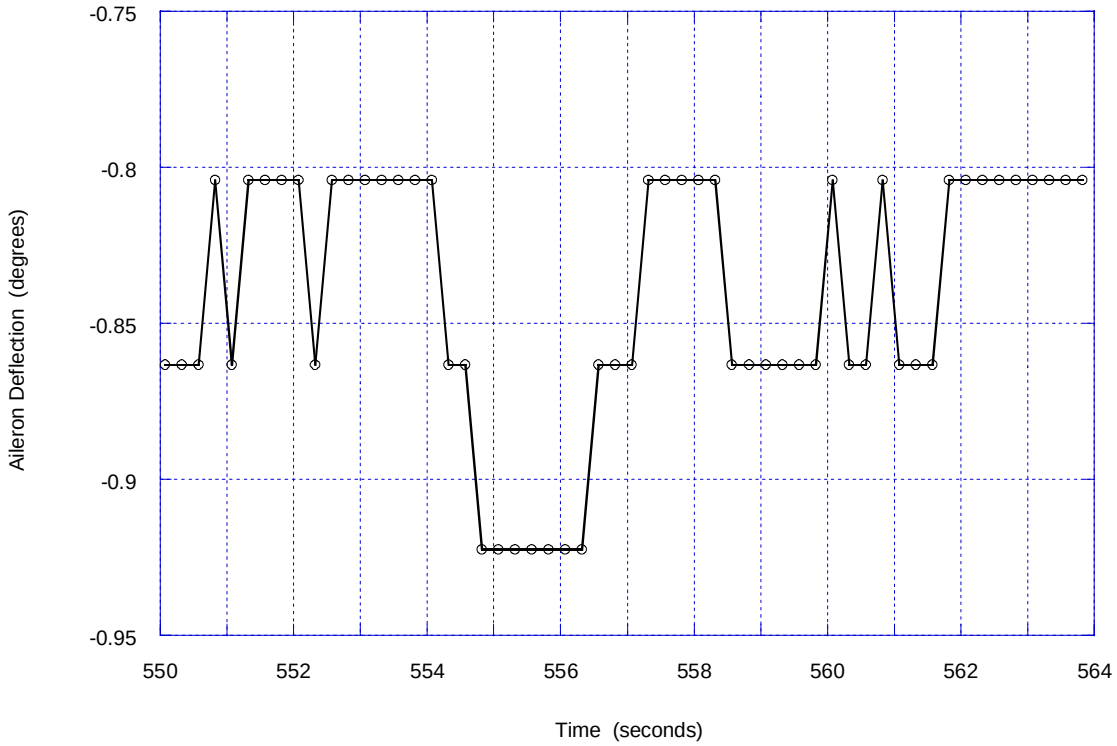

FIGURE 3. PEAK CROPPING DUE TO DIGITIZATION

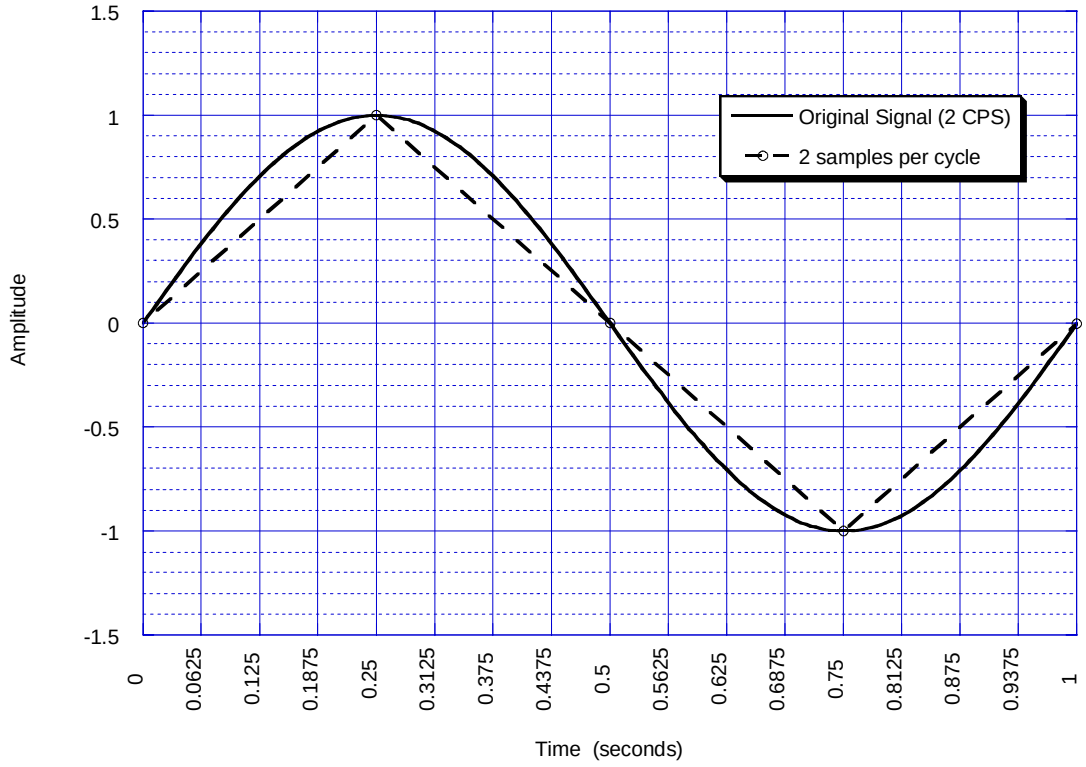

FIGURE 4. SINE WAVE SAMPLED AT TWICE ITS FREQUENCY

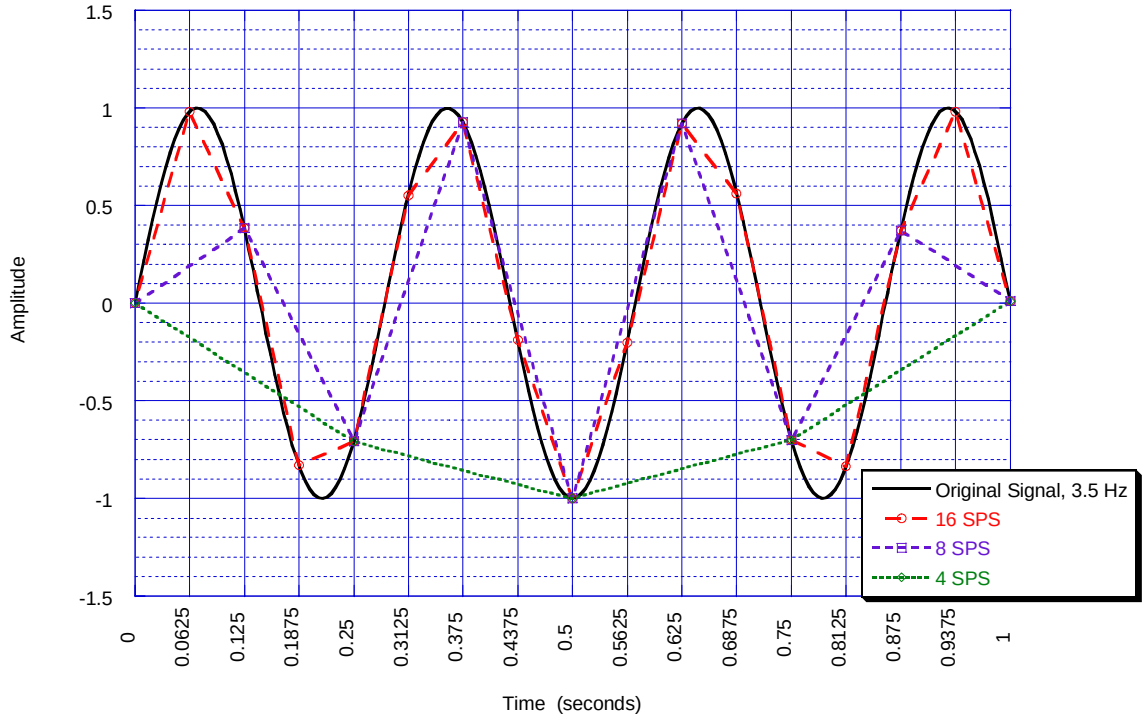

FIGURE 5. ANALOG SIGNAL SAMPLED AT DIFFERENT SAMPLING RATES

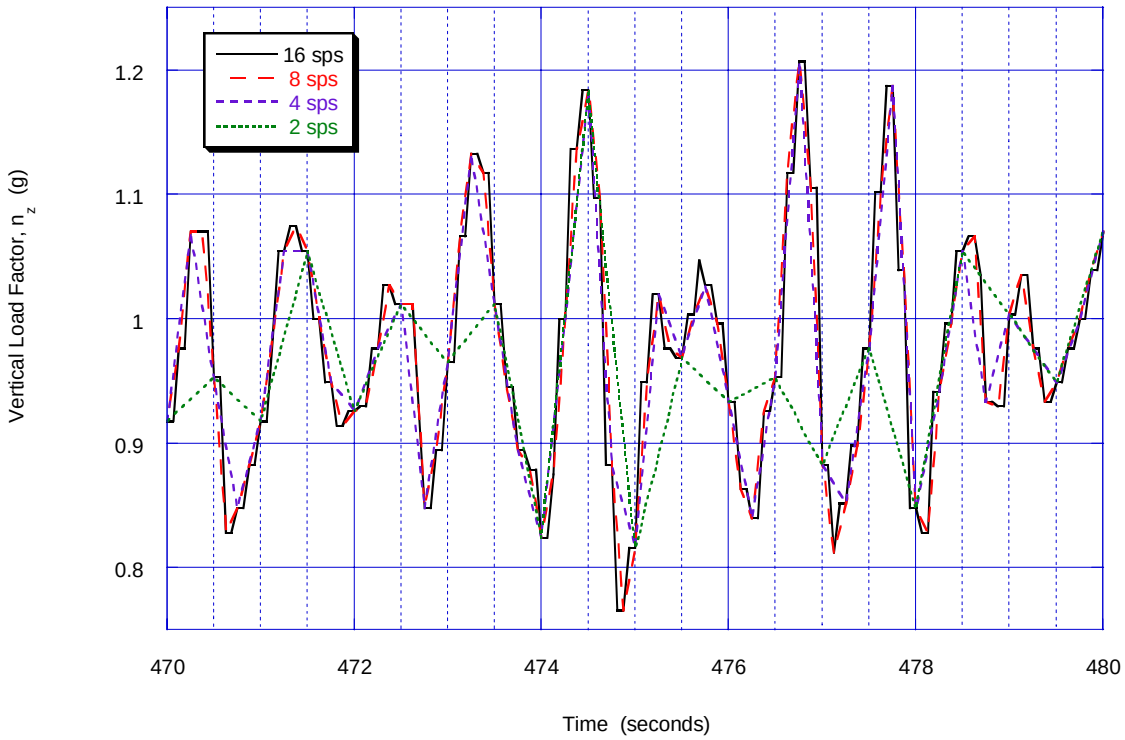

FIGURE 6. VERTICAL LOAD FACTOR TIME HISTORY SAMPLED AT DIFFERENT SAMPLING RATES

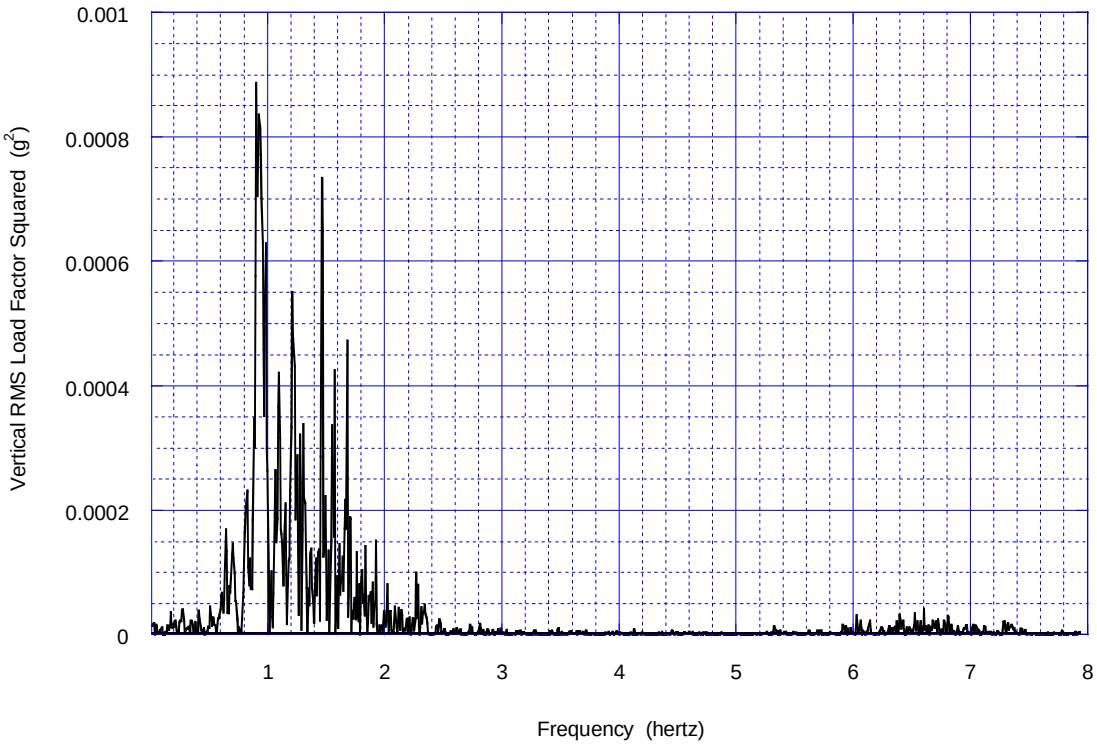

FIGURE 7. VERTICAL LOAD FACTOR PSD, PREFLIGHT

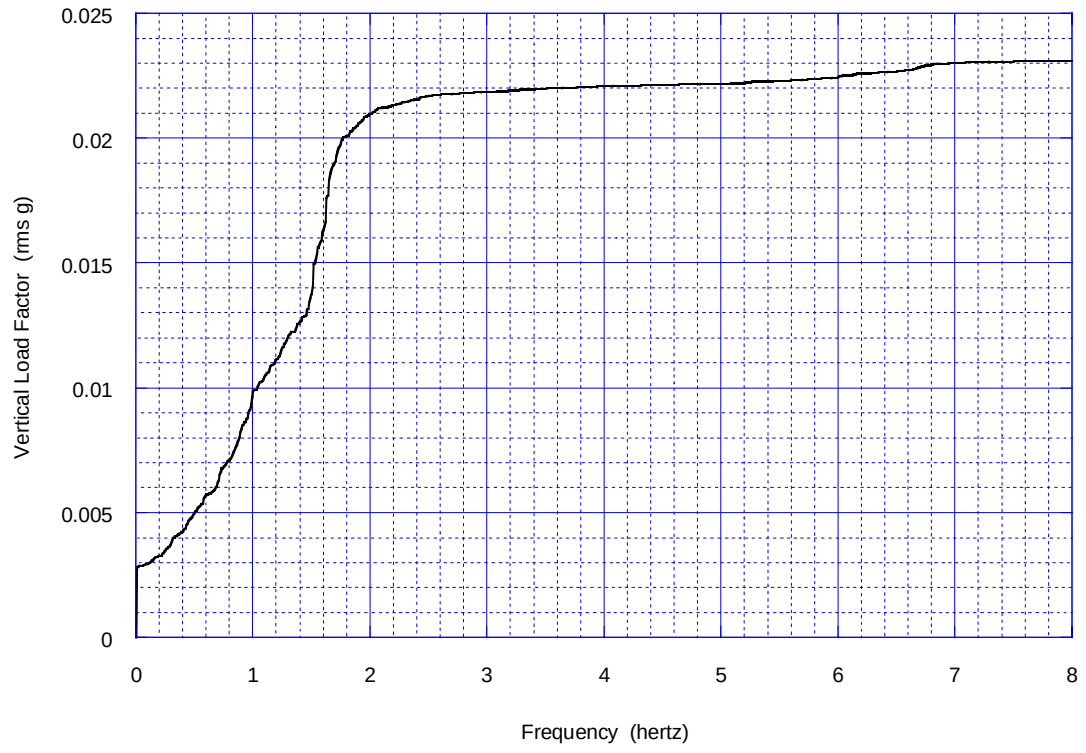

FIGURE 8. VARIATION OF RMS VERTICAL LOAD FACTOR WITH FREQUENCY, POSTFLIGHT

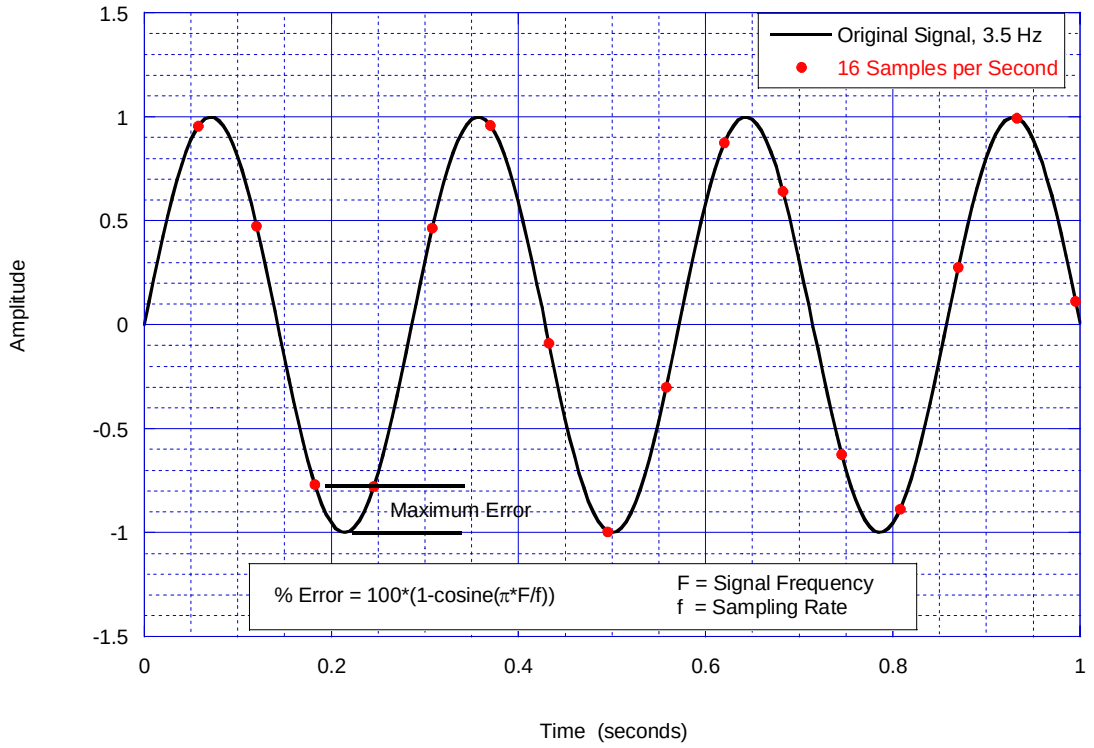

FIGURE 9. CALCULATION OF MAXIMUM PEAK AMPLITUDE ERROR

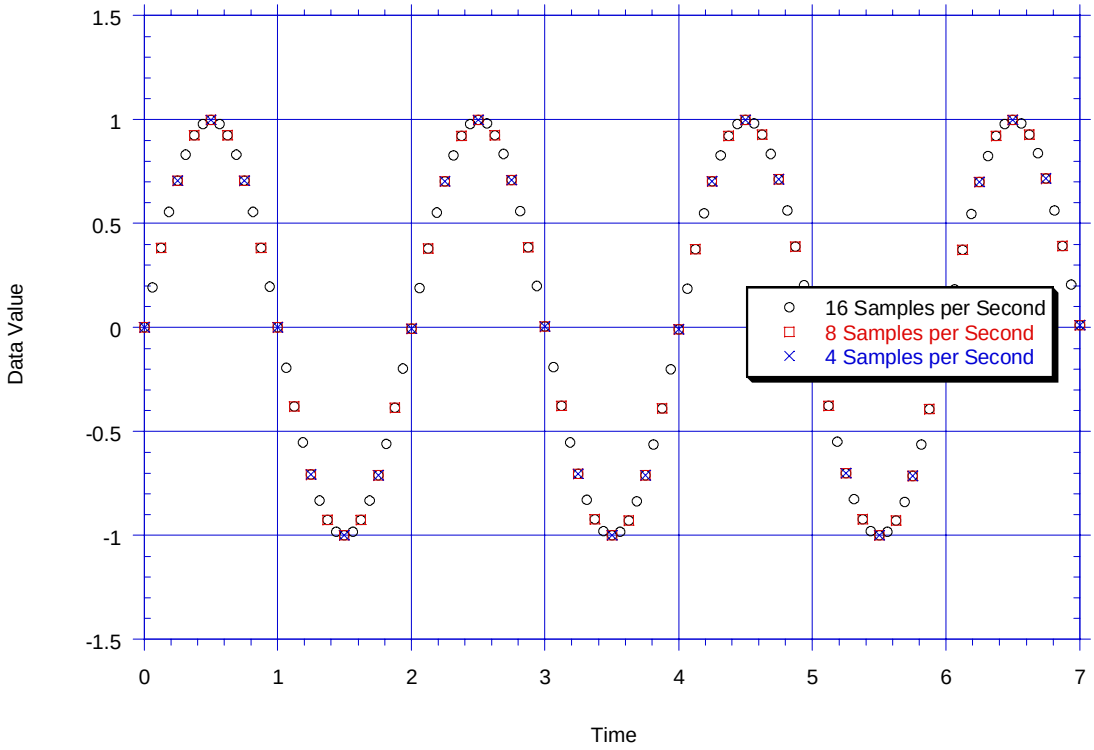

FIGURE 10. DOWNSAMPLING TECHNIQUE

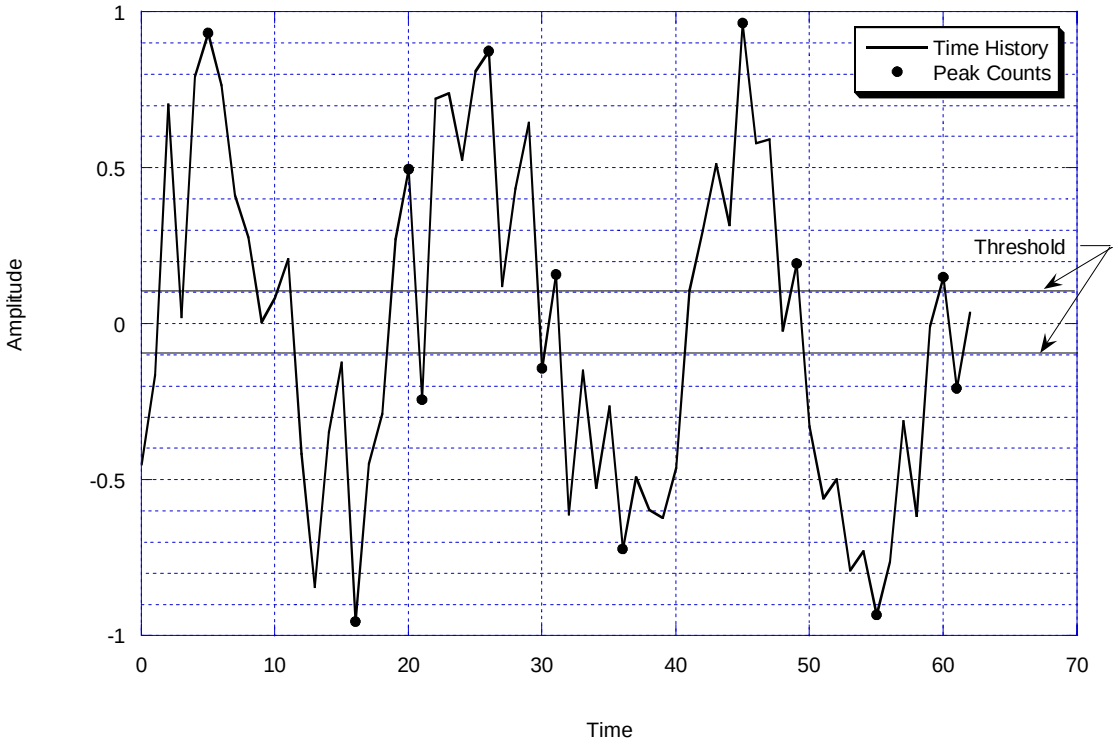

FIGURE 11. PEAK BETWEEN MEAN COUNTING

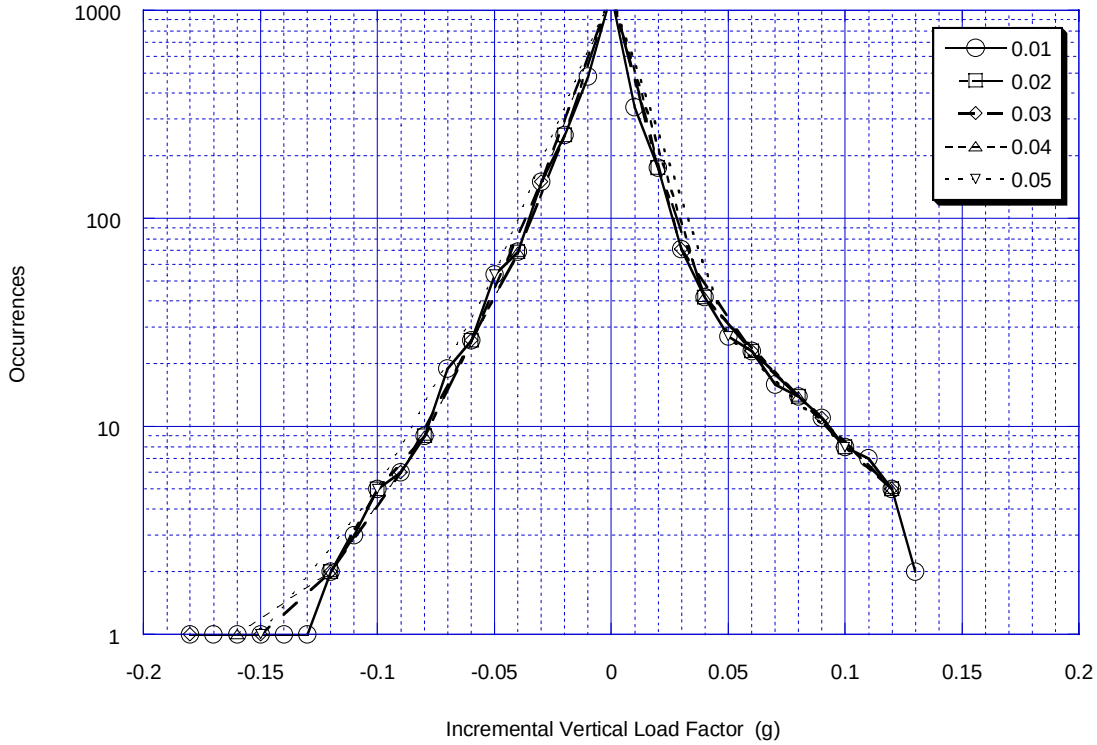

FIGURE 12. EFFECT OF USING DIFFERENT CLASS INTERVALS ON AN INCREMENTAL VERTICAL LOAD FACTOR DISTRIBUTION

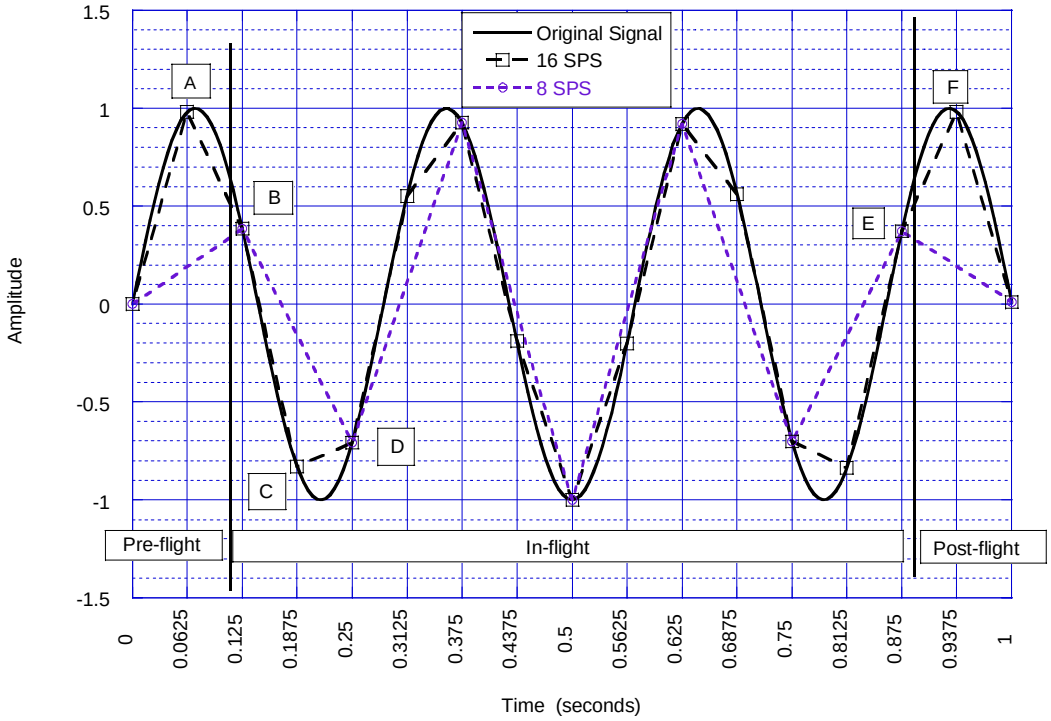

FIGURE 13. EFFECT OF SAMPLING RATE ON PHASE OF FLIGHT BIN COUNT

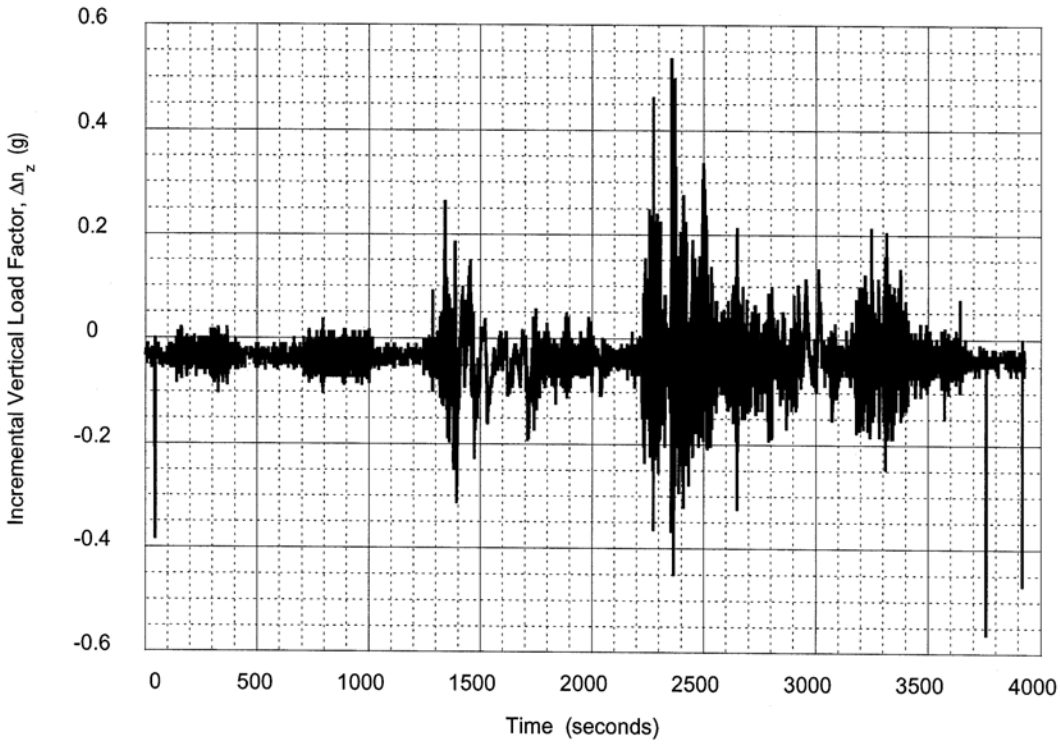

FIGURE 14. INCREMENTAL VERTICAL LOAD FACTOR TIME HISTORY, FLIGHT SEQUENCE 3

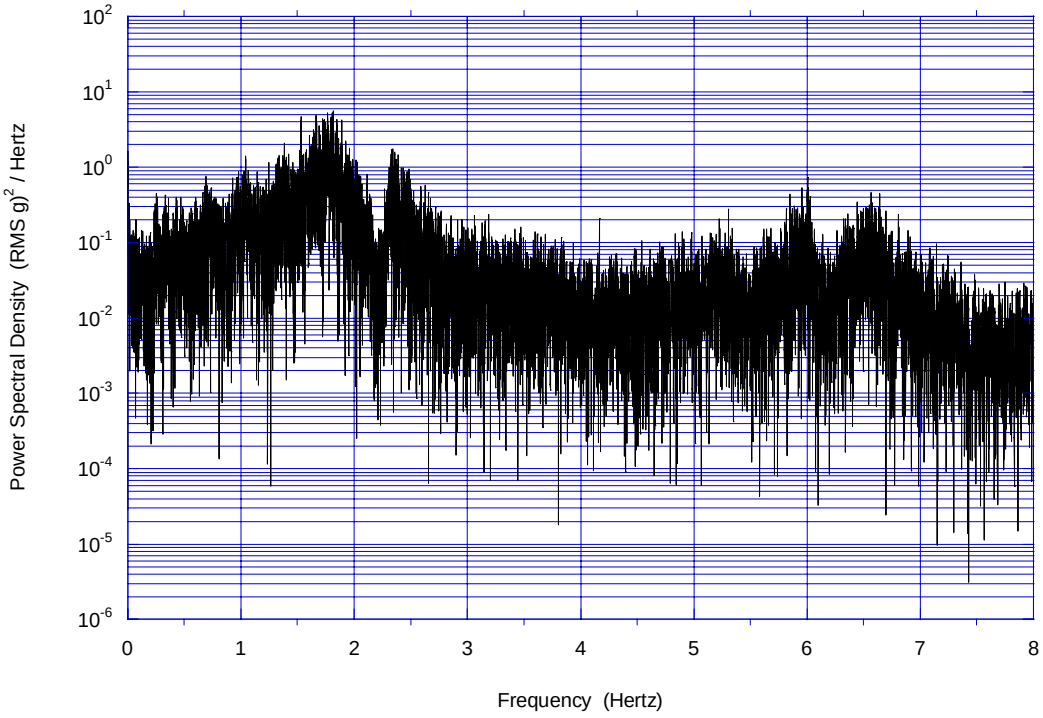

FIGURE 15. NORMALIZED PSD OF INCREMENTAL VERTICAL LOAD FACTOR, FLIGHT SEQUENCE 3, PREFLIGHT

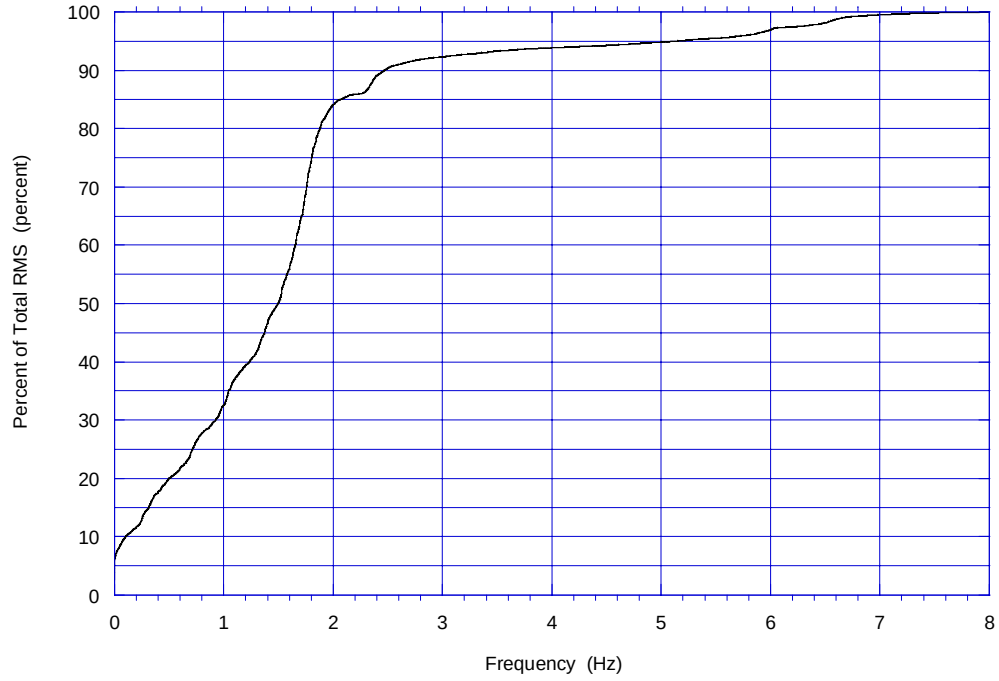

FIGURE 16. PERCENT OF TOTAL INCREMENTAL VERTICAL LOAD FACTOR RMS VS FREQUENCY, FLIGHT SEQUENCE 3, PREFLIGHT

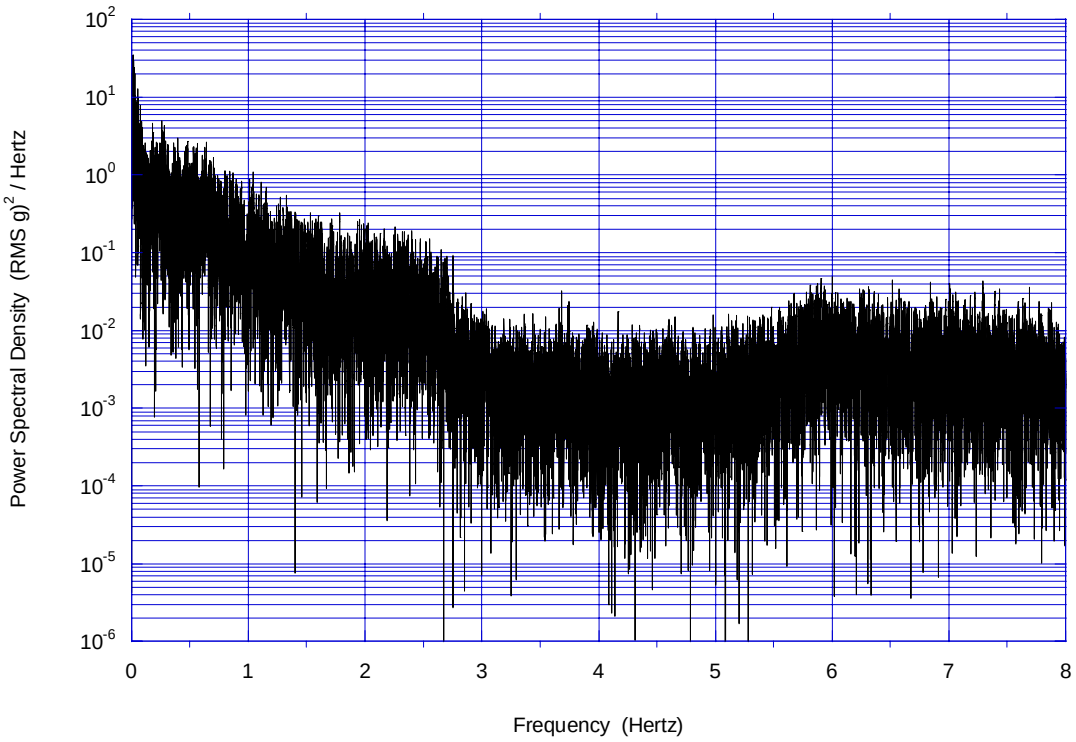

FIGURE 17. NORMALIZED PSD OF INCREMENTAL VERTICAL LOAD FACTOR, FLIGHT SEQUENCE 3, IN FLIGHT

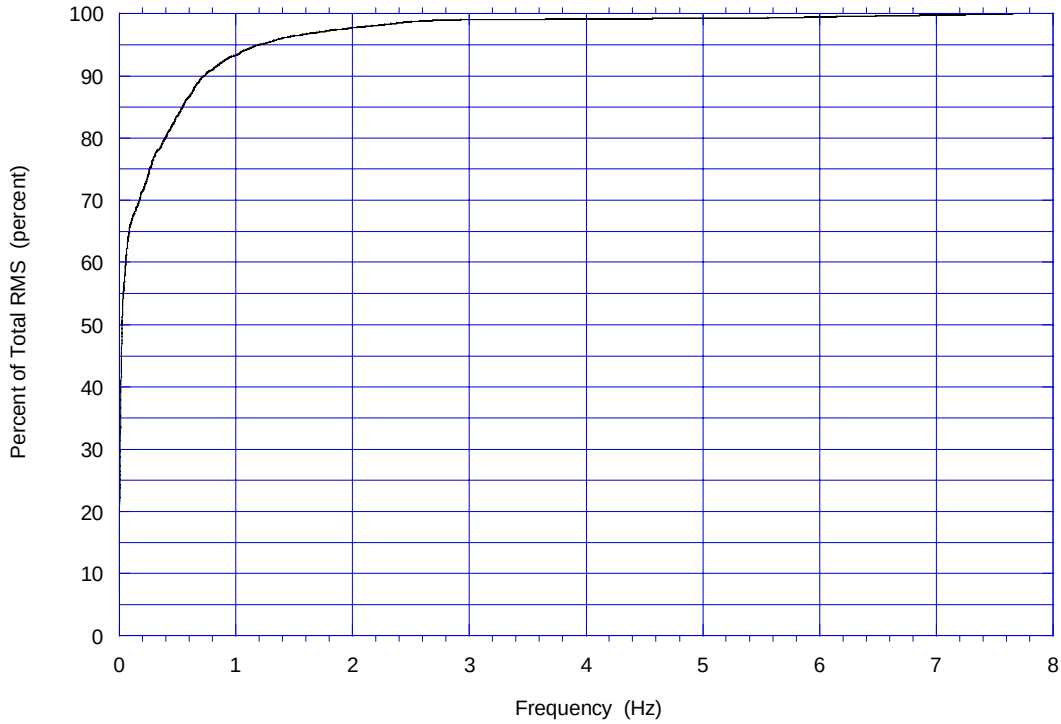

FIGURE 18. PERCENT OF TOTAL INCREMENTAL VERTICAL LOAD FACTOR RMS VS FREQUENCY, FLIGHT SEQUENCE 3, IN FLIGHT

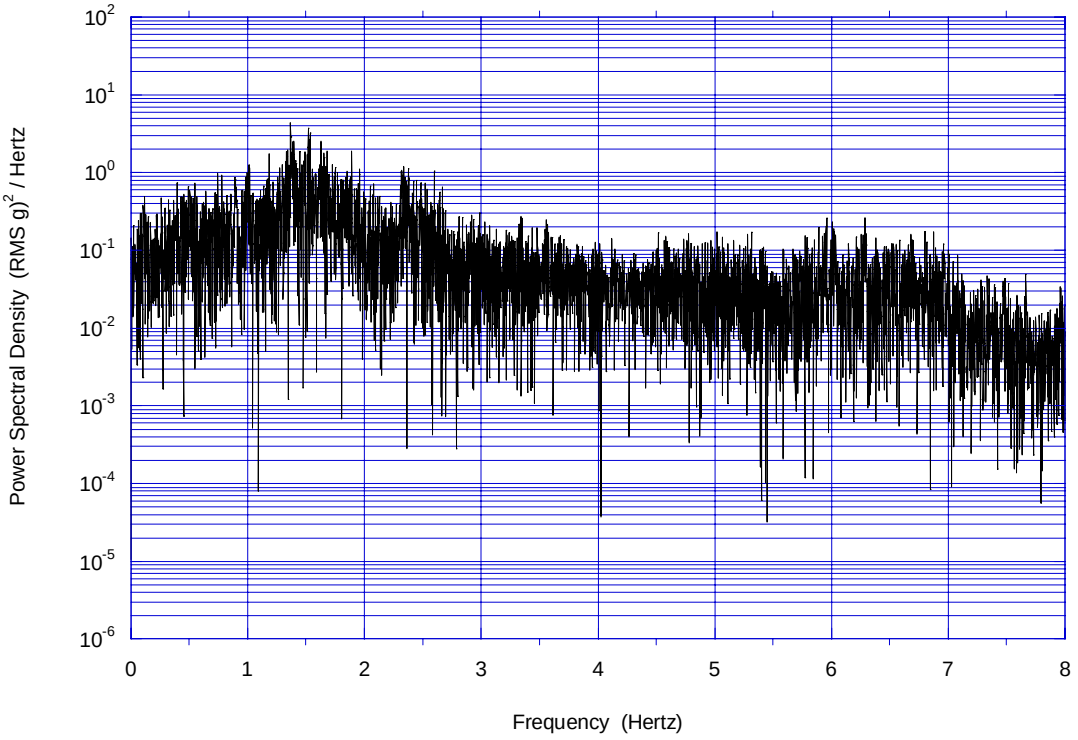

FIGURE 19. NORMALIZED PSD OF INCREMENTAL VERTICAL LOAD FACTOR, FLIGHT SEQUENCE 3, POSTFLIGHT

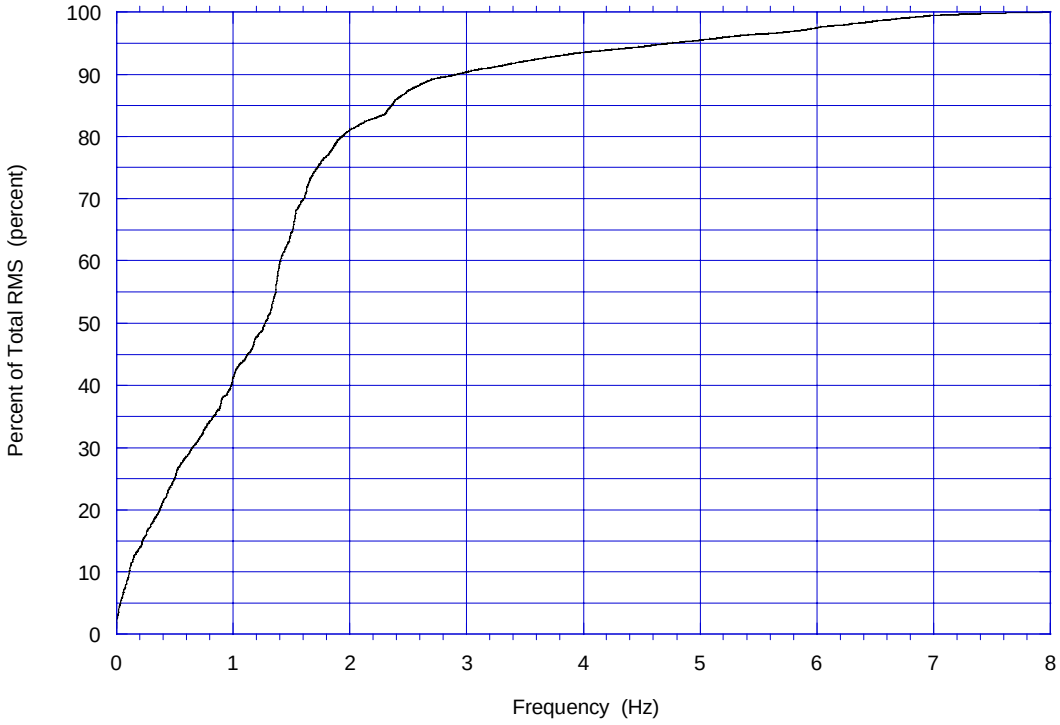

FIGURE 20. PERCENT OF TOTAL INCREMENTAL VERTICAL LOAD FACTOR RMS VS FREQUENCY, FLIGHT SEQUENCE 3, POSTFLIGHT

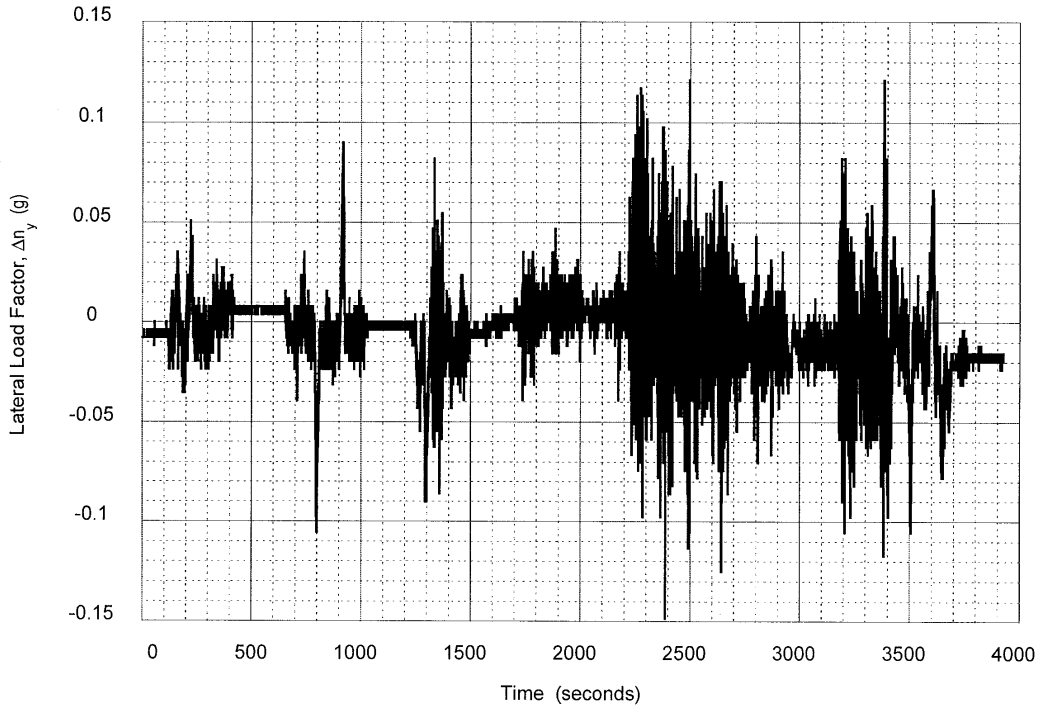

FIGURE 21. LATERAL LOAD FACTOR TIME HISTORY, FLIGHT SEQUENCE 3

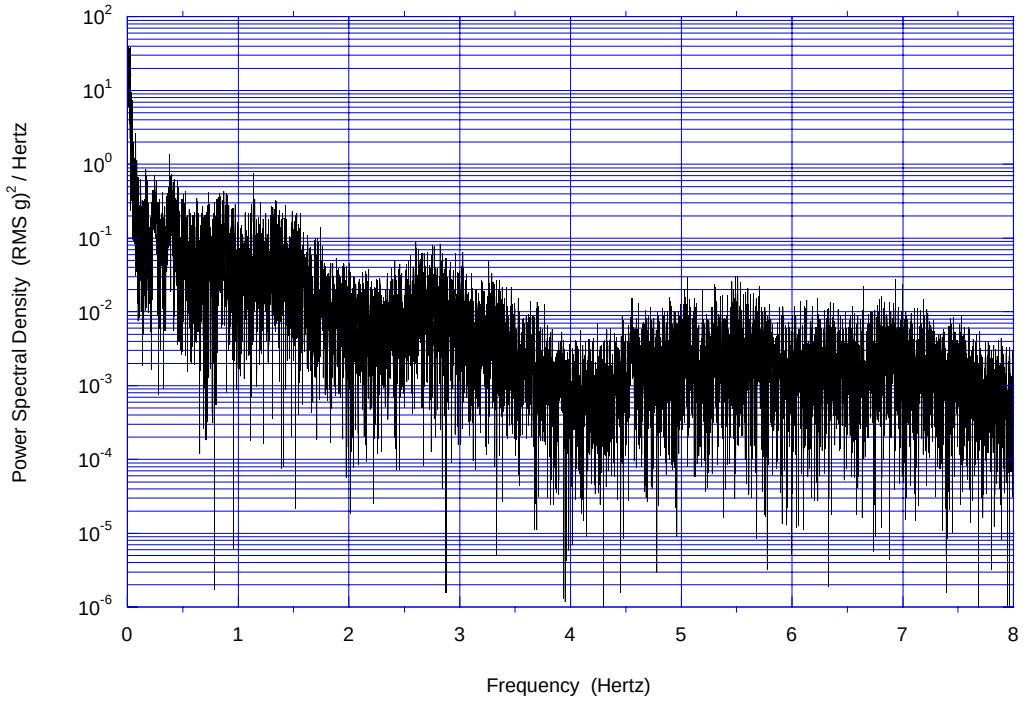

FIGURE 22. NORMALIZED PSD OF LATERAL LOAD FACTOR, FLIGHT SEQUENCE 3, PREFLIGHT

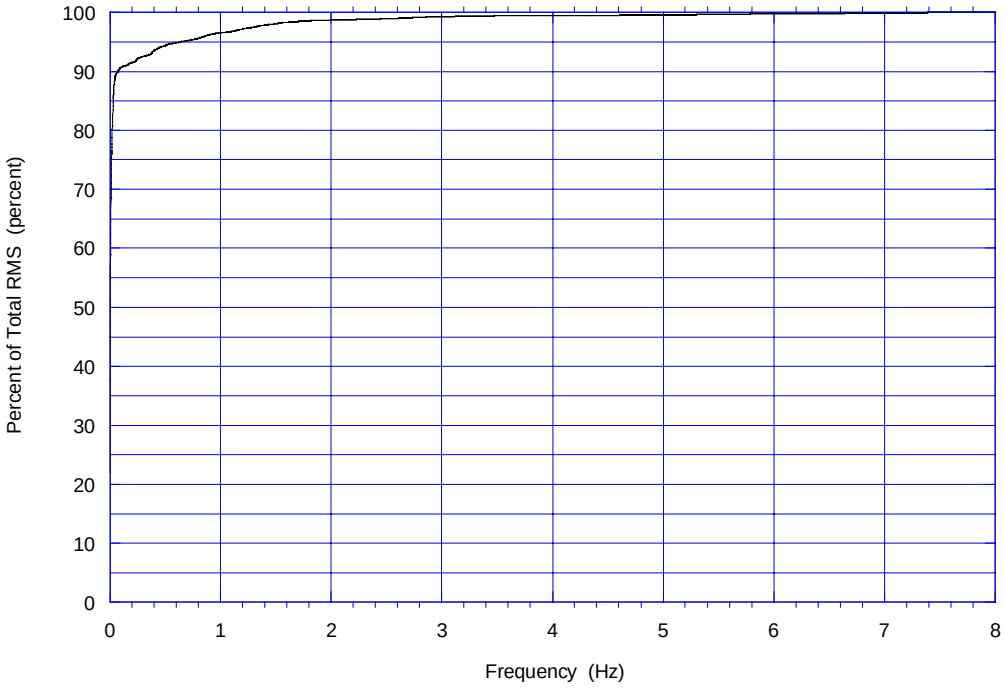

FIGURE 23. PERCENT OF TOTAL LATERAL LOAD FACTOR RMS VS FREQUENCY, FLIGHT SEQUENCE 3, PREFLIGHT

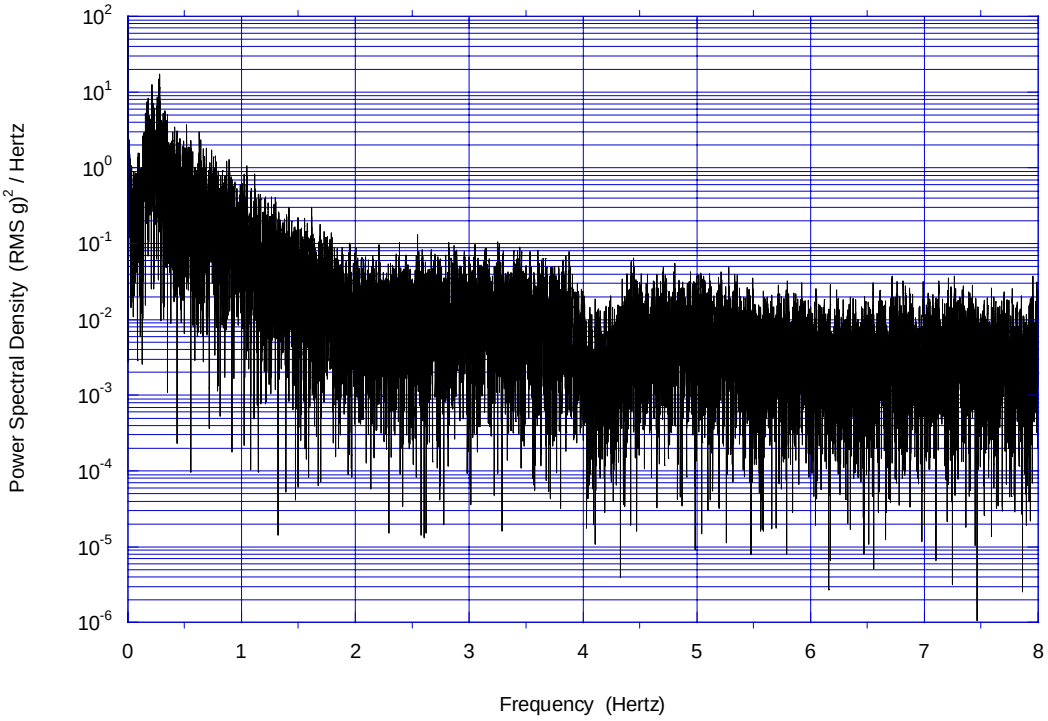

FIGURE 24. NORMALIZED PSD OF LATERAL LOAD FACTOR, FLIGHT SEQUENCE 3, IN FLIGHT

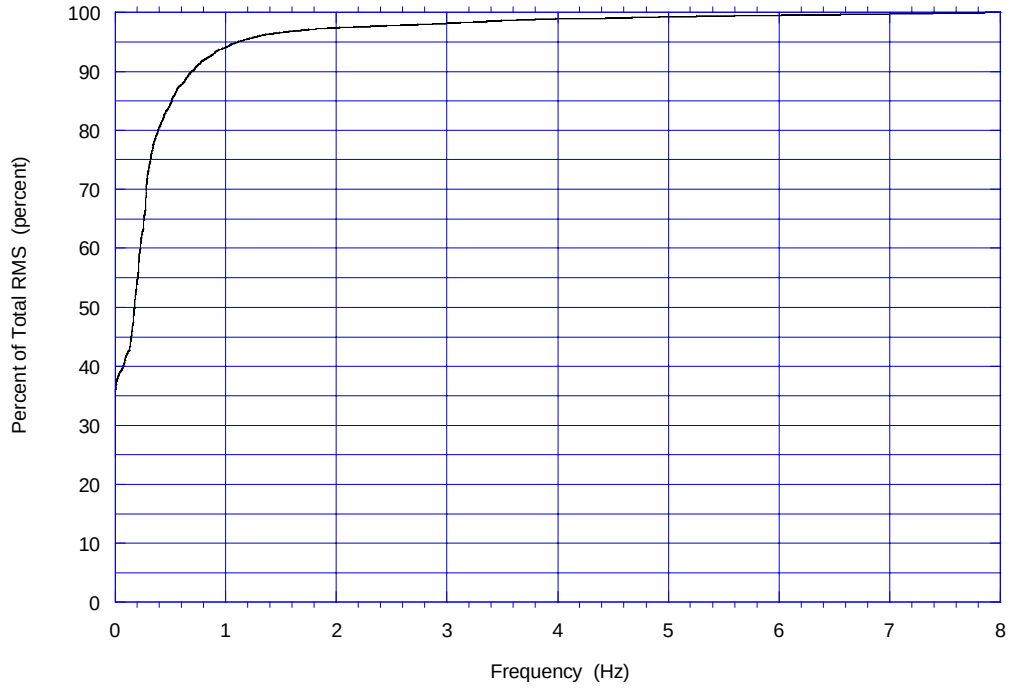

FIGURE 25. PERCENT OF TOTAL LATERAL LOAD FACTOR RMS VS FREQUENCY, FLIGHT SEQUENCE 3, IN FLIGHT

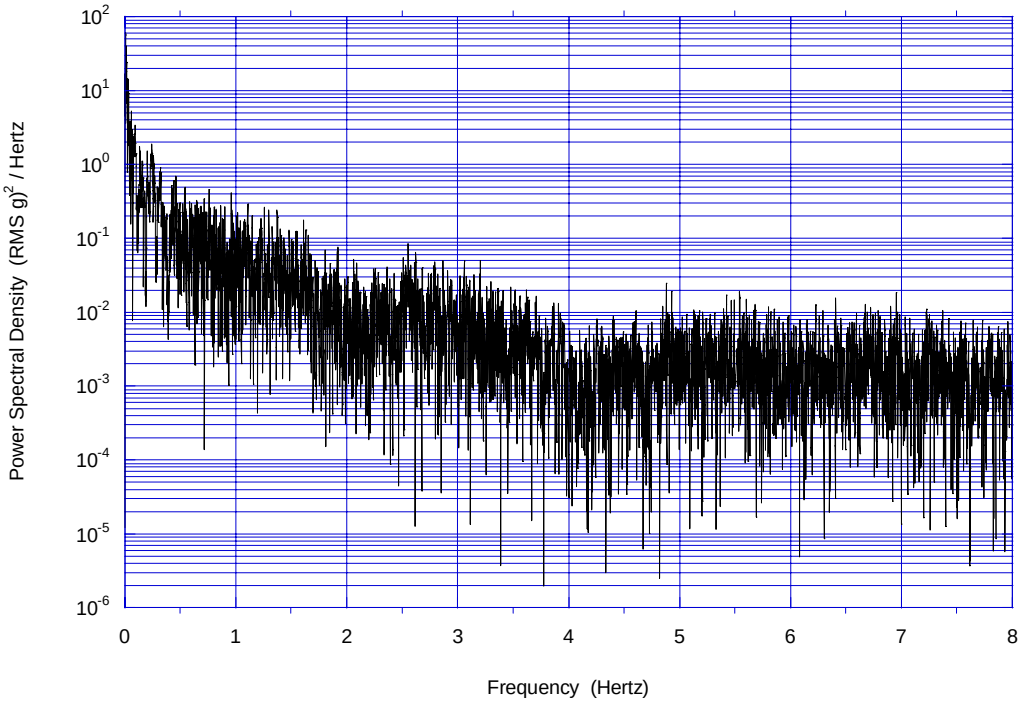

FIGURE 26. NORMALIZED PSD OF LATERAL LOAD FACTOR, FLIGHT SEQUENCE 3, POSTFLIGHT

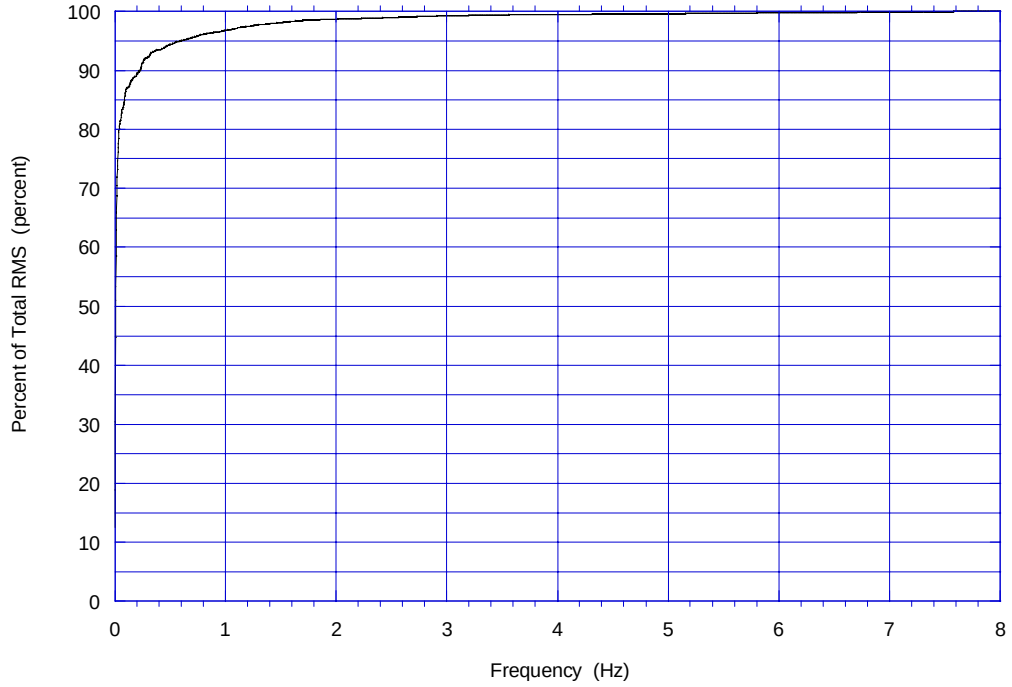

FIGURE 27. PERCENT OF TOTAL LATERAL LOAD FACTOR RMS VS FREQUENCY, FLIGHT SEQUENCE 3, POSTFLIGHT

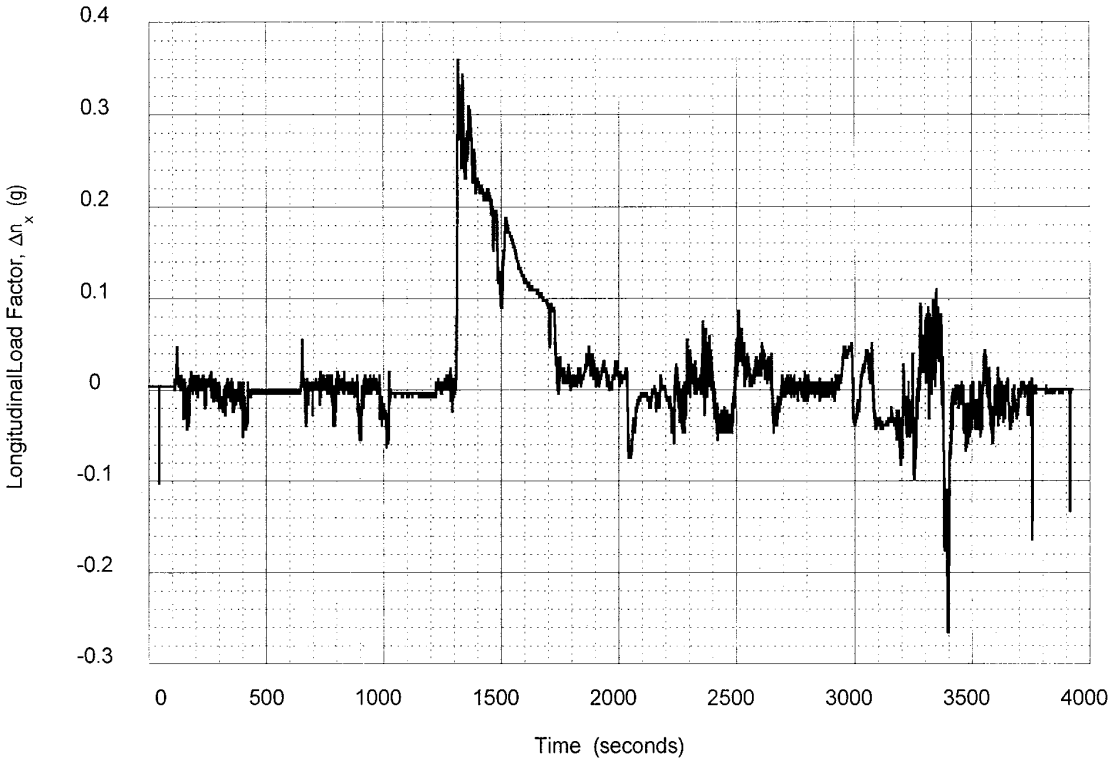

FIGURE 28. LONGITUDINAL LOAD FACTOR TIME HISTORY, FLIGHT SEQUENCE 3

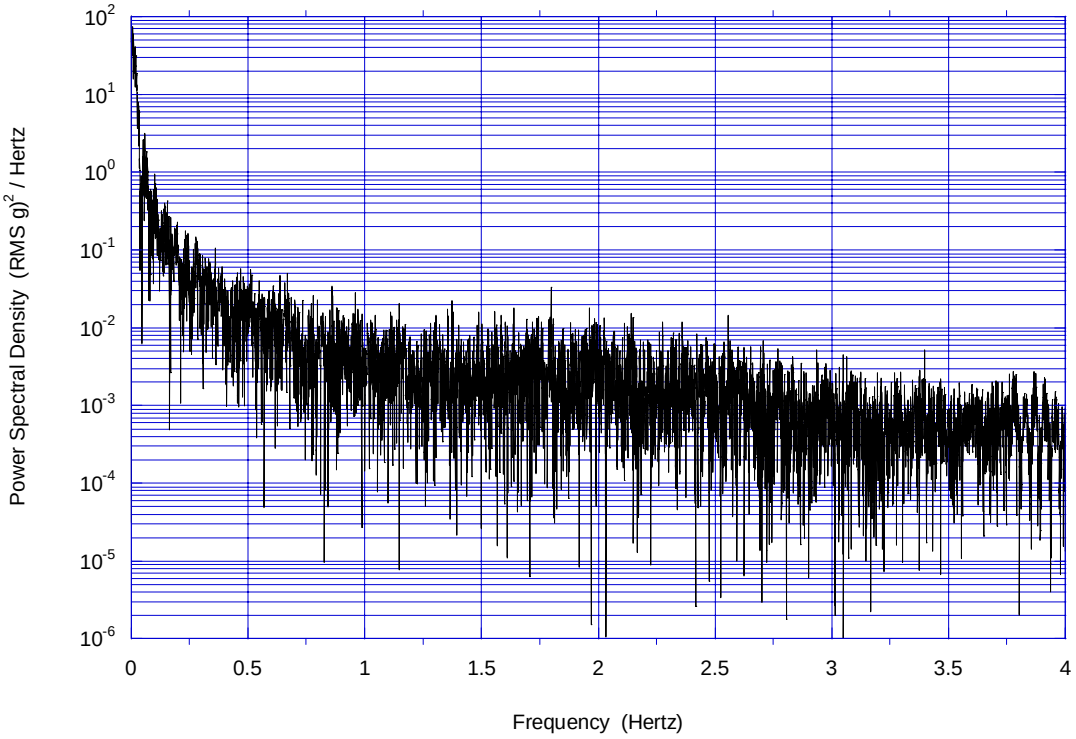

FIGURE 29. NORMALIZED PSD OF LONGITUDINAL LOAD FACTOR, FLIGHT SEQUENCE 3, PREFLIGHT

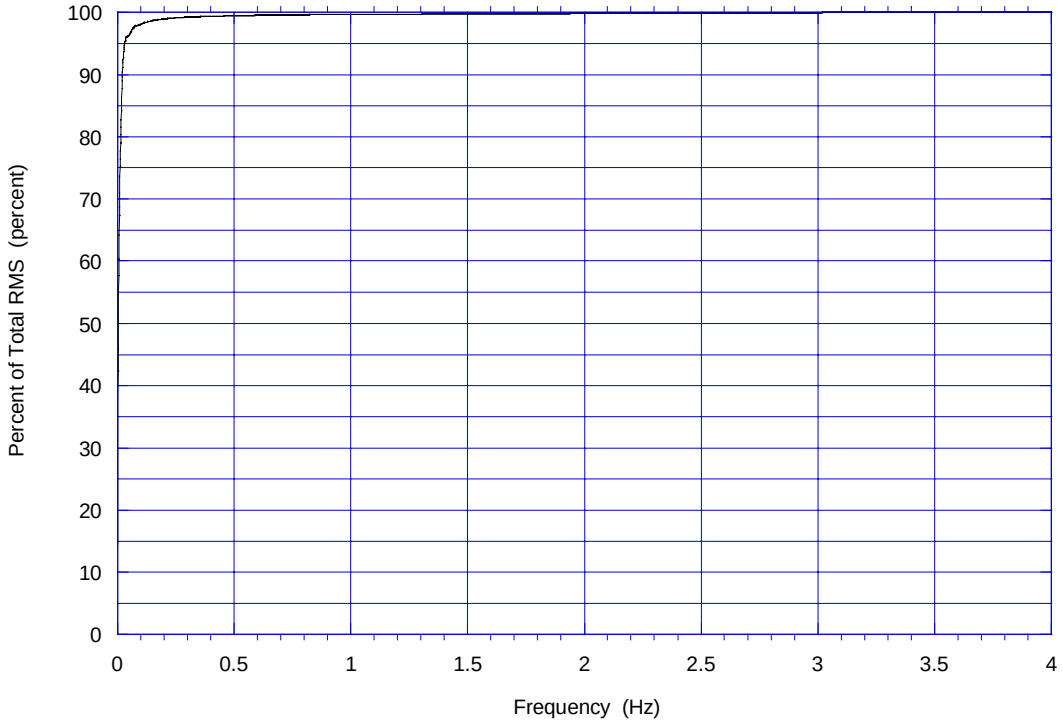

FIGURE 30. PERCENT OF TOTAL LONGITUDINAL LOAD FACTOR RMS VS FREQUENCY, FLIGHT SEQUENCE 3, PREFLIGHT

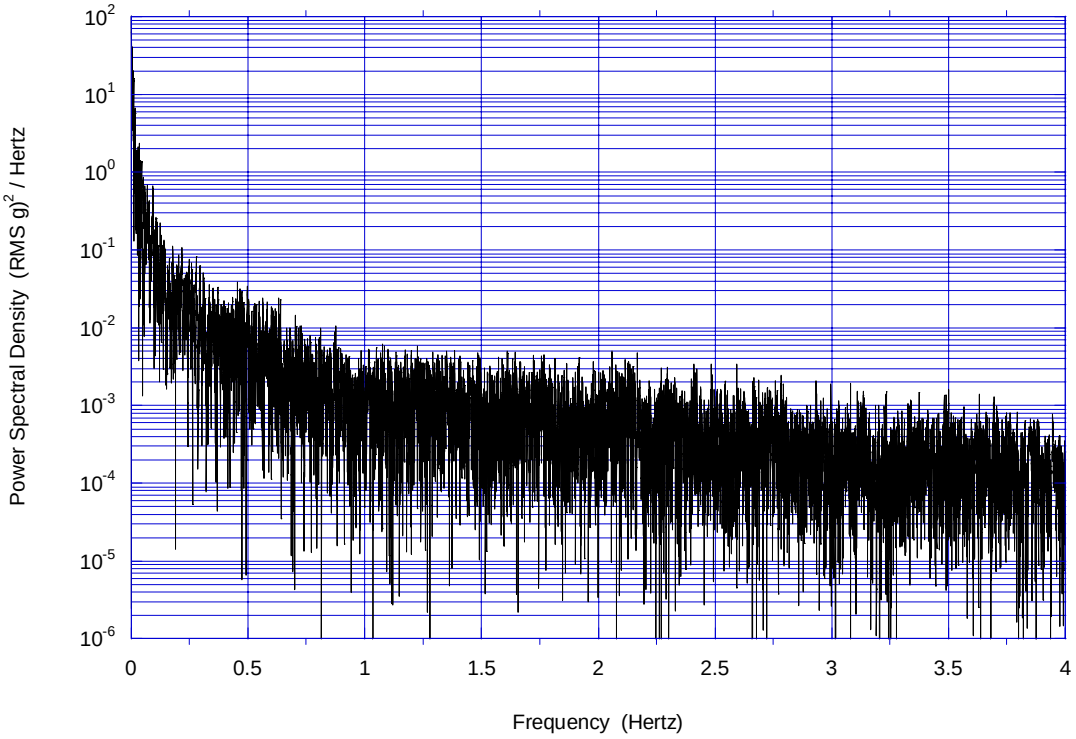

FIGURE 31. NORMALIZED PSD OF LONGITUDINAL LOAD FACTOR, FLIGHT SEQUENCE 3, IN FLIGHT

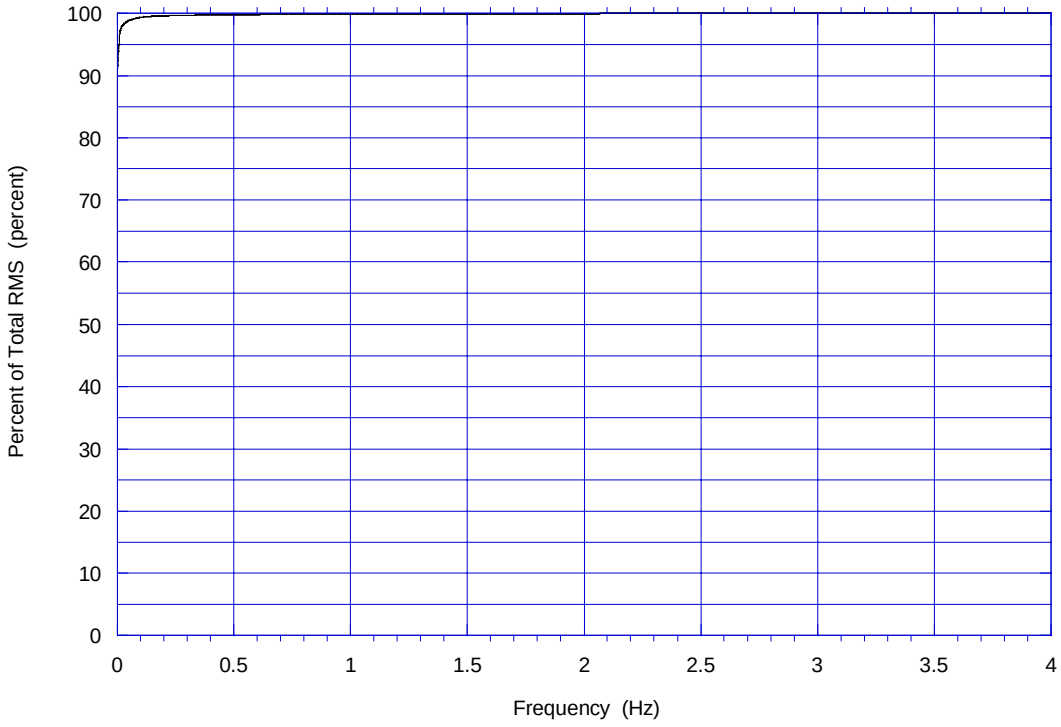

FIGURE 32. PERCENT OF TOTAL LONGITUDINAL LOAD FACTOR RMS VS FREQUENCY, FLIGHT SEQUENCE 3, IN FLIGHT

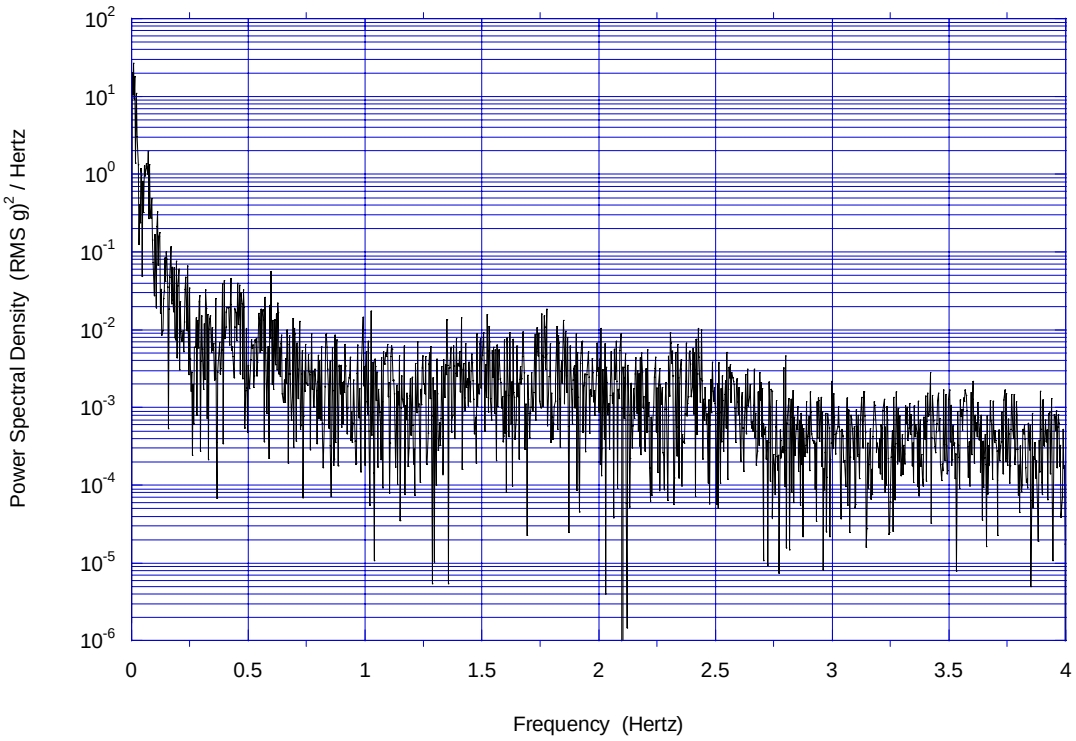

FIGURE 33. NORMALIZED PSD OF LONGITUDINAL LOAD FACTOR, FLIGHT SEQUENCE 3, POSTFLIGHT

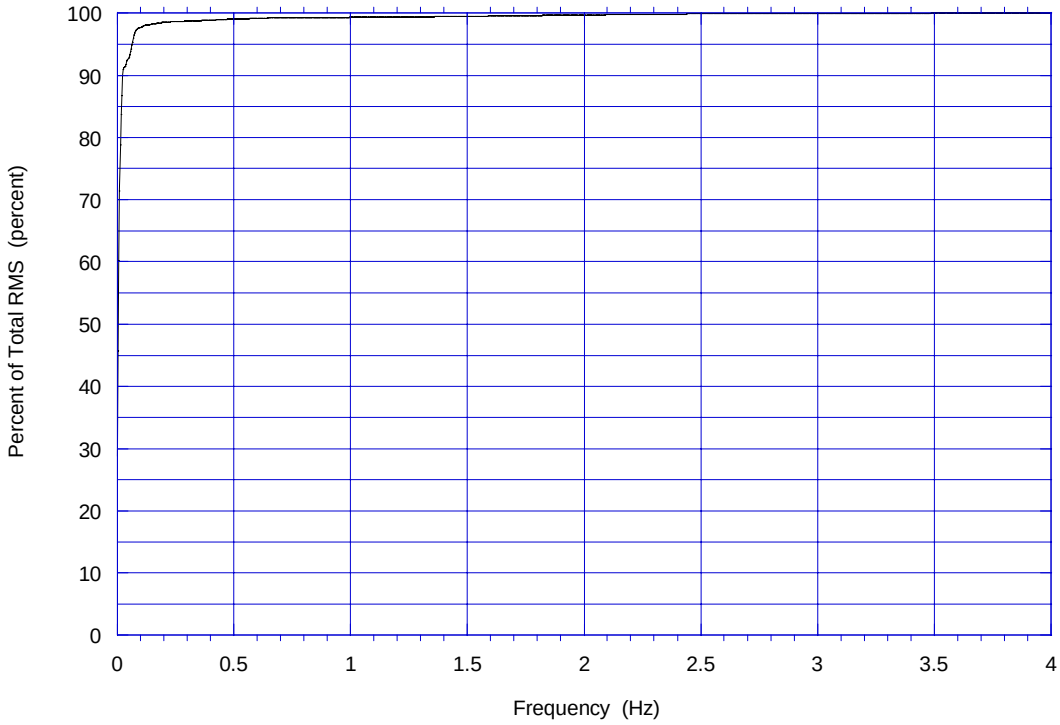

FIGURE 34. PERCENT OF TOTAL LONGITUDINAL LOAD FACTOR RMS VS FREQUENCY, FLIGHT SEQUENCE 3, POSTFLIGHT

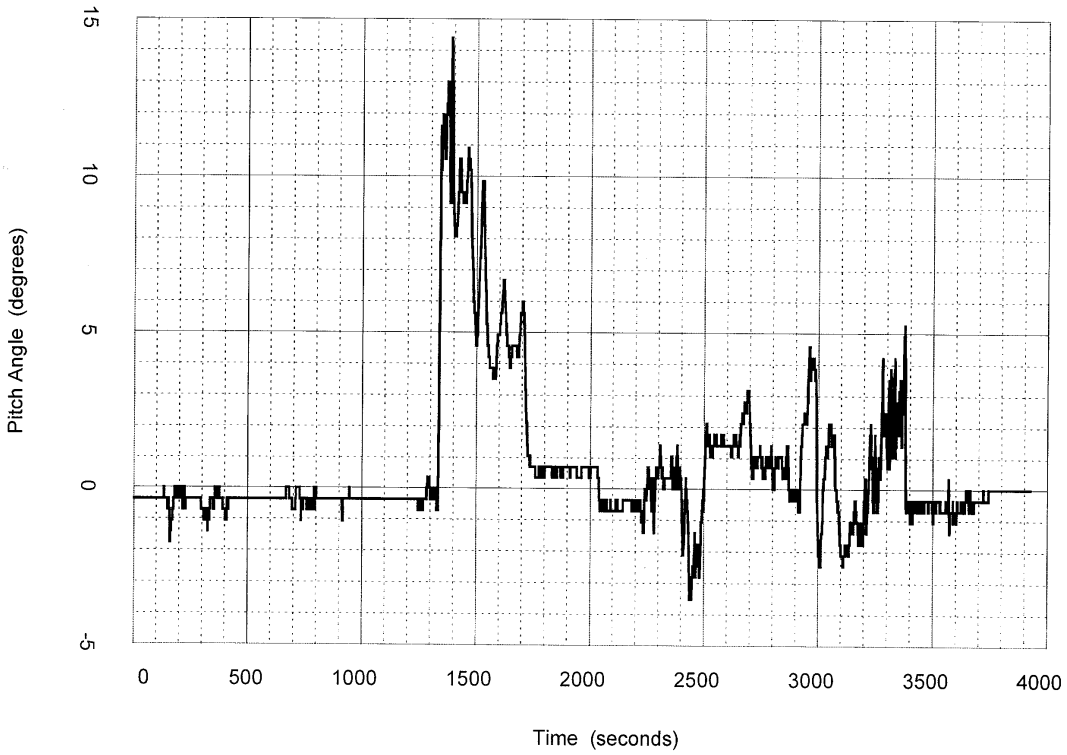

FIGURE 35. PITCH ANGLE TIME HISTORY, FLIGHT SEQUENCE 3

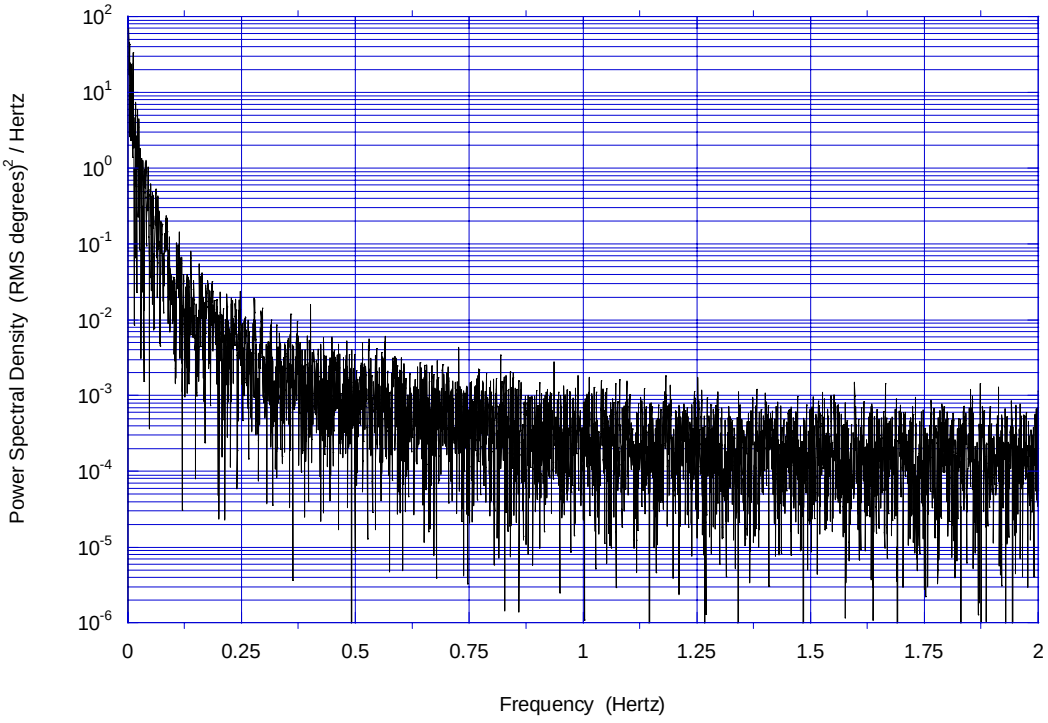

FIGURE 36. NORMALIZED PSD OF PITCH ANGLE,
FLIGHT SEQUENCE 3, IN FLIGHT

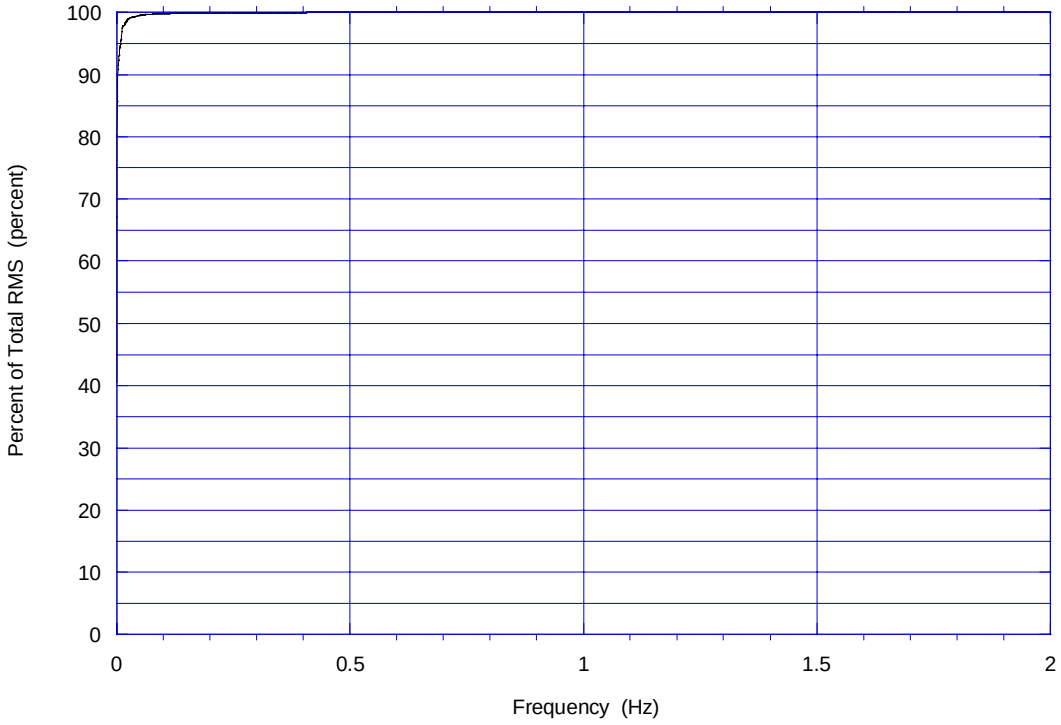

FIGURE 37. PERCENT OF TOTAL PITCH ANGLE RMS VS FREQUENCY, FLIGHT SEQUENCE 3, IN FLIGHT

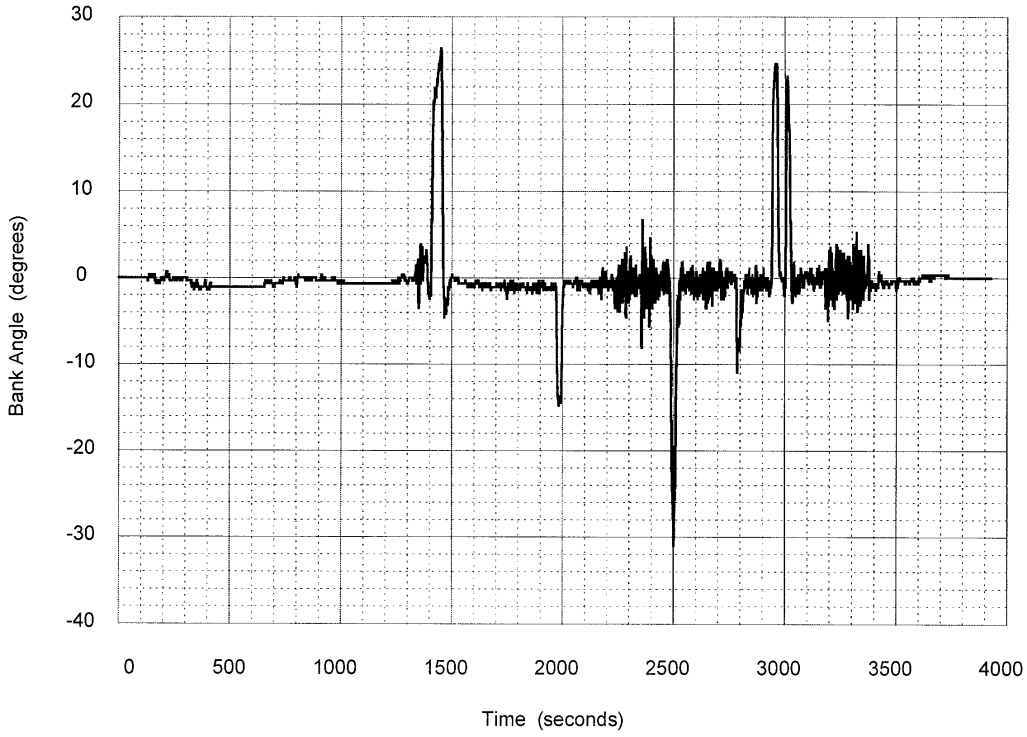

FIGURE 38. BANK ANGLE TIME HISTORY, FLIGHT SEQUENCE 3

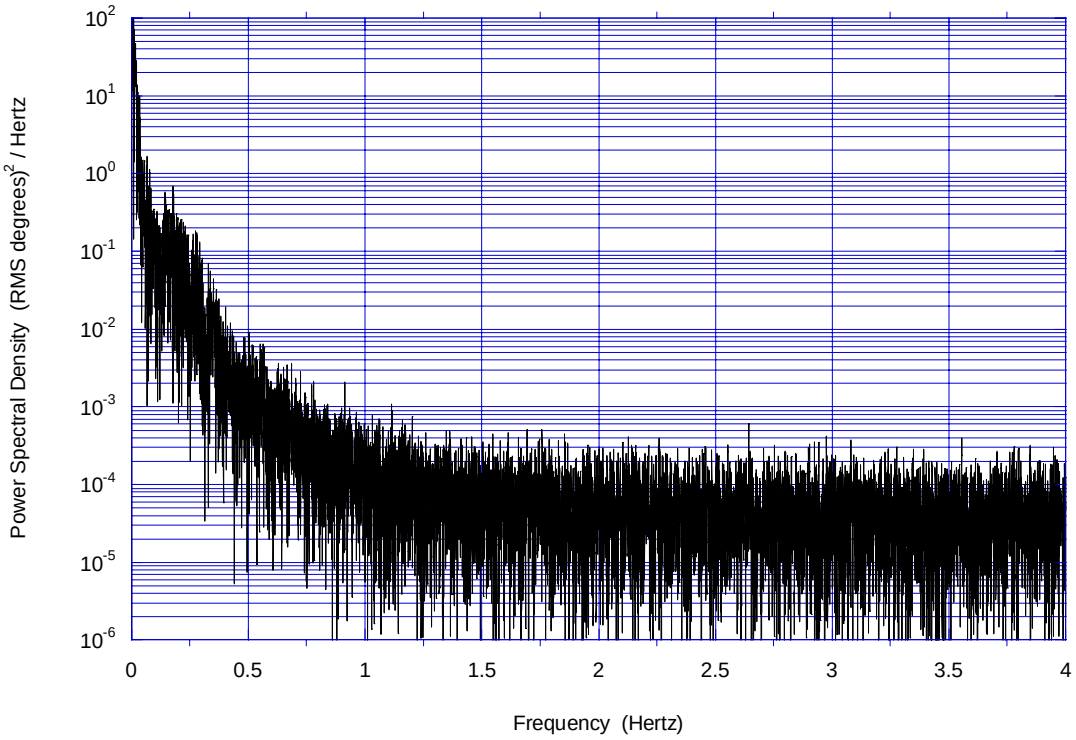

FIGURE 39. NORMALIZED PSD OF BANK ANGLE, FLIGHT SEQUENCE 3, IN FLIGHT

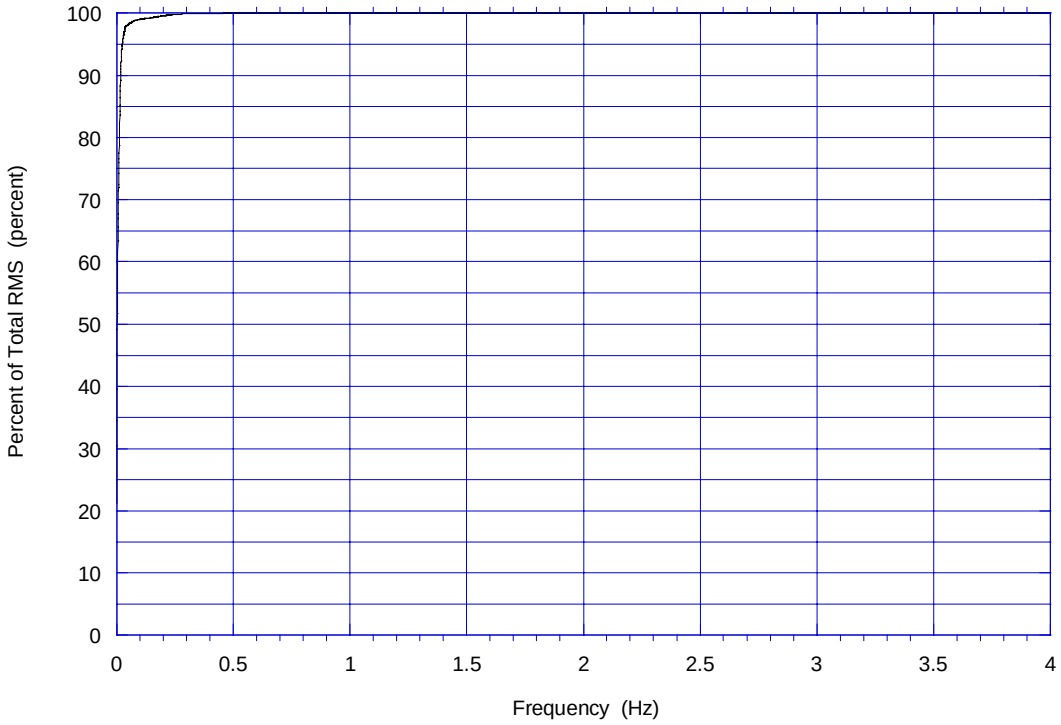

FIGURE 40. PERCENT OF TOTAL BANK ANGLE RMS VS FREQUENCY, FLIGHT SEQUENCE 3, IN FLIGHT

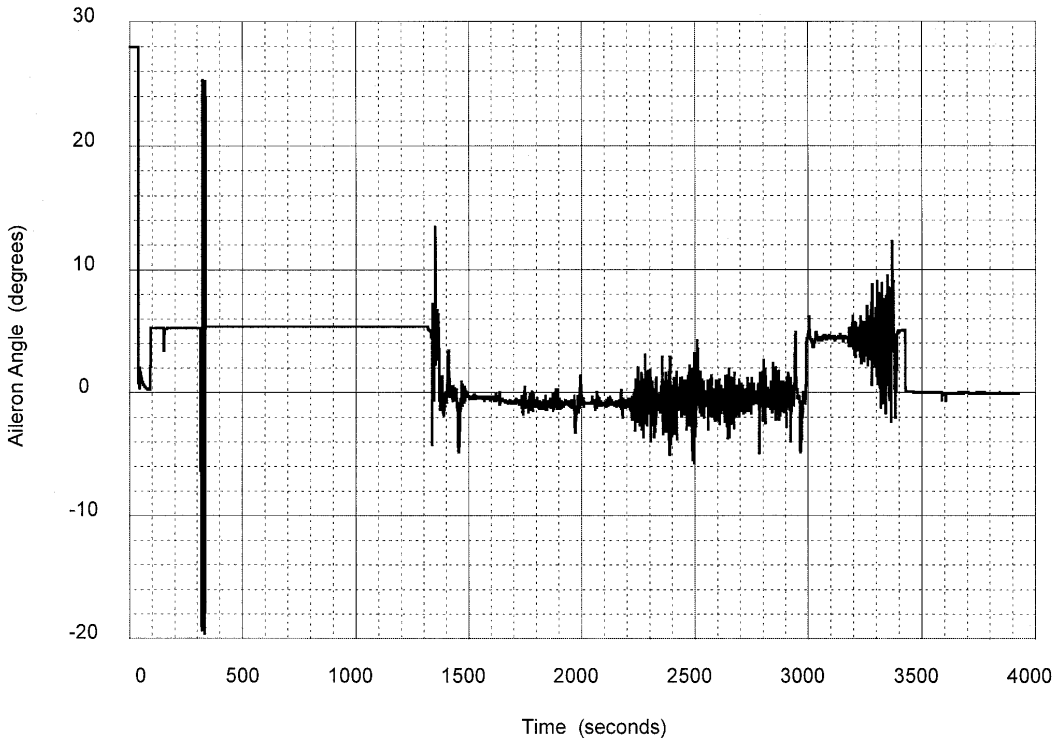

FIGURE 41. AILERON ANGLE TIME HISTORY, FLIGHT SEQUENCE 3

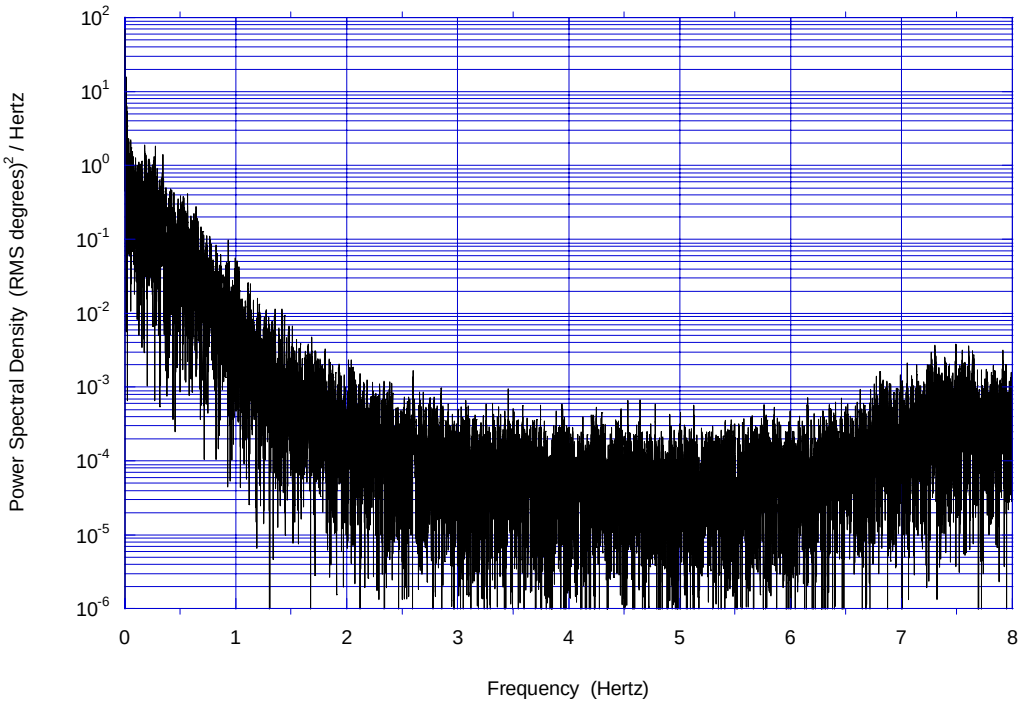

FIGURE 42. NORMALIZED PSD OF AILERON ANGLE, FLIGHT SEQUENCE 3, IN FLIGHT

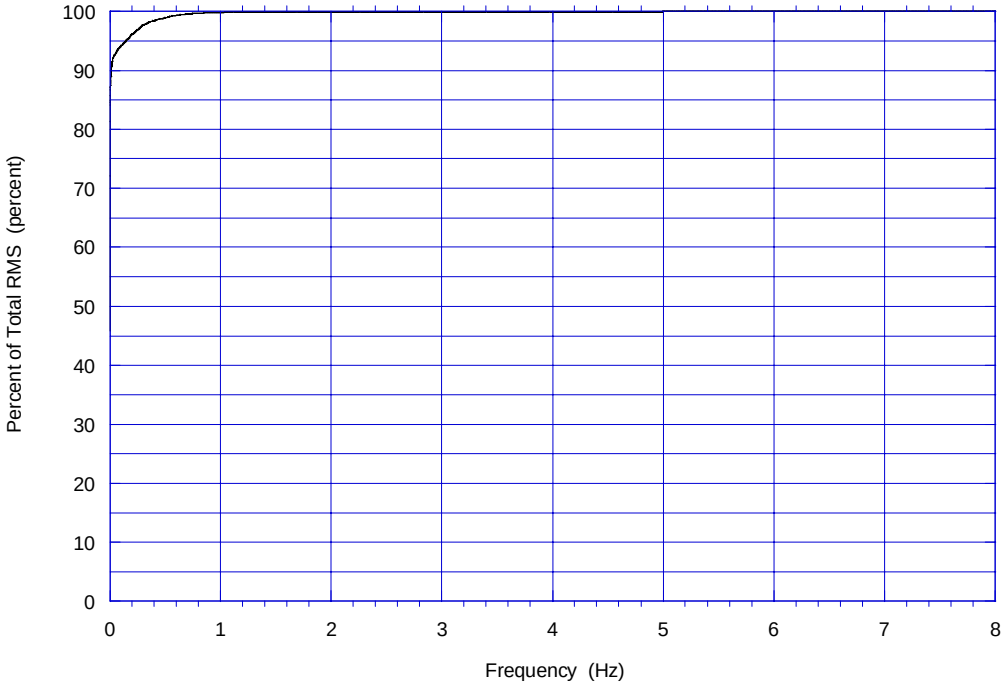

FIGURE 43. PERCENT OF TOTAL AILERON ANGLE RMS VS FREQUENCY, FLIGHT SEQUENCE 3, IN FLIGHT

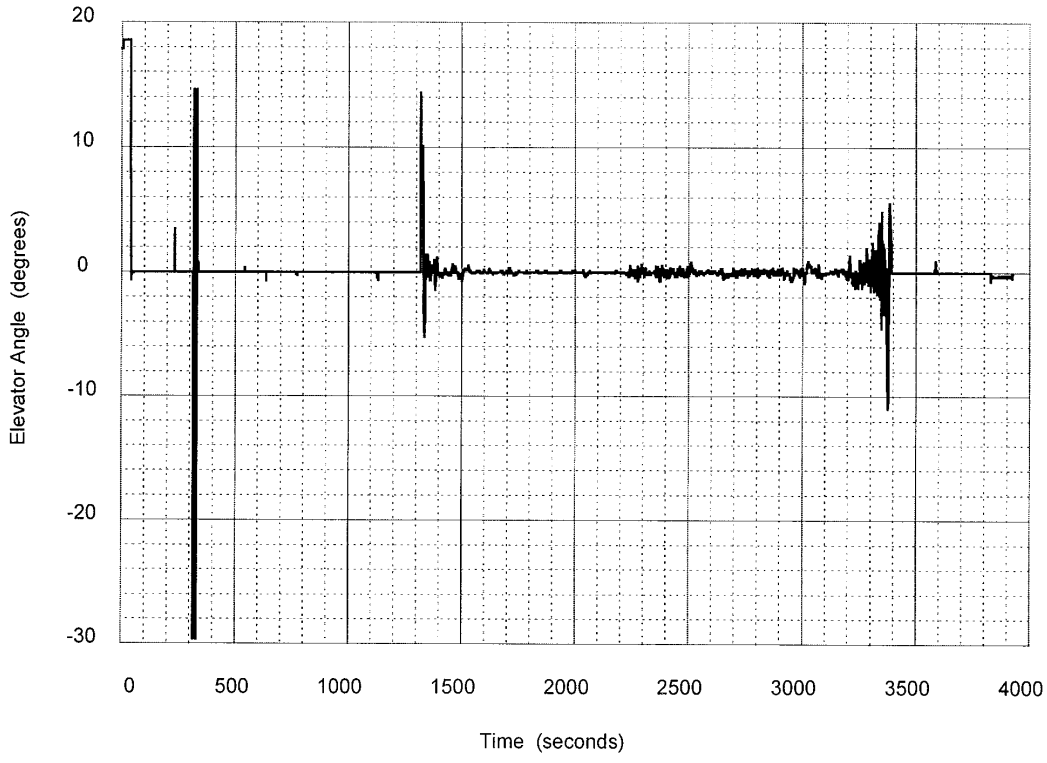

FIGURE 44. ELEVATOR ANGLE TIME HISTORY, FLIGHT SEQUENCE 3

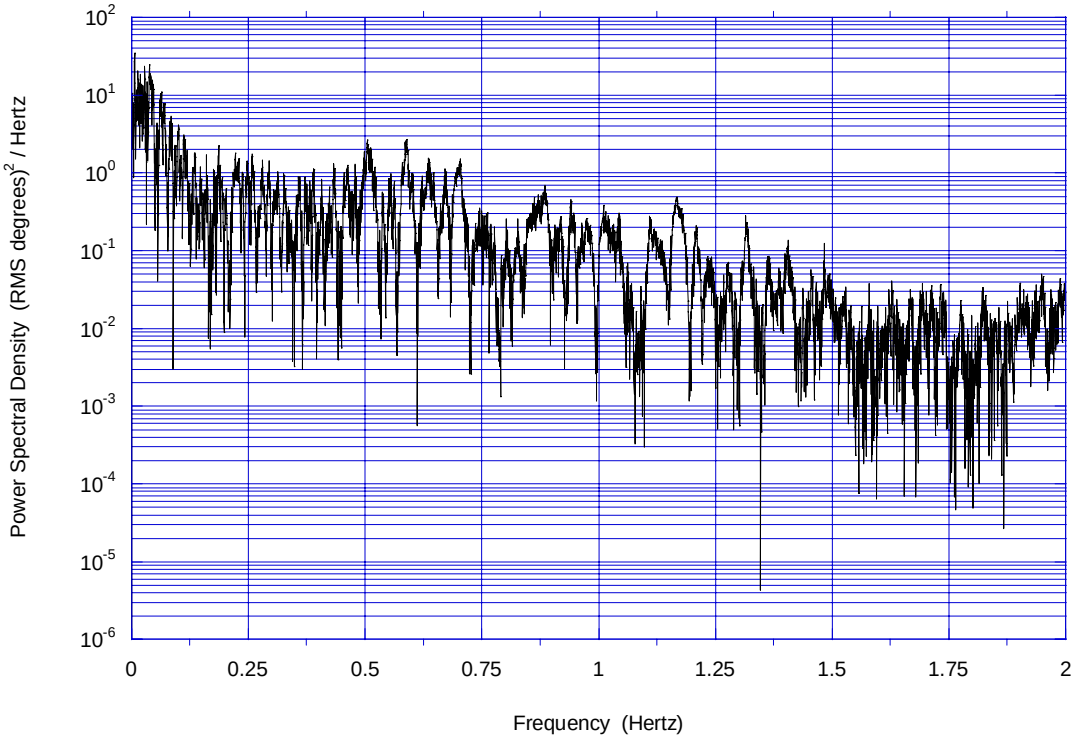

FIGURE 45. NORMALIZED PSD OF ELEVATOR ANGLE, FLIGHT SEQUENCE 3, IN FLIGHT

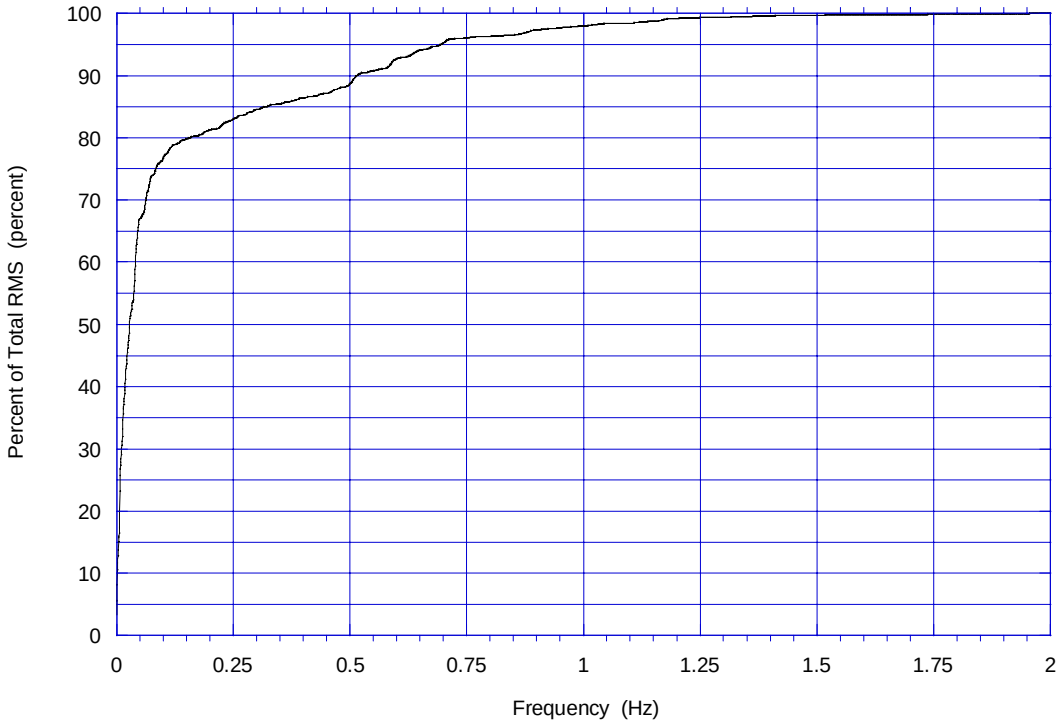

FIGURE 46. PERCENT OF TOTAL ELEVATOR ANGLE RMS VS FREQUENCY, FLIGHT SEQUENCE 3, IN FLIGHT

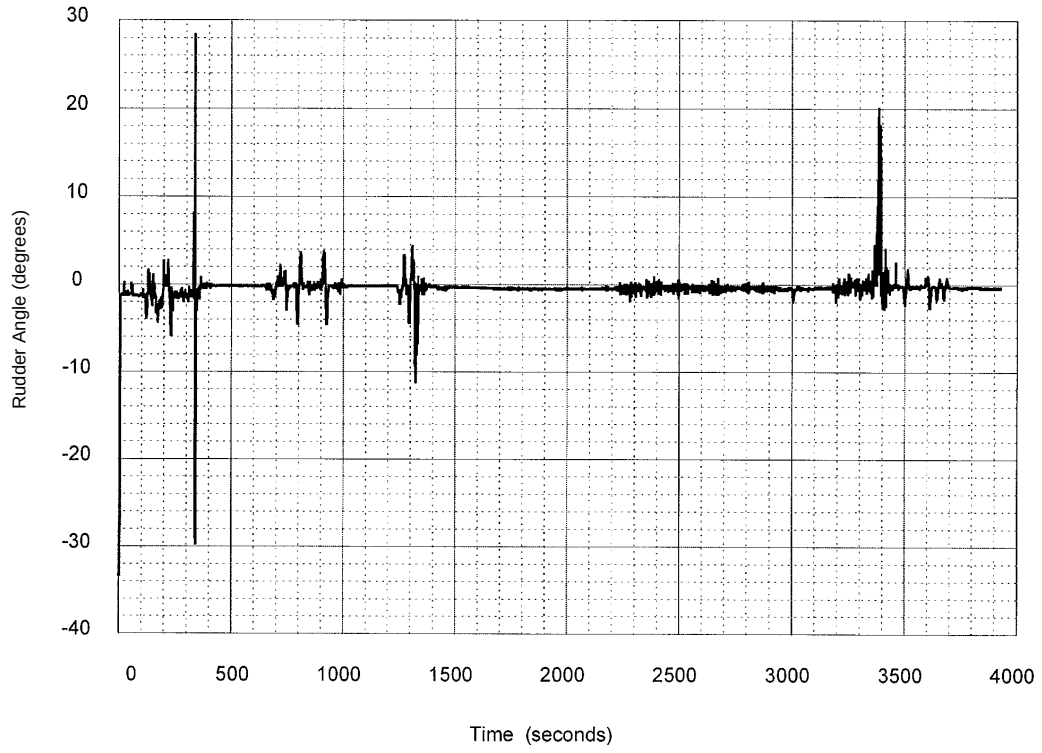

FIGURE 47. RUDDER ANGLE TIME HISTORY, FLIGHT SEQUENCE 3

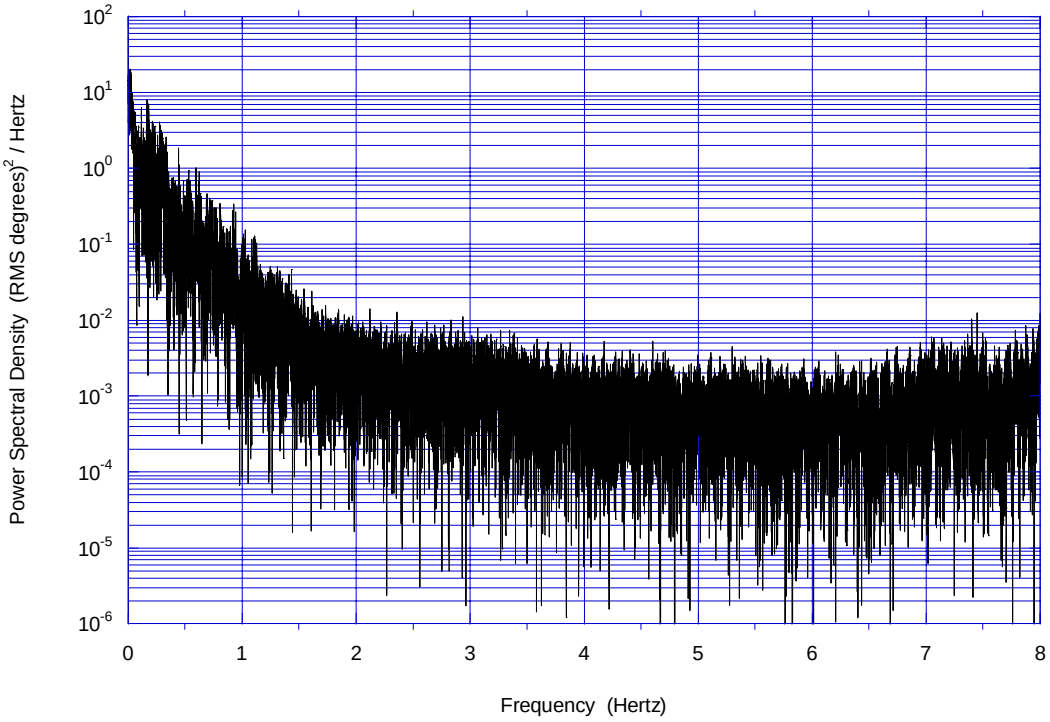

FIGURE 48. NORMALIZED PSD OF RUDDER ANGLE,
FLIGHT SEQUENCE 3, IN FLIGHT

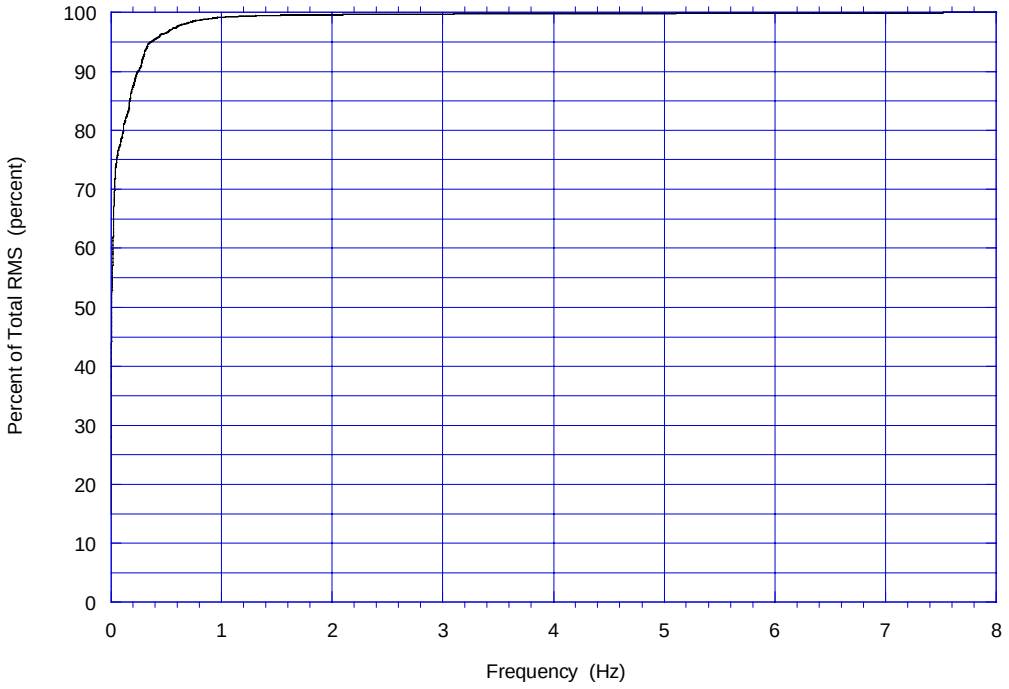

FIGURE 49. PERCENT OF TOTAL RUDDER ANGLE RMS VS FREQUENCY, FLIGHT SEQUENCE 3, IN FLIGHT

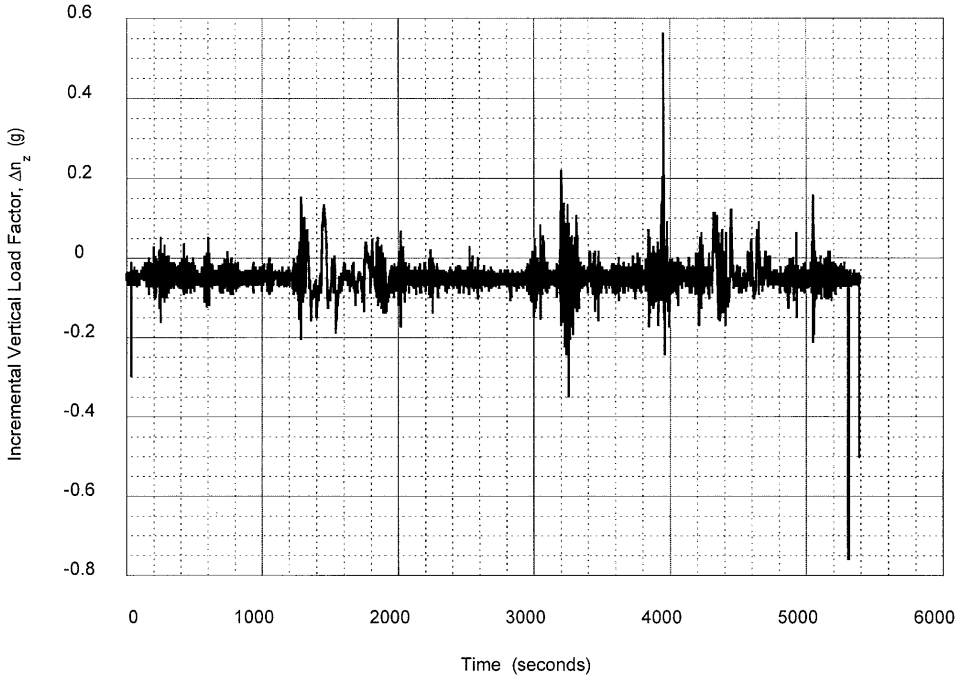

FIGURE 50. INCREMENTAL VERICAL LOAD FACTOR TIME HISTORY, FLIGHT SEQUENCE 35

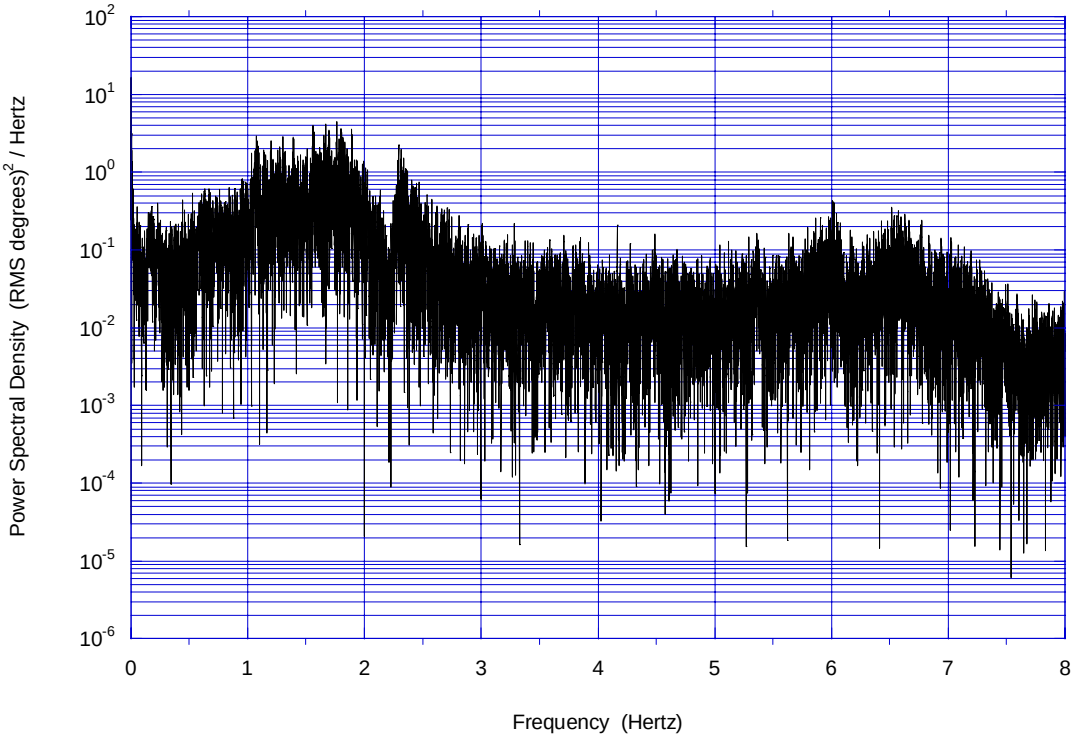

FIGURE 51. NORMALIZED PSD OF INCREMENTAL VERTICAL LOAD FACTOR, FLIGHT SEQUENCE 35, PREFLIGHT

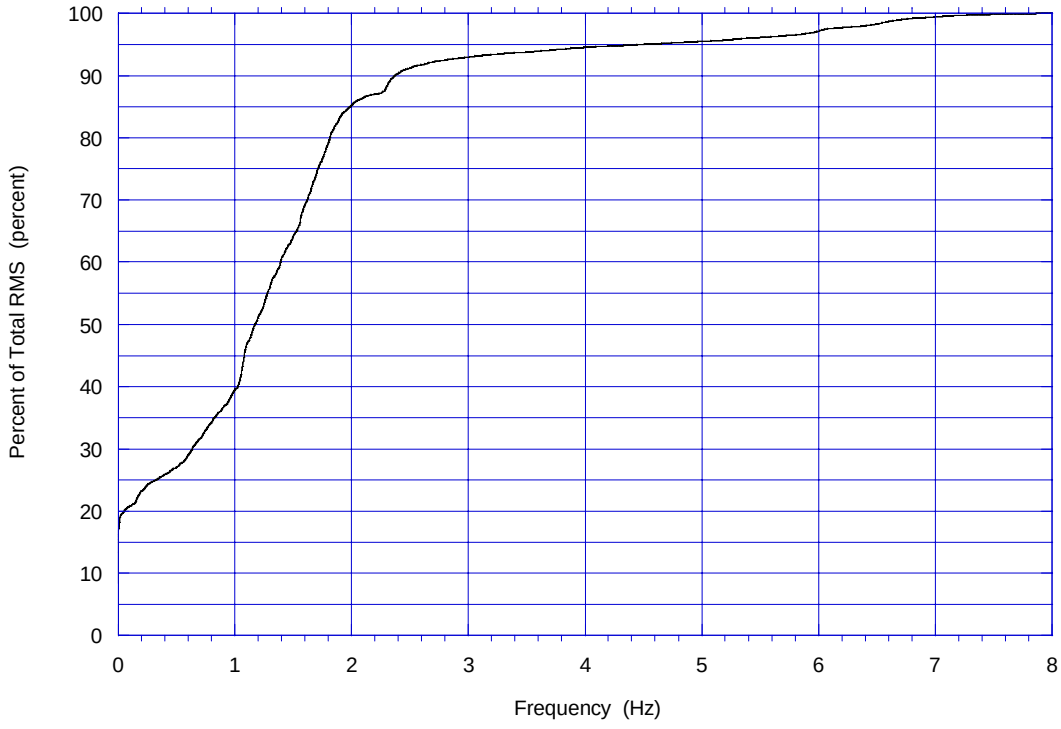

FIGURE 52. PERCENT OF TOTAL INCREMENTAL VERTICAL LOAD FACTOR RMS VS FREQUENCY, FLIGHT SEQUENCE 35, PREFLIGHT

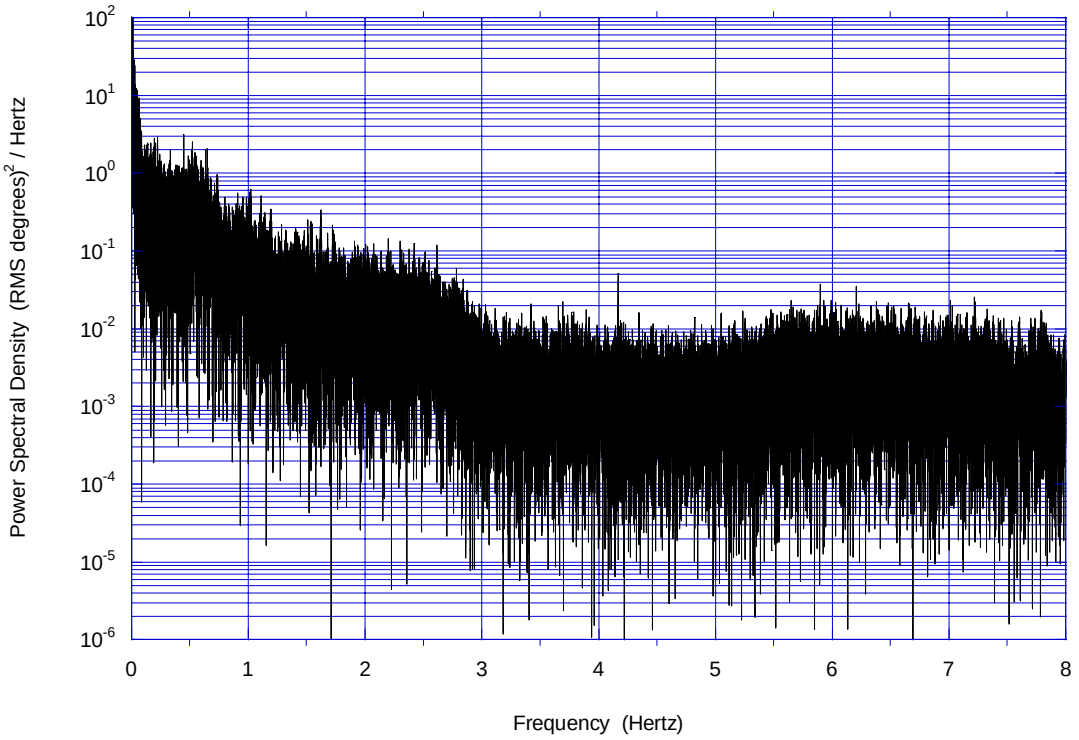

FIGURE 53. NORMALIZED PSD OF INCREMENTAL VERTICAL LOAD FACTOR, FLIGHT SEQUENCE 35, IN FLIGHT

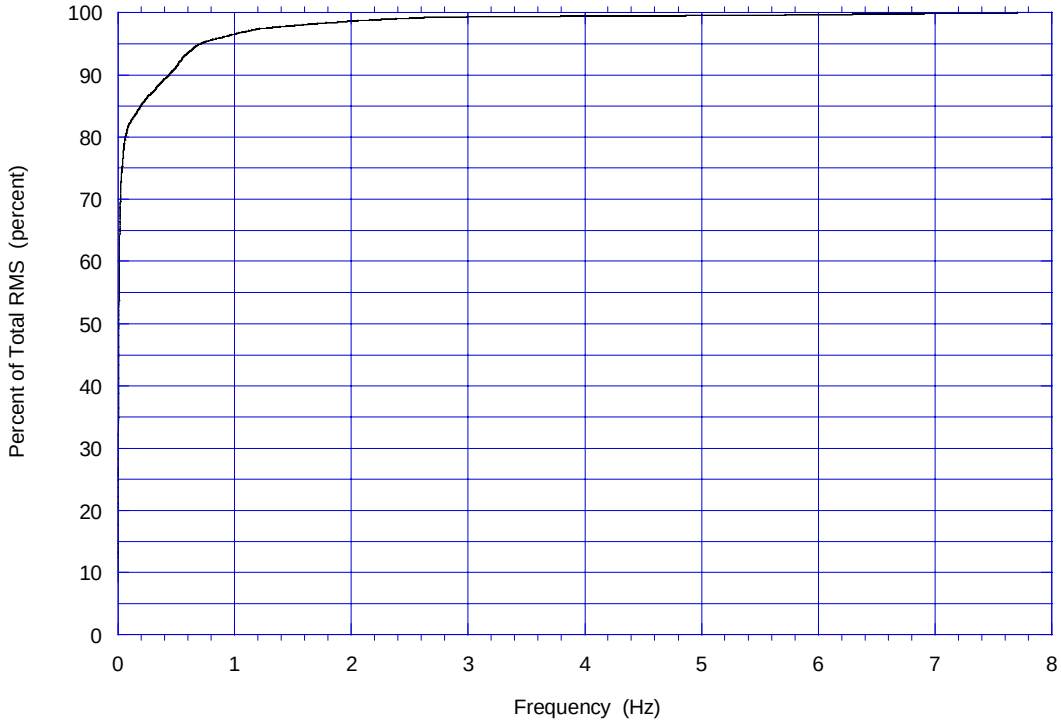

FIGURE 54. PERCENT OF TOTAL INCREMENTAL VERTICAL LOAD FACTOR RMS VS FREQUENCY, FLIGHT SEQUENCE 35, IN FLIGHT

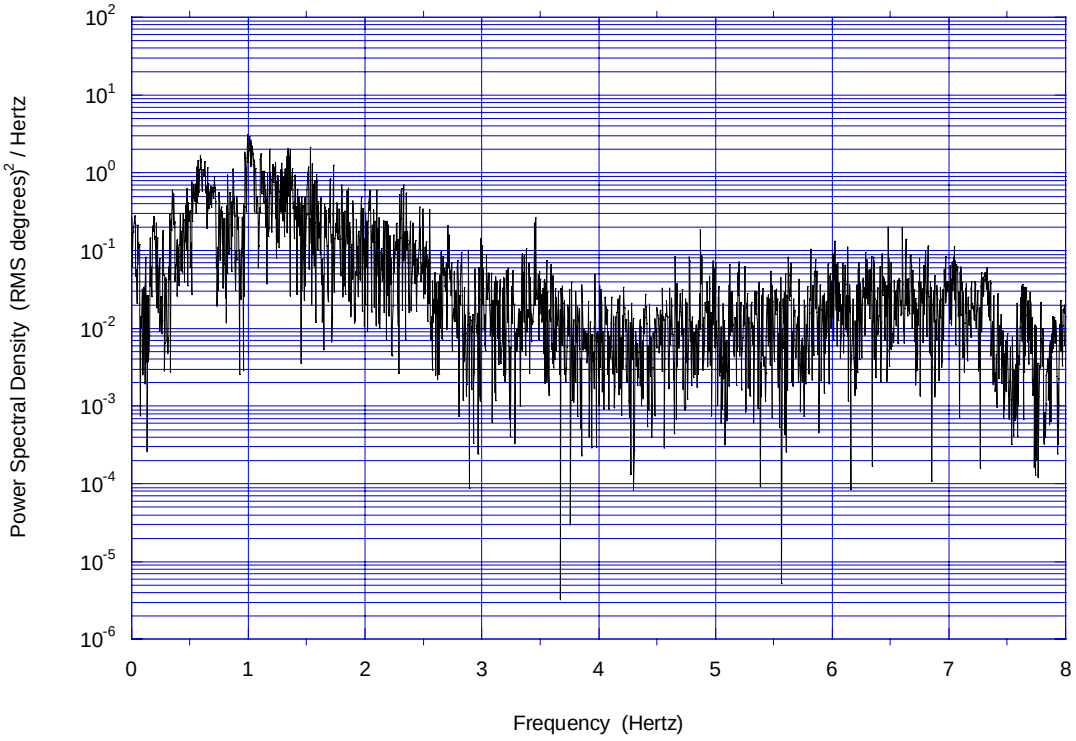

FIGURE 55. NORMALIZED PSD OF INCREMENTAL VERTICAL LOAD FACTOR, FLIGHT SEQUENCE 35, POSTFLIGHT

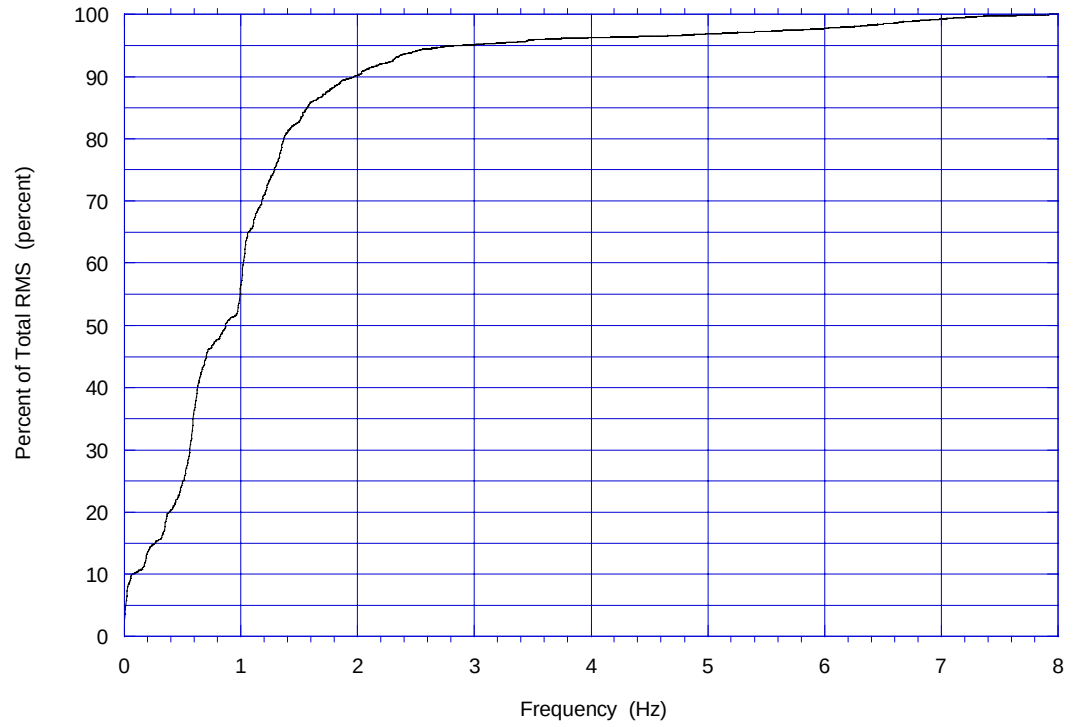

FIGURE 56. PERCENT OF INCREMENTAL VERTICAL LOAD FACTOR RMS VS FREQUENCY, FLIGHT SEQUENCE 35, POSTFLIGHT

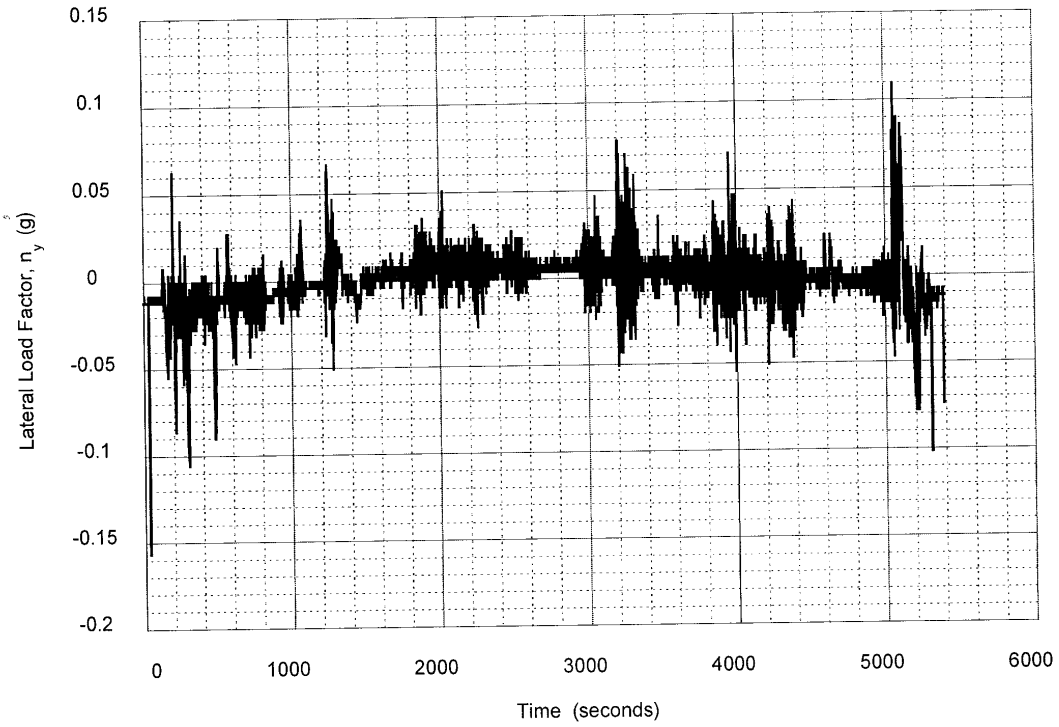

FIGURE 57. LATERAL LOAD FACTOR TIME HISTORY, FLIGHT SEQUENCE 35

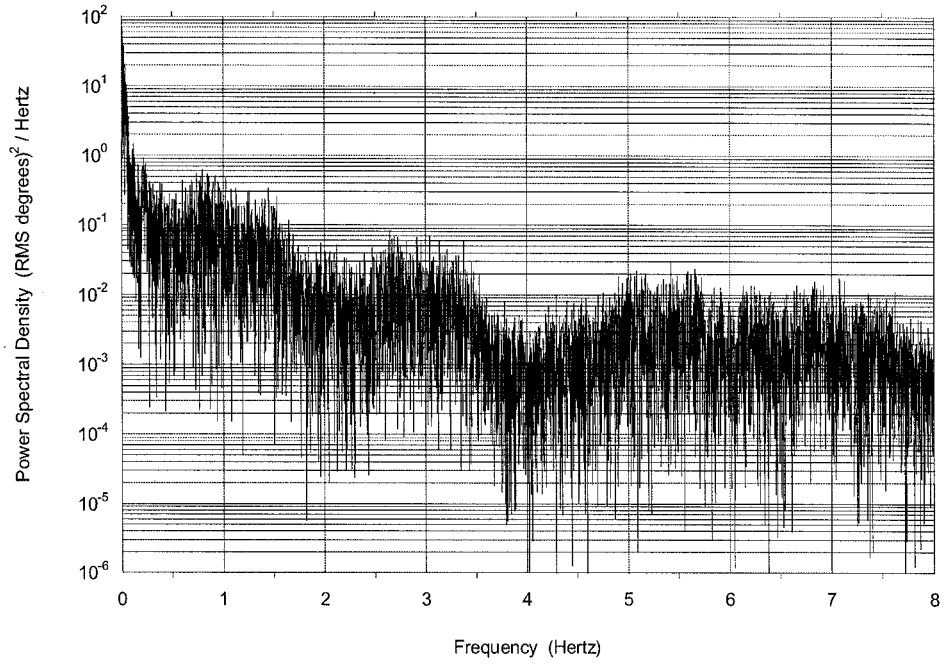

FIGURE 58. NORMALIZED PSD OF LATERAL LOAD FACTOR, FLIGHT SEQUENCE 35, PREFLIGHT

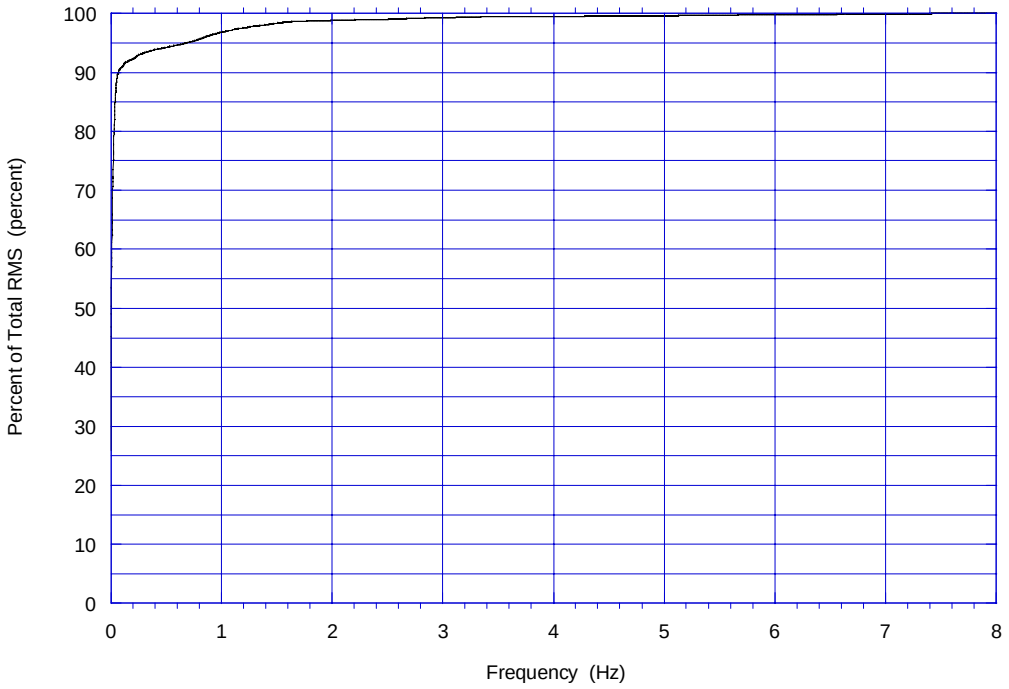

FIGURE 59. PERCENT OF TOTAL LATERAL LOAD FACTOR RMS VS, FREQUENCY, FLIGHT SEQUENCE 35, PREFLIGHT

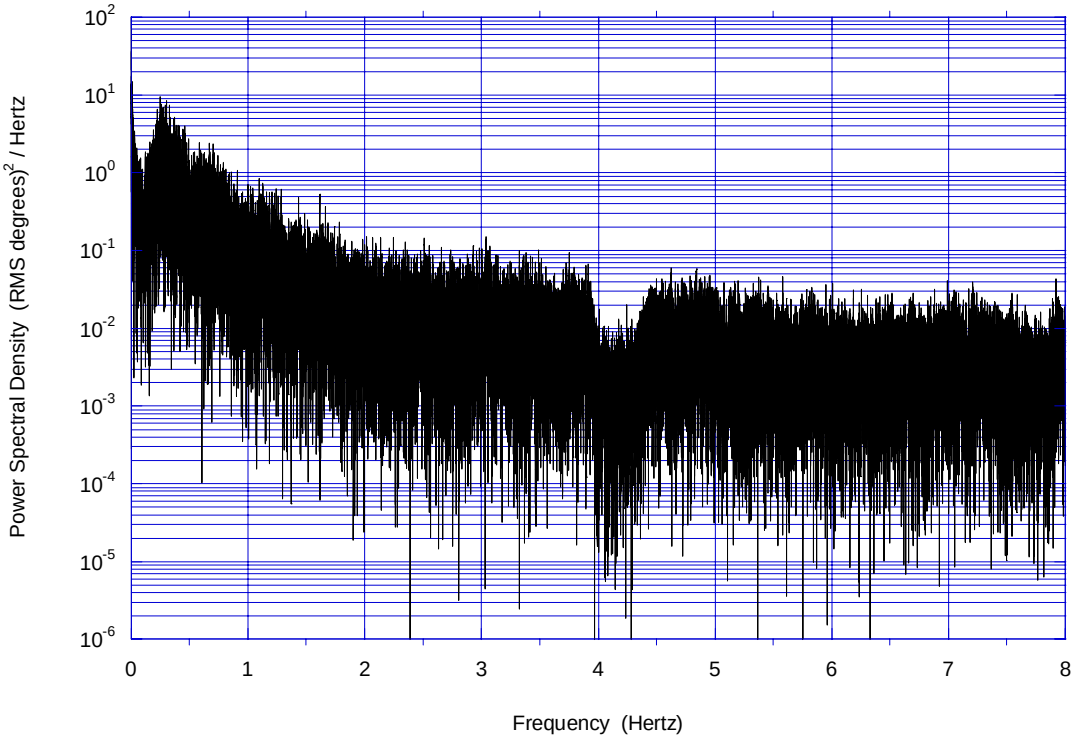

FIGURE 60. NORMALIZED PSD OF LATERAL LOAD FACTOR, FLIGHT SEQUENCE 35, IN FLIGHT

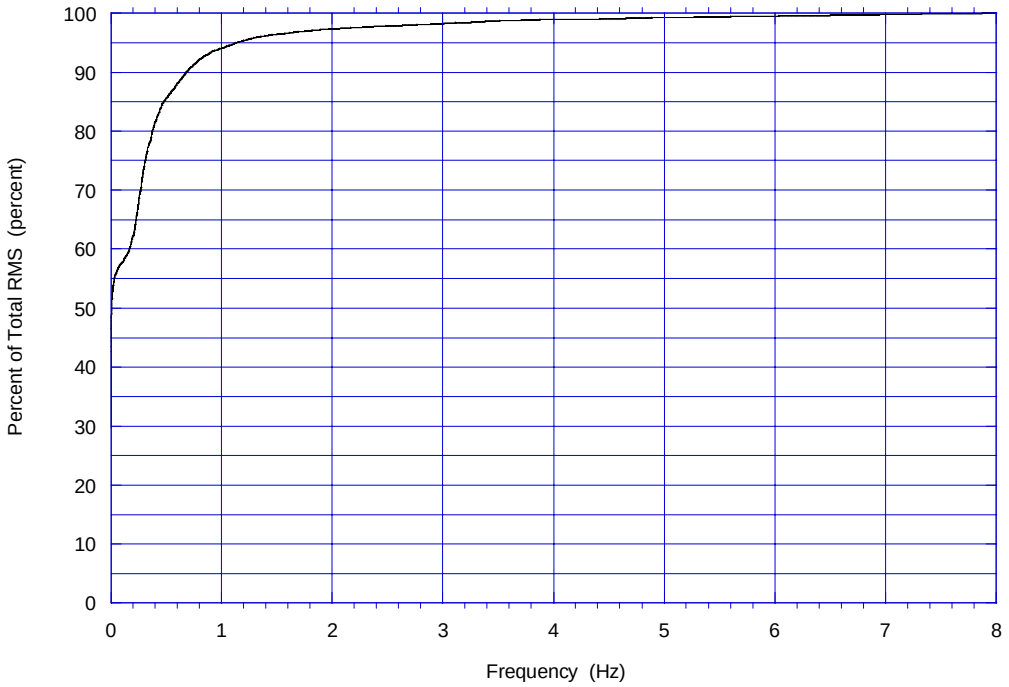

FIGURE 61. PERCENT OF TOTAL LATERAL LOAD FACTOR RMS VS FREQUENCY, FLIGHT SEQUENCE 35, IN FLIGHT

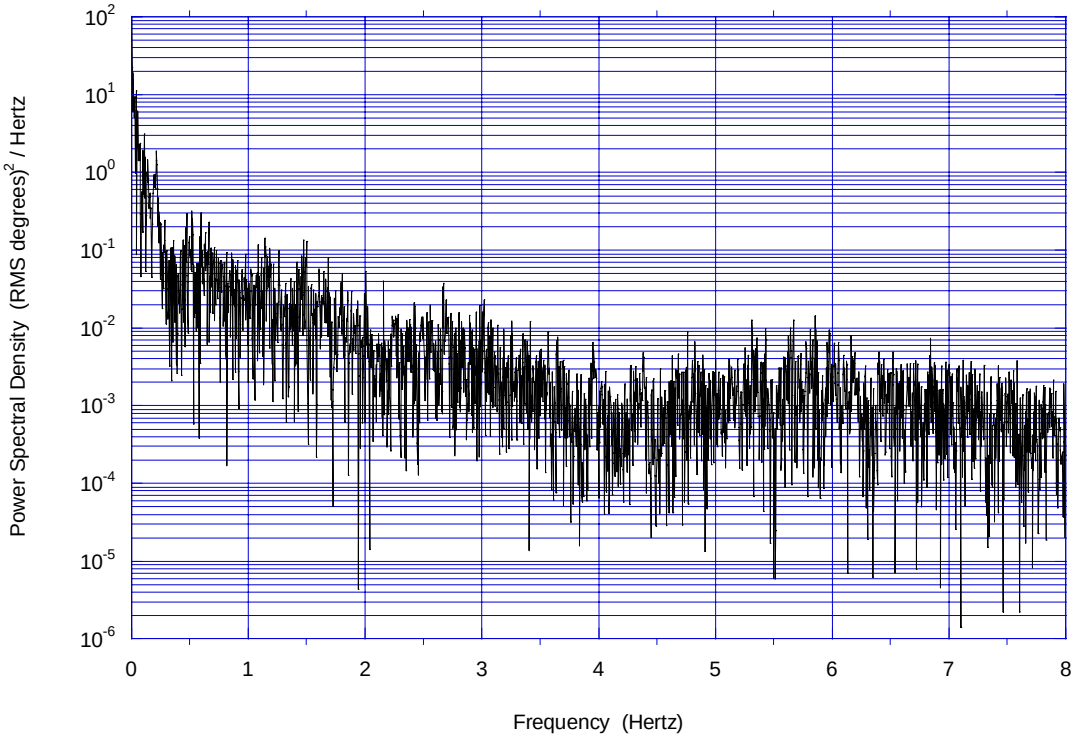

FIGURE 62. NORMALIZED PSD OF LATERAL LOAD FACTOR, FLIGHT SEQUENCE 35, POSTFLIGHT

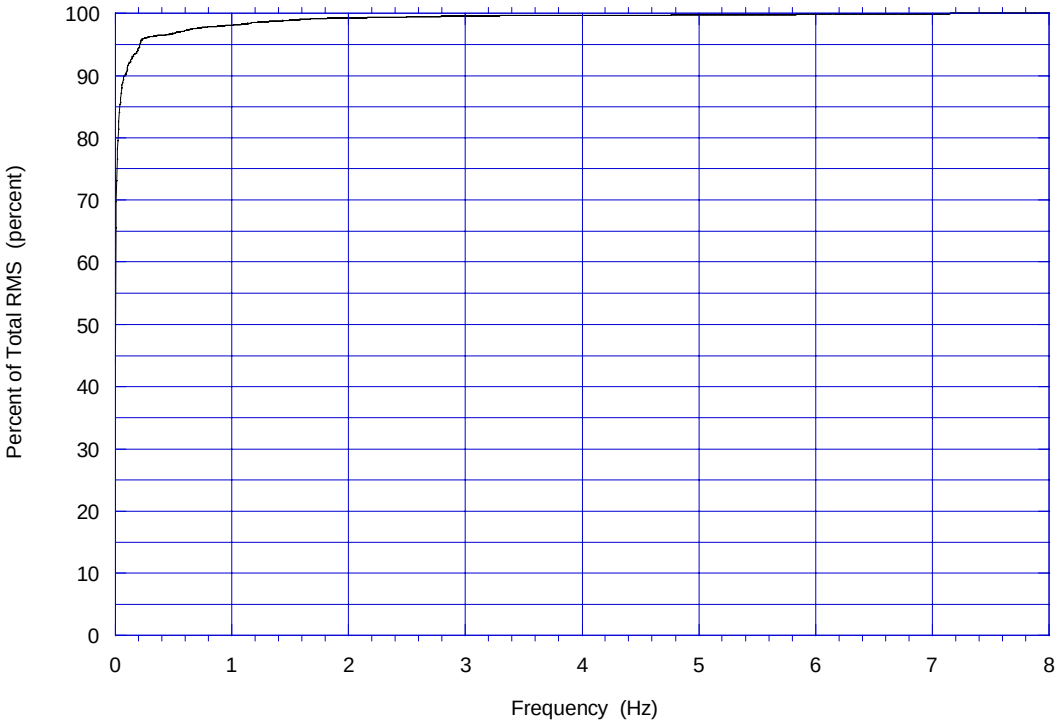

FIGURE 63. PERCENT OF TOTAL LATERAL LOAD FACTOR RMS VS FREQUENCY, FLIGHT SEQUENCE 35, POSTFLIGHT

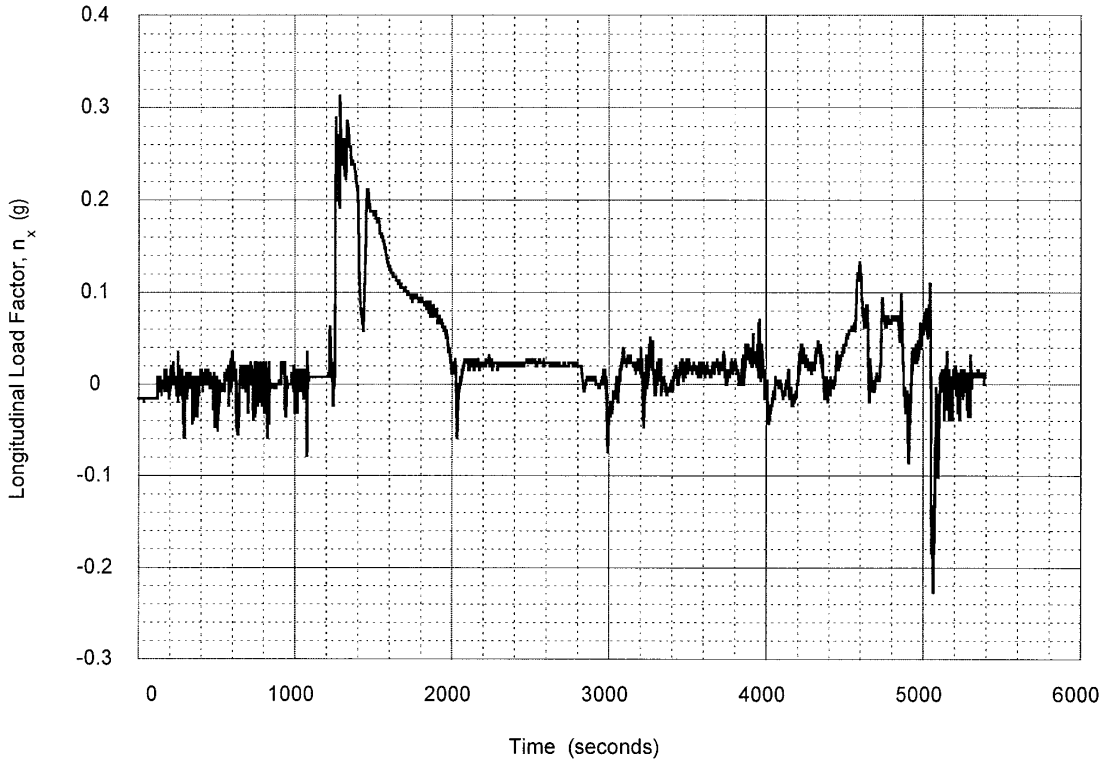

FIGURE 64. LONGITUDINAL LOAD FACTOR TIME HISTORY, FLIGHT SEQUENCE 35

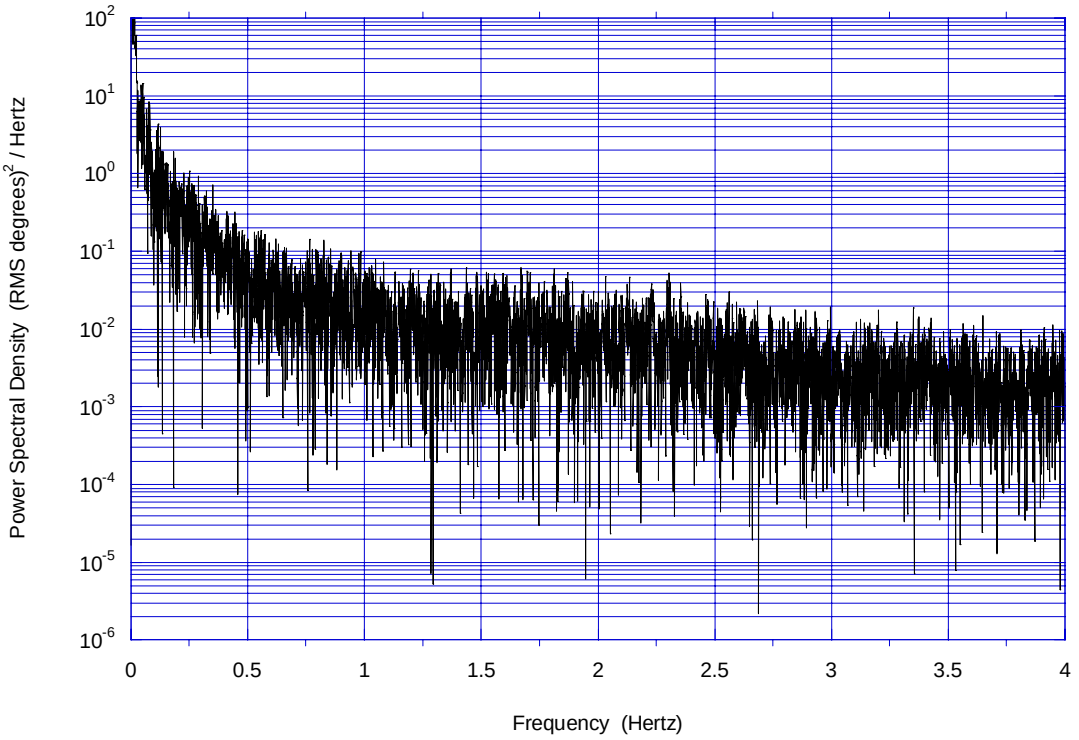

FIGURE 65. NORMALIZED PSD OF LONGITUDINAL LOAD FACTOR, FLIGHT SEQUENCE 35, PREFLIGHT

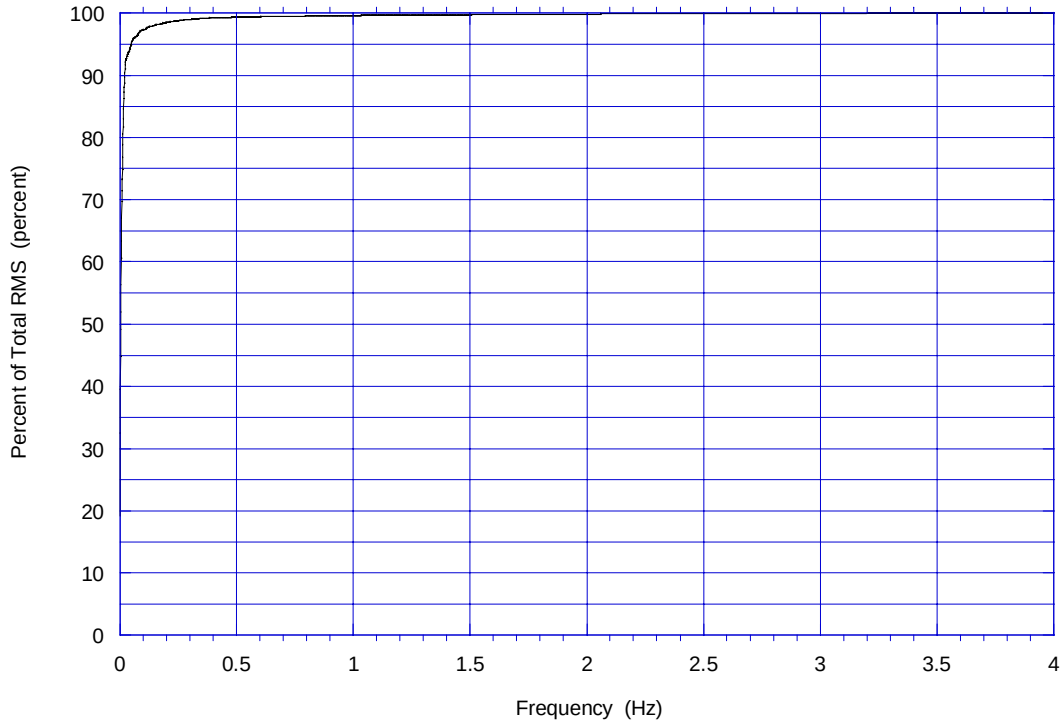

FIGURE 66. PERCENT OF TOTAL LONGITUDINAL LOAD FACTOR RMS VS FREQUENCY, FLIGHT SEQUENCE 35, PREFLIGHT

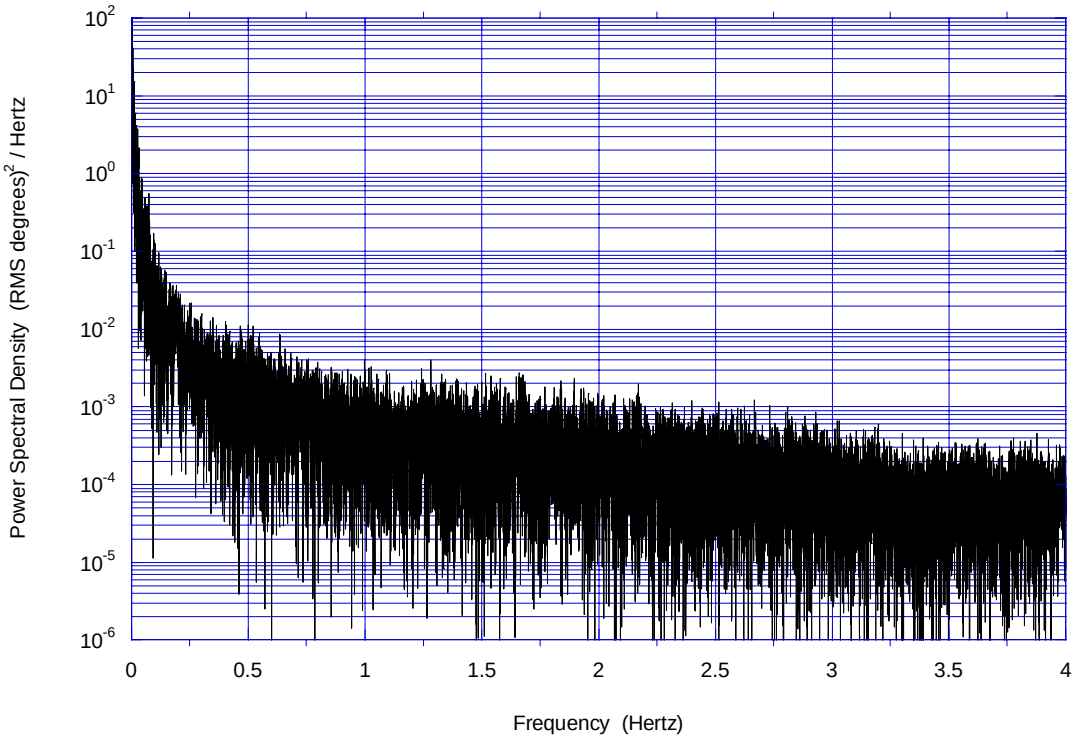

FIGURE 67. NORMALIZED PSD OF LONGITUDINAL LOAD FACTOR, FLIGHT SEQUENCE 35, IN FLIGHT

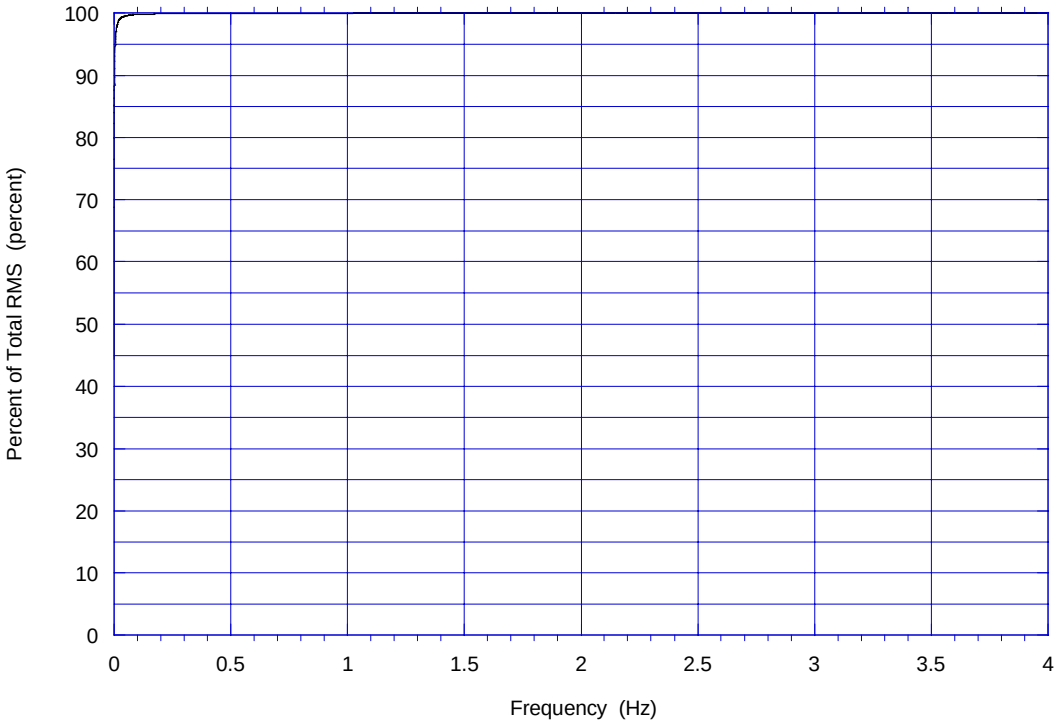

FIGURE 68. PERCENT OF TOTAL LONGITUDINAL LOAD FACTOR RMS VS FREQUENCY, FLIGHT SEQUENCE 35, IN FLIGHT

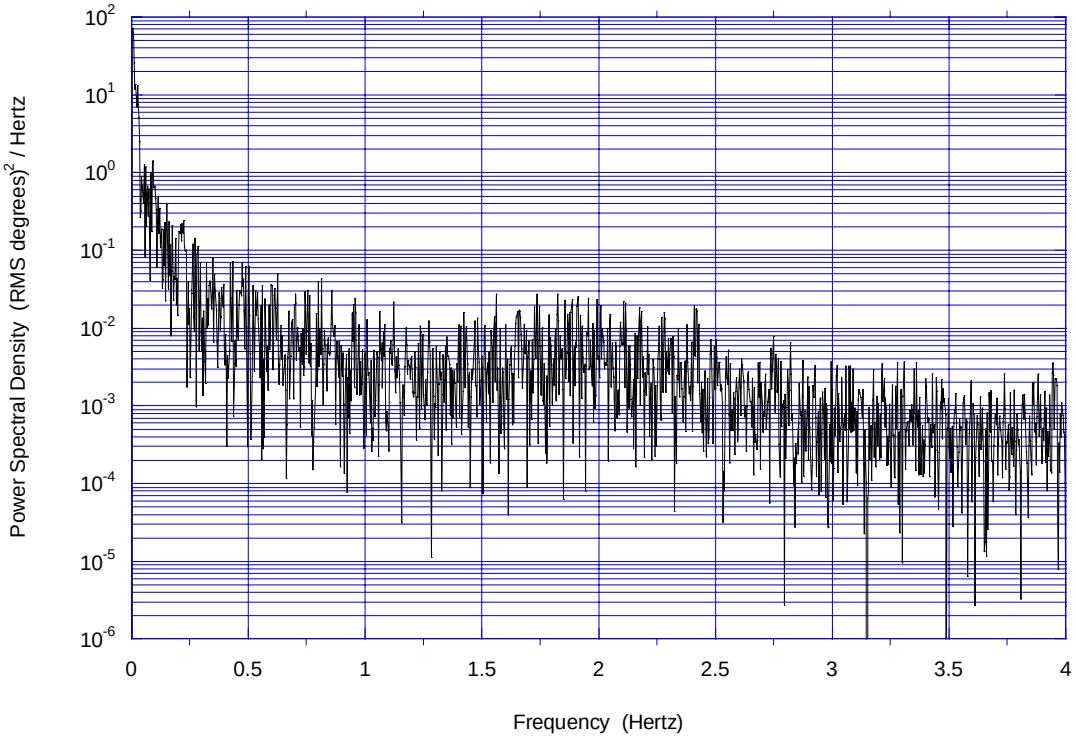

FIGURE 69. NORMALIZED PSD OF LONGITUDINAL LOAD FACTOR, FLIGHT SEQUENCE 35, POSTFLIGHT

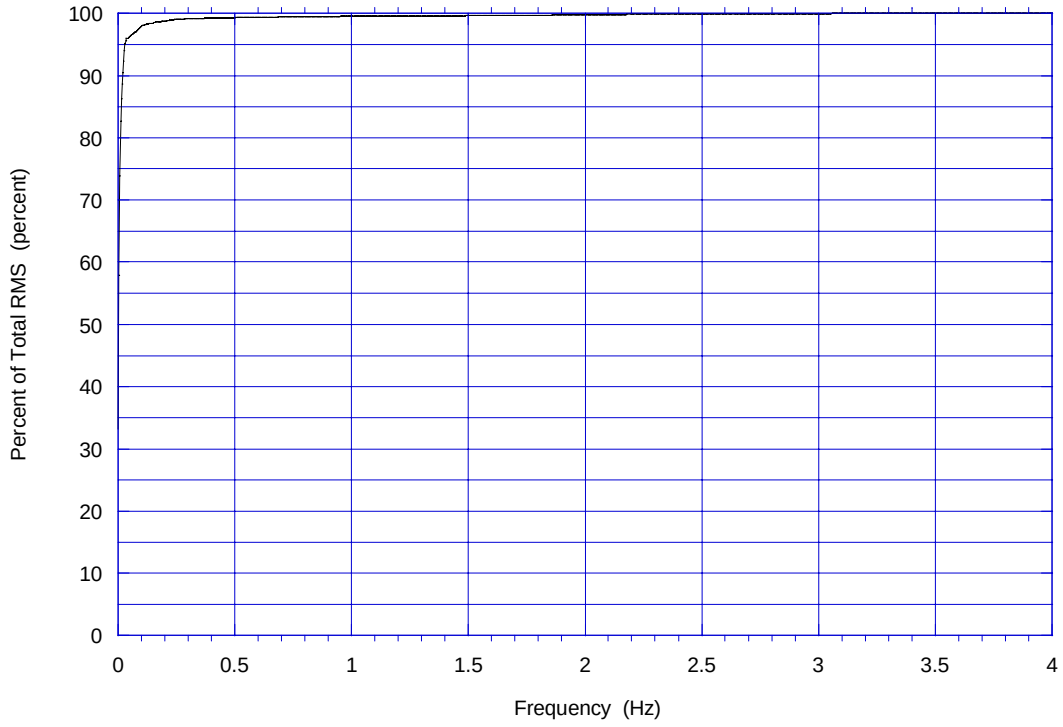

FIGURE 70. PERCENT OF TOTAL LONGITUDINAL LOAD FACTOR RMS VS FREQUENCY, FLIGHT SEQUENCE 35, POSTFLIGHT

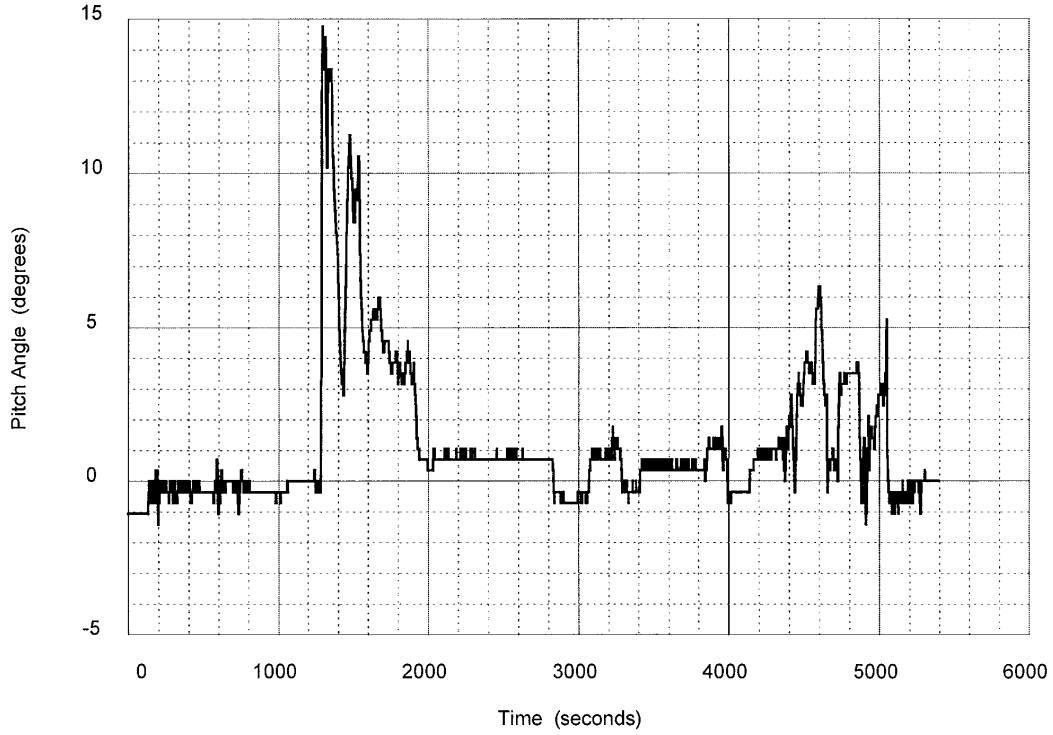

FIGURE 71. PITCH ANGLE TIME HISTORY, FLIGHT SEQUENCE 35

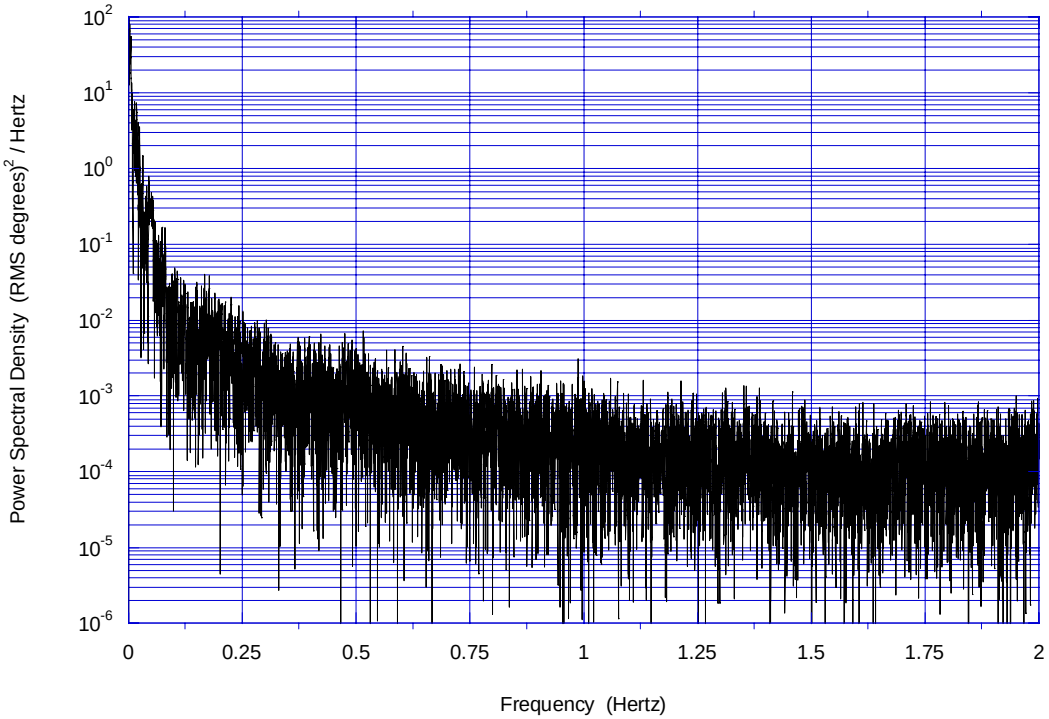

FIGURE 72. NORMALIZED PSD OF PITCH ANGLE,
FLIGHT SEQUENCE 35, IN FLIGHT

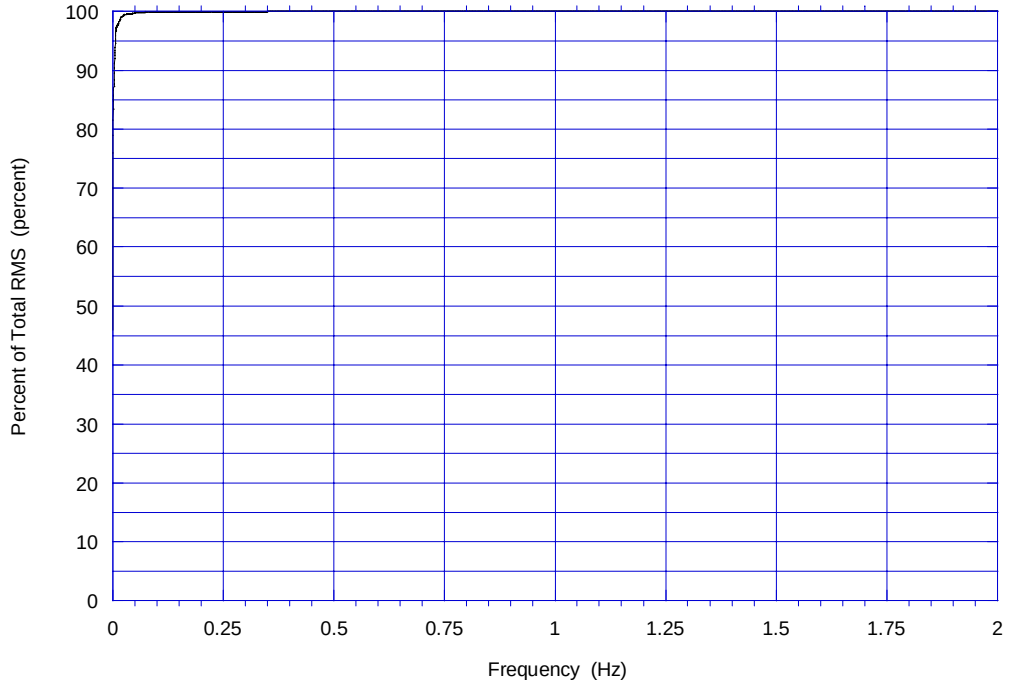

FIGURE 73. PERCENT OF TOTAL PITCH ANGLE RMS VS FREQUENCY, FLIGHT SEQUENCE 35, IN FLIGHT

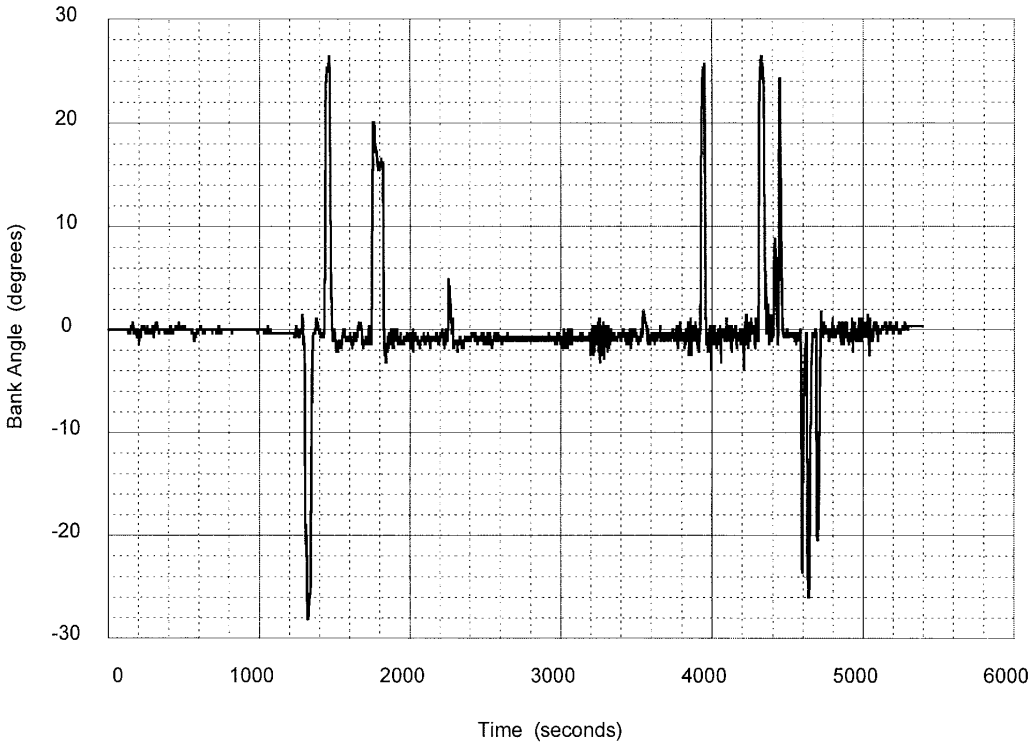

FIGURE 74. BANK ANGLE TIME HISTORY, FLIGHT SEQUENCE 35

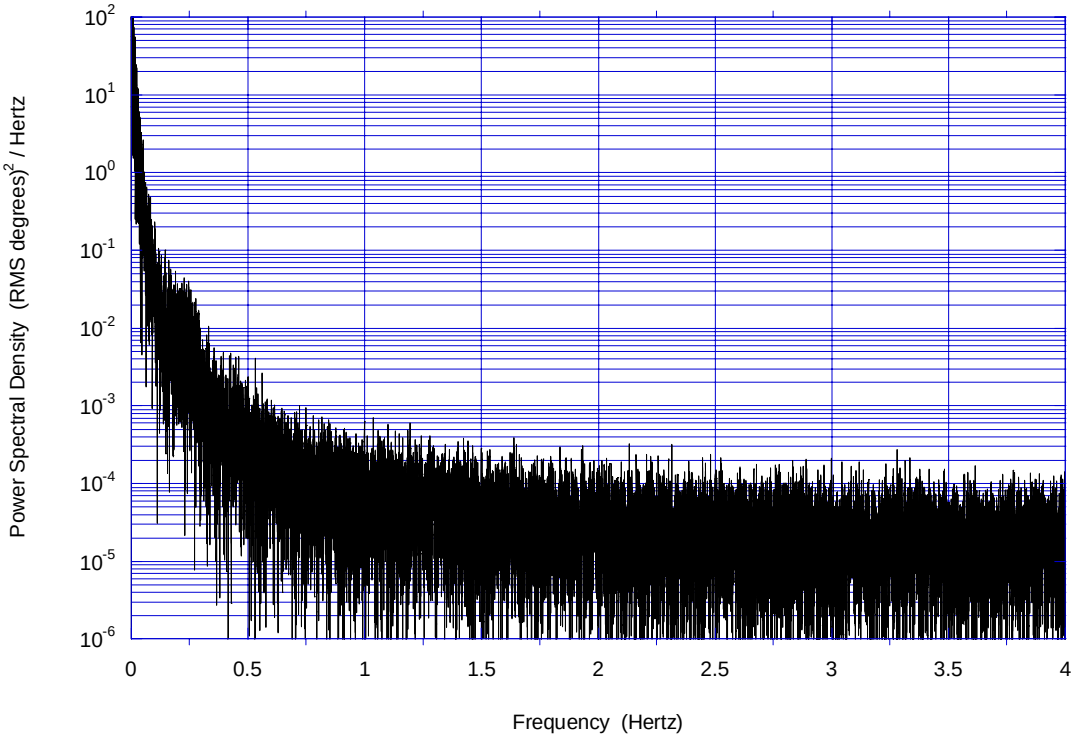

FIGURE 75. NORMALIZED PSD OF BANK ANGLE,
FLIGHT SEQUENCE 35, IN FLIGHT

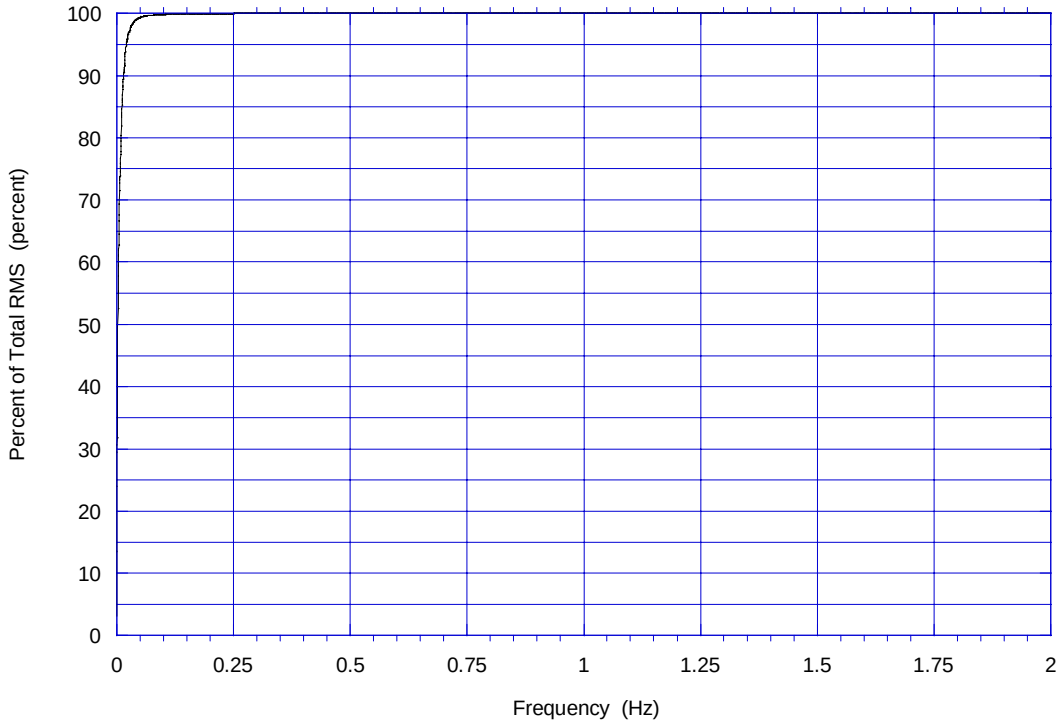

FIGURE 76. PERCENT OF TOTAL BANK ANGLE RMS VS FREQUENCY,
FLIGHT SEQUENCE 35, IN FLIGHT

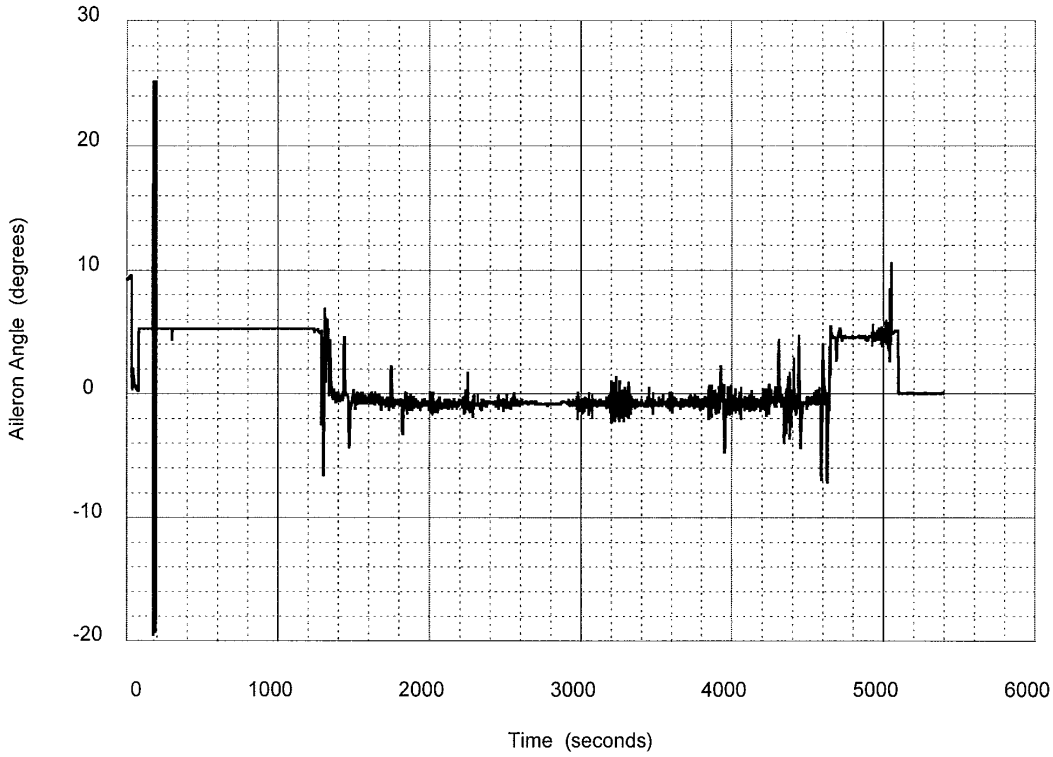

FIGURE 77. AILERON ANGLE TIME HISTORY, FLIGHT SEQUENCE 35

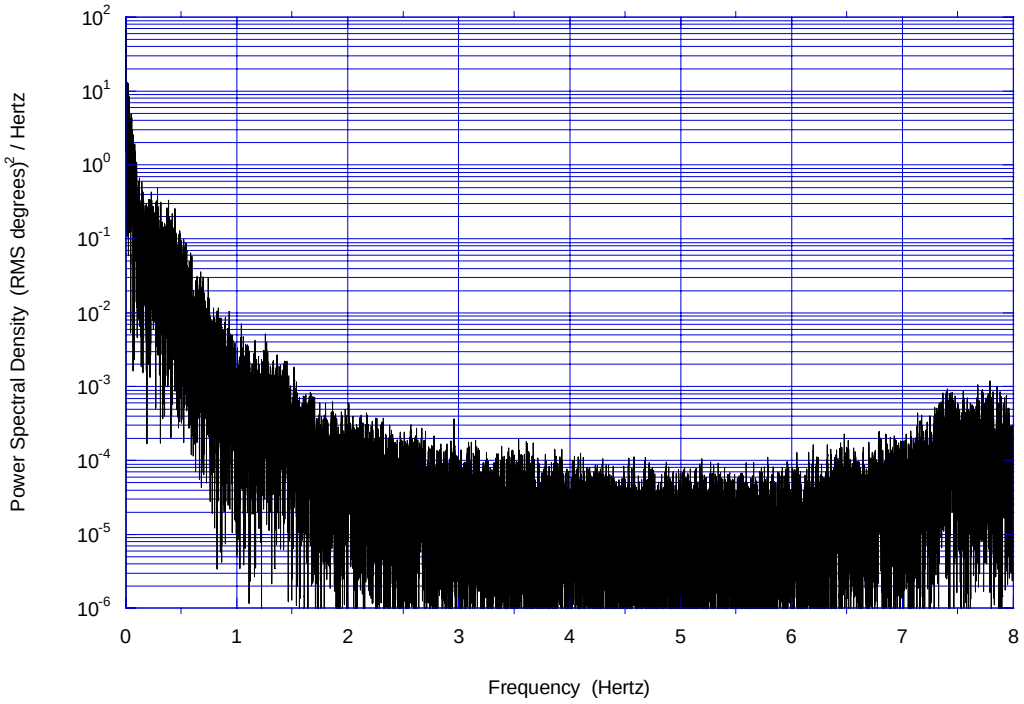

FIGURE 78. NORMALIZED PSD OF AILERON ANGLE,
FLIGHT SEQUENCE 35, IN FLIGHT

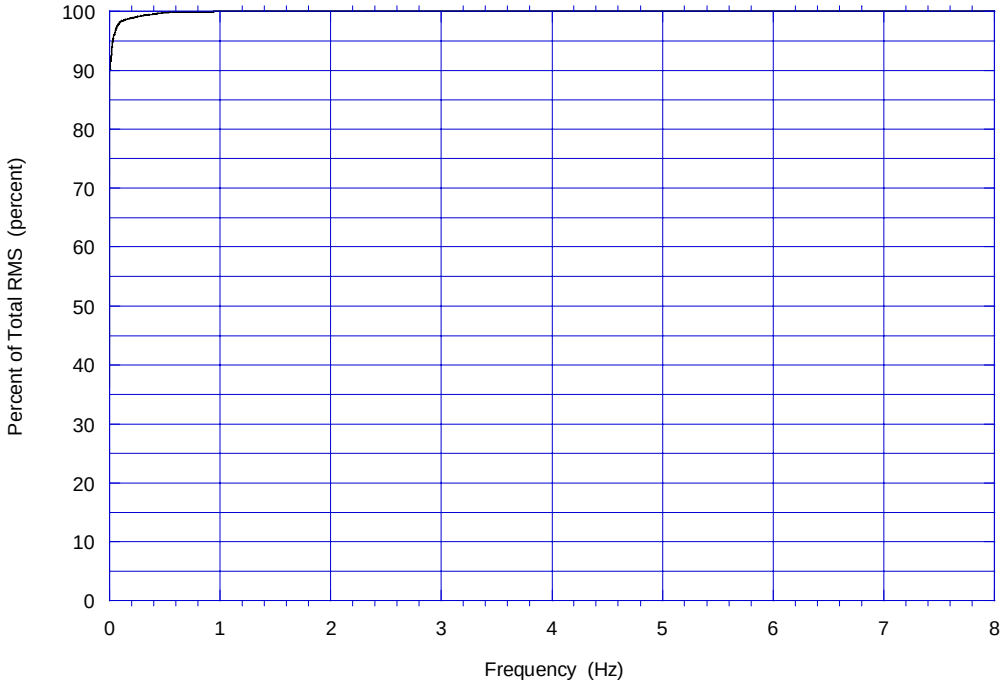

FIGURE 79. PERCENT OF TOTAL AILERON ANGLE RMS VS FREQUENCY, FLIGHT SEQUENCE 35, IN FLIGHT

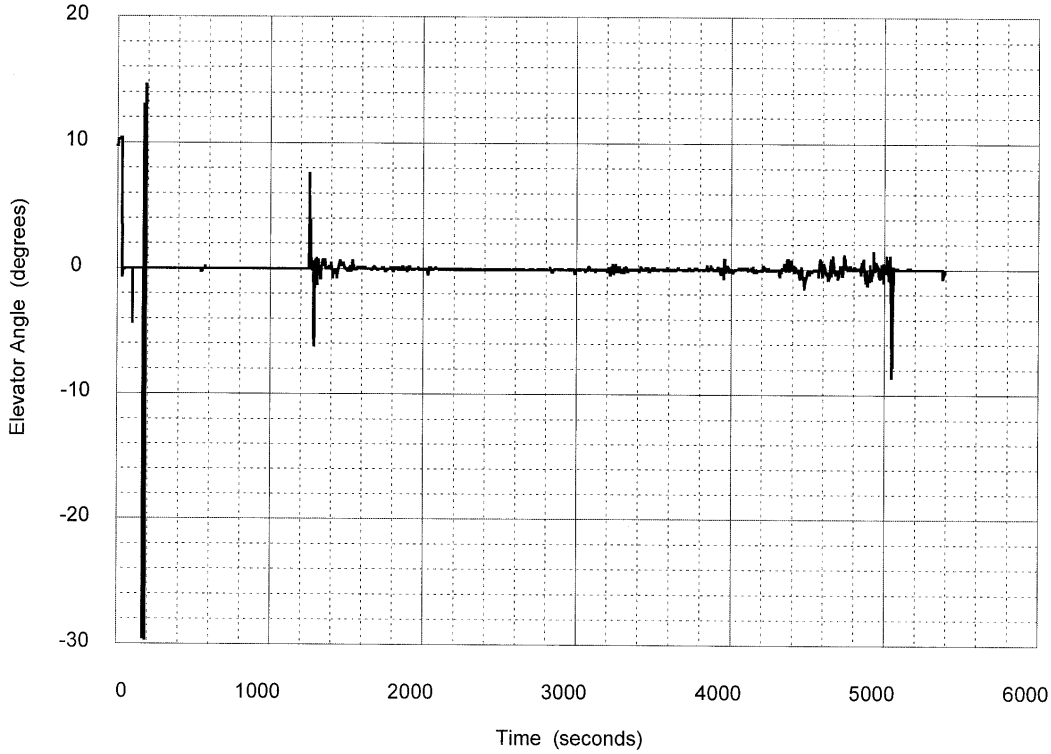

FIGURE 80. ELEVATOR ANGLE TIME HISTORY, FLIGHT SEQUENCE 35

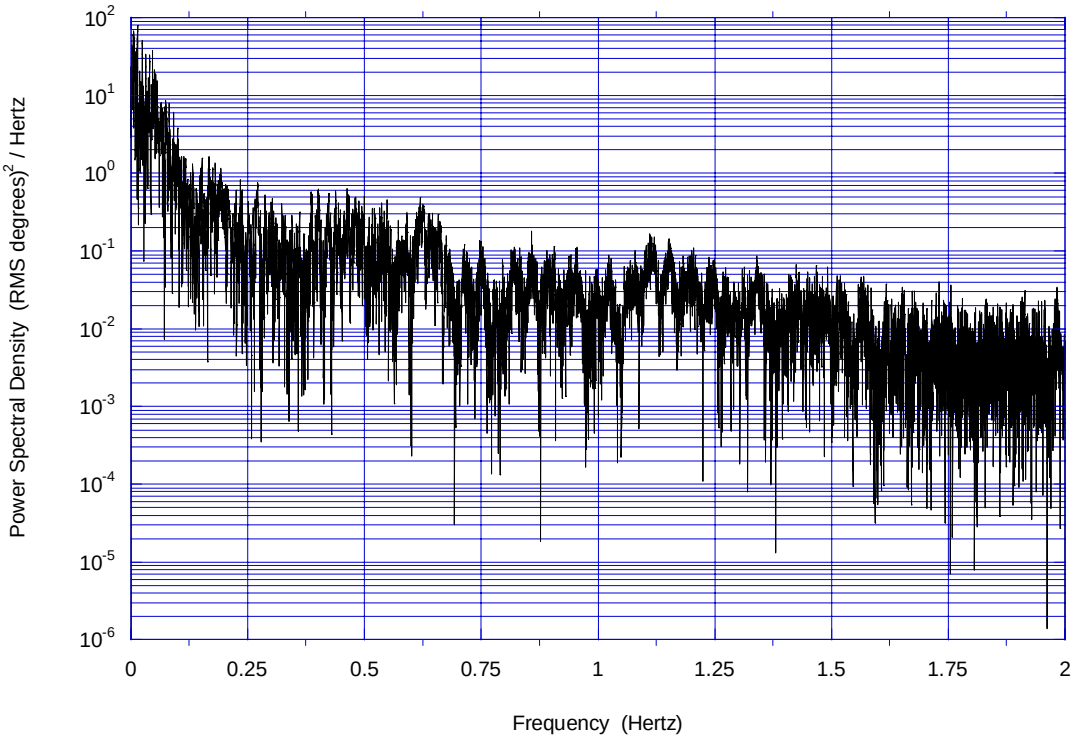

FIGURE 81. NORMALIZED PSD OF ELEVATOR ANGLE,
FLIGHT SEQUENCE 35, IN FLIGHT

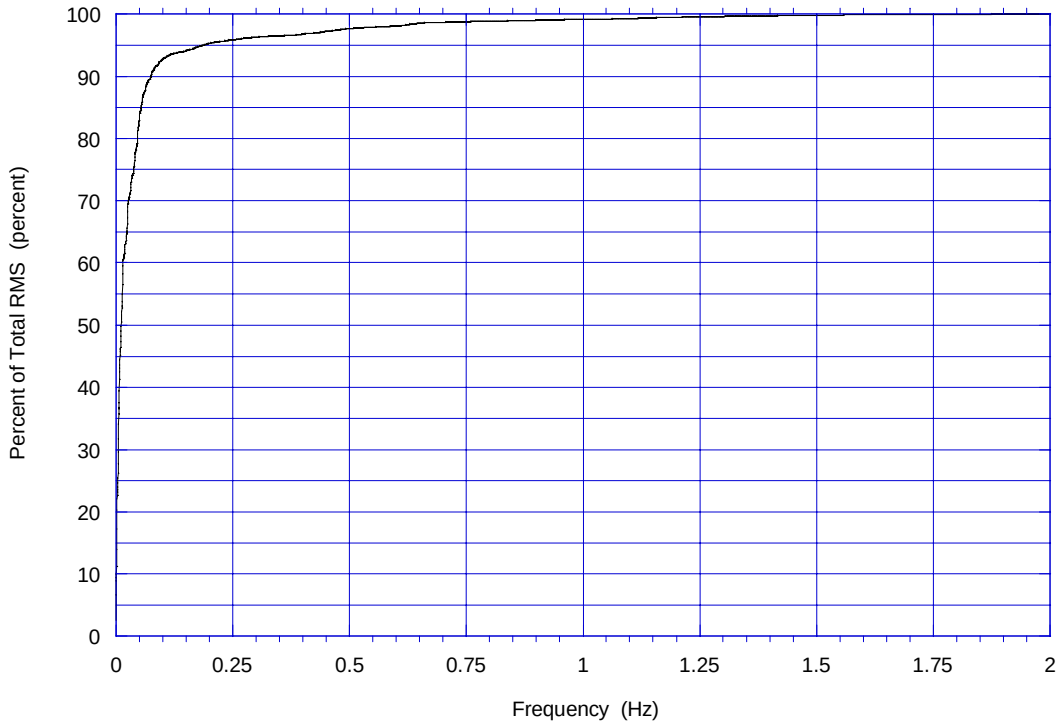

FIGURE 82. PERCENT OF TOTAL ELEVATOR ANGLE RMS VS FREQUENCY,
FLIGHT SEQUENCE 35, IN FLIGHT

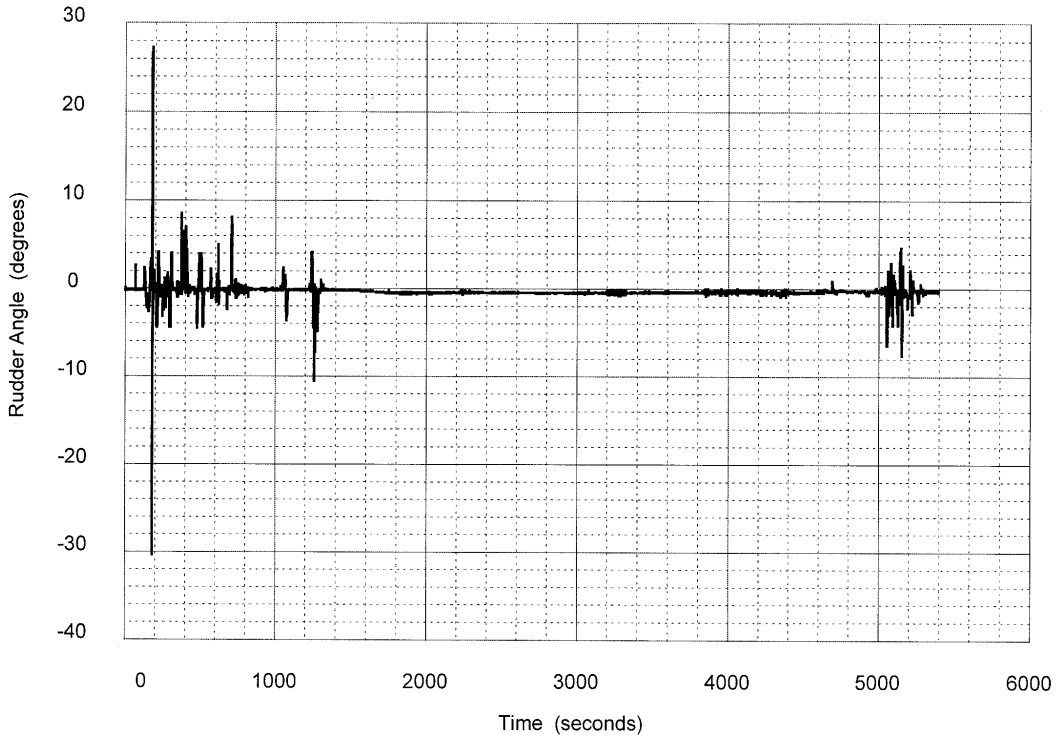

FIGURE 83. RUDDER ANGLE TIME HISTORY, FLIGHT SEQUENCE 35

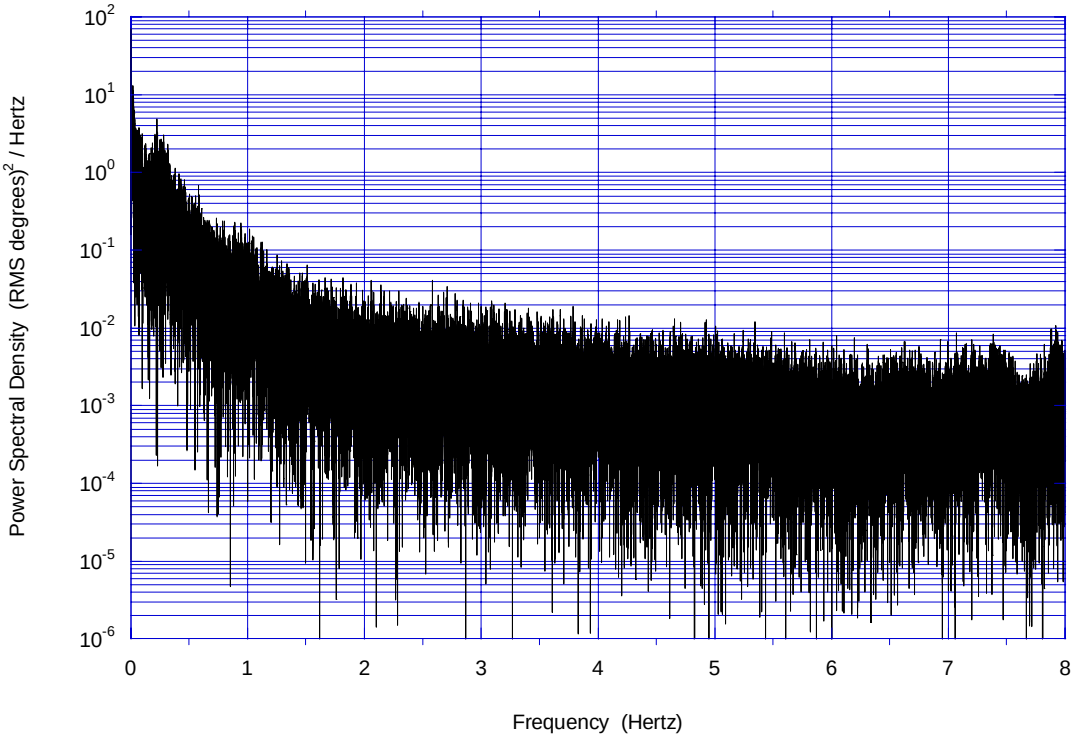

FIGURE 84. NORMALIZED PSD OF RUDDER ANGLE, FLIGHT SEQUENCE 35, IN FLIGHT

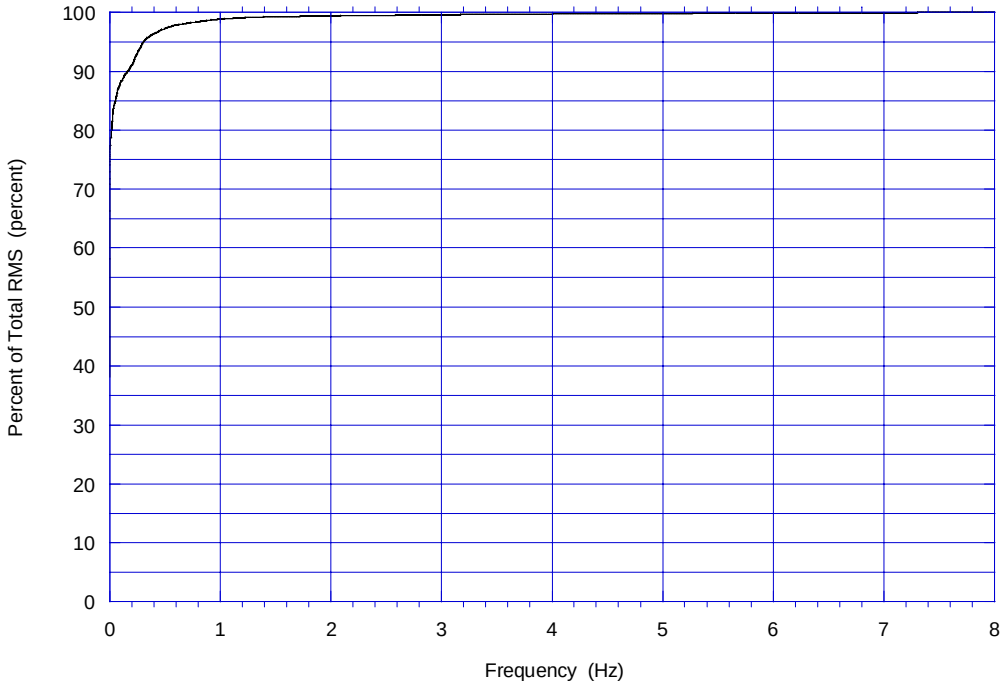

FIGURE 85. PERCENT OF TOTAL RUDDER ANGLE RMS VS FREQUENCY, FLIGHT SEQUENCE 35, IN FLIGHT

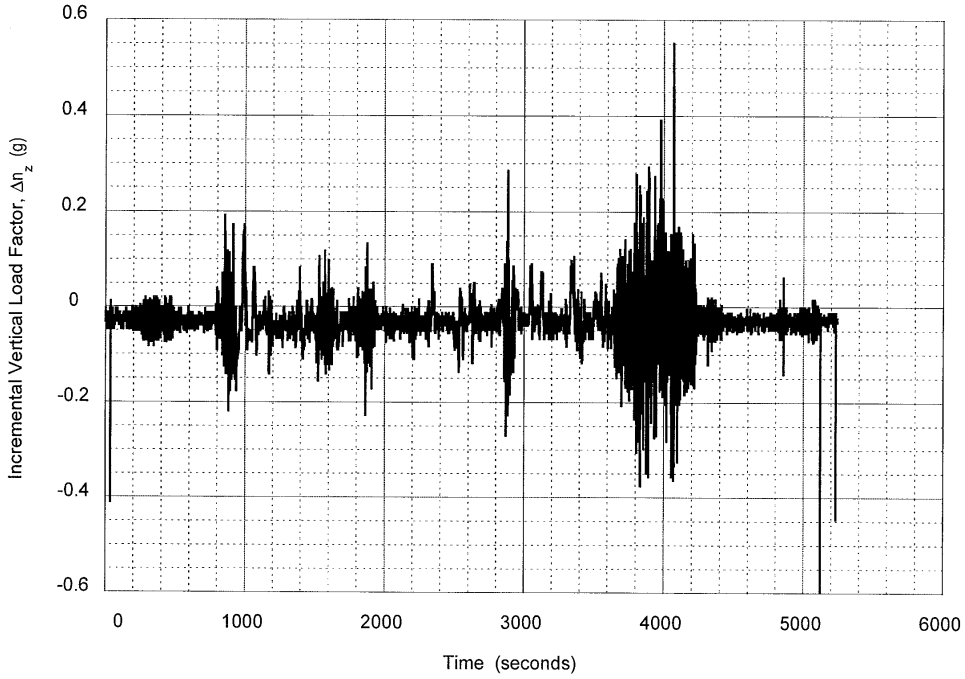

FIGURE 86. INCREMENTAL VERTICAL LOAD FACTOR TIME HISTORY, FLIGHT SEQUENCE 62

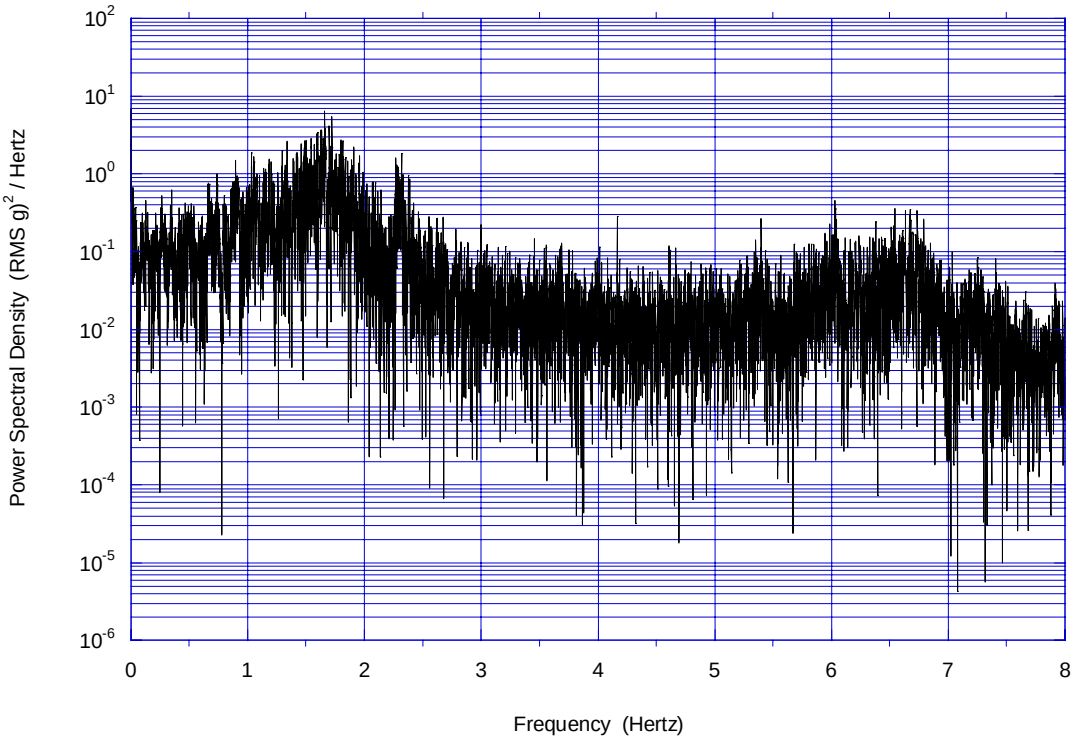

FIGURE 87. NORMALIZED PSD OF INCREMENTAL VERTICAL LOAD FACTOR, FLIGHT SEQUENCE 62, PREFLIGHT

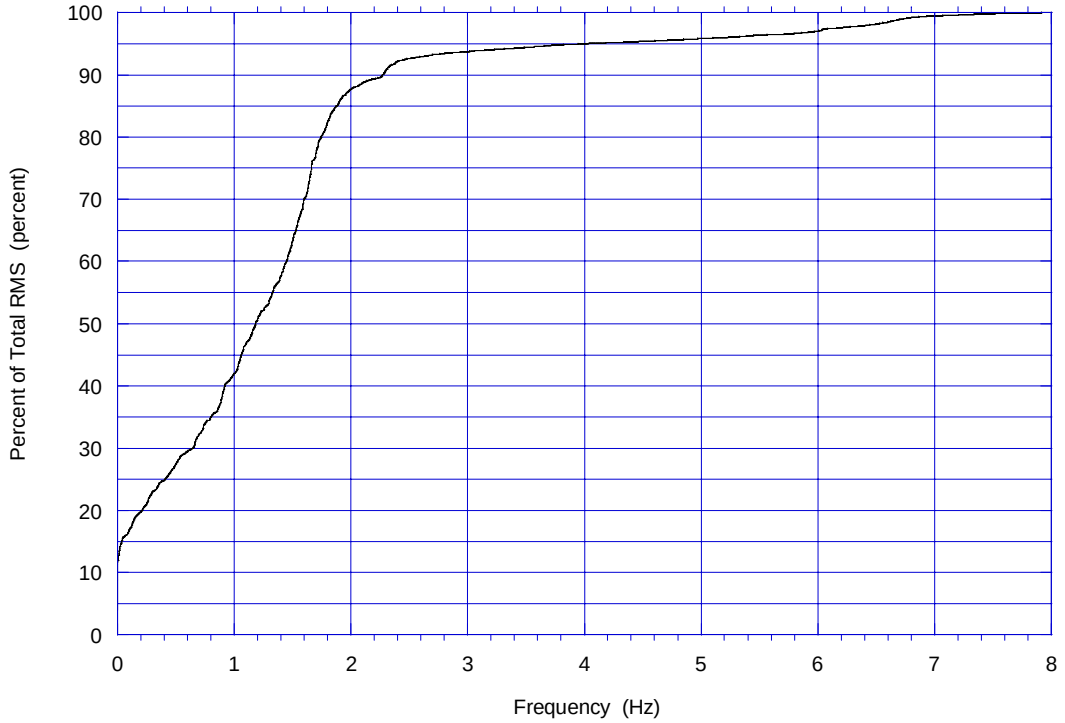

FIGURE 88. PERCENT OF TOTAL INCREMENTAL VERTICAL LOAD FACTOR RMS VS FREQUENCY, FLIGHT SEQUENCE 62, PREFLIGHT

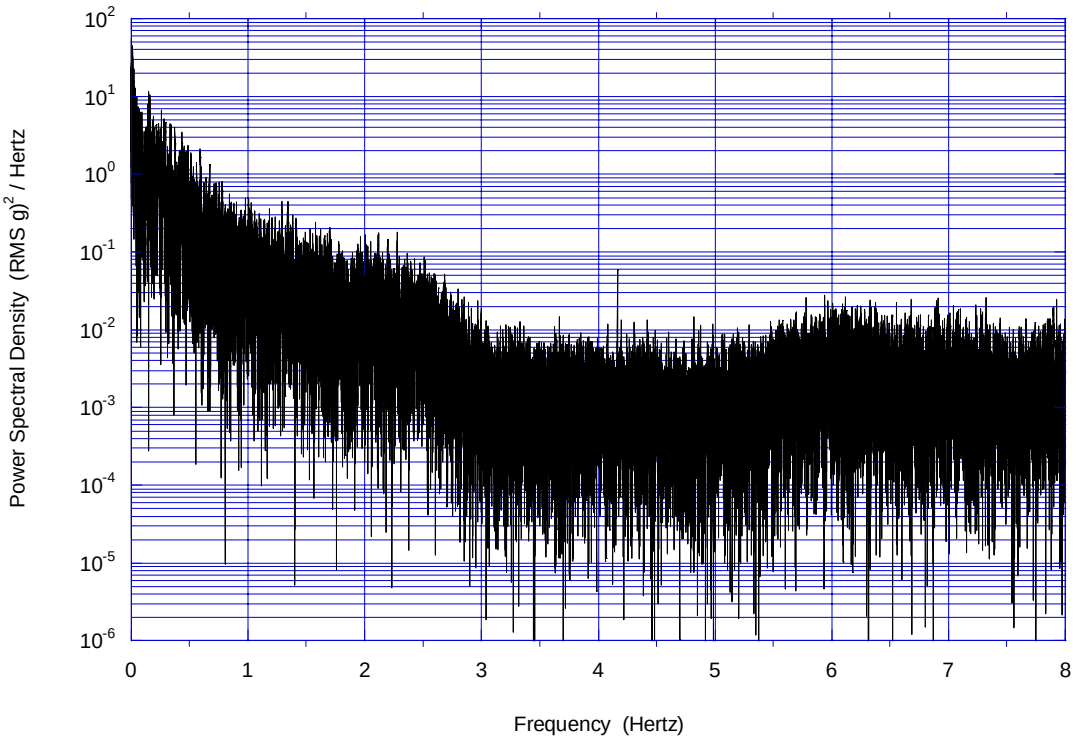

FIGURE 89. NORMALIZED PSD OF INCREMENTAL VERTICAL LOAD FACTOR, FLIGHT SEQUENCE 62, IN FLIGHT

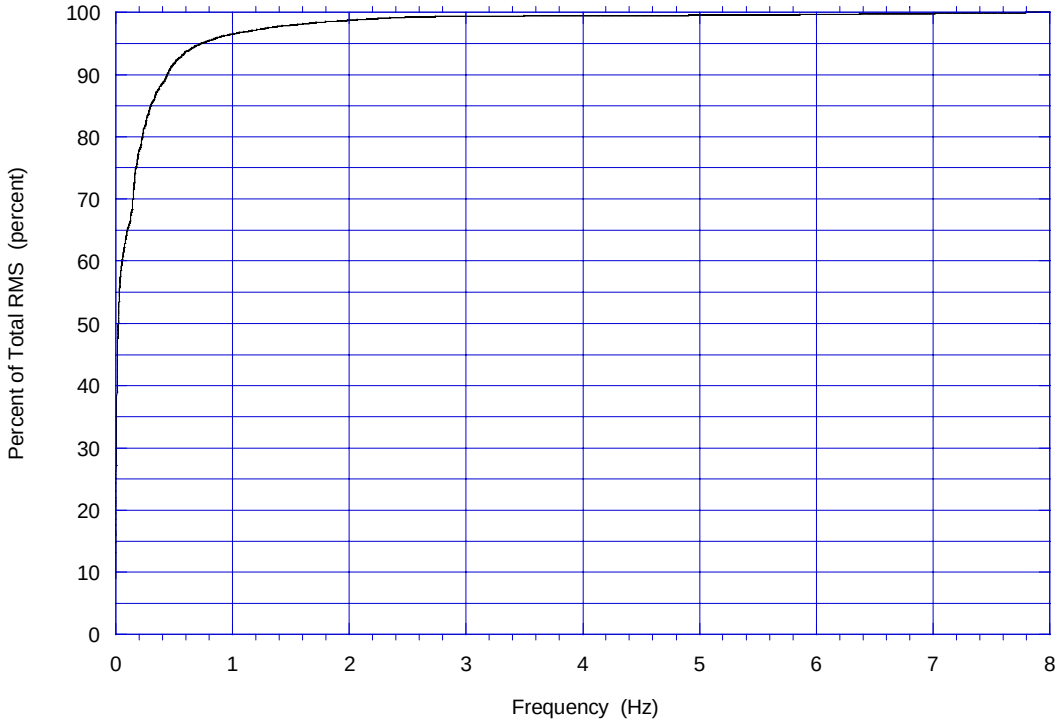

FIGURE 90. PERCENT OF TOTAL INCREMENTAL VERTICAL LOAD FACTOR RMS VS FREQUENCY, FLIGHT SEQUENCE 62, IN FLIGHT

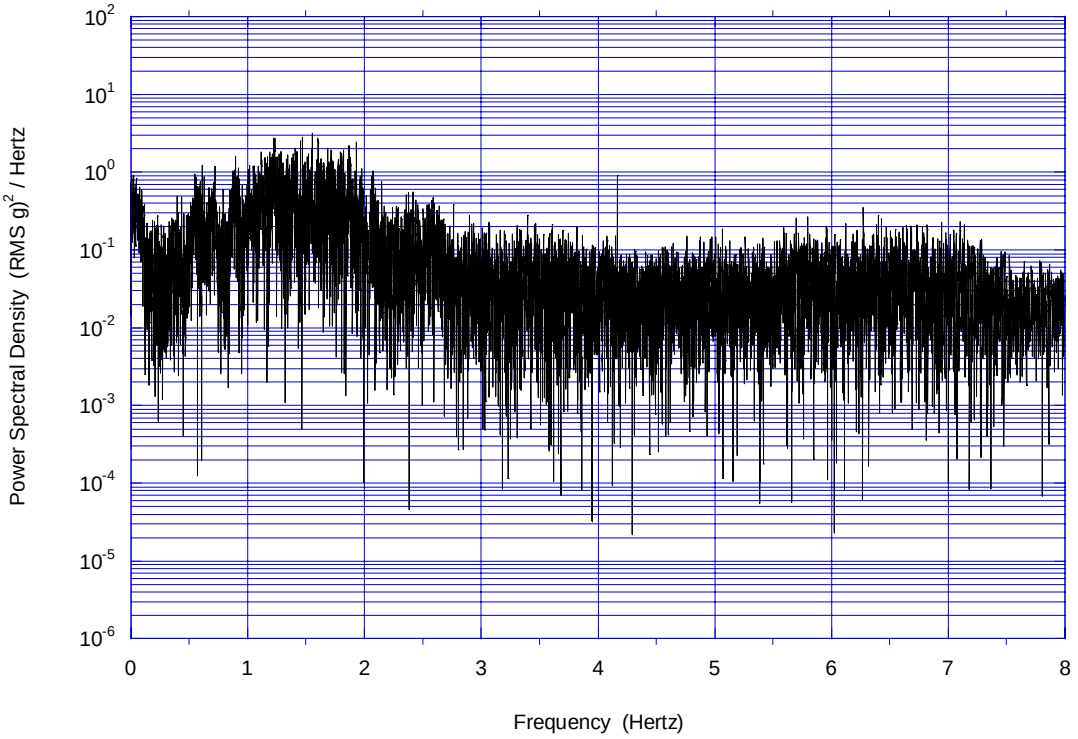

FIGURE 91. NORMALIZED PSD OF INCREMENTAL VERTICAL LOAD FACTOR, FLIGHT SEQUENCE 62, POSTFLIGHT

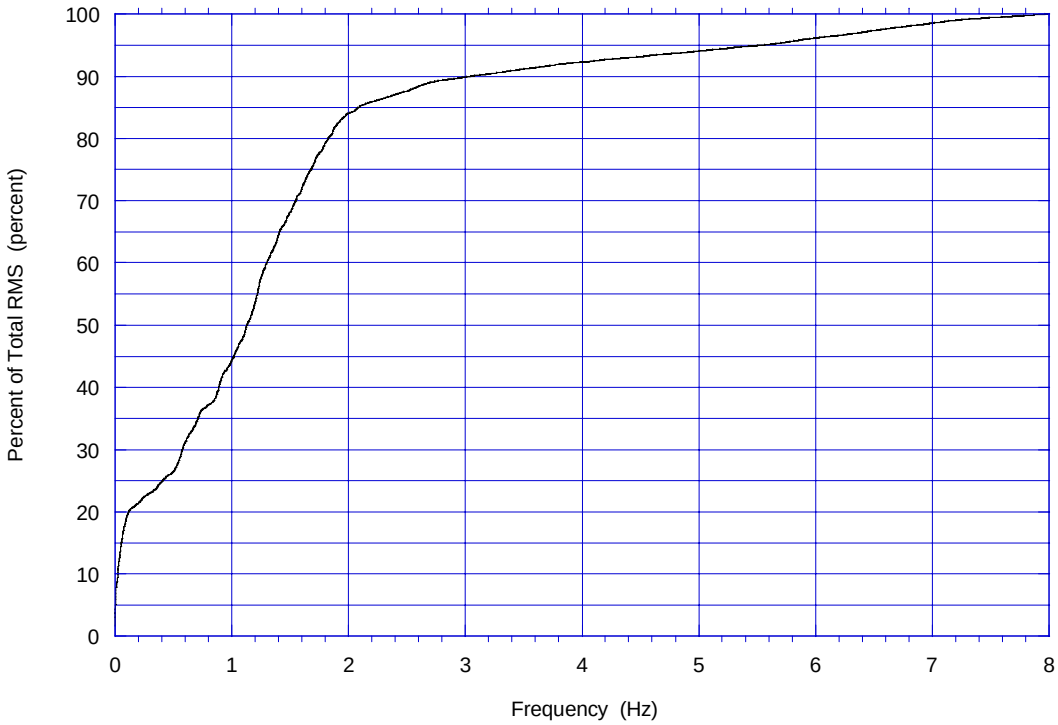

FIGURE 92. PERCENT OF TOTAL INCREMENTAL VERTICAL LOAD FACTOR RMS VS FREQUENCY, FLIGHT SEQUENCE 62, POSTFLIGHT

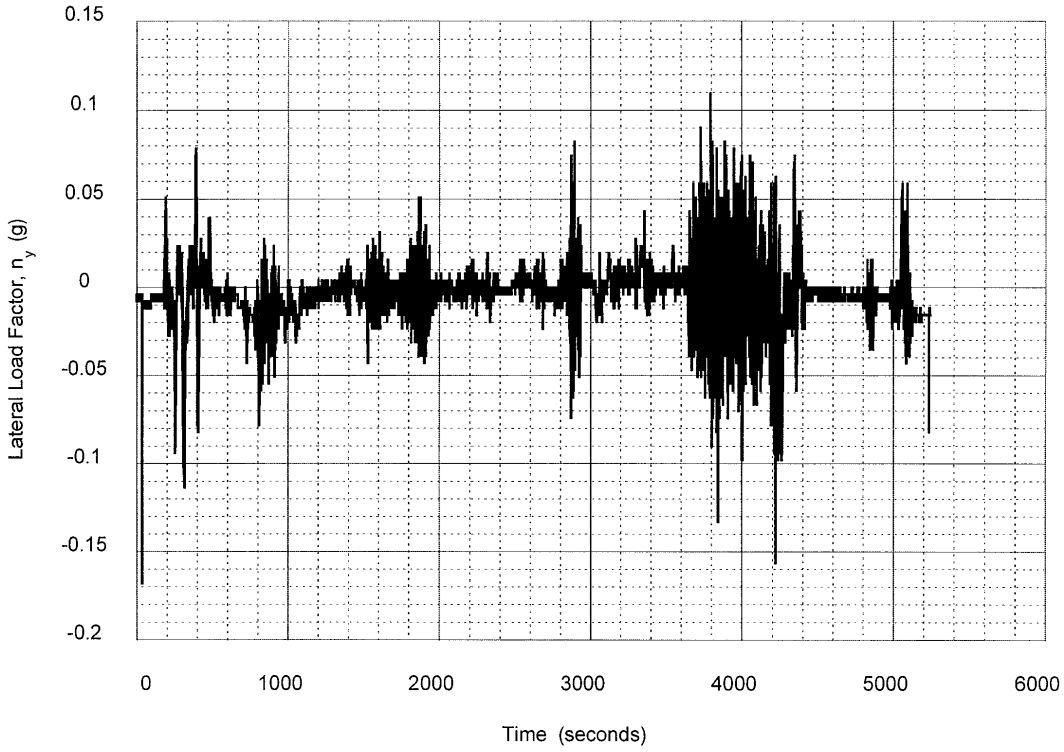

FIGURE 93. LATERAL LOAD FACTOR TIME HISTORY, FLIGHT SEQUENCE 62

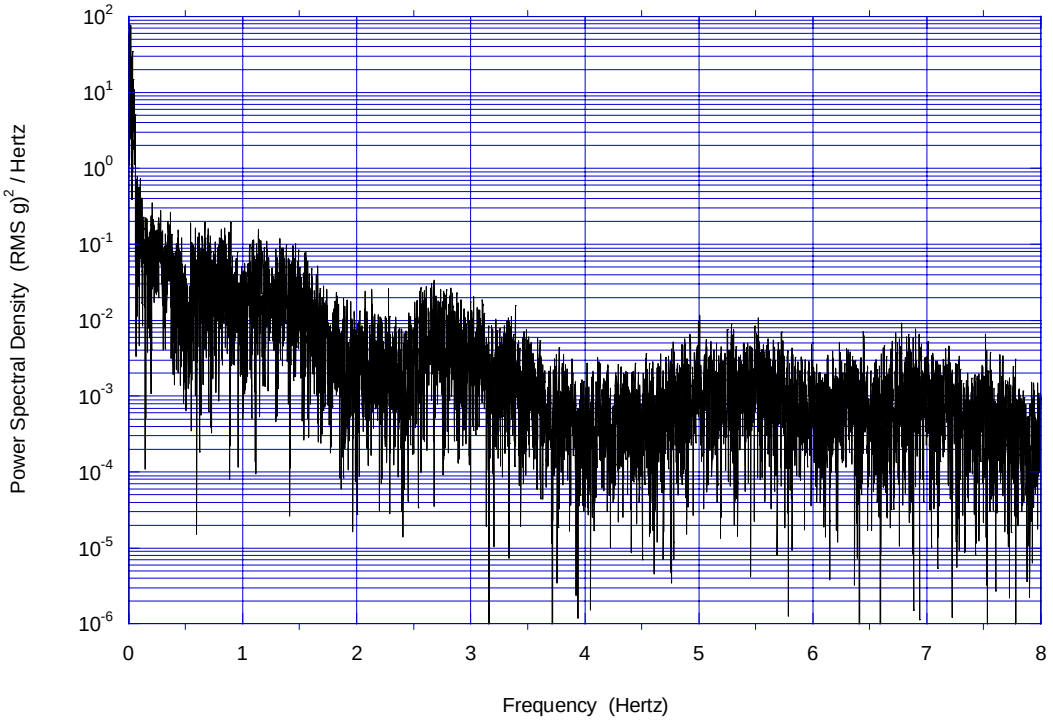

FIGURE 94. NORMALIZED PSD OF LATERAL LOAD FACTOR, FLIGHT SEQUENCE 62, PREFLIGHT

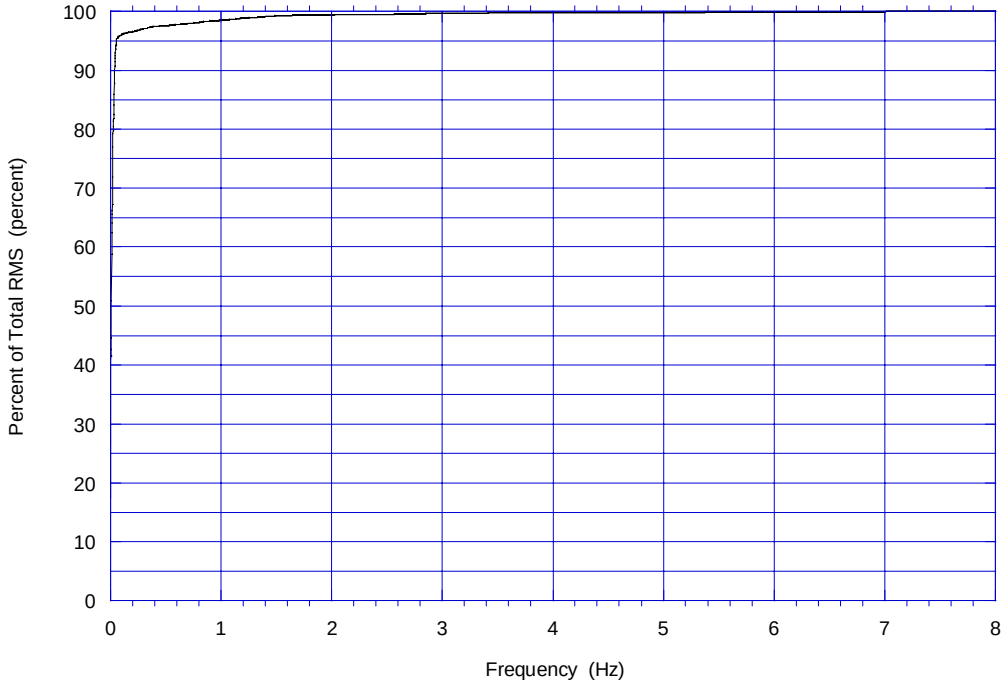

FIGURE 95. PERCENT OF TOTAL LATERAL LOAD FACTOR RMS VS FREQUENCY, FLIGHT SEQUENCE 62, PREFLIGHT

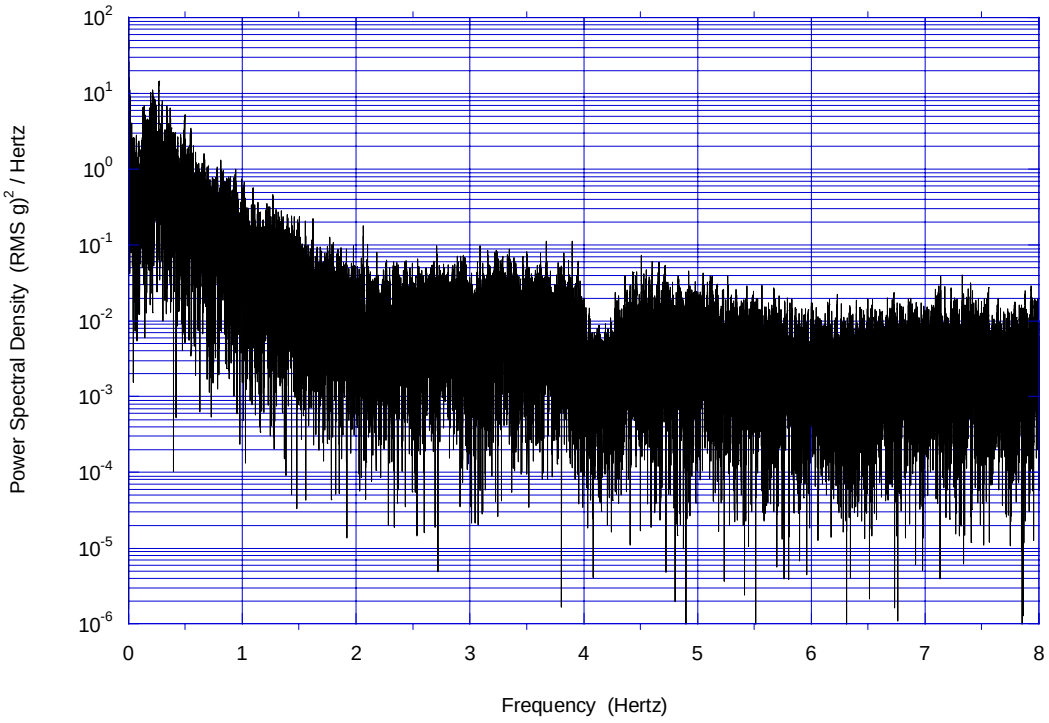

FIGURE 96. NORMALIZED PSD OF LATERAL LOAD FACTOR, FLIGHT SEQUENCE 62, IN FLIGHT

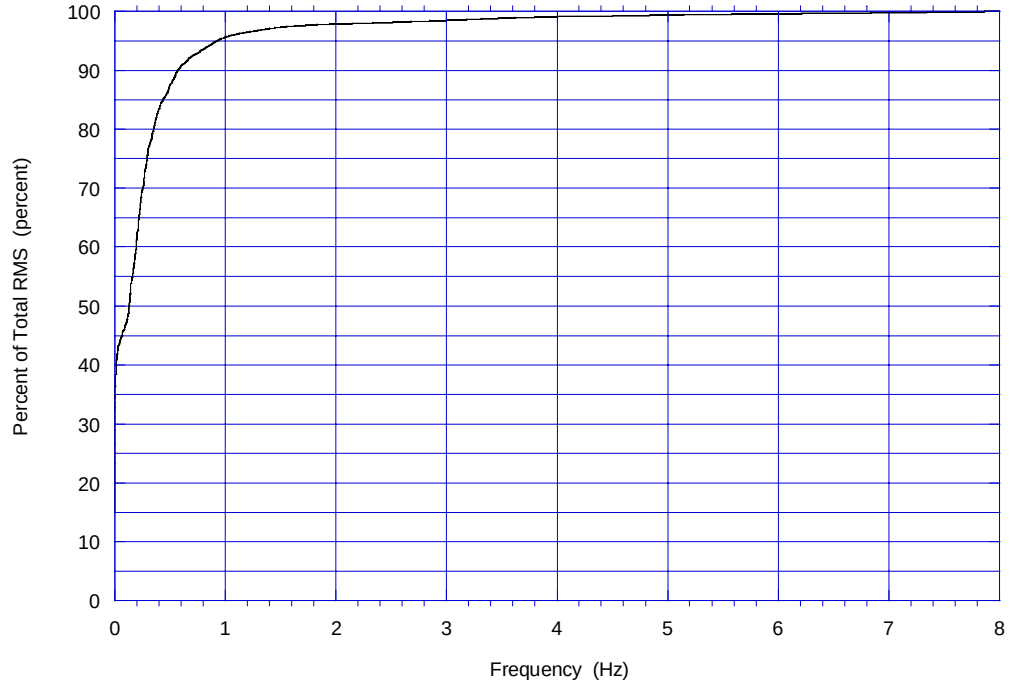

FIGURE 97. PERCENT OF TOTAL LATERAL LOAD FACTOR RMS VS FREQUENCY, FLIGHT SEQUENCE 62, IN FLIGHT

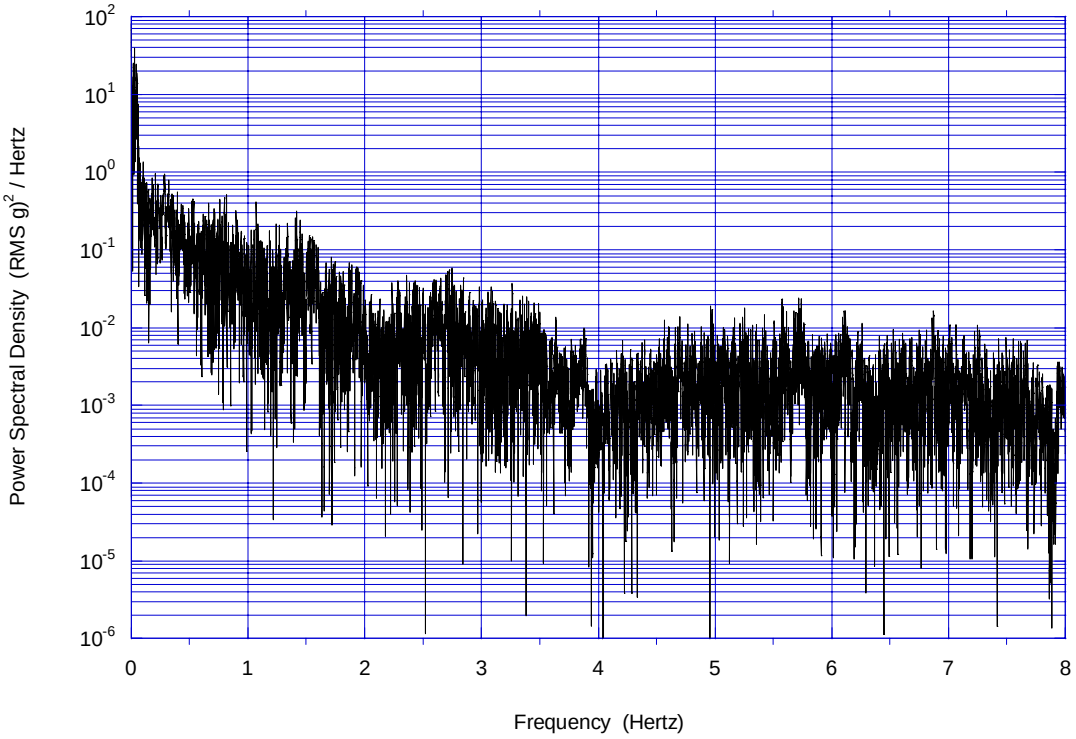

FIGURE 98. NORMALIZED PSD OF LATERAL LOAD FACTOR, FLIGHT SEQUENCE 62, POSTFLIGHT

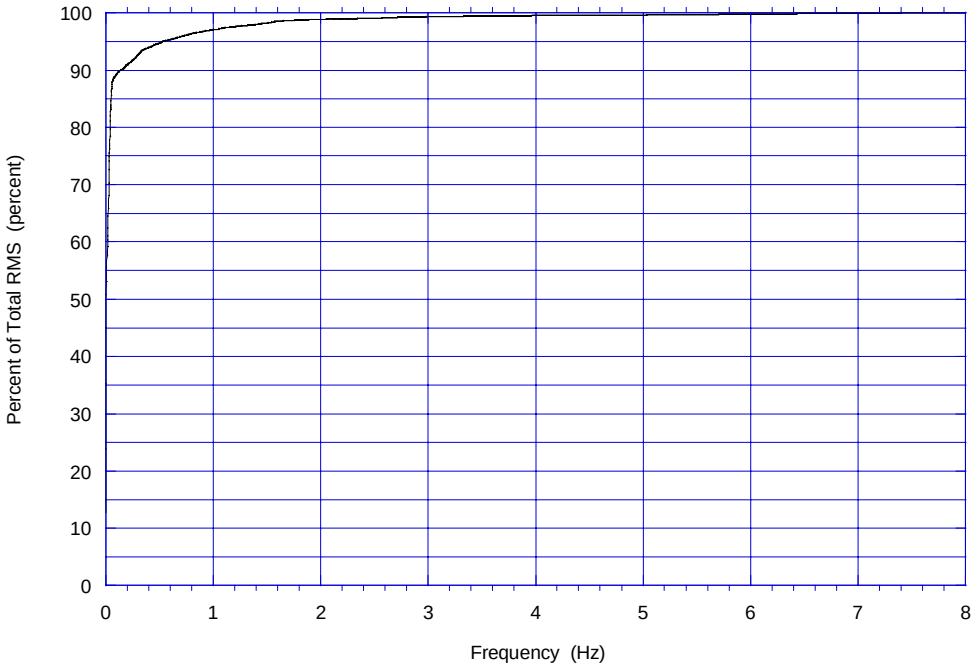

FIGURE 99. PERCENT OF TOTAL LATERAL LOAD FACTOR RMS VS FREQUENCY, FLIGHT SEQUENCE 62, POSTFLIGHT

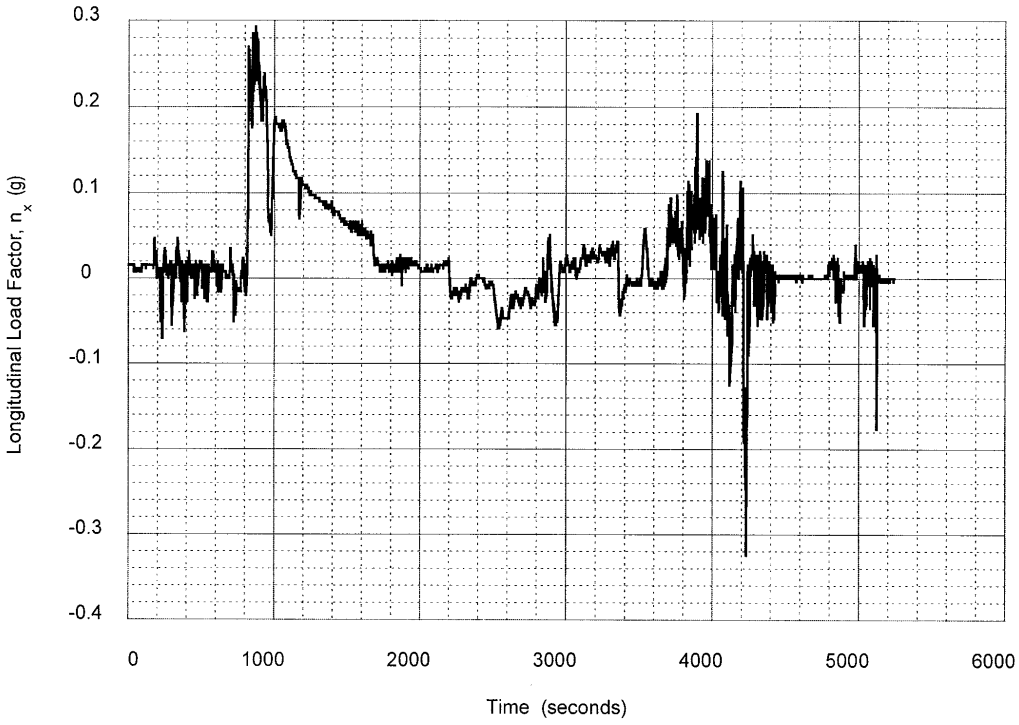

FIGURE 100. LONGITUDINAL LOAD FACTOR TIME HISTORY, FLIGHT SEQUENCE 62

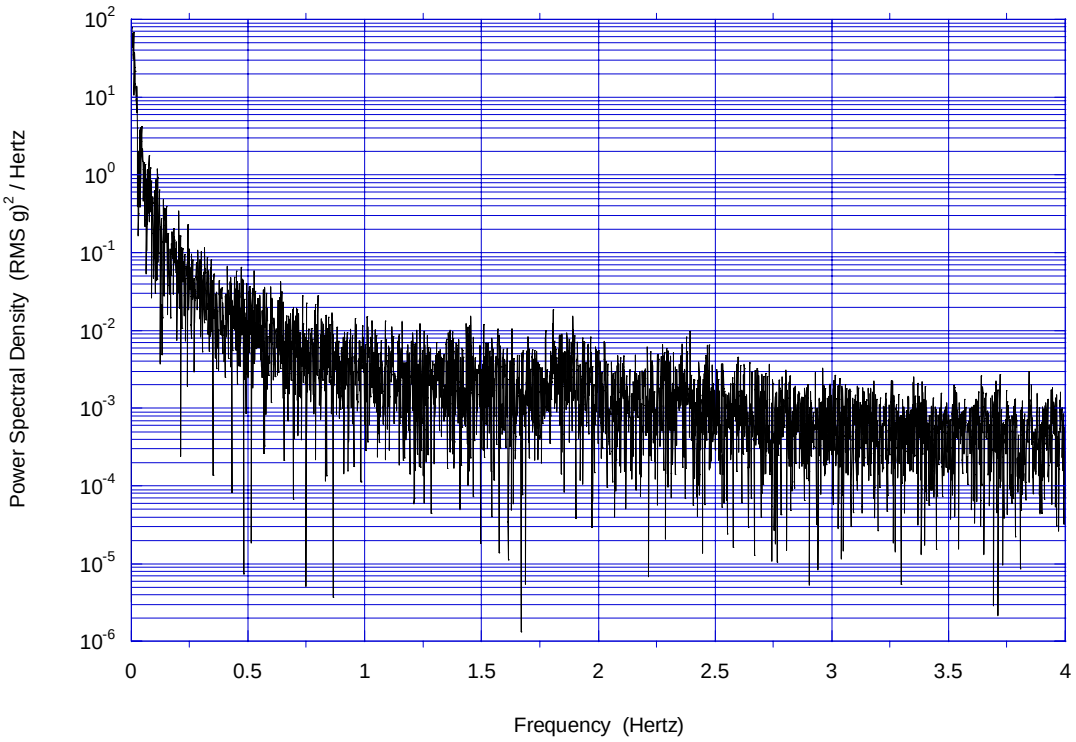

FIGURE 101. NORMALIZED PSD OF LONGITUDINAL LOAD FACTOR, FLIGHT SEQUENCE 62, PREFLIGHT

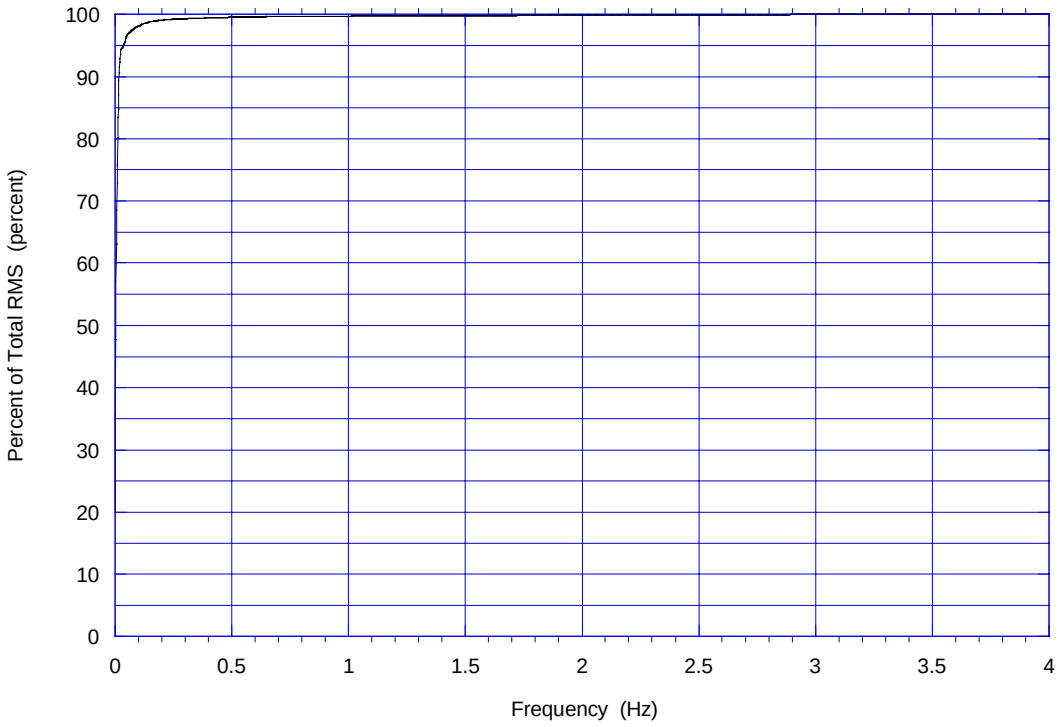

FIGURE 102. PERCENT OF TOTAL LONGITUDINAL LOAD FACTOR RMS VS FREQUENCY, FLIGHT SEQUENCE 62, PREFLIGHT

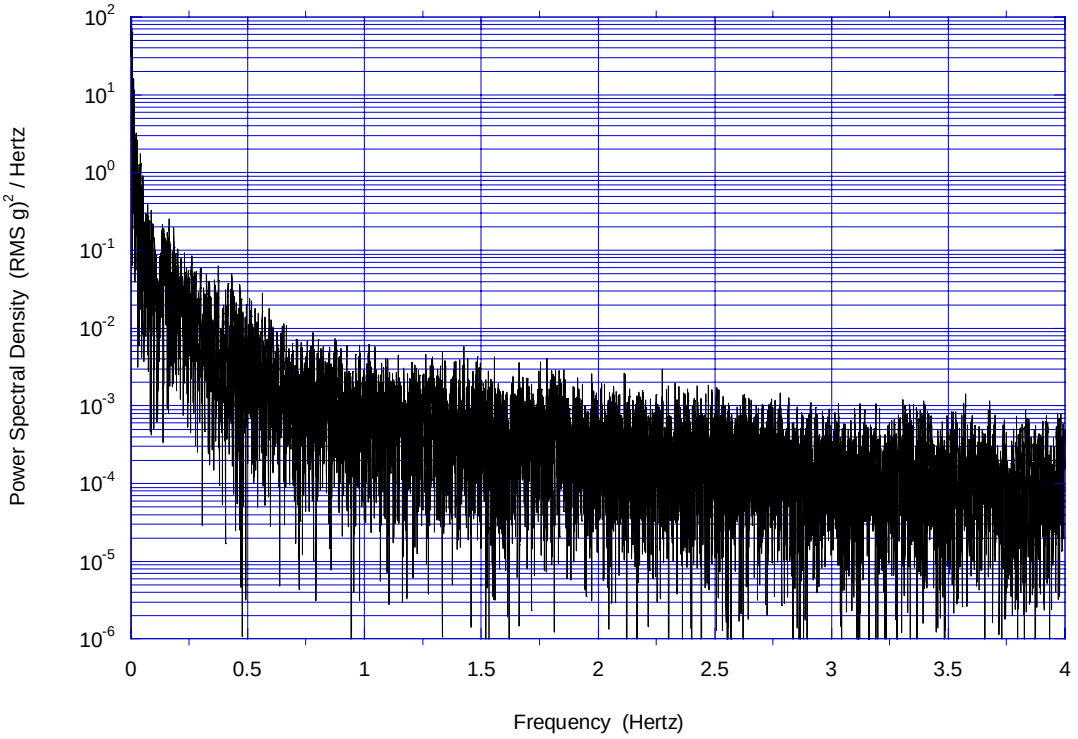

FIGURE 103. NORMALIZED PSD OF LONGITUDINAL LOAD FACTOR, FLIGHT SEQUENCE 62, IN FLIGHT

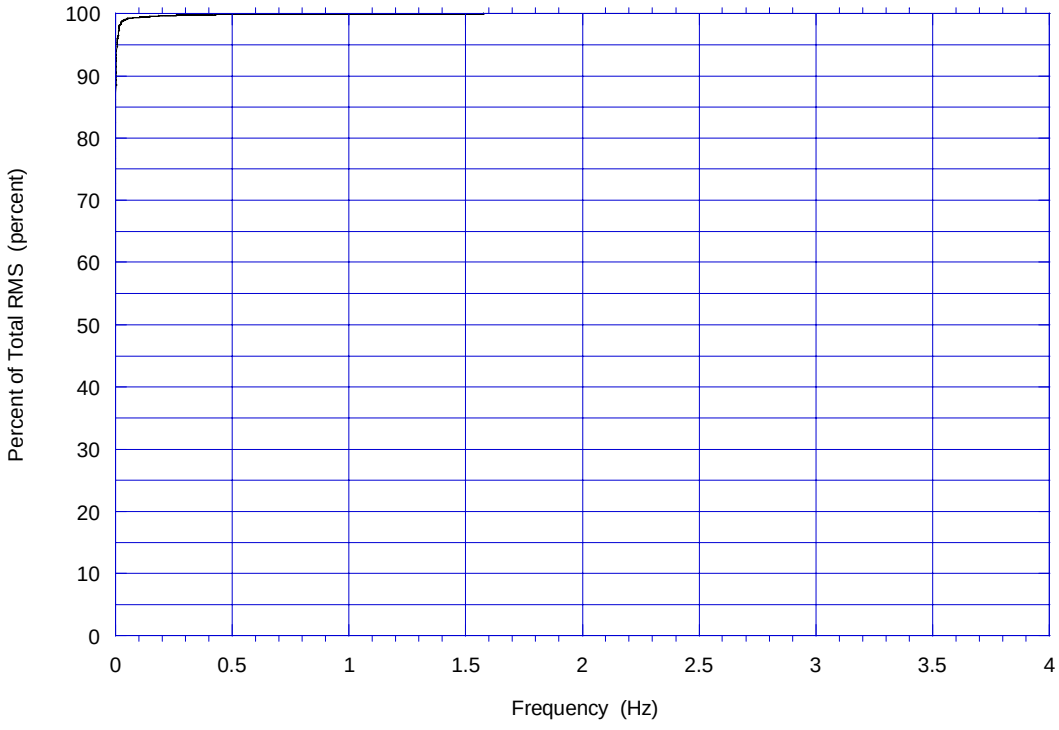

FIGURE 104. PERCENT OF TOTAL LONGITUDINAL LOAD FACTOR RMS VS FREQUENCY, FLIGHT SEQUENCE 62, IN FLIGHT

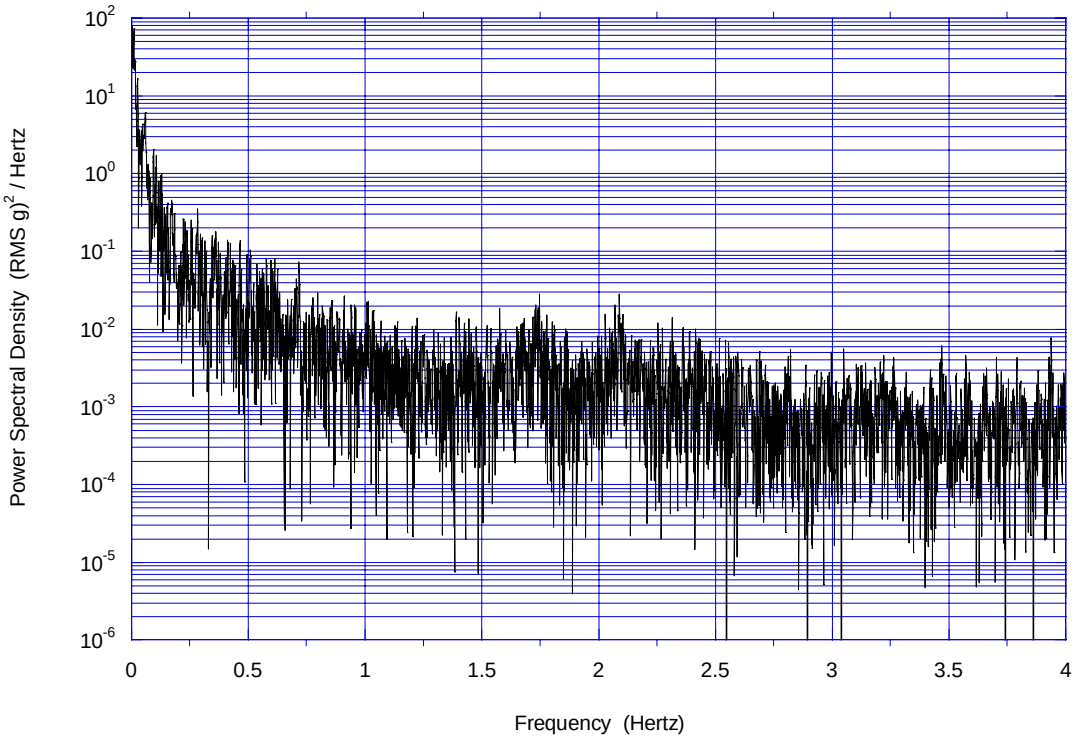

FIGURE 105. NORMALIZED PSD OF LONGITUDINAL LOAD FACTOR, FLIGHT SEQUENCE 62, POSTFLIGHT

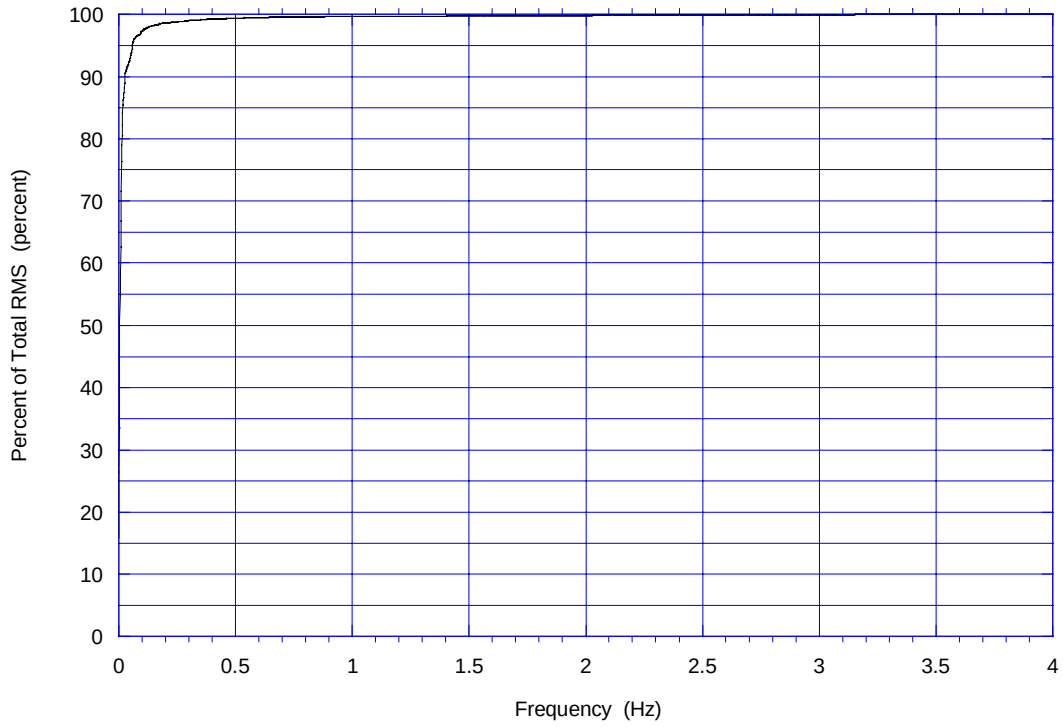

FIGURE 106. PERCENT OF TOTAL LONGITUDINAL LOAD FACTOR RMS VS FREQUENCY, FLIGHT SEQUENCE 62, POSTFLIGHT

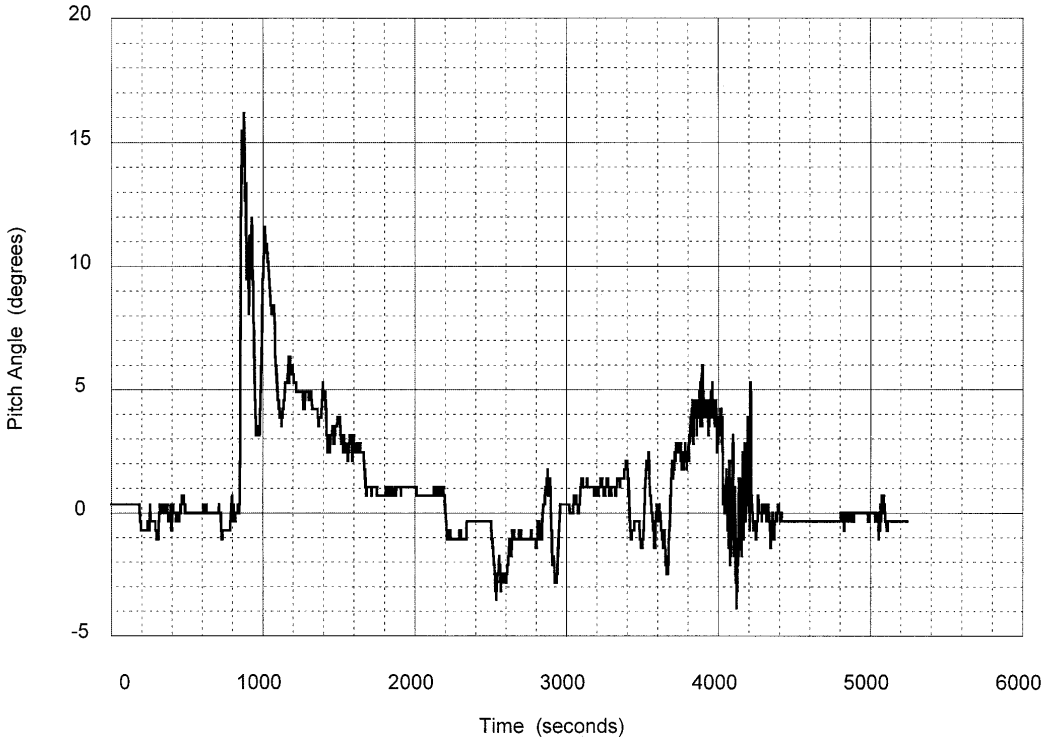

FIGURE 107. PITCH ANGLE TIME HISTORY, FLIGHT SEQUENCE 62

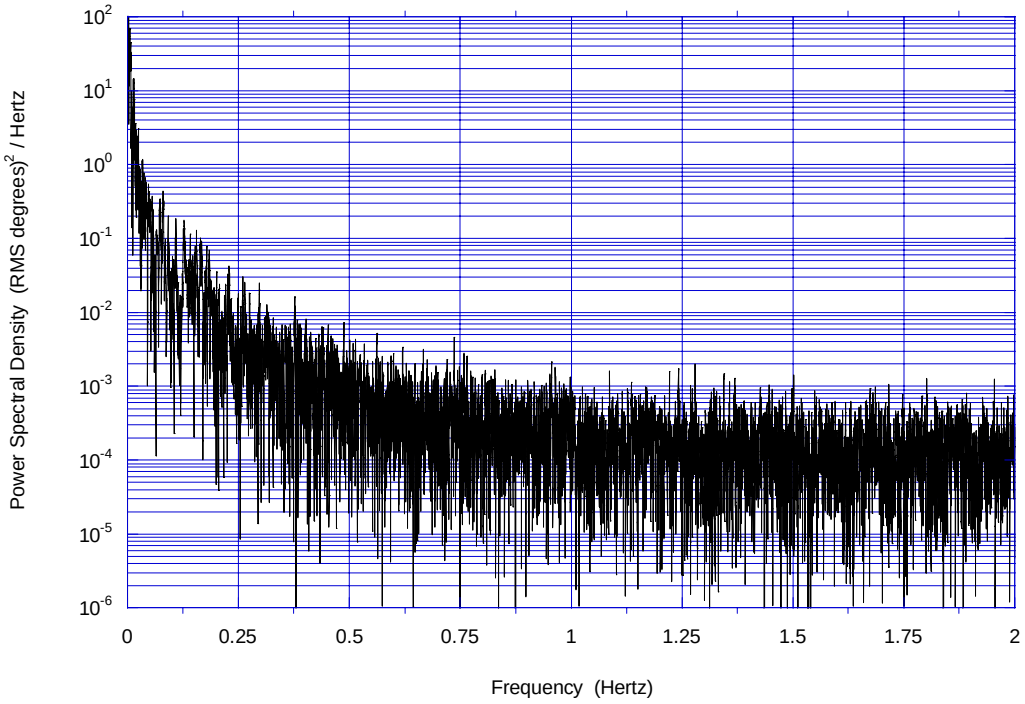

FIGURE 108. NORMALIZED PSD OF PITCH ANGLE,
FLIGHT SEQUENCE 62, IN FLIGHT

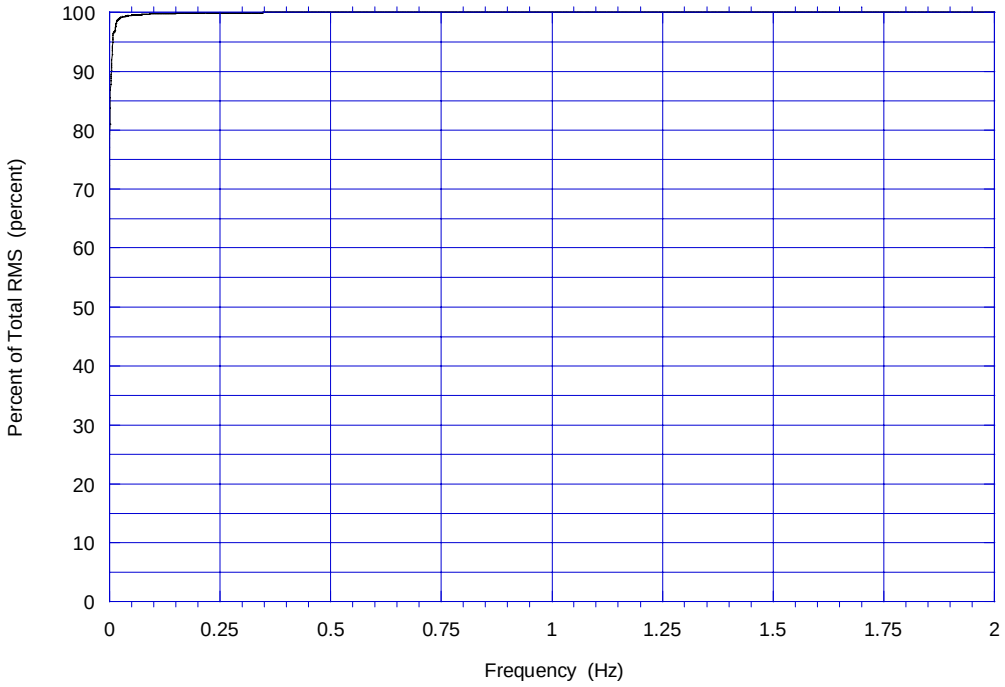

FIGURE 109. PERCENT OF TOTAL PITCH ANGLE RMS VS FREQUENCY, FLIGHT SEQUENCE 62, IN FLIGHT

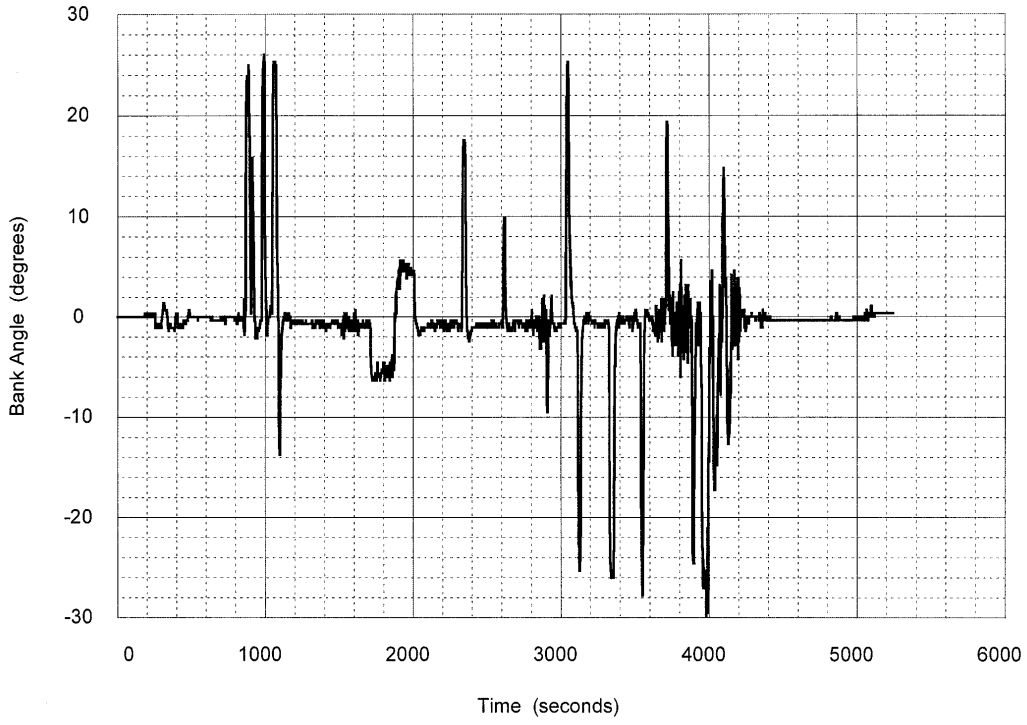

FIGURE 110. BANK ANGLE TIME HISTORY, FLIGHT SEQUENCE 62

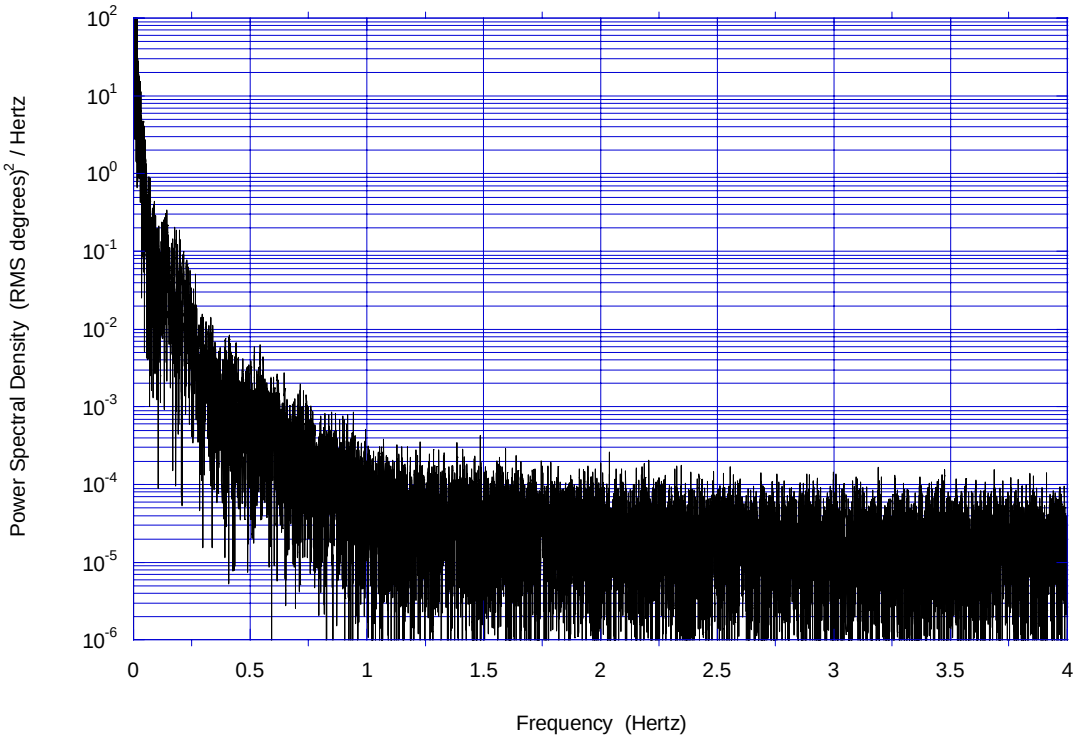

FIGURE 111. NORMALIZED PSD OF BANK ANGLE, FLIGHT SEQUENCE 62, IN FLIGHT

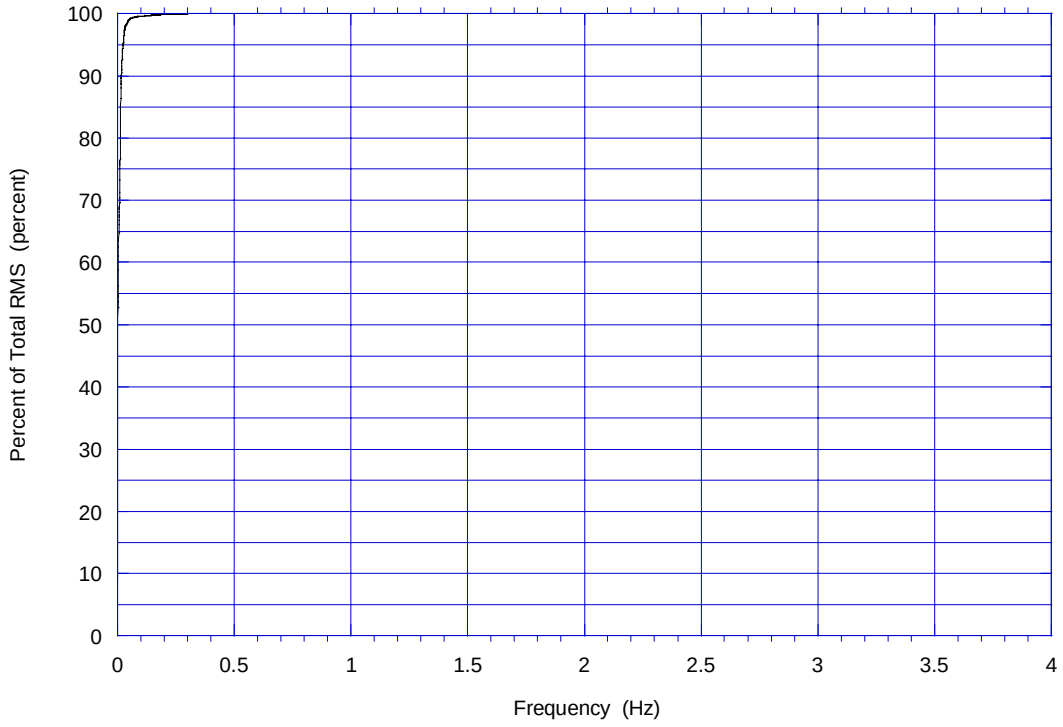

FIGURE 112. PERCENT OF TOTAL BANK ANGLE RMS VS FREQUENCY, FLIGHT SEQUENCE 62, IN FLIGHT

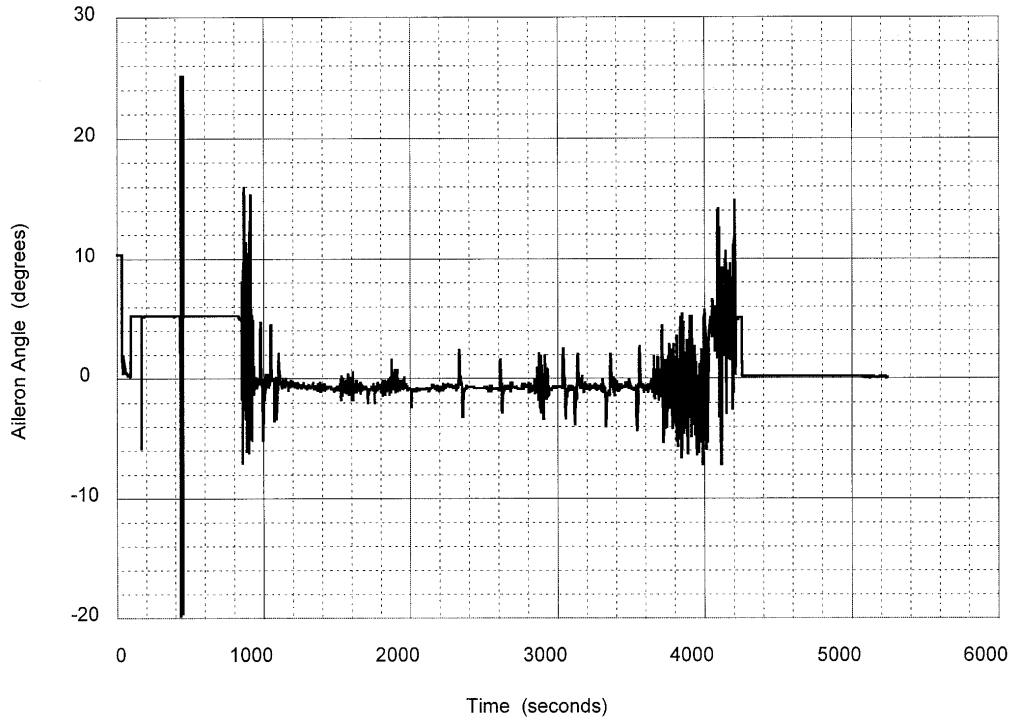

FIGURE 113. AILERON ANGLE TIME HISTORY, FLIGHT SEQUENCE 62

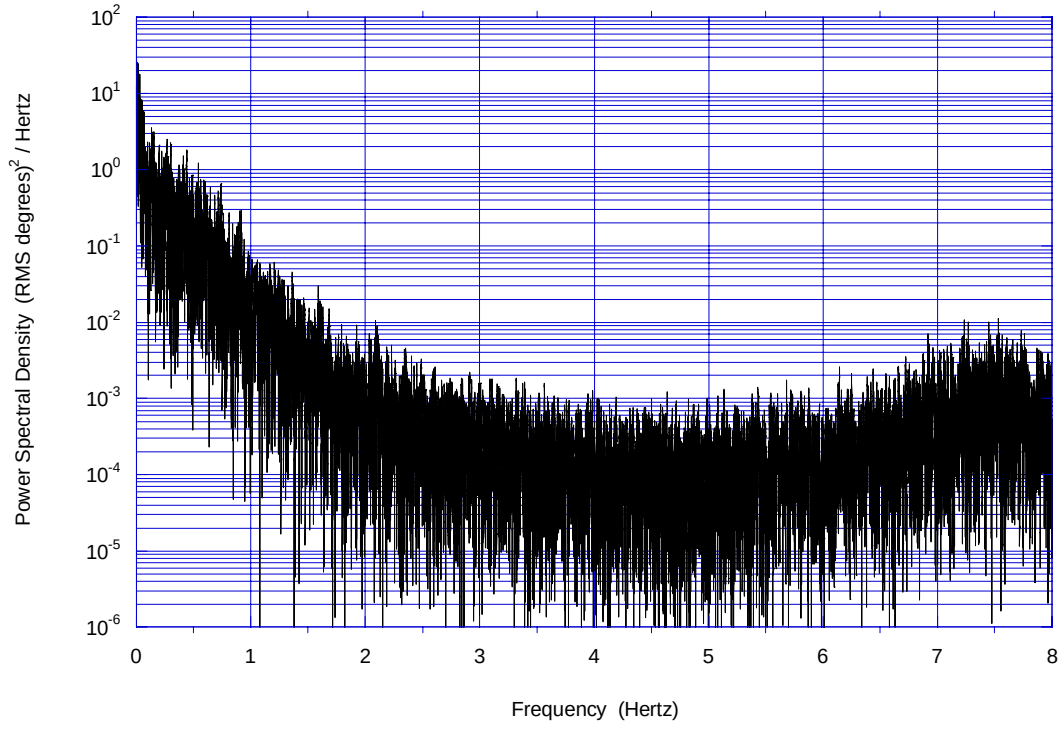

FIGURE 114. NORMALIZED PSD OF AILERON ANGLE, FLIGHT SEQUENCE 62, IN FLIGHT

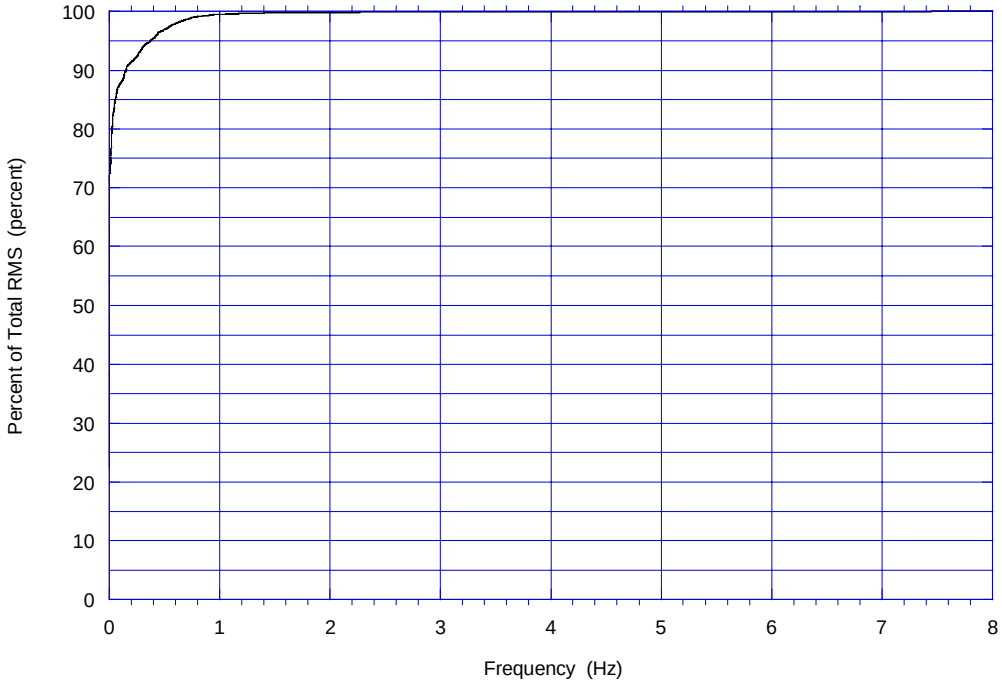

FIGURE 115. PERCENT OF AILERON ANGLE RMS VS FREQUENCY, FLIGHT SEQUENCE 62, IN FLIGHT

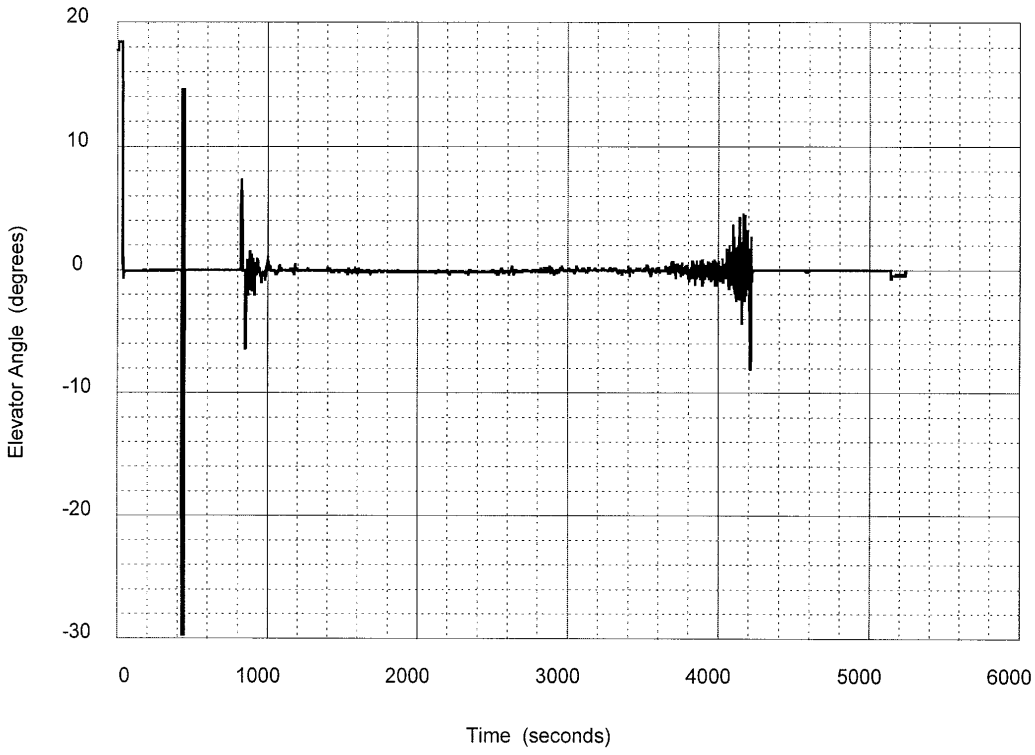

FIGURE 116. ELEVATOR ANGLE TIME HISTORY, FLIGHT SEQUENCE 62

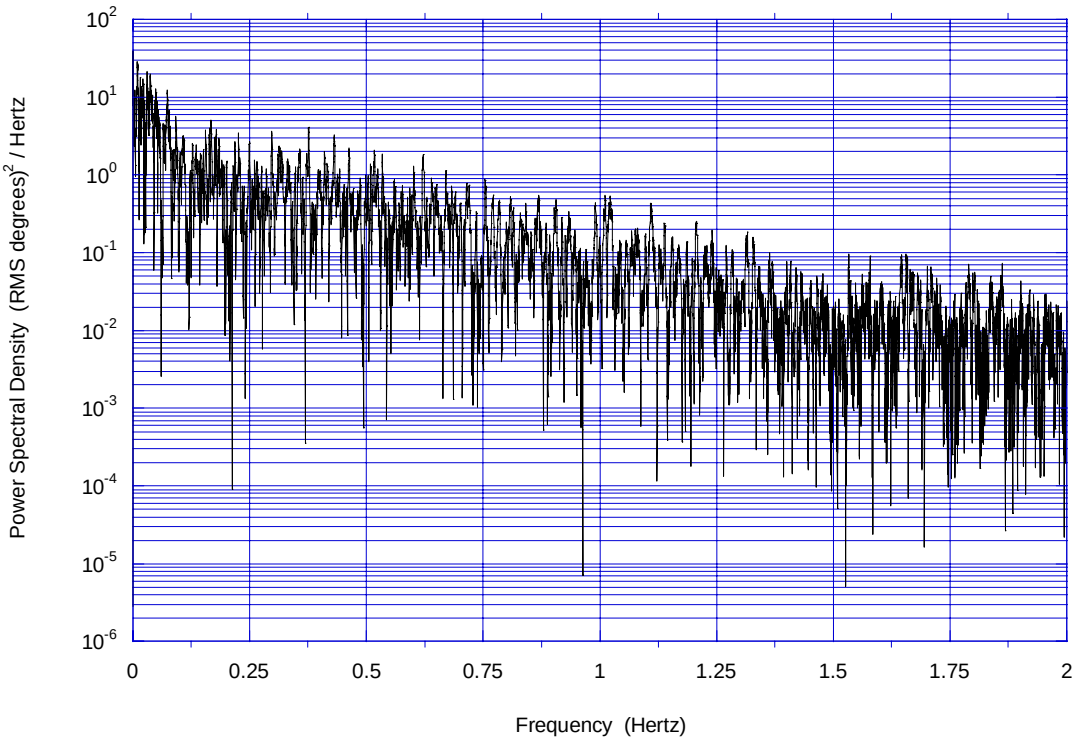

FIGURE 117. NORMALIZED PSD OF ELEVATOR ANGLE, FLIGHT SEQUENCE 62, IN FLIGHT

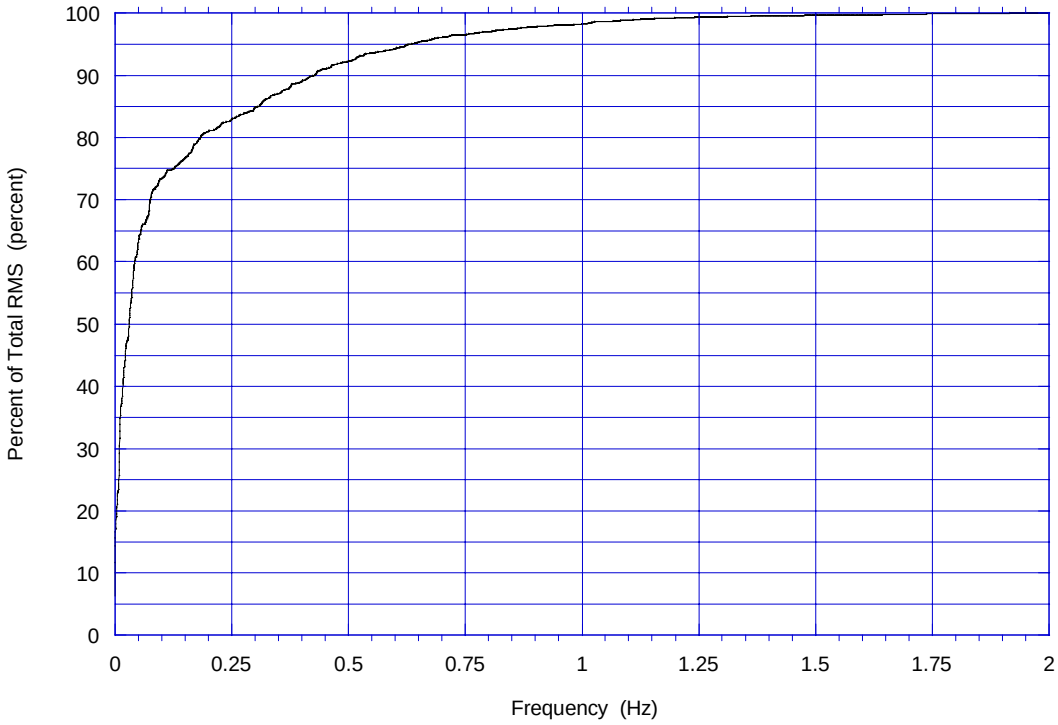

FIGURE 118. PERCENT OF ELEVATOR ANGLE RMS VS FREQUENCY, FLIGHT SEQUENCE 62, IN FLIGHT

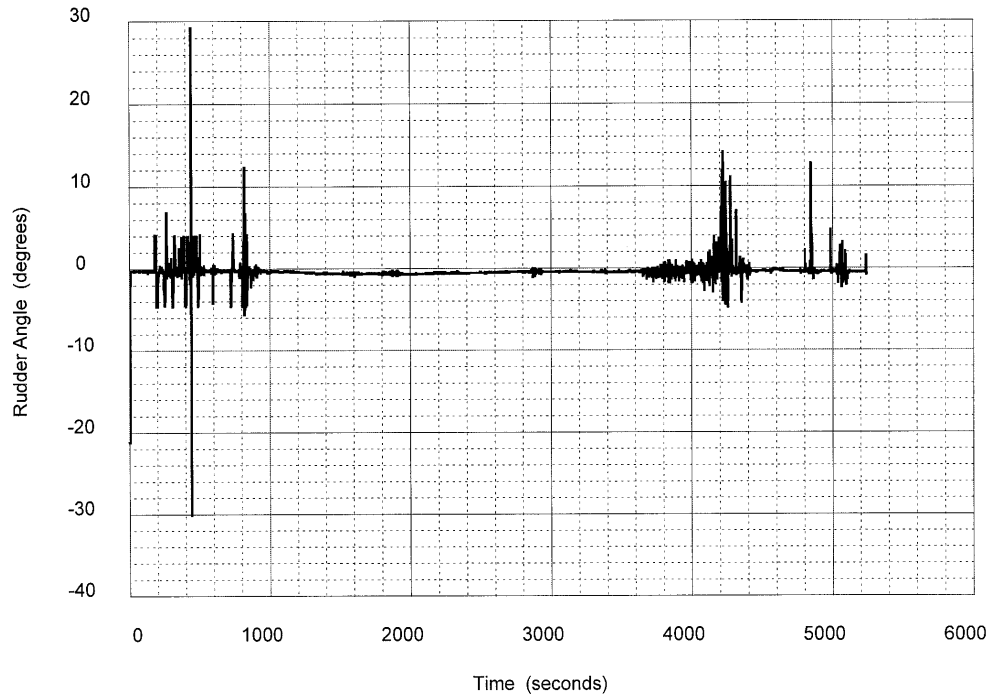

FIGURE 119. RUDDER ANGLE TIME HISTORY, FLIGHT SEQUENCE 62

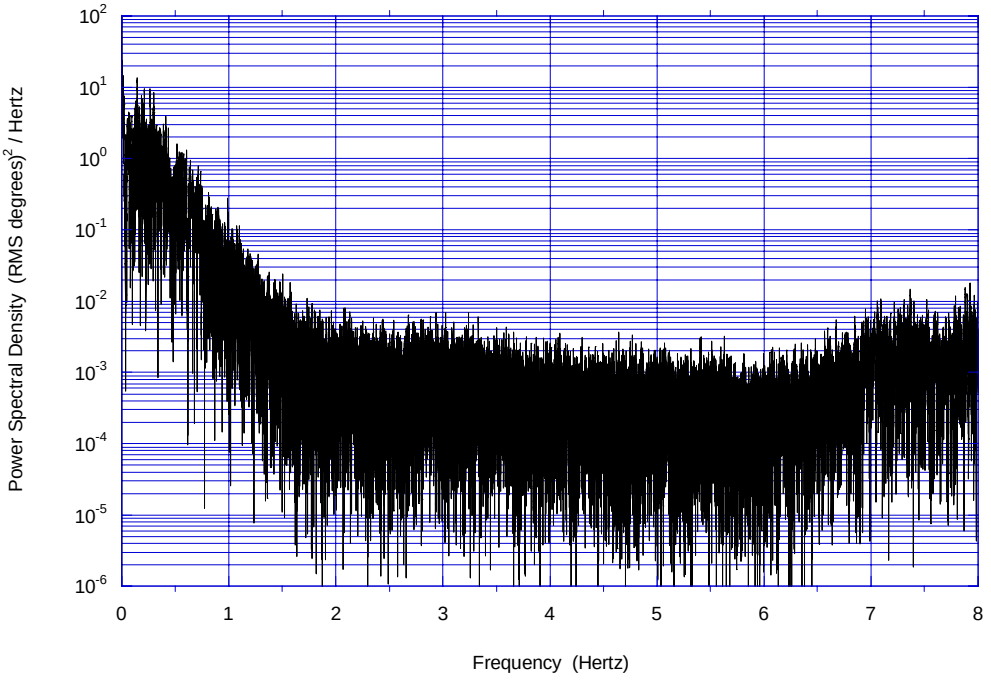

FIGURE 120. NORMALIZED PSD OF RUDDER ANGLE, FLIGHT SEQUENCE 62, IN FLIGHT

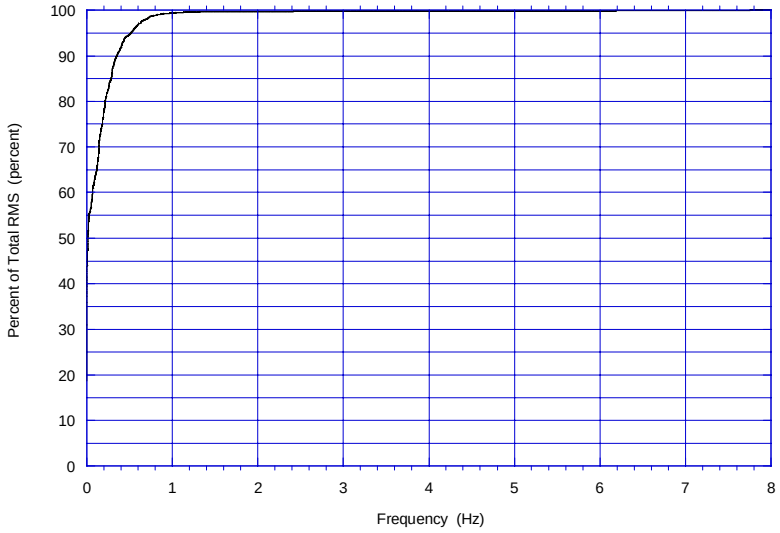

FIGURE 121. PERCENT OF RUDDER ANGLE RMS VS FREQUENCY, FLIGHT SEQUENCE 62, IN FLIGHT

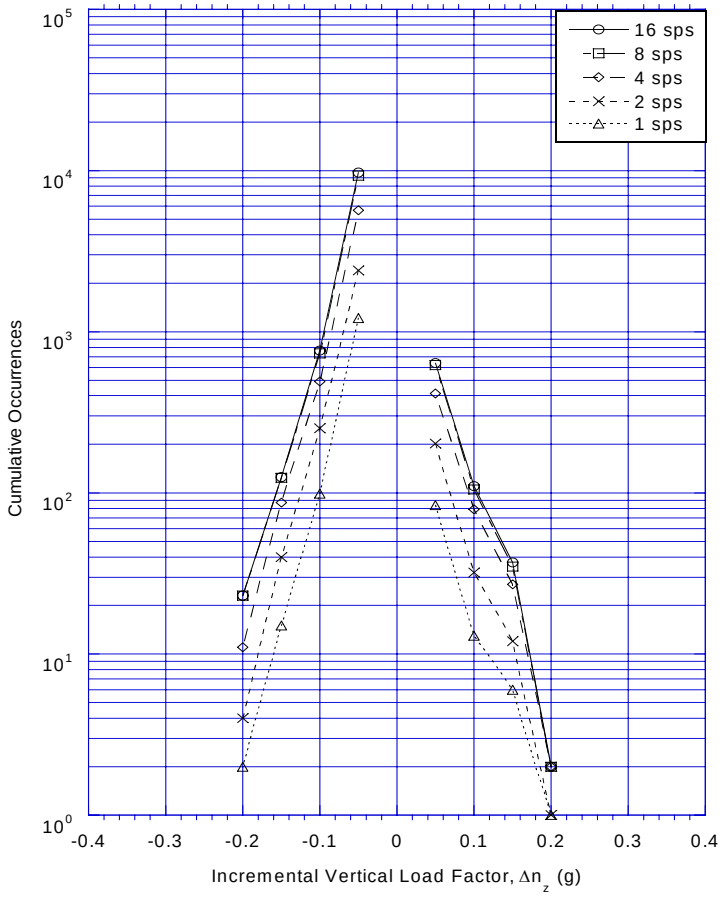

FIGURE 122. CUMULATIVE OCCURRENCES OF INCREMENTAL VERTICAL LOAD FACTOR, PREFLIGHT

Vertical Load Factor n_z	16 Samples per Second		8 Samples per Second		4 Samples per Second		2 Samples per Second		1 Sample per Second	
	Cumulative Occurrences	Percent of 16 sps Cumulative Occurrences	Cumulative Occurrences	Percent of 16 sps Cumulative Occurrences	Cumulative Occurrences	Percent of 16 sps Cumulative Occurrences	Cumulative Occurrences	Percent of 16 sps Cumulative Occurrences	Cumulative Occurrences	Percent of 16 sps Cumulative Occurrences
0.2	2	100	2	100	2	100	1	50	1	50
0.15	37	100	35	94.59	27	72.97	12	32.43	6	16.22
0.1	110	100	105	95.45	79	71.82	32	29.09	13	11.82
0.05	639	100	620	97.03	415	64.95	203	31.77	84	13.15
-0.05	9713	100	9334	96.1	5663	58.3	2395	24.66	1218	12.54
-0.1	767	100	735	95.83	492	64.15	252	32.86	99	12.91
-0.15	125	100	124	99.2	87	69.6	40	32	15	12
-0.2	23	100	23	100	11	47.83	4	17.39	2	8.696

sps = samples per second

FIGURE 123. EFFECT OF SAMPLING RATE ON CUMULATIVE OCCURRENCES OF INCREMENTAL VERTICAL LOAD FACTOR, PREFLIGHT

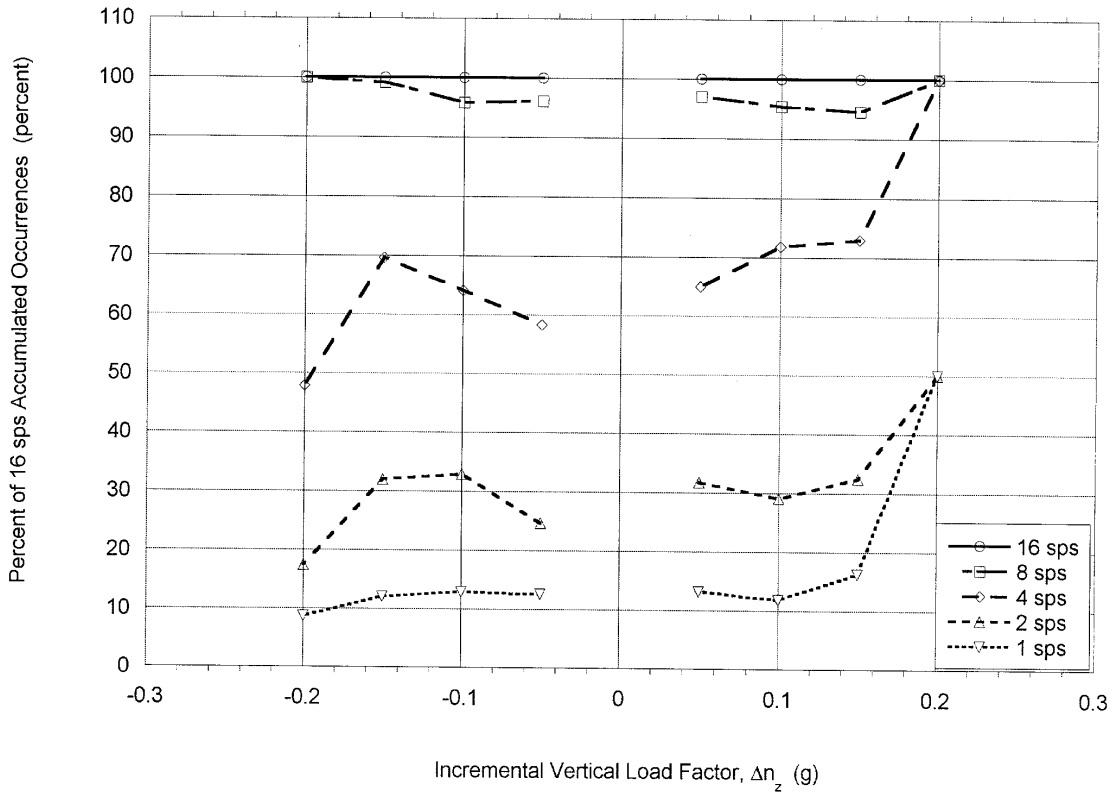

FIGURE 124. PERCENT OF INCREMENTAL VERTICAL ACCELERATION PEAK COUNTS AS A FUNCTION OF SAMPLING RATE, PREFLIGHT

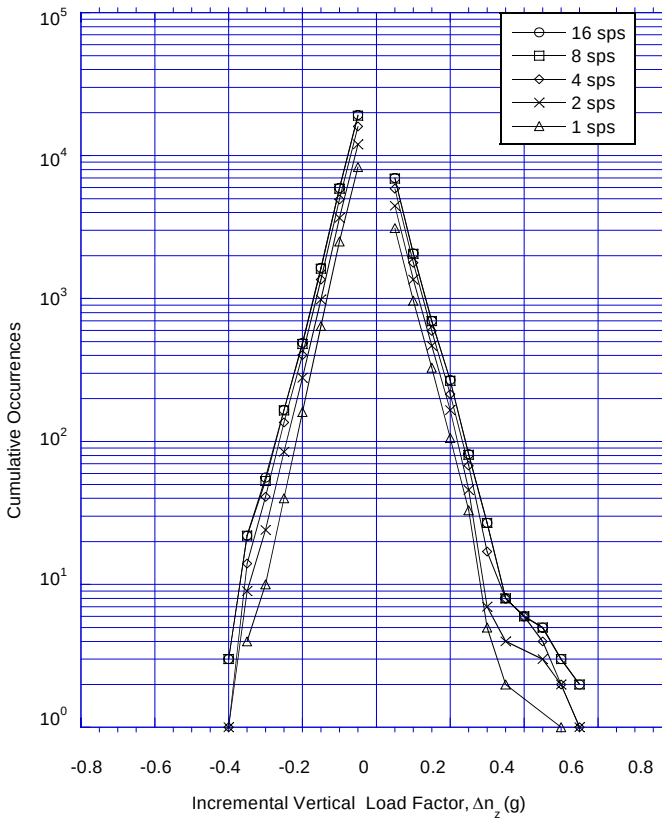

FIGURE 125. CUMULATIVE OCCURRENCES OF INCREMENTAL VERTICAL LOAD FACTOR, IN FLIGHT

Vertical Load Factor n_z	16 Samples per Second		8 Samples per Second		4 Samples per Second		2 Samples per Second		1 Sample per Second	
	Cumulative Occurrences	Percent of 16 sps Cumulative Occurrences	Cumulative Occurrences	Percent of 16 sps Cumulative Occurrences	Cumulative Occurrences	Percent of 16 sps Cumulative Occurrences	Cumulative Occurrences	Percent of 16 sps Cumulative Occurrences	Cumulative Occurrences	Percent of 16 sps Cumulative Occurrences
0.55	2	100	2	100	1	50	1	50		
0.5	3	100	3	100	2	66.67	2	66.67	1	33.33
0.45	5	100	5	100	4	80	3	60	1	20
0.4	6	100	6	100	6	100	3	50	1	16.67
0.35	8	100	8	100	8	100	4	50	2	25
0.3	27	100	27	100	17	62.96	7	25.93	5	18.52
0.25	82	100	81	98.78	68	82.93	46	56.1	33	40.24
0.2	269	100	266	98.88	215	79.93	166	61.71	106	39.41
0.15	702	100	697	99.29	597	85.04	469	66.81	329	46.87
0.1	2072	100	2054	99.13	1787	86.25	1358	65.54	966	46.62
0.05	7000	100	6898	98.54	5877	83.96	4468	63.83	3122	44.6
-0.05	19327	100	19058	98.61	16048	83.03	11980	61.99	8345	43.18
-0.1	5961	100	5878	98.61	4939	82.86	3658	61.37	2517	42.22
-0.15	1639	100	1617	98.66	1365	83.28	988	60.28	644	39.29
-0.2	490	100	483	98.57	402	82.04	279	56.94	161	32.86
-0.25	167	100	165	98.8	136	81.44	85	50.9	40	23.95
-0.3	56	100	53	94.64	41	73.21	24	42.86	10	17.86
-0.35	22	100	22	100	14	63.64	9	40.91	4	18
-0.4	3	100	3	100	1	33.33	1	33.33		

FIGURE 126. EFFECT OF SAMPLING RATE ON CUMULATIVE OCCURRENCES OF INCREMENTAL VERTICAL LOAD FACTOR, IN FLIGHT

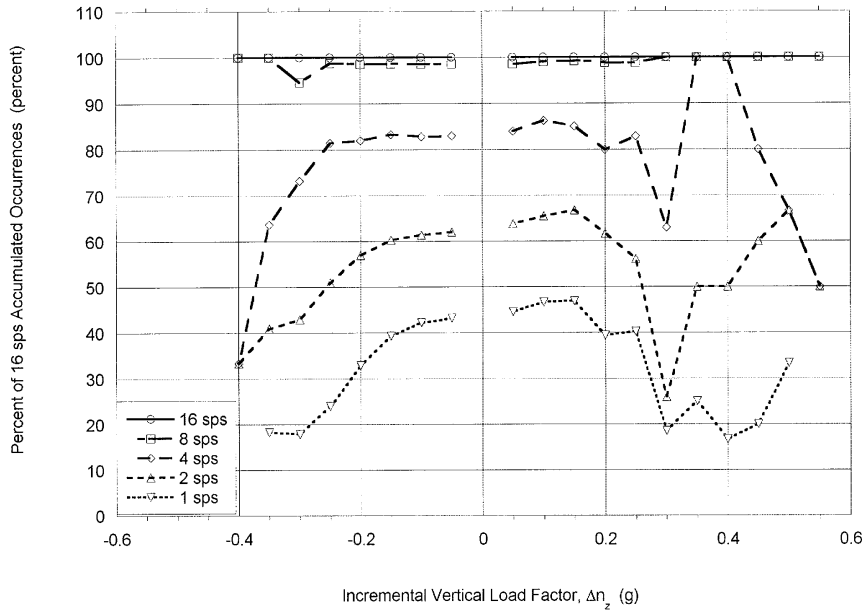

FIGURE 127. PERCENT OF INCREMENTAL VERTICAL ACCELERATION PEAK COUNTS AS A FUNCTION OF SAMPLING RATE, IN FLIGHT

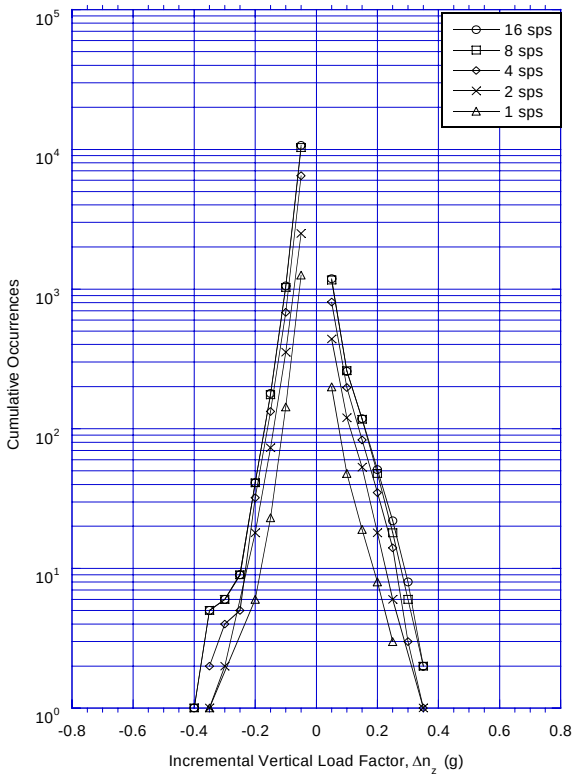

FIGURE 128. CUMULATIVE OCCURRENCES OF INCREMENTAL VERTICAL LOAD FACTOR, POSTFLIGHT

Vertical Load Factor n_z	16 Samples per Second		8 Samples per Second		4 Samples per Second		2 Samples per Second		1 Sample per Second	
	Cumulative Occurrences	Percent of 16 sps Cumulative Occurrences	Cumulative Occurrences	Percent of 16 sps Cumulative Occurrences	Cumulative Occurrences	Percent of 16 sps Cumulative Occurrences	Cumulative Occurrences	Percent of 16 sps Cumulative Occurrences	Cumulative Occurrences	Percent of 16 sps Cumulative Occurrences
0.35	2	100	2	100	1	50	1	50		
0.3	8	100	6	75	3	37.5	1	12.5		
0.25	22	100	18	81.82	14	63.64	6	27.27	3	13.64
0.2	51	100	48	94.12	35	68.63	18	35.29	8	15.69
0.15	118	100	117	99.15	83	70.34	53	44.92	19	16.1
0.1	258	100	260	100.8	197	76.36	120	46.51	48	18.6
0.05	1183	100	118	97.89	809	68.39	440	37.19	199	16.82
-0.05	10717	100	10335	96.44	6494	60.6	2506	23.38	1260	11.76
-0.1	1054	100	1028	97.53	682	64.71	352	33.4	143	13.57
-0.15	179	100	175	97.77	133	74.3	73	40.78	23	12.85
-0.2	41	100	41	100	32	78.05	18	43.9	6	14.63
-0.25	9	100	9	100	5	55.56	2	22.22	1	11.11
-0.3	6	100	6	100	4	66.67	2	33.33	1	16.67
-0.35	5	100	5	100	2	40	1	20	1	20
-0.4	1	100	1	100						

FIGURE 129. EFFECT OF SAMPLING RATE ON CUMULATIVE OCCURRENCES OF INCREMENTAL VERTICAL LOAD FACTOR, POSTFLIGHT

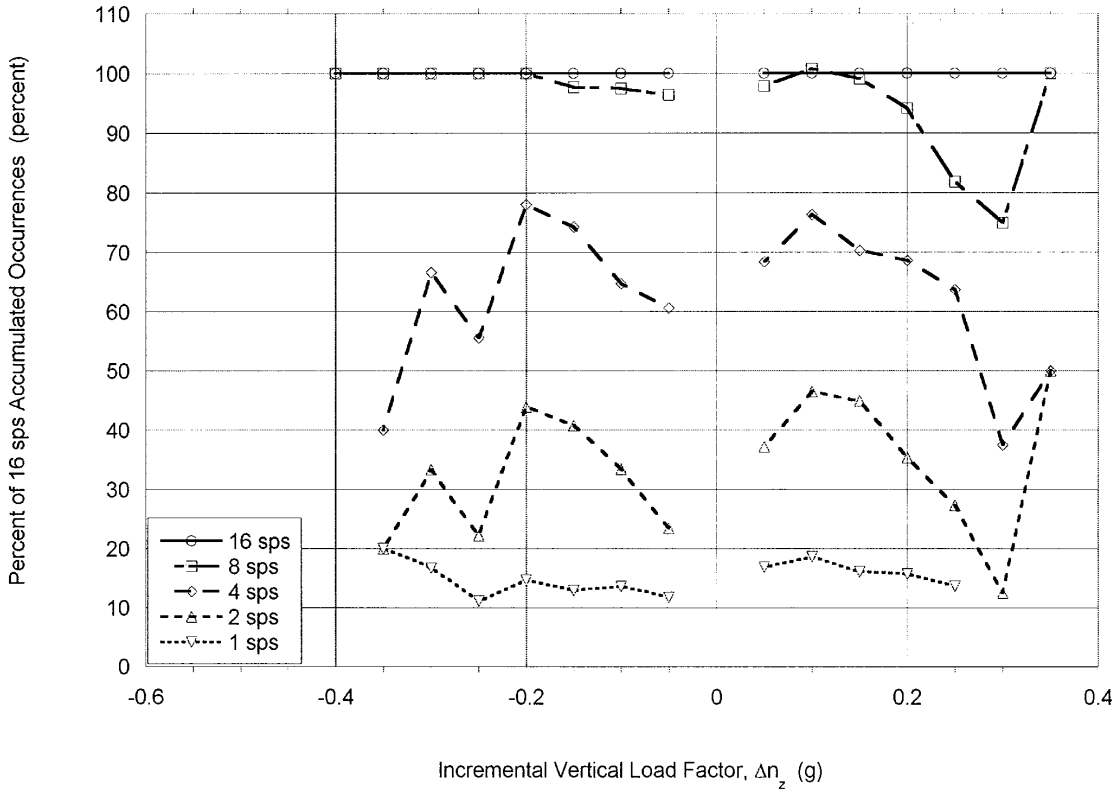

FIGURE 130. PERCENT OF INCREMENTAL VERTICAL ACCELERATION PEAK COUNTS AS A FUNCTION OF SAMPLING RATE, POSTFLIGHT

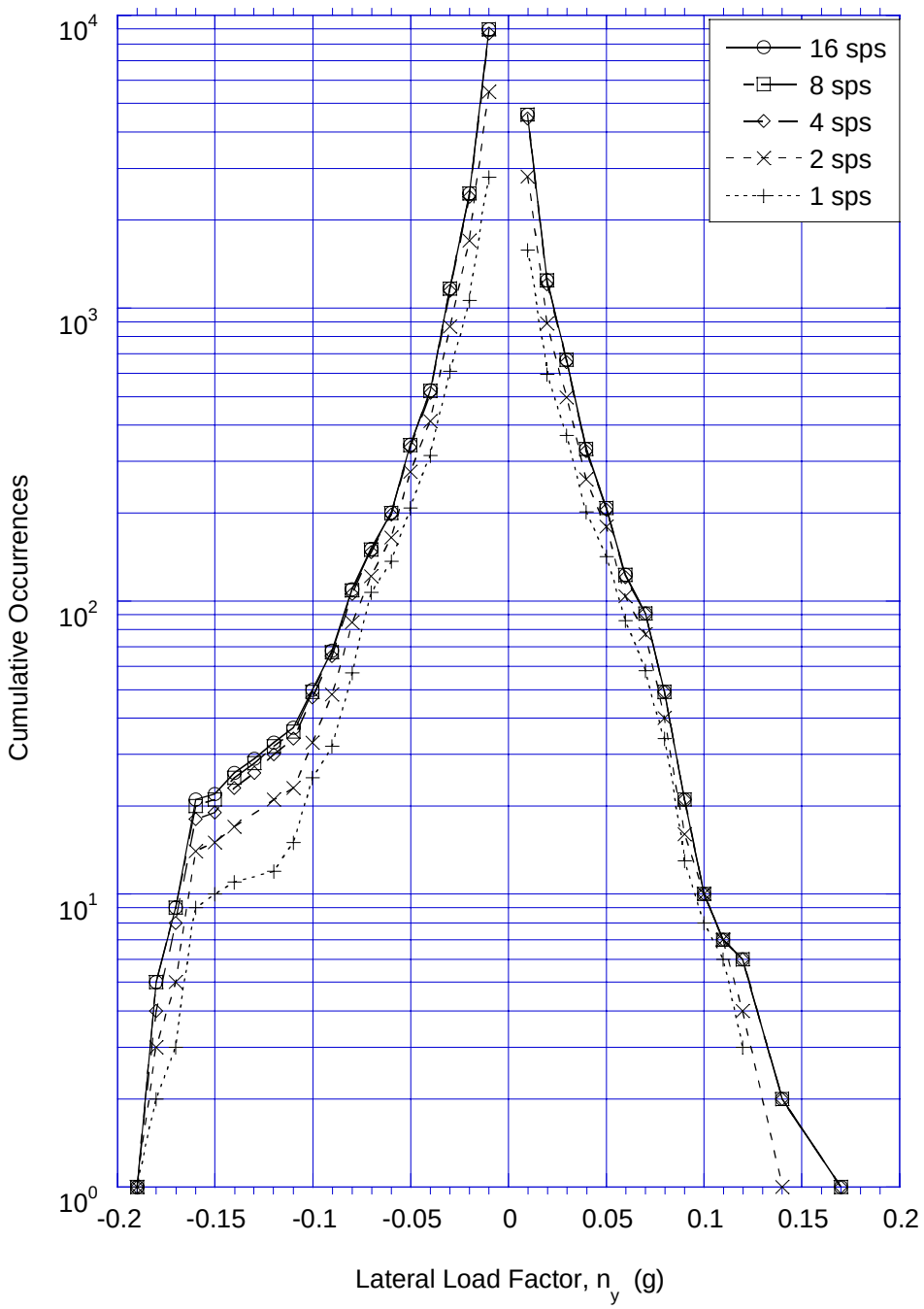

FIGURE 131. CUMULATIVE OCCURRENCES OF LATERAL LOAD FACTOR, PREFLIGHT

Lateral Load Factor n_y	16 Samples per Second		8 Samples per Second		4 Samples per Second		2 Samples per Second		1 Sample per Second	
	Cumulative Occurrences	Percent of 16 sps Cumulative Occurrences	Cumulative Occurrences	Percent of 16 sps Cumulative Occurrences	Cumulative Occurrences	Percent of 16 sps Cumulative Occurrences	Cumulative Occurrences	Percent of 16 sps Cumulative Occurrences	Cumulative Occurrences	Percent of 16 sps Cumulative Occurrences
0.17	1	100	1	100	1	100				
0.16	1	100	1	100	1	100				
0.15	1	100	1	100	1	100				
0.14	2	100	2	100	2	100	1	50		
0.13	2	100	2	100	2	100	1	50		
0.12	6	100	6	100	6	100	4	66.67	3	50
0.11	7	100	7	100	7	100	7	100	6	85.71
0.1	10	100	10	100	10	100	10	100	8	80
0.09	21	100	21	100	21	100	16	76.19	13	61.9
0.08	49	100	49	100	49	100	40	81.63	34	69.39
0.07	91	100	91	100	91	100	77	84.62	58	63.74
0.06	123	100	123	100	121	98.37	104	84.55	86	69.92
0.05	208	100	208	100	205	98.56	180	86.54	142	68.27
0.04	331	100	331	100	326	98.49	261	78.85	202	61.03
0.03	667	100	667	100	656	98.35	497	74.51	369	55.32
0.02	1244	100	1244	100	1210	97.27	889	71.46	595	47.83
0.01	4577	100	4576	99.98	4436	96.92	2811	61.42	1583	34.59
-0.01	8963	100	8961	99.98	8663	96.65	5497	61.33	2805	31.3
-0.02	2467	100	2465	99.92	2409	97.65	1694	68.79	1063	43.09
-0.03	1168	100	1167	99.91	1149	98.37	865	74.06	609	52.14
-0.04	524	100	523	99.81	514	98.09	412	78.63	314	59.92
-0.05	342	100	341	99.71	336	98.25	277	80.99	208	60.82
-0.06	201	100	200	99.5	197	98.01	165	82.09	137	68.16
-0.07	151	100	150	99.34	147	97.35	122	80.79	107	70.86
-0.08	110	100	109	99.09	106	96.36	85	77.27	57	51.82
-0.09	68	100	67	98.53	65	95.59	48	70.59	32	47.06
-0.1	50	100	49	98	47	94	33	66	25	50
-0.11	37	100	36	97.3	34	91.89	23	62.16	15	40.54
-0.12	33	100	32	96.97	30	90.91	21	63.64	12	36.36
-0.13	29	100	28	96.55	26	89.66				
-0.14	26	100	25	96.15	23	88.46	17	65.38	11	42.31
-0.15	22	100	21	95.45	19	86.36	15	68.18	10	45.45
-0.16	21	100	20	95.24	18	85.71	14	66.67	9	42.86
-0.17	9	100	9	100	8	88.89	5	55.56	3	33.33
-0.18	5	100	5	100	4	80	3	60	2	40
-0.19	1	100	1	100	1	100	1	100	1	100

FIGURE 132. EFFECT OF SAMPLING RATE ON CUMULATIVE OCCURRENCES OF LATERAL LOAD FACTOR, PREFLIGHT

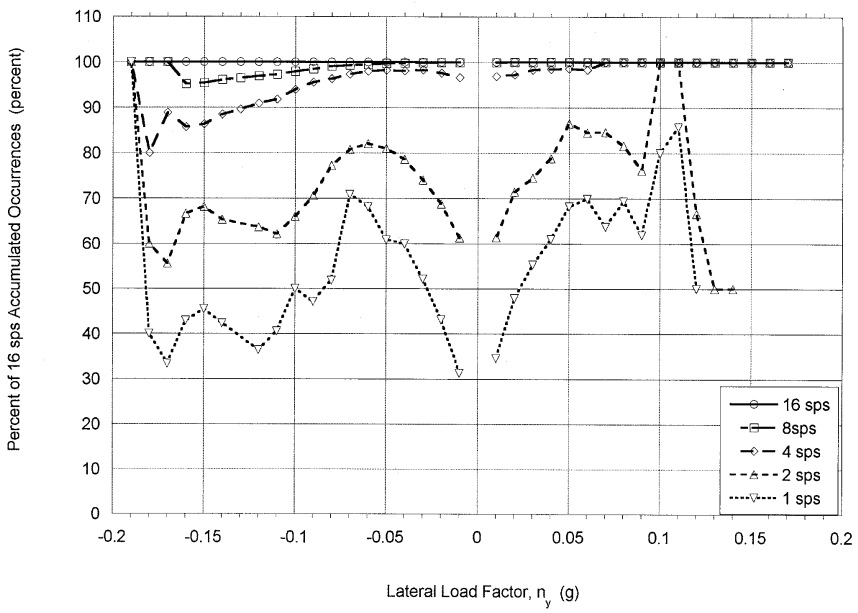

FIGURE 133. PERCENT OF LATERAL LOAD FACTOR PEAK COUNTS AS A FUNCTION OF SAMPLING RATE, PREFLIGHT

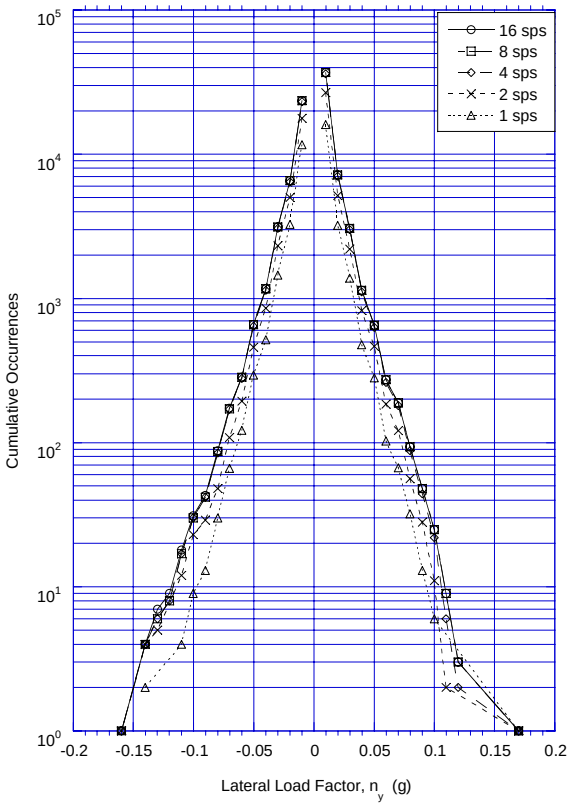

FIGURE 134. CUMULATIVE OCCURRENCES OF LATERAL LOAD FACTOR, IN FLIGHT

Lateral Load Factor n_y	16 Samples per Second		8 Samples per Second		4 Samples per Second		2 Samples per Second		1 Sample per Second	
	Cumulative Occurrences	Percent of 16 sps Cumulative Occurrences	Cumulative Occurrences	Percent of 16 sps Cumulative Occurrences	Cumulative Occurrences	Percent of 16 sps Cumulative Occurrences	Cumulative Occurrences	Percent of 16 sps Cumulative Occurrences	Cumulative Occurrences	Percent of 16 sps Cumulative Occurrences
0.17	1	100	1	100	1	100	1	100	1	100
0.16	1	100	1	100	1	100	1	100	1	100
0.14	1	100	1	100	1	100	1	100	1	100
0.13	1	100	1	100	1	100	1	100	1	100
0.12	3	100	3	100	2	66.67	1	33.33	1	33.33
0.11	9	100	9	100	6	66.67	2	22.22	1	11.11
0.1	25	100	25	100	22	88	11	44	6	24
0.09	48	100	48	100	44	91.67	28	58.33	13	27.08
0.08	94	100	94	100	88	93.62	56	59.57	32	34.04
0.07	188	100	188	100	181	96.28	121	64.36	67	35.64
0.06	273	100	273	100	261	95.6	185	67.77	103	37.73
0.05	649	100	649	100	631	97.23	466	71.8	282	43.45
0.04	1138	100	1138	100	1113	97.8	823	72.32	478	42
0.03	3067	100	3066	99.97	3003	97.91	2205	71.89	1382	45.06
0.02	7211	100	7206	99.93	7046	97.71	5173	71.74	3219	44.64
0.01	36810	100	36805	99.99	36047	97.93	26718	72.58	16074	43.87
-0.01	23608	100	23607	100	23142	98.03	17742	75.15	11667	49.42
-0.02	6559	100	6558	99.98	6434	98.09	4997	76.19	3273	49.9
-0.03	3126	100	3125	99.97	3067	98.11	2318	74.15	1455	46.55
-0.04	1166	100	1165	99.91	1142	97.94	856	73.41	518	44.43
-0.05	658	100	657	99.85	639	97.11	459	69.76	294	44.68
-0.06	285	100	284	99.65	278	97.54	194	68.07	122	42.81
-0.07	173	100	172	99.42	170	98.27	108	62.43	66	38.15
-0.08	88	100	87	98.86	85	96.59	48	54.55	30	34.09
-0.09	43	100	42	97.67	42	97.67	29	67.44	13	30.23
-0.1	31	100	30	96.77	30	96.77	23	74.19	9	29.03
-0.11	18	100	17	94.44	17	94.44	12	66.67	4	22.22
-0.12	9	100	8	88.89	8	88.89	5	55.56	2	22.22
-0.13	7	100	6	85.71	6	85.71	5	71.43	2	28.57
-0.14	4	100	4	100	4	100	4	100	2	50
-0.15	1	100	1	100	1	100	1	100		
-0.16	1	100	1	100	1	100	1	100		

FIGURE 135. EFFECT OF SAMPLING RATE ON CUMULATIVE OCCURRENCES OF LATERAL LOAD FACTOR, IN FLIGHT

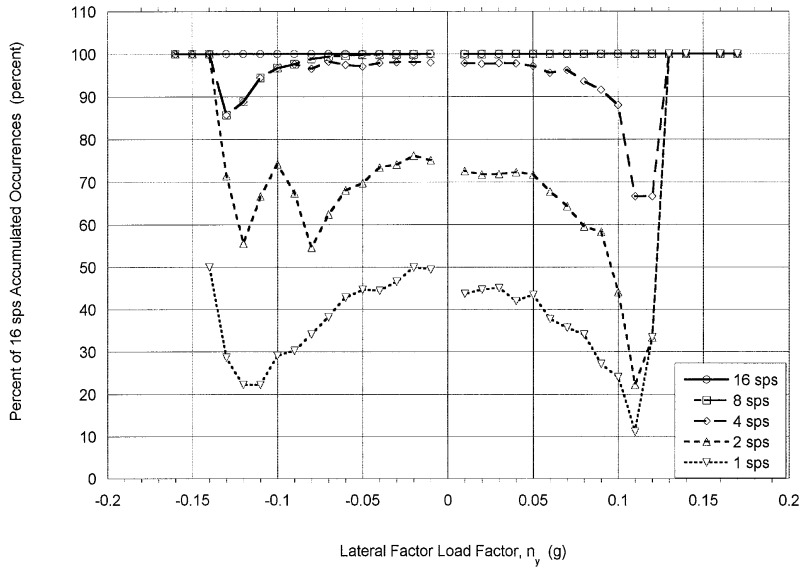

FIGURE 136. PERCENT OF LATERAL LOAD FACTOR PEAK COUNTS AS A FUNCTION OF SAMPLING RATE, IN FLIGHT

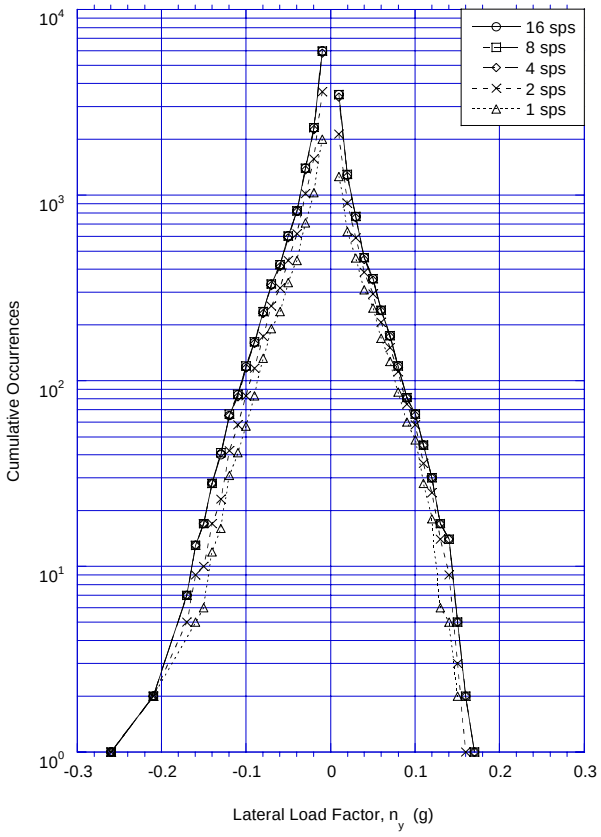

FIGURE 137. CUMULATIVE OCCURRENCES OF LATERAL LOAD FACTOR, POSTFLIGHT

Lateral Load Factor n_y	16 Samples per Second		8 Samples per Second		4 Samples per Second		2 Samples per Second		1 Sample per Second	
	Cumulative Occurrences	Percent of 16 sps Cumulative Occurrences	Cumulative Occurrences	Percent of 16 sps Cumulative Occurrences	Cumulative Occurrences	Percent of 16 sps Cumulative Occurrences	Cumulative Occurrences	Percent of 16 sps Cumulative Occurrences	Cumulative Occurrences	Percent of 16 sps Cumulative Occurrences
0.17	1	100	1	100	1	100				
0.16	2	100	2	100	2	100	1	50		
0.15	5	100	5	100	5	100	3	60	2	40
0.14	14	100	14	100	14	100	9	64.29	5	35.71
0.13	17	100	17	100	17	100	14	82.35	6	35.29
0.12	30	100	30	100	30	100	25	83.33	18	60
0.11	45	100	45	100	45	100	36	80	28	62.22
0.1	66	100	66	100	65	98.48	58	87.88	48	72.73
0.09	81	100	81	100	81	100	75	92.59	60	74.07
0.08	120	100	120	100	119	99.17	112	93.33	87	72.5
0.07	175	100	175	100	173	98.86	151	86.29	127	72.57
0.06	240	100	240	100	238	99.17	207	86.25	169	70.42
0.05	355	100	355	100	349	98.31	294	82.82	247	69.58
0.04	461	100	461	100	450	97. 61	384	83.3	309	67.03
0.03	768	100	769	100.13	756	98.44	589	76.69	459	59.77
0.02	1289	100	1292	100.23	1263	97.98	905	70.21	636	49.34
0.01	3476	100	3480	100.12	3374	97.07	2132	61.33	1261	36.28
-0.01	5988	100	5989	100.02	5807	96.98	3606	60.22	2000	33.4
-0.02	2305	100	2306	100.04	2256	97.87	1569	68.07	1032	44.77
-0.03	1395	100	1396	100.07	1370	98.21	1018	72.97	708	50.75
-0.04	824	100	825	100.12	815	98.91	620	75.24	445	54
-0.05	601	100	602	100.17	590	98.17	445	74.04	339	56.41
-0.06	422	100	423	100.24	412	97.63	316	74.88	236	55.92
-0.07	331	100	332	100.3	325	98.19	253	76.44	191	57.7
-0.08	235	100	236	100.43	230	97.87	174	74.04	132	56.17
-0.09	161	100	162	100.62	159	98.76	117	72.67	83	51.55
-0.1	119	100	120	100.84	117	98.32	83	69.75	57	47.9
-0.11	84	100	85	101.19	82	97.62	58	69.05	41	48.81
-0.12	65	100	66	101.54	65	100	42	64.62	31	47.69
-0.13	40	100	41	102.5	41	102.5	23	57.5	16	40
-0.14	28	100	28	100	28	100	17	60.71	12	42.86
-0.15	17	100	17	100	17	100	10	58.82	6	35.29
-0.16	13	100	13	100	13	100	9	69.23	5	38.46
-0.17	7	100	7	100	7	100	5	71.43	2	28.57
-0.18	2	100	2	100	2	100	2	100	2	100
-0.19	2	100	2	100	2	100	2	100	2	100
-0.2	2	100	2	100	2	100	2	100	2	100
-0.21	2	100	2	100	2	100	2	100	2	100
-0.22	1	100	1	100	1	100	1	100	1	100
-0.23	1	100	1	100	1	100	1	100	1	100
-0.24	1	100	1	100	1	100	1	100	1	100
-0.25	1	100	1	100	1	100	1	100	1	100
-0.26	1	100	1	100	1	100	1	100	1	100

FIGURE 138. EFFECT OF SAMPLING RATE ON CUMULATIVE OCCURRENCES OF LATERAL LOAD FACTOR, POSTFLIGHT

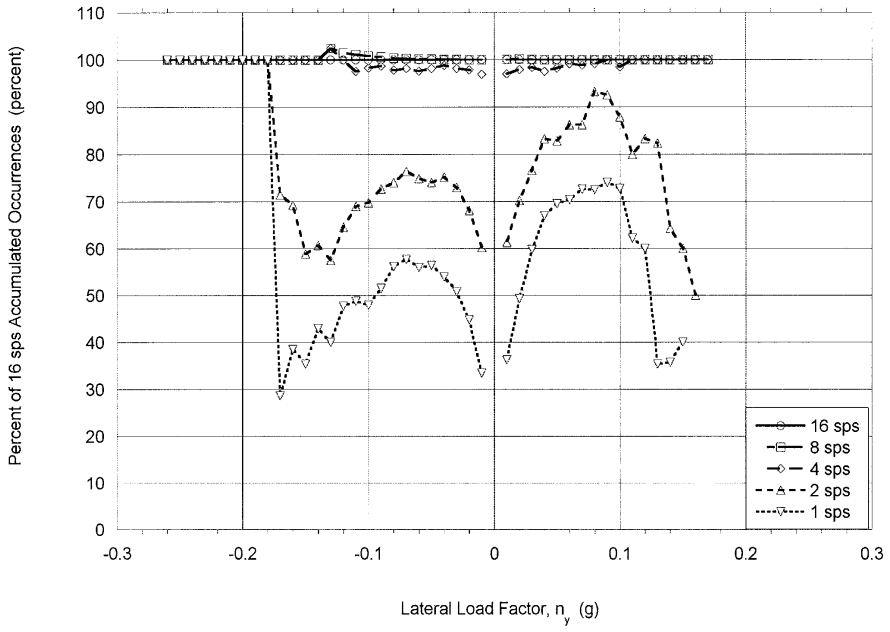

FIGURE 139. PERCENT OF LATERAL LOAD FACTOR PEAK COUNTS AS A FUNCTION OF SAMPLING RATE, POSTFLIGHT

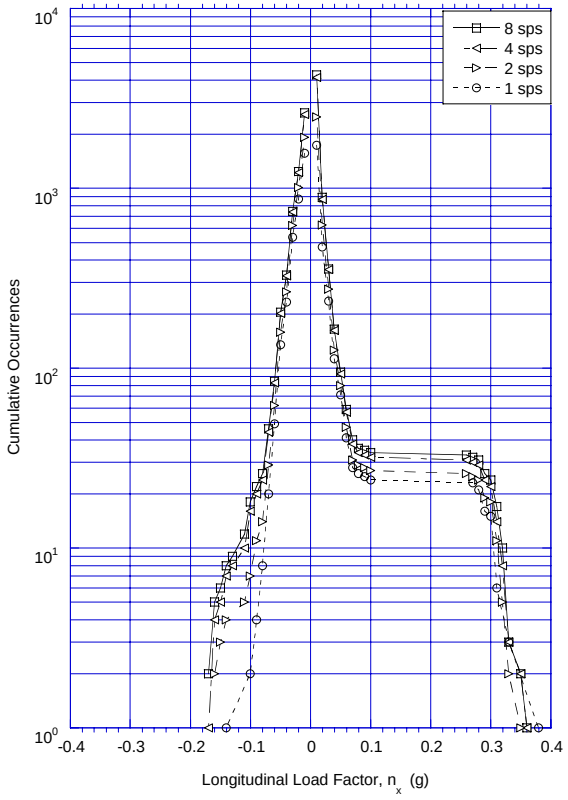

FIGURE 140. CUMULATIVE OCCURRENCES OF LONGITUDINAL LOAD FACTOR, PREFLIGHT

Longitudinal Load Factor n_x	8 Samples per Second		4 Samples per Second		2 Samples per Second		1 Sample per Second	
	Cumulative Occurrences	Percent of 8 sps Cumulative Occurrences	Cumulative Occurrences	Percent of 8 sps Cumulative Occurrences	Cumulative Occurrences	Percent of 8 sps Cumulative Occurrences	Cumulative Occurrences	Percent of 8 sps Cumulative Occurrences
0.38							1	
0.36	1	100	1	100			1	100
0.35	2	100	2	100	1	50	1	50
0.34	2	100	2	100	1	50	1	50
0.33	3	100	3	100	2	66.67	3	100
0.32	10	100	8	80	5	50	3	30
0.31	17	100	14	82.35	11	64.71	6	35.29
0.3	24	100	22	91.67	18	75	15	62.5
0.29	26	100	24	92.31	19	73.08	16	61.54
0.28	31	100	29	93.55	24	77.42	21	67.74
0.27	32	100	30	93.75	25	78.12	23	71.87
0.26	33	100	31	93.94	26	78.79	23	69.7
0.25	33	100	31	93.94	26	78.79	23	69.7
0.24	33	100	31	93.94	26	78.79	23	69.7
0.23	33	100	31	93.94	26	78.79	23	69.7
0.22	33	100	31	93.94	26	78.79	23	69.7
0.21	33	100	31	93.94	26	78.79	23	69.7
0.2	33	100	31	93.94	26	78.79	23	69.7
0.19	33	100	31	93.94	26	78.79	23	69.7
0.18	33	100	31	93.94	26	78.79	23	69.7
0.17	33	100	31	93.94	26	78.79	23	69.7
0.16	33	100	31	93.94	26	78.79	23	69.7
0.15	33	100	31	93.94	26	78.79	23	69.7
0.14	33	100	31	93.94	26	78.79	23	69.7
0.13	33	100	31	93.94	26	78.79	23	69.7
0.12	33	100	31	93.94	26	78.79	23	69.7
0.11	33	100	31	93.94	26	78.79	23	69.7
0.1	34	100	32	94.12	27	79.41	24	70.59
0.09	35	100	33	94.29	28	80	25	71.43
0.08	36	100	34	94.44	29	80.56	26	72.22
0.07	40	100	38	95	31	77.5	28	70
0.06	59	100	57	96.61	47	79.66	41	69.49
0.05	95	100	93	97.89	80	84.21	71	74.74
0.04	165	100	162	98.18	126	76.36	113	68.48
0.03	357	100	352	98.6	276	77.31	237	66.39
0.02	894	100	869	97.2	625	69.91	471	52.68
0.01	4272	100	4137	96.84	2500	58.52	1740	40.73
-0.01	2629	100	2579	98.1	1928	73.34	1571	59.76
-0.02	1241	100	1225	98.71	1009	81.31	874	70.43
-0.03	746	100	740	99.2	624	83.65	534	71.58
-0.04	330	100	327	99.09	267	80.91	233	70.61
-0.05	205	100	202	98.54	159	77.56	135	65.85
-0.06	85	100	83	97.65	62	72.94	49	57.65
-0.07	46	100	44	95.65	29	63.04	20	43.48
-0.08	26	100	24	92.31	14	53.85	8	30.77
-0.09	22	100	20	90.91	11	50	4	18.18
-0.1	18	100	16	88.89	7	38.89	2	11.11
-0.11	12	100	10	83.33	5	41.67	1	8.333
-0.13	9	100	8	88.89	4	44.44	1	11.11
-0.14	8	100	7	87.5	4	50	1	12.5
-0.15	6	100	5	83.33	3	50		
-0.16	5	100	4	80	2	40		
-0.17	2	100	1	50				

FIGURE 141. EFFECT OF SAMPLING RATE ON CUMULATIVE OCCURRENCES OF LONGITUDINAL LOAD FACTOR, PREFLIGHT

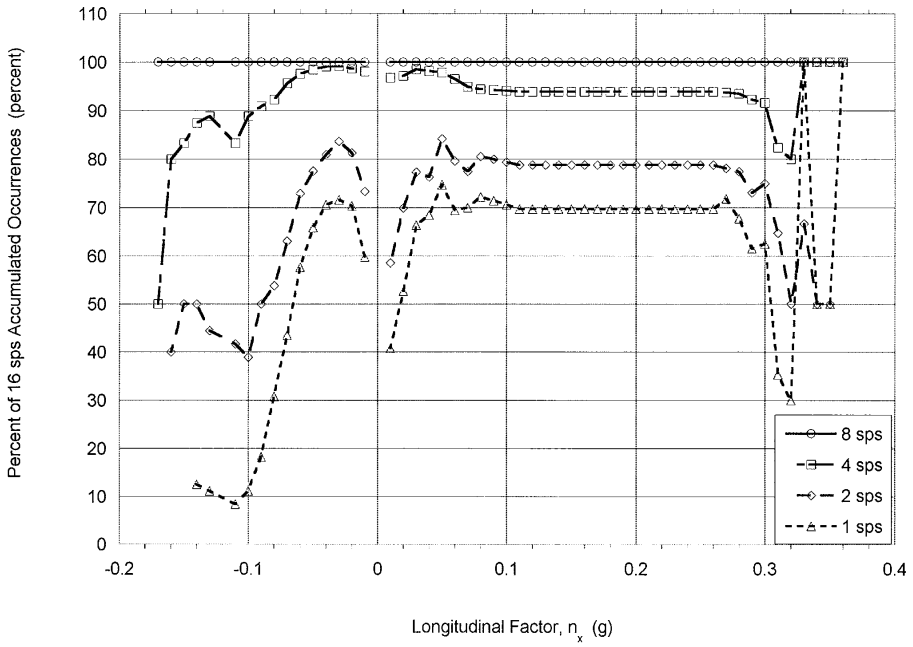

FIGURE 142. PERCENT OF LONGITUDINAL LOAD FACTOR PEAK COUNTS AS A FUNCTION OF SAMPLING RATE, PREFLIGHT

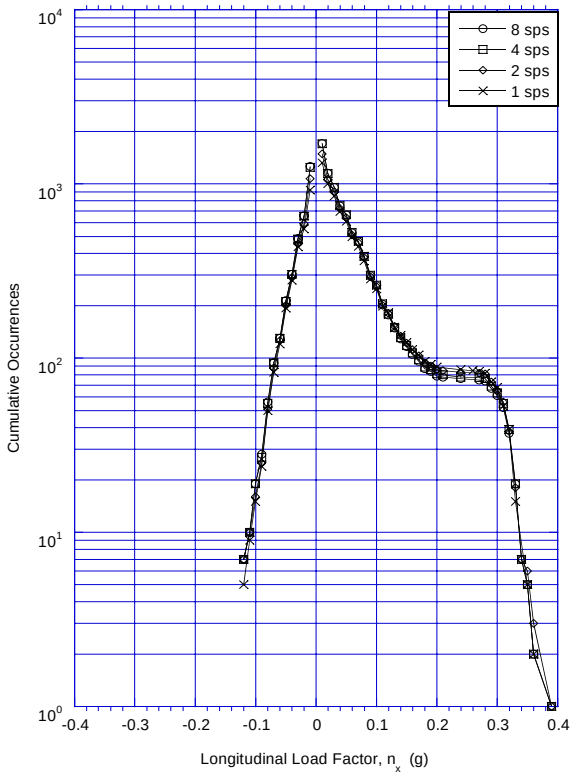

FIGURE 143. CUMULATIVE OCCURRENCES OF LONGITUDINAL LOAD FACTOR, IN FLIGHT

Longitudinal Load Factor n_x	8 Samples per Second		4 Samples per Second		2 Samples per Second		1 Sample per Second	
	Cumulative Occurrences	Percent of 8 sps Cumulative Occurrences	Cumulative Occurrences	Percent of 8 sps Cumulative Occurrences	Cumulative Occurrences	Percent of 8 sps Cumulative Occurrences	Cumulative Occurrences	Percent of 8 sps Cumulative Occurrences
0.39	1	100	1	100	1	100		
0.38	1	100	1	100	1	100		
0.37	1	100	1	100	1	100		
0.36	2	100	2	100	3	150	2	100
0.35	5	100	5	100	6	120	5	100
0.34	7	100	7	100	7	100	5	71.43
0.33	19	100	19	100	18	94.74	15	78.95
0.32	37	100	39	105.4	38	102.7	39	105.4
0.31	52	100	55	105.8	56	107.7	53	101.9
0.3	61	100	63	103.3	65	106.6	68	111.5
0.29	67	100	69	103	73	109	73	109
0.28	74	100	76	102.7	81	109.5	82	110.8
0.27	75	100	77	102.7	82	109.3	84	112
0.26	75	100	77	102.7	82	109.3	85	113.3
0.25	75	100	77	102.7	82	109.3	85	113.3
0.24	76	100	78	102.6	83	109.2	86	113.2
0.23	76	100	78	102.6	83	109.2	86	113.2
0.22	76	100	78	102.6	83	109.2	86	113.2
0.21	78	100	80	102.6	85	109	86	110.3
0.2	79	100	81	102.5	86	108.9	89	112.7
0.19	84	100	86	102.4	90	107.1	92	109.5
0.18	87	100	89	102.3	94	108	96	110.3
0.17	96	100	98	102.1	103	107.3	104	108.3
0.16	105	100	107	101.9	112	106.7	112	106.7
0.15	116	100	118	101.7	122	105.2	123	106
0.14	129	100	131	101.6	134	103.9	135	104.7
0.13	149	100	150	100.7	152	102	149	100
0.12	177	100	179	101.1	181	102.3	182	102.8
0.11	204	100	205	100.5	201	98.53	198	97.06
0.1	261	100	263	100.8	257	98.47	250	95.79
0.09	297	100	299	100.7	294	98.99	284	95.62
0.08	384	100	385	100.3	377	98.18	362	94.27
0.07	466	100	468	100.4	460	98.71	438	93.99
0.06	525	100	527	100.4	511	97.33	497	94.67
0.05	663	100	665	100.3	640	96.53	611	92.16
0.04	750	100	752	100.3	722	96.27	693	92.4
0.03	956	100	957	100.1	902	94.35	853	89.23
0.02	1150	100	1146	99.65	1064	92.52	1001	87.04
0.01	1707	100	1698	99.47	1487	87.11	1322	77.45
-0.01	1261	100	1246	98.81	1072	85.01	921	73.04
-0.02	657	100	652	99.24	592	90.11	554	84.32
-0.03	484	100	482	99.59	453	93.6	435	89.88
-0.04	303	100	303	100	290	95.71	280	92.41
-0.05	214	100	211	98.6	201	93.93	194	90.65
-0.06	130	100	130	100	126	96.92	121	93.08
-0.07	94	100	94	100	88	93.62	83	88.3
-0.08	56	100	55	98.21	51	91.07	50	89.29
-0.09	28	100	27	96.43	25	89.29	24	85.71
-0.1	19	100	19	100	16	84.21	15	78.95
-0.11	10	100	10	100	10	100	9	90
-0.12	7	100	7	100	7	100	5	71.43

FIGURE 144. EFFECT OF SAMPLING RATE ON CUMULATIVE OCCURRENCES OF LONGITUDINAL LOAD FACTOR, IN FLIGHT

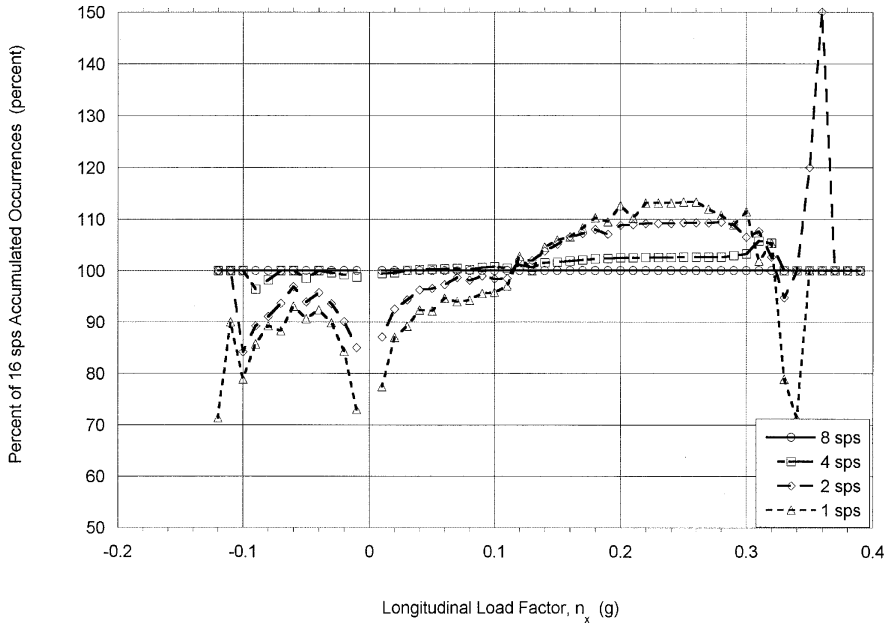

FIGURE 145. PERCENT OF LONGITUDINAL LOAD FACTOR PEAK COUNTS AS A FUNCTION OF SAMPLING RATE, IN FLIGHT

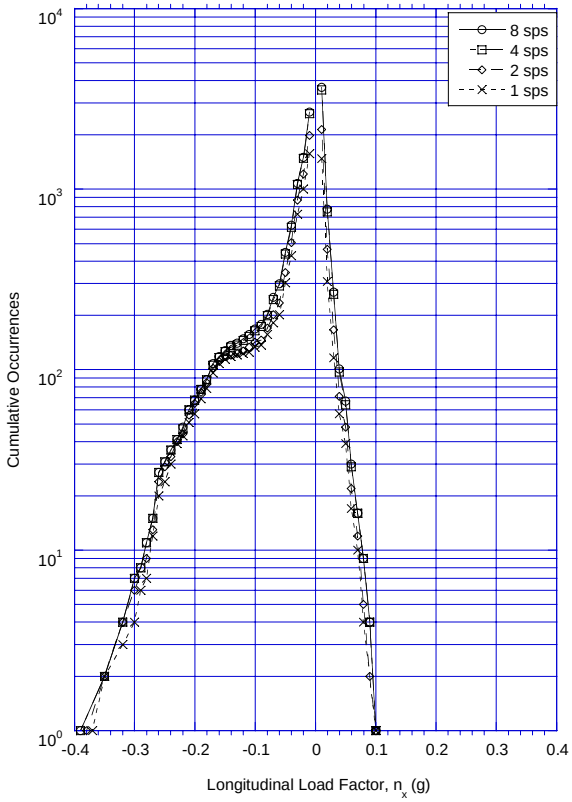

FIGURE 146. CUMULATIVE OCCURRENCES OF LONGITUDINAL LOAD FACTOR, POSTFLIGHT

Longitudinal Load Factor n_x	8 Samples per Second		4 Sa16les per Second		2 Samples per Second		1 Sample per Second	
	Cumulative Occurrences	Percent of 8 sps Cumulative Occurrences	Cumul9tive Occurrences	Percent of 8 sps Cumulative Occurrences	Cumulative Occurrences	Percent of 8 sps Cumulative Occurrences	Cumulative Occurrences	Percent of 8 sps Cumulative Occurrences
0.1	1	100	1	100	1	100	1	100
0.09	4	100	4	100	2	50	1	25
0.08	9	100	9	100	5	55.56	4	44.44
0.07	16	100	16	100	12	75	10	62.5
0.06	30	100	29	96.67	22	73.33	17	56.67
0.05	67	100	64	95.52	48	71.64	39	58.21
0.04	101	100	97	96.04	71	70.3	57	56.44
0.03	268	100	262	97.76	166	61.94	116	43.28
0.02	773	100	747	96.64	464	60.03	308	39.84
0.01	3670	100	3545	96.59	2147	58.5	1478	40.27
-0.01	2676	100	2612	97.61	1980	73.99	1572	58.74
-0.02	1504	100	1479	98.34	1211	80.52	1000	66.49
-0.03	1077	100	1063	98.7	869	80.69	725	67.32
-0.04	631	100	617	97.78	505	80.03	427	67.67
-0.05	447	100	438	97.99	346	77.4	302	67.56
-0.06	299	100	291	97.32	234	78.26	202	67.56
-0.07	252	100	245	97.22	202	80.16	182	72.22
-0.08	203	100	199	98.03	170	83.74	157	77.34
-0.09	178	100	174	97.75	146	82.02	137	76.97
-0.1	168	100	164	97.62	142	84.52	133	79.17
-0.11	157	100	153	97.45	133	84.71	125	79.62
-0.12	148	100	145	97.97	127	85.81	123	83.11
-0.13	140	100	137	97.86	123	87.86	121	86.43
-0.14	136	100	133	97.79	120	88.24	118	86.76
-0.15	128	100	126	98.44	118	92.19	114	89.06
-0.16	118	100	117	99.15	111	94.07	108	91.53
-0.17	108	100	106	98.15	102	94.44	96	88.89
-0.18	88	100	88	100	85	96.59	79	89.77
-0.19	78	100	78	100	75	96.15	69	88.46
-0.2	68	100	68	100	65	95.59	57	83.82
-0.21	60	100	60	100	56	93.33	51	85
-0.22	48	100	47	97.92	44	91.67	43	89.58
-0.23	41	100	41	100	40	97.56	39	95.12
-0.24	36	100	36	100	33	91.67	30	83.33
-0.25	31	100	31	100	29	93.55	24	77.42
-0.26	27	100	27	100	24	88.89	20	74.07
-0.27	15	100	15	100	13	86.67	12	80
-0.28	11	100	11	100	9	81.82	7	63.64
-0.29	8	100	8	100	6	75	6	75
-0.3	7	100	7	100	6	85.71	4	57.14
-0.31	4	100	4	100	4	100	3	75
-0.32	4	100	4	100	4	100	3	75
-0.33	2	100	2	100	2	100	2	100
-0.34	2	100	2	100	2	100	2	100
-0.35	2	100	2	100	2	100	2	100
-0.36	1	100	1	100	1	100	1	100
-0.37	1	100	1	100	1	100	1	100
-0.38	1	100	1	100	1	100		
-0.39	1	100	1	100				

FIGURE 147. EFFECT OF SAMPLING RATE ON CUMULATIVE OCCURRENCES OF LONGITUDINAL LOAD FACTOR, POSTFLIGHT

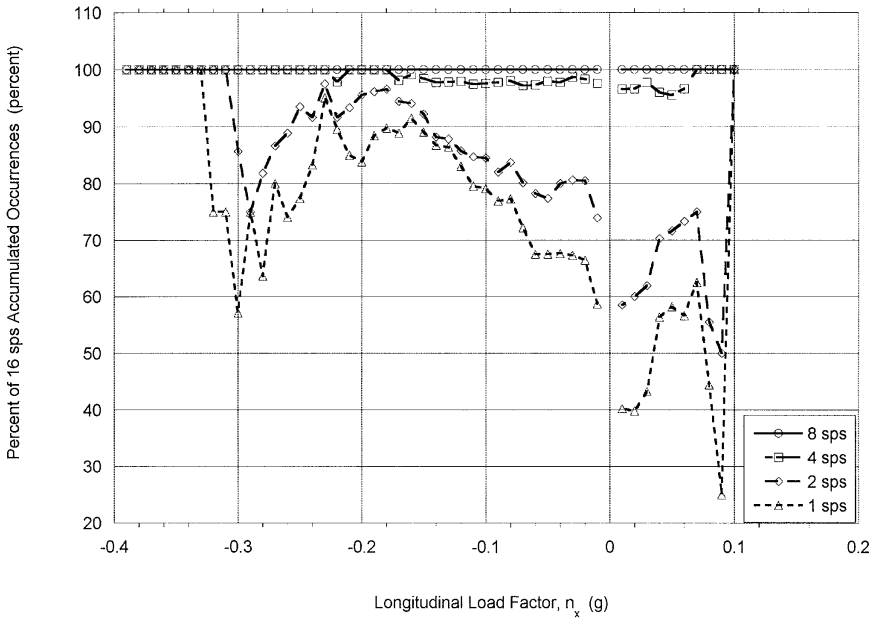

FIGURE 148. PERCENT OF LONGITUDINAL LOAD FACTOR PEAK COUNTS AS A FUNCTION OF SAMPLING RATE, POSTFLIGHT

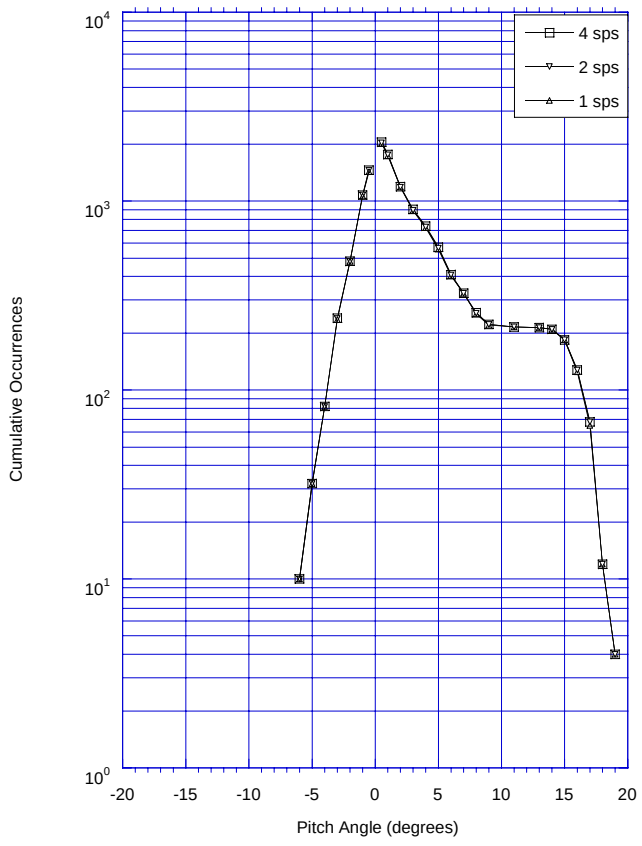

FIGURE 149. CUMULATIVE OCCURRENCES OF PITCH ANGLE

Pitch Angle (degrees)	4 Samples per Second		2 Samples per Second		1 Sample per Second	
	Cumulative Occurrences	Percent of 4 sps Cumulative Occurrences	Cumulative Occurrences	Percent of 4 sps Cumulative Occurrences	Cumulative Occurrences	Percent of 4 sps Cumulative Occurrences
19	4	100	4	100	4	100
18	12	100	12	100	12	100
17	68	100	68	100	65	95.59
16	128	100	128	100	125	97.66
15	184	100	184	100	184	100
14	210	100	210	100	210	100
13	214	100	214	100	214	100
12	214	100	214	100	214	100
11	216	100	216	100	216	100
10	216	100	216	100	216	100
9	222	100	222	100	221	99.55
8	256	100	255	99.61	253	98.83
7	326	100	325	99.69	325	99.69
6	408	100	407	99.75	403	98.77
5	568	100	566	99.65	558	98.24
4	734	100	731	99.59	724	98.64
3	902	100	898	99.56	894	99.11
2	1194	100	1189	99.58	1185	99.25
1	1766	100	1761	99.72	1750	99.09
0.5	2048	100	2039	99.56	2022	98.73
-0.5	1456	100	1454	99.86	1435	98.56
-1	1076	100	1076	100	1065	98.98
-2	480	100	480	100	479	99.79
-3	240	100	239	99.58	237	98.75
-4	82	100	82	100	82	100
-5	32	100	32	100	32	100
-6	10	100	10	100	10	100

FIGURE 150. EFFECT OF SAMPLING RATE ON CUMULATIVE OCCURRENCES OF PITCH ANGLE, IN FLIGHT

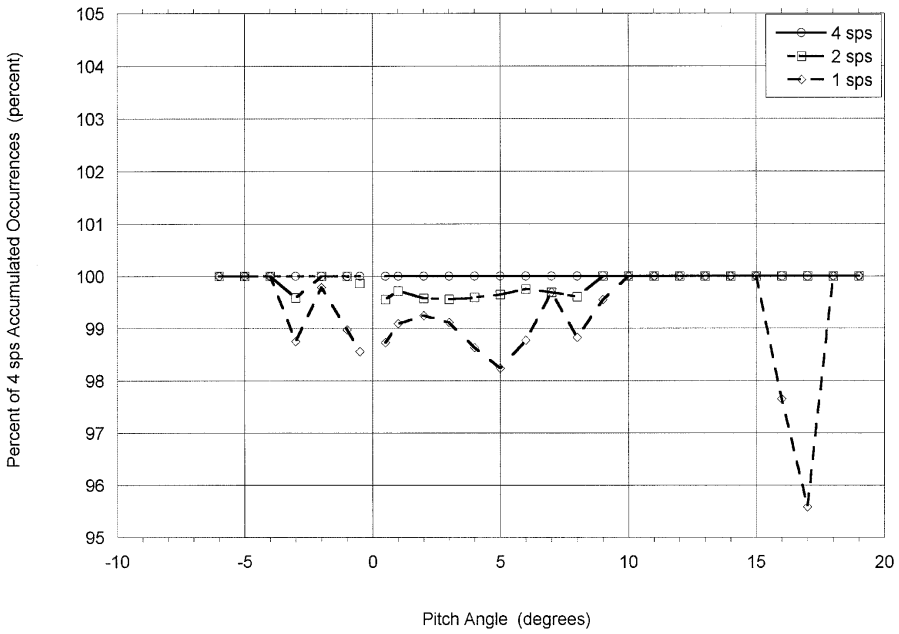

FIGURE 151. PERCENT OF PITCH ANGLE PEAK COUNTS AS A FUNCTION OF SAMPLING RATE, IN FLIGHT

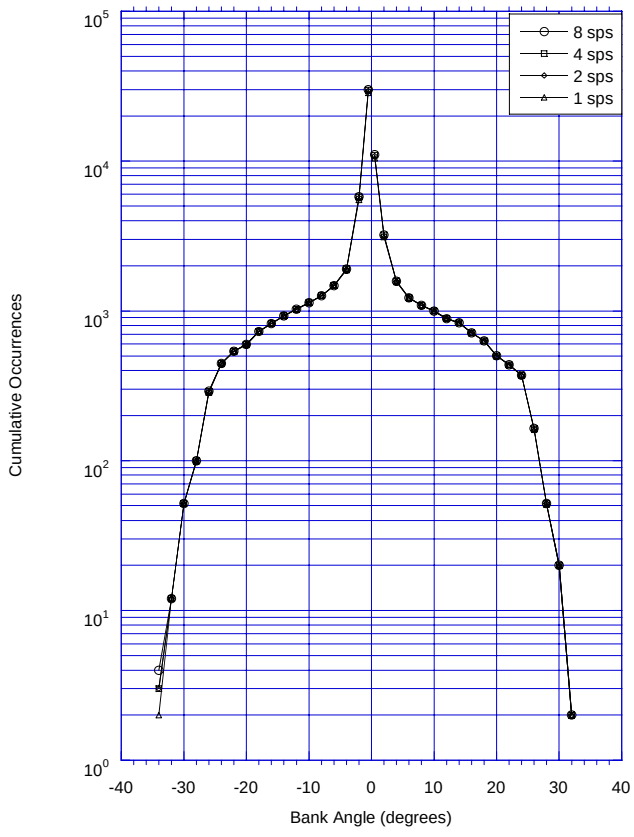

FIGURE 152. CUMULATIVE OCCURRENCES OF BANK ANGLE

Bank Angle (degrees)	8 Samples per Second		4 Samples per Second		2 Samples per Second		1 Sample per Second	
	Cumulative Occurrences	Percent of 8 sps Cumulative Occurrences	Cumulative Occurrences	Percent of 8 sps Cumulative Occurrences	Cumulative Occurrences	Percent of 8 sps Cumulative Occurrences	Cumulative Occurrences	Percent of 8 sps Cumulative Occurrences
32	2	100	2	100	2	100	2	100
30	20	100	20	100	20	100	20	100
28	52	100	52	100	52	100	51	98.08
26	164	100	163	99.39	163	99.39	161	98.17
24	372	100	372	100	372	100	372	100
22	436	100	436	100	436	100	435	99.77
20	502	100	502	100	502	100	502	100
18	632	100	632	100	632	100	631	99.84
16	714	100	713	99.86	712	99.72	712	99.72
14	832	100	832	100	832	100	832	100
12	890	100	890	100	890	100	890	100
10	1000	100	1000	100	1000	100	999	99.9
8	1088	100	1088	100	1086	99.82	1086	99.82
6	1224	100	1222	99.84	1221	99.75	1218	99.51
4	1586	100	1582	99.75	1576	99.37	1565	98.68
2	3218	100	3212	99.81	3180	98.82	3105	96.49
0.5	11018	100	10970	99.56	10836	98.35	10461	94.94
-0.5	29972	100	29861	99.63	29523	98.5	28531	95.19
-2	5780	100	5760	99.65	5695	98.53	5515	95.42
-4	1904	100	1902	99.89	1894	99.47	1877	98.58
-6	1478	100	1478	100	1476	99.86	1472	99.59
-8	1260	100	1260	100	1259	99.92	1258	99.84
-10	1136	100	1136	100	1135	99.91	1134	99.82
-12	1024	100	1024	100	1024	100	1023	99.9
-14	928	100	928	100	928	100	927	99.89
-16	822	100	822	100	822	100	822	100
-18	730	100	730	100	730	100	730	100
-20	596	100	596	100	596	100	593	99.5
-22	536	100	536	100	536	100	536	100
-24	446	100	446	100	445	99.78	444	99.55
-26	290	100	290	100	289	99.66	285	98.28
-28	100	100	100	100	100	100	99	99
-30	52	100	52	100	52	100	52	100
-32	12	100	12	100	12	100	12	100
-34	4	100	3	75	3	75	2	50

FIGURE 153. EFFECT OF SAMPLING RATE ON CUMULATIVE OCCURRENCES OF BANK ANGLE, IN FLIGHT

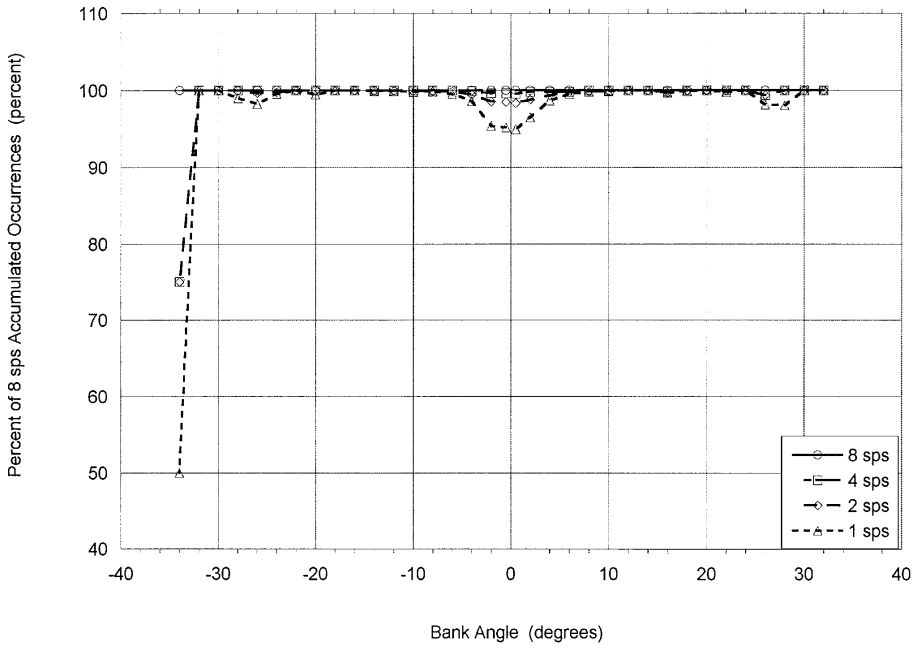

FIGURE 154. PERCENT BANK ANGLE PEAK COUNTS AS A FUNCTION OF SAMPLING RATE, IN FLIGHT

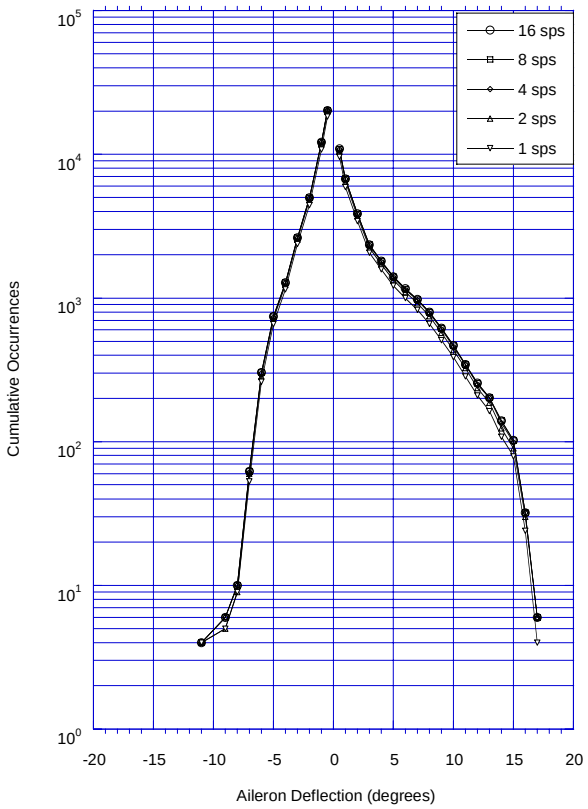

FIGURE 155. CUMULATIVE OCCURRENCES OF AILERON DEFLECTION ANGLE

Aileron Angle (degrees)	16 Samples per Second		8 Samples per Second		4 Samples per Second		2 Samples per Second		1 Sample per Second	
	Cumulative Occurrences	Percent of 16 sps Cumulative Occurrences	Cumulative Occurrences	Percent of 16 sps Cumulative Occurrences	Cumulative Occurrences	Percent of 16 sps Cumulative Occurrences	Cumulative Occurrences	Percent of 16 sps Cumulative Occurrences	Cumulative Occurrences	Percent of 16 sps Cumulative Occurrences
17	6	100	6	100	6	100	6	100	4	66.67
16	32	100	32	100	32	100	30	93.75	24	75
15	102	100	102	100	99	97.06	90	88.24	79	77.45
14	140	100	140	100	135	96.43	124	88.57	108	77.14
13	202	100	202	100	201	99.5	187	92.57	163	80.69
12	256	100	256	100	251	98.05	237	92.58	210	82.03
11	346	100	346	100	342	98.84	325	93.93	285	82.37
10	468	100	468	100	459	98.08	433	92.52	388	82.91
9	618	100	618	100	608	98.38	574	92.88	511	82.69
8	798	100	797	99.87	784	98.25	747	93.61	661	82.83
7	978	100	976	99.8	966	98.77	923	94.38	828	84.66
6	1156	100	1154	99.83	1141	98.7	1097	94.9	997	86.25
5	1406	100	1404	99.86	1395	99.22	1333	94.81	1214	86.34
4	1806	100	1804	99.89	1790	99.11	1717	95.07	1583	87.65
3	2350	100	2348	99.91	2325	98.94	2233	95.02	2062	87.74
2	3864	100	3862	99.95	3840	99.38	3695	95.63	3426	88.66
1	6754	100	6750	99.94	6703	99.24	6444	95.41	5919	87.64
0.5	10880	100	10875	99.95	10824	99.49	10497	96.48	9608	88.31
-0.5	20208	100	20207	100	20168	99.8	19803	98	18380	90.95
-1	12154	100	12153	99.99	12128	99.79	11845	97.46	10819	89.02
-2	4972	100	4971	99.98	4949	99.54	4805	96.64	4429	89.08
-3	2628	100	2627	99.96	2615	99.51	2544	96.8	2378	90.49
-4	1280	100	1280	100	1271	99.3	1229	96.02	1149	89.77
-5	742	100	742	100	734	98.92	716	96.5	657	88.54
-6	304	100	304	100	299	98.36	284	93.42	261	85.86
-7	62	100	62	100	61	98.39	60	96.77	53	85.48
-8	10	100	10	100	10	100	9	90	9	90
-9	6	100	6	100	6	100	5	83.33	5	83.33
-10	4	100	4	100	4	100	4	100	4	100
-11	4	100	4	100	4	100	4	100	4	100

FIGURE 156. EFFECT OF SAMPLING RATE ON CUMULATIVE OCCURRENCES OF AILERON DEFLECTION ANGLE, IN FLIGHT

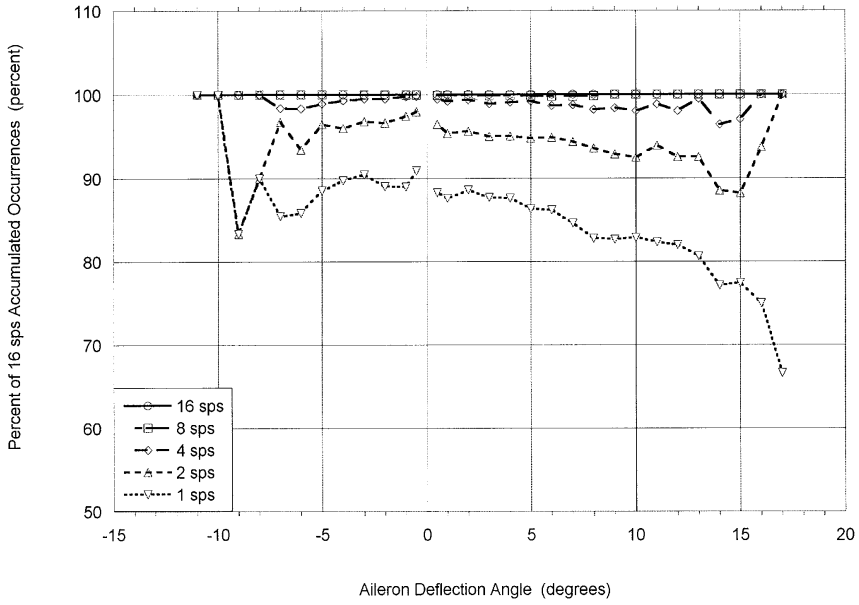

FIGURE 157. PERCENT AILERON DEFLECTION ANGLE PEAK COUNTS AS A FUNCTION OF SAMPLING RATE, IN FLIGHT

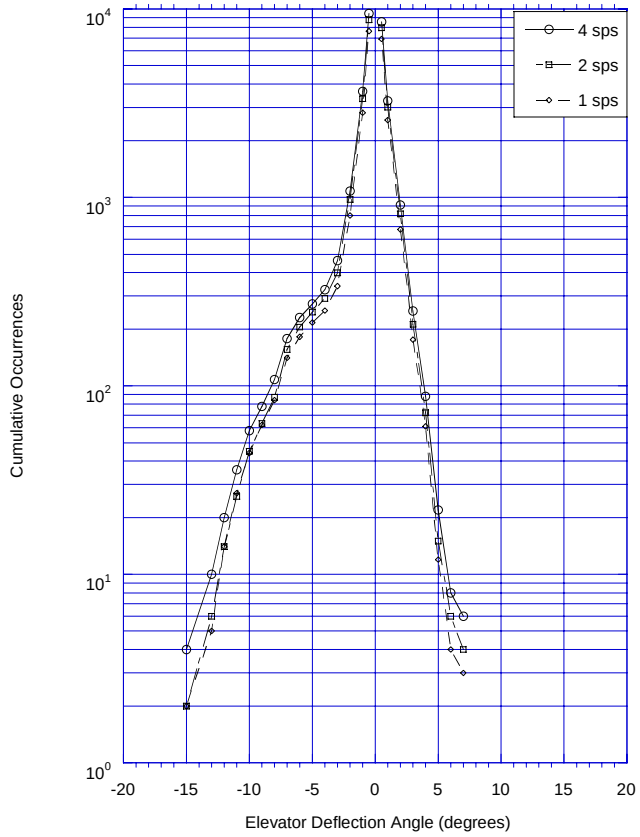

FIGURE 158. CUMULATIVE OCCURRENCES OF ELEVATOR DEFLECTION ANGLE

Elevator Angle (degrees)	4 Samples per Second		2 Samples per Second		1 Sample per Second	
	Cumulative Occurrences	Percent of 4 sps Cumulative Occurrences	Cumulative Occurrences	Percent of 4 sps Cumulative Occurrences	Cumulative Occurrences	Percent of 4 sps Cumulative Occurrences
7	6	100	4	66.67	3	50
6	8	100	6	75	4	50
5	22	100	15	68.18	12	54.55
4	88	100	72	81.82	61	69.32
3	250	100	212	84.8	176	70.4
2	912	100	819	89.8	674	73.9
1	3250	100	3017	92.83	2578	79.32
0.5	8570	100	7967	92.96	6931	80.88
-0.5	9466	100	8770	92.65	7619	80.49
-1	3654	100	3347	91.6	2813	76.98
-2	1084	100	977	90.13	802	73.99
-3	462	100	397	85.93	339	73.38
-4	324	100	291	89.81	251	77.47
-5	272	100	247	90.81	214	79.78
-6	230	100	205	89.13	182	79.13
-7	178	100	156	87.64	141	79.21
-8	108	100	87	80.56	84	77.78
-9	78	100	63	80.77	62	79.49
-10	58	100	45	77.59	44	75.86
-11	36	100	26	72.22	27	75
-12	20	100	14	70	14	70
-13	10	100	6	60	5	50
-14	4	100	2	50	2	50
-15	4	100	2	50	2	50

FIGURE 159. EFFECT OF SAMPLING RATE ON CUMULATIVE OCCURRENCES OF ELEVATOR DEFLECTION ANGLE, IN FLIGHT

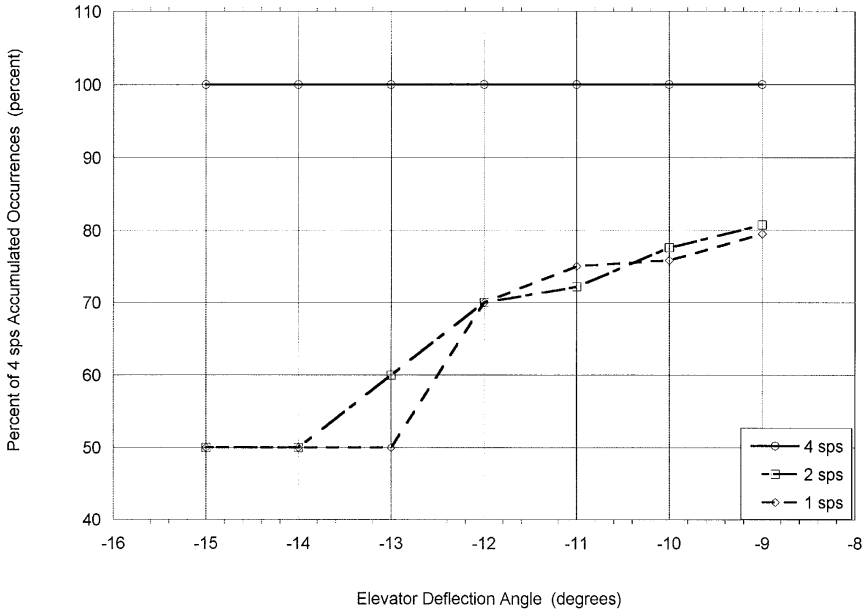

FIGURE 160. PERCENT ELEVATOR DEFLECTION ANGLE PEAK COUNTS AS A FUNCTION OF SAMPLING RATE, IN FLIGHT

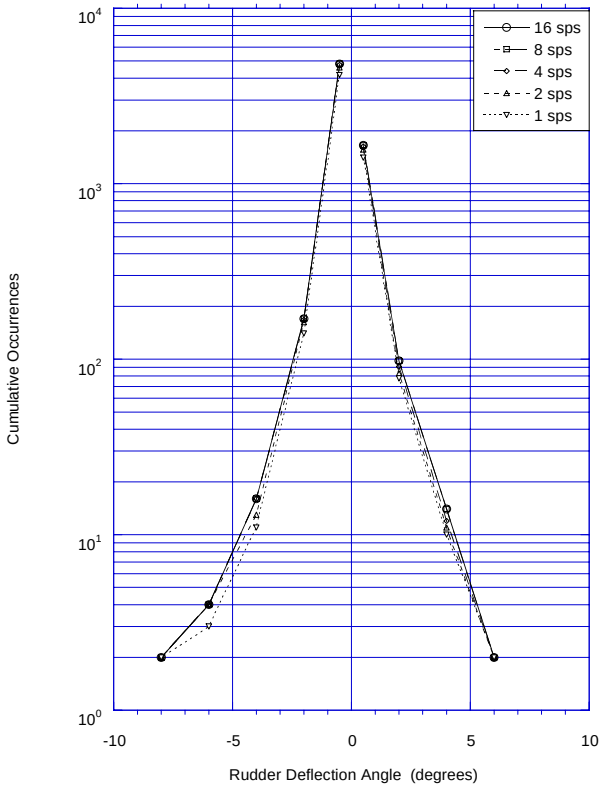

FIGURE 161. CUMULATIVE OCCURRENCES OF RUDDER DEFLECTION ANGLE

Rudder Angle (degrees)	16 Samples per Second		8 Samples per Second		4 Samples per Second		2 Samples per Second		1 Sample per Second	
	Cumulative Occurrences	Percent of 16 sps Cumulative Occurrences	Cumulative Occurrences	Percent of 16 sps Cumulative Occurrences	Cumulative Occurrences	Percent of 16 sps Cumulative Occurrences	Cumulative Occurrences	Percent of 16 sps Cumulative Occurrences	Cumulative Occurrences	Percent of 8 sps Cumulative Occurrences
6	2	100	2	100	2	100	2	100	2	100
4	14	100	14	100	12	85.71	11	78.57	10	71.43
2	98	100	98	100	91	92.86	83	84.69	78	79.59
0.5	1658	100	1658	99.88	1632	98.43	1567	94.51	1406	84.8
-0.5	4826	100	4823	99.94	4762	98.67	4590	95.11	41.81	86.63
-2	170	100	170	100	168	98.82	163	95.88	140	82.35
-4	16	100	16	100	16	100	13	81.25	11	68.75
-6	4	100	4	100	4	100	4	100	3	75
-8	2	100	2	100	2	100	2	100	2	100

FIGURE 162. EFFECT OF SAMPLING RATE ON CUMULATIVE OCCURRENCES OF RUDDER DEFLECTION ANGLE, IN FLIGHT

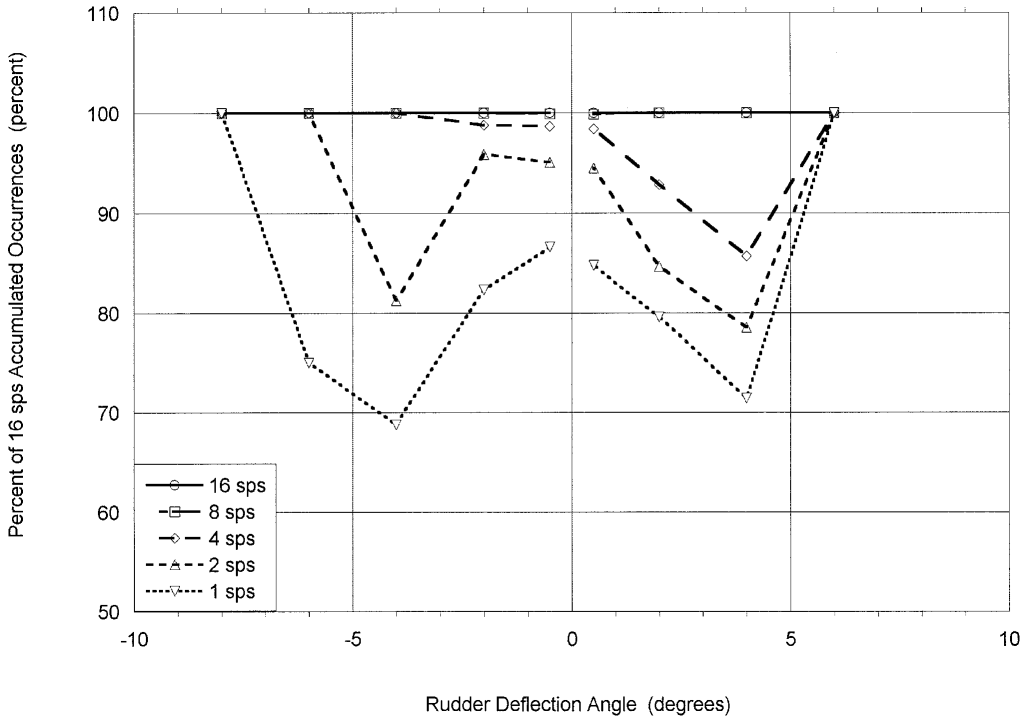

FIGURE 163. PERCENT RUDDER DEFLECTION ANGLE PEAK COUNTS AS A FUNCTION OF SAMPLING RATE, IN FLIGHT

TABLE 1. PARAMETER SAMPLING RATES

Parameter	Units	Sampling Rate
Vertical Load Factor	g	16
Lateral Load Factor	g	16
Longitudinal Load Factor	g	8
Pitch Angle	degrees	4
Bank Angle	degrees	8
Aileron Position	degrees	16
Elevator Position	degrees	4
Rudder Position	degrees	16
Spoiler Position	degrees	2
Radio Height	feet	16
Gear Compressed	discrete	16
N1 and N2	% rpm	1
Ground Speed	knots	1
Airspeed	knots	1

TABLE 2. FIGURE LAYOUT FOR THREE FLIGHTS

Parameter	Figure Description	Figure Number		
		Flight Sequence 3	Flight Sequence 35	Flight Sequence 62
Vertical Load Factor	Time History	14	50	86
	Preflight PSD	15	51	87
	Preflight rms	16	52	88
	In-flight PSD	17	53	89
	In-flight rms	18	54	90
	Postflight PSD	19	55	91
	Postflight rms	20	56	92
Lateral Load Factor	Time History	21	57	93
	Preflight PSD	22	58	94
	Preflight rms	23	59	95
	In-flight PSD	24	60	96
	In-flight rms	25	61	97
	Postflight PSD	26	62	98
	Postflight rms	27	63	99
Longitudinal Load Factor	Time History	28	64	100
	Preflight PSD	30	65	101
	Preflight rms	31	66	102
	In-flight PSD	31	67	103
	In-flight rms	32	68	104
	Postflight PSD	33	70	105
	Postflight rms	34	70	106
Pitch Angle	Time History	35	71	107
	In-flight PSD	36	72	108
	In-flight rms	37	73	109
Bank Angle	Time History	38	74	110
	In-flight PSD	39	75	111
	In-flight rms	40	76	112
Aileron Angle	Time History	41	77	113
	In-flight PSD	42	78	114
	In-flight rms	43	79	115
Elevator Angle	Time History	44	80	116
	In-flight PSD	45	81	117
	In-flight rms	46	82	118
Rudder Angle	Time History	47	83	119
	In-flight PSD	48	84	120
	In-flight rms	49	85	121

TABLE 3. PEAK COUNTING CRITERIA

Parameter	Sampling Rate Studied	Threshold	Binning Increment
Vertical Acceleration	16, 8, 4, 2, 1	±0.05	0.05
Lateral Acceleration	16, 8, 4, 2, 1	±0.01	0.01
Longitudinal Acceleration	8, 4, 2, 1	±0.01	0.01
Pitch Angle	4, 2, 1	±0.5	1.0
Bank Angle	8, 4, 2, 1	±0.5	2.0
Aileron Position	16, 8, 4, 2, 1	±0.5	1
Elevator Position	4, 2, 1	±0.5	1
Rudder Position	16, 8, 4, 2, 1	±0.5	2

TABLE 4. FIGURE LAYOUT FOR CUMULATIVE OCCURRENCE DATA

Parameter	Figure Description	Figure Number		
		Cumulative Occurrences in Graphical Format	Cumulative Occurrences in Tabular Format	Cumulative Occurrences in Relative Percent
Vertical Load Factor	Preflight	122	123	124
	In flight	125	126	127
	Postflight	128	129	130
Lateral Load Factor	Preflight	131	132	133
	In flight	134	135	136
	Postflight	137	138	139
Longitudinal Load Factor	Preflight	140	141	142
	In flight	143	144	145
	Postflight	146	147	148
Pitch Angle	In flight	149	150	151
Bank Angle	In flight	152	153	154
Aileron Angle	In flight	155	156	157
Elevator Angle	In flight	158	159	160
Rudder Angle	In flight	161	162	163

TABLE 5. SAMPLING RATE REQUIREMENTS

Parameter	Frequency Bandwidth Required to Include 95% of Total rms	Minimum Sampling Rate Required From PSD Analysis	Minimum Sampling Rate Required From Peak Count Statistics	Sampling Rate Required for Maximum 10% Error in Amplitude Measurement	Part 121-Specified Sampling Rate
Vertical Load Factor	Ground < 6 Flight < 1.5	12 3	Ground ≥16 Flight ≥ 8	40 10	8[1,2,3]
Lateral Load Factor	< 1.5	3	Ground ≥8 Flight ≥16	10	4[1,2,3]
Longitudinal Load Factor	< 0.1	1	Ground ≥8 Flight ≥4	1	4[1,2,3]
Pitch Angle	<0.05	1	2	1	1[1], 4 [2,3]
Bank Angle	< 0.05	1	4	1	1[1], 2 [2,3]
Aileron Deflection	< 0.3	1	4	2	1[1], 2[2], 4[3]
Elevator Deflection	< 1.0	2	4	7	1[1], 2[2], 4[3]
Rudder Deflection	<0.5	1	8	4	1[1], 2[2]

[1] For aircraft manufactured prior to July 1996
[2] For aircraft manufactured after July 1996 and before August 2002
[3] For aircraft manufactured after August 2002

APPENDIX A—APPENDIX B TO 14 CFR PART 121, AIRPLANE FLIGHT RECORDER SPECIFICATION

APPENDIX B TO PART 121—AIRPLANE FLIGHT RECORDER SPECIFICATION

Parameters	Range	Accuracy sensor input to DFDR readout	Sampling interval (per second)	Resolution [4] readout
Time (GMT or Frame Counter) (range 0 to 4095, sampled 1 per frame).	24 Hrs	±0.125% Per Hour	0.25 (1 per 4 seconds).	1 sec.
Altitude	−1,000 ft to max certificated altitude of aircraft.	±100 to ±700 ft (See Table 1, TSO–C51a).	1	5′ to 35′ [1]
Airspeed	50 KIAS to V_{so}, and V_{so} to 1.2 V_D.	±5%, ±3%	1	1 kt.
Heading	360°	±2°	1	0.5°
Normal Acceleration (Vertical)	−3g to +6g	±1% of max range excluding datum error of ±5%.	8	0.01g.
Pitch Attitude	±75°	±2°	1	0.5°
Roll Attitude	±180°	±2°	1	0.5°
Radio Transmitter Keying	On-Off (Discrete)	±2°	±2%	
Thrust/Power on Each Engine	Full Range Forward	±2°	1 (per engine)	0.2% [2]
Trailing Edge Flap or Cockpit Control Selection.	Full Range or Each Discrete Position.	±3° or as Pilot's Indicator	0.5	0.5% [2]
Leading Edge Flap or Cockpit Control Selection.	Full Range or Each Discrete Position.	±3° or as Pilot's Indicator	0.5	0.5% [2]
Thrust Reverser Position	Stowed, In Transit, and Reverse (Discrete).		1 (per 4 seconds per engine).	
Ground Spoiler Position/ Speed Brake Selection.	Full Range or Each Discrete Position.	±2% Unless Higher Accuracy Uniquely Required.	1	0.2% [2].
Marker Beacon Passage	Discrete		1	
Autopilot Engagement	Discrete		1	
Longitudinal Acceleration	±1g	±1.5% max range excluding datum error of ±5%.	4	0.01g.
Pilot Input and/or Surface Position—Primary Controls (Pitch, Roll, Yaw) [3].	Full Range	±2° Unless Higher Accuracy Uniquely Required.	1	0.2% [2].
Lateral Acceleration	±1g	±1.5% max range excluding datum error of ±5%.	4	0.01g.
Pitch Trim Position	Full Range	±3% Unless Higher Accuracy Uniquely Required.	1	0.3% [2].
Glideslope Deviation	±400 Microamps	±3%	1	0.3% [2].
Localizer Deviation	±400 Microamps	±3%	1	0.3% [2].
AFCS Mode and Engagement Status.	Discrete		1	
Radio Altitude	−20 ft to 2,500 ft	±2 Ft or ±3% Whichever is Greater Below 500 Ft and ±5% Above 500 Ft.	1	1 ft + 5% [2] above 500′.
Master Warning	Discrete		1	
Main Gear Squat Switch Status.	Discrete		1	
Angle of Attack (if recorded directly)..	As installed	As installed	2	0.3% [2]
Outside Air Temperature or Total Air Temperature..	−50° C to +90° C	±2° c	0.5	0.3° c
Hydraulics, Each System Low Pressure.	Discrete		0.5	or 0.5% [2]
Groundspeed.	As installed	Most Accurate Systems Installed (IMS Equipped Aircraft Only).	1	0.2% [2]

APPENDIX B—APPENDIX M TO 14 CFR PART 121, AIRPLANE FLIGHT RECORDER SPECIFICATIONS

APPENDIX M TO PART 121—AIRPLANE FLIGHT RECORDER SPECIFICATIONS

The recorded values must meet the designated range, resolution, and accuracy requirements during dynamic and static conditions. All data recorded must be correlated in time to within one second.

Parameters	Range	Accuracy (sensor input)	Seconds per sampling interval	Resolution	Remarks
1. Time or Relative Times Counts.[1].	24 Hrs, 0 to 4095.	±0.125% Per Hour.	4	1 sec	UTC time preferred when available. Count increments each 4 second of system operation.
2. Pressure Altitude.	−1000 ft to max certificated altitude of aircraft. +5000 ft.	±100 to ±700 ft (see table, TSO C124a or TSO C51a).	1	5′ to 35′	Data should be obtained from the air data computer when practicable.
3. Indicated airspeed or Calibrated airspeed.	50 KIAS or minimum value to Max V_{so} to 1.2 V_{D}.	±5% and ±3%	1	1 kt	Data should be obtained from the air data computer when practicable.
4. Heading (Primary flight crew reference).	0–360° and Discrete "true" or "mag".	±2°	1	0.5°	When true or magnetic heading can be selected as the primary heading reference, a discrete indicating selection must be recorded.
5. Normal acceleration (vertical)[9].	−3g to +6g	±1% of max range excluding datum error of ±5%.	0.125	0.004g.	
6. Pitch Attitude	±75°	±2°	1 or 0.25 for airplanes operated under §121.344(f).	0.5°	A sampling rate of 0.25 is recommended.
7. Roll attitude[2]	±180°	±2°	1 or 0.5 for airplanes operated under §121.344(f).	0.5	A sampling rate of 0.5 is recommended.
8. Manual Radio Transmitter Keying or CVR/DFDR synchronization reference.	On-Off (Discrete) None		1		Preferably each crew member but one discrete acceptable for all transmission provided the CVR/FDR system complies with TSO C124a CVR synchronization requirements (paragraph 4.2.1 ED–55).

The recorded values must meet the designated range, resolution, and accuracy requirements during dynamic and static conditions. All data recorded must be correlated in time to within one second.

Parameters	Range	Accuracy (sensor input)	Seconds per sampling interval	Resolution	Remarks
9. Thrust/power on each engine—primary flight crew reference.	Full range forward.	±2%	1 (per engine)	0.3% of full range.	Sufficient parameters (*e.g.* EPR, N1 or Torque, NP) as appropriate to the particular engine being recorded to determine power in forward and reverse thrust, including potential overspeed condition.
10. Autopilot Engagement.	Discrete "on" or "off".		1		
11. Longitudinal Acceleration.	±1g	±1.5% max. range excluding datum error of ±5%.	0.25	0.004g	
12a. Pitch control(s) (non fly-by-wire systems).	Full range	±2% Unless higher accuracy uniquely required.	0.5 or 0.25 for airplanes operated under §121.344(f).	0.5% of full range.	For airplanes that have a flight control break away capability that allows either pilot to operate the controls independently, record both control inputs. The control inputs may be sampled alternately once per second to produce the sampling interval of 0.5 or 0.25, as applicable.
12b. Pitch Control(s) position (fly-by-wire systems).[3].	Full Range	±2° Unless Higher Accuracy Uniquely Required..	0.5 or 0.25 for airplanes operated under §121.344(f)..	0.2% of full range.	
13a. Lateral Control position(s) (non-fly-by-wire).	Full Range	±2° Unless Higher Accuracy Uniquely Required.	0.5 or 0.25 for airplanes operated under §121.344(f).	0.2% of full range.	For airplanes that have a flight control break away capability that allows either pilot to operate the controls independently, record both control inputs. The control inputs may be sampled alternately once per second to produce the sampling interval of 0.5 or 0.25, as applicable.
13b. Lateral Control position(s) (fly-by-wire).[4].	Full Range	±2° Unless Higher Accuracy Uniquely Required.	0.5 or 0.25 for airplanes operated under §121.344(f).	0.2% of full range.	
14a. Yaw control position(s) (non-fly-by-wire)[5].	Full range	±2° Unless higher accuracy uniquely required.	0.5	0.3% of full range.	For airplanes that have a flight control break away capability that allows either pilot to operate the controls independently, record both control inputs. The control inputs may be sampled alternately once per second to produce the sampling interval of 0.5.
14b. Yaw Control position(s) (fly-by-wire).	Full Range	±2° Unless Higher Accuracy Uniquely Required.	0.5	0.2% of full range.	
15. Pitch Control Surface(s) Position.[6].	Full Range	±2° Unless Higher Accuracy Uniquely Required..	0.5 or 0.25 for airplanes operated under §121.344(f)..	0.3% of full range..	For airplanes fitted with multiple or split surfaces, a suitable combination of inputs is acceptable in lieu of recording each surface separately. The control surfaces may be sampled alternately to produce the sampling interval of 0.5 or 0.25.

The recorded values must meet the designated range, resolution, and accuracy requirements during dynamic and static conditions. All data recorded must be correlated in time to within one second.

Parameters	Range	Accuracy (sensor input)	Seconds per sampling interval	Resolution	Remarks
16. Lateral control surface(s) position[7].	Full range	±2° Unless higher accuracy uniquely required.	0.5 or 0.25 for airplanes operated under §121.344(f).	0.3% of full range.	A suitable combination of surface position sensors is acceptable in lieu of recording each surface separately. The control surfaces may be sampled alternately to produce the sampling interval of 0.5 or 0.25.
17. Yaw Control Surface(s) Position.[8].	Full Range	±2° Unless Higher Accuracy Uniquely Required.	0.5	0.2% of full range.	For airplanes with multiple or split surfaces, a suitable combination of surface position sensors is acceptable in lieu of recording each surface separately. The control surfaces may be sampled alternately to produce the sapling interval of 0.5.
18. Lateral Acceleration.	±1g	±1.5% max. range excluding datum error of ±5%.	0.25	0.004g	
19. Pitch trime surface position.	Full range	±3° Unless higher accuracy uniquely required.	1	0.6% of full range.	
20. Trailing Edge Flap or Cockpit Control Selection.[10].	Full Range or Each Position (discrete).	±3° or as Pilot's indicator.	2	0.5% of full range.	Flap position and cockpit control may each be sampled at 4 second intervals, to give a data point every 2 seconds.
21. Leading Edge Flap or Cockpit Control Selection.[11].	Full Range or Each Discrete Position.	±3° or as Pilot's indicator and sufficient to determine each discrete position.	2	0.5% of full range.	Left and right sides, or flap position and cockpit control may each be sampled at 4 second intervals, so as to give a data point every 2 seconds.
22. Each Thrust Reverser Position (or equivalent for propeller airplane).	Stowed, In Transit, and Reverse (Discrete).	.....	1 (per engine) ...	.....	Turbo-jet—2 discretes enable the 3 states to be determined. Turbo-prop—discrete.
23. Ground spoiler position or brake selection[12].	Full range or each position (discrete).	±2° Unless higher accuracy uniquely required.	1 or 0.5 for airplanes operated under §121.344(f).	0.5% of full range.	
24. Outside Air Temperature or Total Air Temperature.[13].	−50 °C to +90 °C.	±2 °C	2	0.3 °C	
25. Autopilot/ Autothrottle/ AFCS Mode and Engagement Status.	A suitable combination of discretes.	.....	1	.....	Discretes should show which systems are engaged and which primary modes are controlling the flight path and speed of the aircraft.
26. Radio Altitude[14].	−20 ft to 2,500 ft.	±2 ft or ±3% whichever is greater below 500 ft and ±5% above 500 ft.	1	1 ft +5% above 500 ft.	For autoland/category 3 operations. Each radio altimeter should be recorded, but arranged so that at least one is recorded each second.

The recorded values must meet the designated range, resolution, and accuracy requirements during dynamic and static conditions. All data recorded must be correlated in time to within one second.

Parameters	Range	Accuracy (sensor input)	Seconds per sampling interval	Resolution	Remarks
27. Localizer Deviation, MLS Azimuth, or GPS Latitude Deviation.	±400 Microamps or available sensor range as installed. ±62°	As installed ±3% recommended.	1	0.3% of full range.	For autoland/category 3 operations. Each system should be recorded but arranged so that at least one is recorded each second. It is not necessary to record ILS and MLS at the same time, only the approach aid in use need be recorded.
28. Glideslope Deviation, MLS Elevation, or GPS Vertical Deviation.	±400 Microamps or available sensor range as installed 0.9 to +30°	As installed +/ 3 – 3% recommended.	1	0.3% of full range.	For autoland/category 3 operations. Each system should be recorded but arranged so that at least one is recorded each second. It is not necessary to record ILS and MLS at the same time, only the approach aid in use need be recorded.
29. Marker Beacon Passage.	Discrete "on" or "off".		1		A single discrete is acceptable for all markers.
30. Master Warning.	Discrete		1		Record the master warning and record each "red" warning that cannot be determined from other parameters or from the cockpit voice recorder.
31. Air/ground sensor (primary airplane system reference nose or main gear).	Discrete "air" or "ground".		1 (0.25 recommended).		
32. Angle of Attack (If measured directly).	As installed	As installed	2 or 0.5 for airplanes operated under §121.344(f).	0.3% of full range.	If left and right sensors are available, each may be recorded at 4 or 1 second intervals, as appropriate, so as to give a data point at 2 seconds or 0.5 second, as required.
33. Hydraulic Pressure Low, Each System.	Discrete or available sensor range, "low" or "normal".	±5%	2	0.5% of full range.	
34. Groundspeed	As Installed	Most Accurate Systems Installed.	1	0.2% of full range.	
35. GPWS (ground proximity warning system).	Discrete "warning" or "off".		1		A suitable combination of discretes unless recorder capacity is limited in which case a single discrete for all modes is acceptable.
36. Landing Gear Position or Landing gear cockpit control selection.	Discrete		4		A suitable combination of discretes should be recorded.
37. Drift Angle.[15]	As installed	As installed	4	0.1°	
38. Wind Speed and Direction.	As installed	As installed	4	1 knot, and 1.0°.	
39. Latitude and Longitude.	As installed	As installed	4	0.002°, or as installed.	Provided by the Primary Navigation System Reference. Where capacity permits Latitude/longitude resolution should be 0.0002°.
40. Stick shaker and pusher activation.	Discrete(s) "on" or "off".		1		A suitable combination of discretes to determine activation.
41. Windshear Detection.	Discrete "warning" or "off".		1.		

The recorded values must meet the designated range, resolution, and accuracy requirements during dynamic and static conditions. All data recorded must be correlated in time to within one second.

Parameters	Range	Accuracy (sensor input)	Seconds per sampling interval	Resolution	Remarks
42. Throttle/power Leverl position.[16].	Full Range	±2%	1 for each lever	2% of full range	For airplanes with non-mechanically linked cockpit engine controls.
43. Additional Engine Parameters.	As installed	As installed	Each engine each second.	2% of full range	Where capacity permits, the preferred priority is indicated vibration level, N2, EGT, Fuel Flow, Fuel Cut-off lever position and N3, unless engine manufacturer recommends otherwise.
44. Traffic Alert and Collision Avoidance System (TCAS).	Discretes	As installed	1		A suitable combination of discretes should be recorded to determine the status of—Combined Control, Vertical Control, Up Advisory, and Down Advisory. (ref. ARINC Characteristic 735 Attachment 6E, TCAS VERTICAL RA DATA OUTPUT WORD.)
45. DME 1 and 2 Distance.	0–200 NM	As installed	4	1 NM	1 mile
46. Nav 1 and 2 Selected Frequency.	Full Range	As installed	4		Sufficient to determine selected frequency
47. Selected barometric setting.	Full Range	±5%	(1 per 64 sec.)	0.2% of full range	
48. Selected Altitude.	Full Range	±5%	1	100 ft	
49. Selected speed.	Full Range	±5%	1	1 knot	
50. Selected Mach.	Full Range	±5%	1	.01	
51. Selected vertical speed.	Full Range	±5%	1	100 ft/min	
52. Selected heading.	Full Range	±5%	1	1°	
53. Selected flight path.	Full Range	±5%	1	1°	
54. Selected decision height.	Full Range	±5%	64	1 ft	
55. EFIS display format.	Discrete(s)		4		Discretes should show the display system status (e.g., off, normal, fail, composite, sector, plan, nav aids, weather radar, range, copy.
56. Multi-function/Engine Alerts Display format.	Discrete(s)		4		Discretes should show the display system status (e.g., off, normal, fail, and the identity of display pages for emergency procedures, need not be recorded.
57. Thrust command.[17].	Full Range	±2%	2	2% of full range.	
58. Thrust target	Full Range	±2%	4	2% of full range	
59. Fuel quantity in CG trim tank.	Full Range	±5%	(1 per 64 sec.)	1% of full range	
60. Primary Navigation System Reference.	Discrete GPS, INS, VOR/DME, MLS, Loran C, Omega, Localizer Glideslope.		4		A suitable combination of discretes to determine the Primary Navigation System reference.
61. Ice Detection	Discrete "ice" or "no ice".		4		
62. Engine warning each engine vibration	Discrete		1		

The recorded values must meet the designated range, resolution, and accuracy requirements during dynamic and static conditions. All data recorded must be correlated in time to within one second.

Parameters	Range	Accuracy (sensor input)	Seconds per sampling interval	Resolution	Remarks
63. Engine warning each engine over temp.	Discrete		1		
64. Engine warning each engine oil pressure low.	Discrete		1		
65. Engine warning each engine over speed.	Discrete		1		
66. Yaw Trim Surface Position.	Full Range	±3% Unless Higher Accuracy Uniquely Required.	2	0.3% of full range.	
67. Roll Trim Surface Position.	Full Range	±3% Unless Higher Accuracy Uniquely Required.	2	0.3% of full range.	
68. Brake Pressure (left and right).	As installed	±5%	1		To determine braking effort applied by pilots or by autobrakes.
69. Brake Pedal Application (left and right).	Discrete or Analog "applied" or "off".	±5% (Analog)	1		To determine braking applied by pilots.
70. Yaw or sideslip angle.	Full Range	±5%	1	0.5°	
71. Engine bleed valve position.	Discrete "open" or "closed".		4		
72. De-icing or anti-icing system selection.	Discrete "on" or "off".		4		
73. Computed center of gravity.	Full Range	±5%	(1 per 64 sec.)	1% of full range	
74. AC electrical bus status.	Discrete "power" or "off".		4		Each bus.
75. DC electrical bus status.	Discrete "power" or "off".		4		Each bus.
76 APU bleed valve position.	Discrete "open" or "closed".		4		
77. Hydraulic Pressure (each system).	Full range	±5%	2	100 psi	
78. Loss of cabin pressure.	Discrete "loss" or "normal".		1		
79. Computer failure (critical flight and engine control systems).	Discrete "fail" or "normal".		4		
80. Heads-up display (when an information source is installed).	Discrete(s) "on" or "off".		4		
81. Para-visual display (when an information source is installed).	Discrete(s) "on" or "off".				
82. Cockpit trim control input position—pitch.	Full Range	±5%	1	0.2% of full range.	Where mechanical means for control inputs are not available, cockpit display trim positions should be recorded.
83. Cockpit trim control input position—roll.	Full Range	±5%	1	0.7% of full range.	Where mechanical means for control inputs are not available, cockpit display trim position should be recorded.

The recorded values must meet the designated range, resolution, and accuracy requirements during dynamic and static conditions. All data recorded must be correlated in time to within one second.

Parameters	Range	Accuracy (sensor input)	Seconds per sampling interval	Resolution	Remarks
84. Cockpit trim control input position—yaw.	Full range	±5%	1	0.3% of full range.	Where mechanical means for control input are not available, cockpit display trim positions should be recorded.
85. Trailing edge flap and cockpit flap control position.	Full Range	±5%	2	0.5% of full range.	Trailing edge flaps and cockpit flap control position may each be sampled alternately at 4 second intervals to provide a sample each 0.5 second.
86. Leading edge flap and cockpit flap control position.	Full Range or Discrete.	±5%	1	0.5% of full range	
87. Ground spoiler position and speed brake selection.	Full range or discrete.	±5%	0.5	0.3% of full range.	
88. All cockpit flight control input forces (control wheel, control column, rudder pedal).	Full range control wheel ±70 lb control column ±85 rudder pedal ±165.	±5%	1	0.3% full range ..	For fly-by-wire flight control systems, where flight control surface position is a function of the displacement of the control input device only, it is not necessary to record this parameter. For airplanes that have a flight control break away). capability that allows either pilot to operate the control independently, record both control force inputs. The control force inputs may be sampled alternately once per 2 seconds to produce the sampling interval of 1.

[1] For A300 B2/B4 airplanes, resolution=6 seconds.
[2] For A330/A340 series airplanes, resolution=0.703°.
[3] For A318/A319/A320/A321 series airplanes, resolution=0.275% (0.088°>0.064°).
For A330/A340 series airplanes, resolution=2.20%(0.703°>0.064°).
[4] For A318/A319/A320/A321 series airplanes, resolution=0.22% (0.088°>0.080°).
For A330/A340 series airplanes, resolution=1.76% (0.703°>0.080°).
[5] For A330/A340 series airplanes, resolution = 1.18% (0.703°>0.120°).
[6] For A330/A340 series airplanes, resolution=0.783% (0.352°>0.090°).
[7] For A330/A340 series airplanes, aileron resolution = 0.704% (0.352°>0.100°). For A330/A340 series airplanes, spoiler resolution = 1.406% (0.703°>0.100°).
[8] For A330/A340 series airplanes, resolution=0.30% (0.176°>0.12°).
For A330/A340 series airplanes, seconds per sampling interval=1.
[9] For B–717 series airplanes, resolution = .005g. For Dassault F900C/F900EX airplanes, resolution = .007g.
[10] For A330/A340 series airplanes, resolution=1.05% (0.250°>0.120°).
[11] For A330/A340 series airplanes, resolution = 1.05% (0.250°>0.120°). For A300 B2/B4 series airplanes, resolution = 0.92% (0.230°>0.125°).
[12] For A330/A340 series airplanes, spoiler resolution = 1.406% (0.703°>0.100°).
[13] For A330/A340 series airplanes, resolution=0.5°C.
[14] For Dassault F900C/F900EX airplanes, Radio altitude resolution = 1.25 ft.
[15] For A330/A340 series airplanes, resolution = 0.352 degrees.
[16] For A318/A319/A320/A321 series airplanes, resolution = 4.32%. For A330/A340 series airplanes, resolution is 3.27% of full range for throttle lever angle (TLA); for reverse thrust, reverse throttle lever angle (RLA) resolution is nonlinear over the active reverse thrust range, which is 51.54 degrees to 96.14 degrees. The resolved element is 2.8 degrees uniformly over the entire active reverse thrust range, or 2.9% of the full range value of 96.14 degrees.
[17] For A318/A319/A320/A321 series airplanes, with IAE engines, resolution = 2.58%.

[Doc. No. 28109, 62 FR 38382, July 17, 1997; 62 FR 48135, Sept. 12, 1997, as amended by Amdt. 121–271, 64 FR 46120, Aug. 24, 1999; Amdt. 121–278, 65 FR 51745, Aug. 24, 2000; 65 FR 81733, Dec. 27, 2000; Amdt. 121–292, 67 FR 54323, Aug. 21, 2002; Amdt. 121–300, 68 FR 42936, July 18, 2003; 68 FR 50069, Aug. 20, 2003; 68 FR 53877, Sept. 15, 2003]

APPENDIX N TO PART 121—DESIGN-LIFE GOALS

Airplane type	Number of seats	Type certificate data sheet	Design-life goal (hours)
Raytheon (Beech) Aircraft Co.:			
—Beech 99 (all models)	15+2	A14CE	46,000
—Beech 1900 and 1900C	19+2	A24CE	45,000
—Beech 300 and 300LW	13+2	A24CE	30,000
—Beech B300 and B300C	15+2	A24CE	30,000
—Beech 1900D	19+2	A24CE	45,000
British Aerospace Ltd.:			
—BAe Jetstream 3101	19+2	A21EU	45,000
—BAe Jetstream 3201	19+2	A56EU	30,000
deHavilland Aircraft Co.: DHC–6	22+2	A9EA	33,000
Dornier Luftfahrt GmbH:			
—Dornier 228–100 and –200	19+2	A16EU	42,800
—Dornier 228–101 and –201	19+2	A16EU	32,800
—Dornier 228–202	19+2	A16EU	29,600
—Dornier 228–212 (Except SN 155 & 191 and up)	19+2	A16EU	26,400
—Dornier 228–212 (SN 155 and 191 and up)	19+2	A16EU	42,800
Empresa Brasileira de Aeronautica (Embraer): Embraer EMB–110	19+2	A21SO	30,000
Fairchild Aircraft Corporation:			
—SA226–TC	20+2	A8SW	35,000
—SA227–AT	14+2	A5SW	35,000
—SA227–TT	9+2	A5SW	35,000
—SA227–AC	20+2	A8SW	35,000
—SA227–PC	20+2	A8SW	35,000
—SA227–BC	20+2	A8SW	35,000
—SA227–CC	19+2	A18SW	35,000
—SA227–DC	19+2	A18SW	35,000
Pilatus Britten-Norman: PBN BN–2 Mk III (all models)	16+2	A29EU	20,480
Short Brothers PLC:			
—SD3–30	39+2	A41EU	57,600
—SD3–60	39+2	A41EU	28,800
—SD3–Sherpa	39+2	A41EU	40,000

[Doc. No. FAA-1999-5401, 67 FR 72762, Dec. 6, 2002]

PART 125—CERTIFICATION AND OPERATIONS: AIRPLANES HAVING A SEATING CAPACITY OF 20 OR MORE PASSENGERS OR A MAXIMUM PAYLOAD CAPACITY OF 6,000 POUNDS OR MORE; AND RULES GOVERNING PERSONS ON BOARD SUCH AIRCRAFT

SPECIAL FEDERAL AVIATION REGULATION NO. 89 [NOTE]

SPECIAL FEDERAL AVIATION REGULATION NO. 97 [NOTE]

Subpart A—General

Sec.

125.1 Applicability.
125.3 Deviation authority.
125.5 Operating certificate and operations specifications required.
125.7 Display of certificate.
125.9 Definitions.
125.11 Certificate eligibility and prohibited operations.

Subpart B—Certification Rules and Miscellaneous Requirements

125.21 Application for operating certificate.
125.23 Rules applicable to operations subject to this part.
125.25 Management personnel required.
125.27 Issue of certificate.
125.29 Duration of certificate.
125.31 Contents of certificate and operations specifications.
125.33 Operations specifications not a part of certificate.
125.35 Amendment of operations specifications.
125.37 Duty period limitations.
125.39 Carriage of narcotic drugs, marihuana, and depressant or stimulant drugs or substances.
125.41 Availability of certificate and operations specifications.
125.43 Use of operations specifications.
125.45 Inspection authority.
125.47 Change of address.
125.49 Airport requirements.
125.51 En route navigational facilities.
125.53 Flight locating requirements.

APPENDIX C—DERIVATION OF FLIGHT CONTROL DEFLECTION STATISTICS FROM DATA OBTAINED AT LOW SAMPLING RATES

C.1 INTRODUCTION.

The main body of this report provides the results of a study of sampling rate effects on load parameter statistics including flight control surface deflections. The results of the study showed that lower sampling rates affect the resulting cumulative occurrence spectra of the parameters. The extent of the effect is related to the frequency content of the parameter time history. The inclination is to interpret this effect as a reduction in the number of peaks counted due to the lower sampling rates. Table 5 of the report shows that the minimum sampling rate required to identify a peak amplitude within a maximum error of 10 percent is greater than the sampling rate required to identify the existence of a peak. Since the sampling rate required to capture the correct amplitude is higher than that needed to capture the existence of a peak, the differences seen in the peak count statistics are more likely due to the inability to record the correct peak amplitudes than it is to record the existence of a peak. If it is assumed that the correct number of peaks is counted, then using the approach of reference C-1, the cumulative occurrence spectra derived at low sampling rates can be corrected to account for the errors in peak amplitude due to low sampling rates.

C.2 GENERAL POWER SPECTRAL DENSITY DISCUSSION.

The power spectral density (PSD) of a time history displays the variation in parameter root mean square (rms) magnitude (power) as a function of the frequencies inherent in the time history. Figure C-1 shows a sinusoidal time history of 0.05 cycles per second. The PSD of the sinusoidal signal is presented in figure C-2. As can be seen, the signal's primary power is centered at the signal's frequency of 0.05 Hertz (Hz). While the total power of the sinusoid is in truth centered exactly at 0.05 Hz, the fast Fourier transform (FFT) technique used to calculate the PSD tends to average this total power that exists at a distinct frequency over a fixed frequency window, dependent on the sampling rate of the signal. Nevertheless, it still shows the important frequency peak. Figure C-3 shows the same sinusoidal time history, but with secondary random frequencies, such as noise, superimposed on the basic signal. Figure C-4 shows the PSD for this noisy sinusoidal time history. Note that the primary sinusoidal frequency is still shown as a power peak, but the power associated with the superimposed frequencies in the signal is shown at the higher frequencies at considerably lower levels of power. The same PSD presented on a linear scale would show the power at these higher frequencies to be insignificant. These higher frequencies would not be counted as separate peaks in the derivation of a cumulative occurrence curve. The higher frequencies shown in the example are representative of the frequencies seen in the control surface deflection time histories. They represent control surface deflections of small magnitude and high frequency experienced at fixed control surface positions during level cruise or superimposed on large, slower frequency deflections associated with maneuvers.

As shown in section 3.1, integration of the PSD provides insight into a possible choice for a cutoff frequency to be considered for data sampling.

Figures C-5 and C-6 show the increase in power as frequency increases for the PSDs of figures C-2 and C-4, respectively. In both figures, a frequency cutoff associated with 90% of rms accounts for the primary frequency.

C.3 PEAK AMPLITUDE ERROR DISCUSSION.

Table C-1 presents the frequencies at which the rms level reaches 90 percent of its total value for the aileron, elevator, and rudder from the three flights shown previously.

According to the Nyquist theorem, a sampling rate of twice the cutoff frequency would detect the peaks existing in the signal below the cutoff frequency, if not the correct magnitude. From the cutoff frequencies shown in the table, a sampling rate of once per second would appear to be adequate to identify the existence of a peak within the frequency range of interest. Reference C-1 provides a means to estimate the maximum error in peak magnitude as a function of the sampling rate for bandwidths below the cutoff frequency.

$$\%error = 100 * (1 - \cos\frac{2\pi F}{2f} \qquad \text{(C-1)}$$

where: F = bandwidth or cutoff frequency
f = sampling rate

As pointed out in section 3.3 in this report, the actual error may be anywhere from zero percent error to maximum error. Assuming an average error equal to one-half the maximum possible error, figure C-7 shows the average peak error as a function of signal bandwidth and sampling rate.

Figures C-8 through C-10, reproduced from figures 155, 158, and 161, present the cumulative occurrence counts at different sampling rates for aileron, elevator, and rudder respectively. If the primary signal frequency is less than or equal to one-half the sampling frequency, then no peaks should be lost. The sampling rates presented in the figure are faster than twice the cutoff frequency at 95 percent of rms, as shown in table C-1. Thus, the differences shown in the cumulative occurrence spectra are likely due to errors in the magnitude of the counted peaks rather than the number of peaks counted.

Figure C-11 shows the percent change in peak count magnitude that can be expected when changing the sampling rate to 2 samples per second from 4 and 16 samples per second. These curves are based on the information shown in figure C-7.

From figure C-11, for an aileron frequency cutoff equal to or less than 0.15 Hz, a sampling rate of two samples per second would be expected to result in an average error change in peak magnitude from 16 samples per second of approximately 1.25 percent. For the elevator cutoff frequency of 0.5 Hz, a sampling rate of two samples per second would be expected to result in an average change in peak magnitude form of four samples per second of approximately 10.44 percent. For the rudder cutoff frequency of 0.35 Hz, a sampling rate of two samples per second would be expected to result in an average change in peak magnitude form of 16 samples per second of approximately 7.4 percent.

C.4 APPLICATION OF ERROR CORRECTION.

In the procedure discussed in section 3.3, the selected cutoff frequency is determined by the frequency at which the rms reaches 90 percent of the total rms or 90 percent of the area under the PSD curve. At the same time, the overall PSD curve is defined by the sampling rate and the frequency content of the time history. Figure C-12 presents the variation of rms as a function of sampling rate for an aileron time history. The figure shows that the frequency at which the rms reaches 90 percent of the total rms under the PSD curve is little affected by sampling rates of two samples per second or faster. Figures C-13 and C-14 show similar results for the elevator and rudder. This suggests that the primary frequency of the flight control surface deflections, at least for the A-319 on which this study was based, is below one cycle per second, and that the two samples per second is adequate to capture the primary peaks. It is a fair assumption that the flight control surface deflections rates on other aircraft are similar, and that flight control deflection data based on sampling rates of two samples per second can be used to calculate necessary PSDs and determine the desired cutoff frequencies for the 90 percent rms level for the aileron, elevator, and rudder. Given this cutoff frequency, the average expected error can be obtained from figure C-7 and used as a correction to the counted peak magnitudes. The procedure would be as follows:

- Use the time histories for a control surface deflection for a number of random flights to calculate the PSDs.
- For each PSD, determine the increase in rms as a percent of the total rms as a function of frequency.
- Select the cutoff frequencies at the 90 percent rms level.
- Select the highest cutoff frequency from the randomly selected flights and determine the expected maximum error in peak magnitudes from figure C-7.
- Increase the peak magnitudes in the cumulative occurrence graphs to account for the error in magnitude.

$$\delta_{corrected} = \delta_{recorded}\left(1 + \frac{\%error}{100}\right) \tag{C-2}$$

Because the records sampled at 16 samples per second also contain some error, this correction will provide cumulative occurrence spectra slightly more severe than would be obtained from the 16 samples per second time history.

Figures C-15 through C-17 show comparison of the spectra adjusted from two samples per second to the spectra measured at the maximum sampling rates for the aileron, elevator, and rudder respectively. The corrections were based on the 1.25, 10.44, and 7.4 percent errors discussed in section C.3.

C.5 CONCLUSIONS.

The study discussed in this report concluded that the sampling rates used for load parameter recording, including flight control surface deflections, were too low to ensure that correct peak magnitudes were counted. However, it was shown that the approach of reference C-1 might provide reasonable estimates of the average expected magnitude errors. Depending on the selected cutoff frequency, figure C-7 will provide an estimate of the expected average error for the sampling rate of interest. Increasing the peak count magnitudes to account for this error should improve the cumulative occurrence spectra to levels more consistent with those expected from faster sampling rates.

C.6 REFERENCES.

C-1. Anonymous, "Analysis of Relationship Between Sample Rate, Data Bandwidth and Accuracy for Flight Data Recorders with A/D Converters," Technical Note EER-912, Esprit Technology Inc., September 1991.

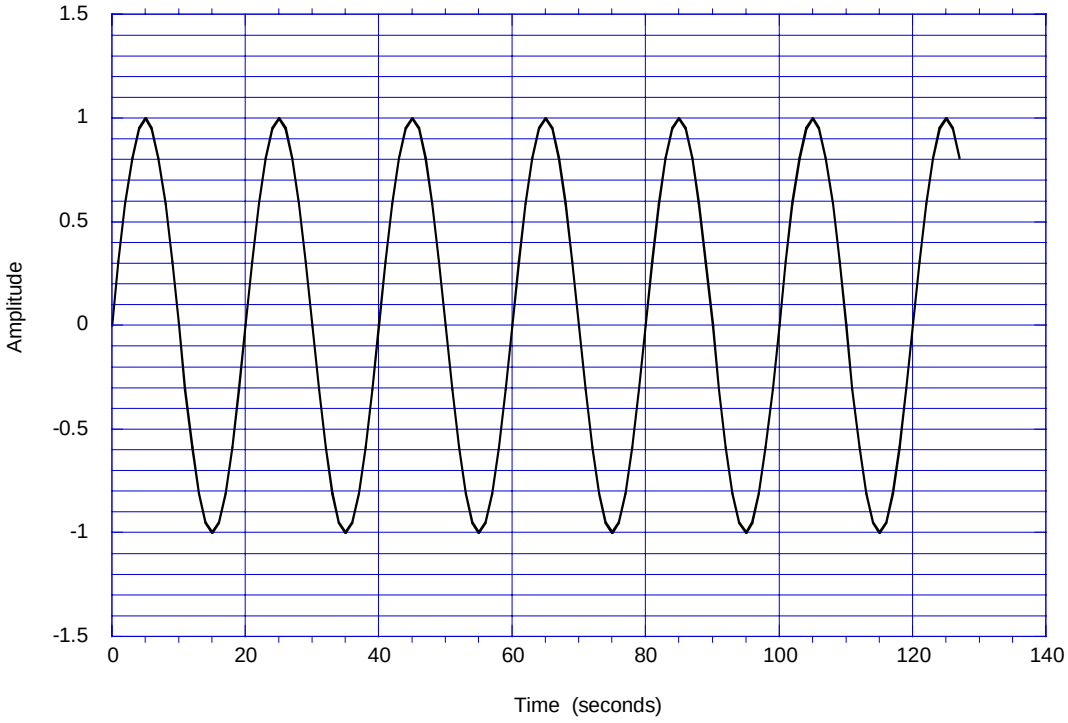

FIGURE C-1. TIME WAVEFORM OF A PURE SINUSOID

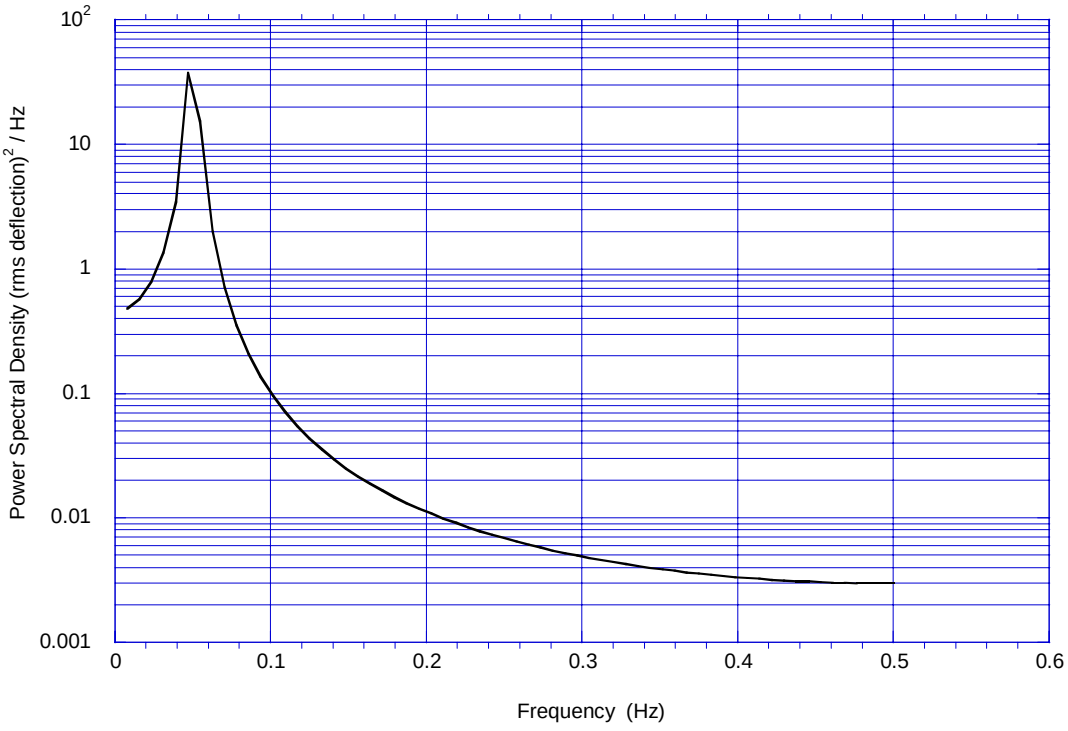

FIGURE C-2. POWER SPECTRAL DENSITY OF A PURE SINUSOID

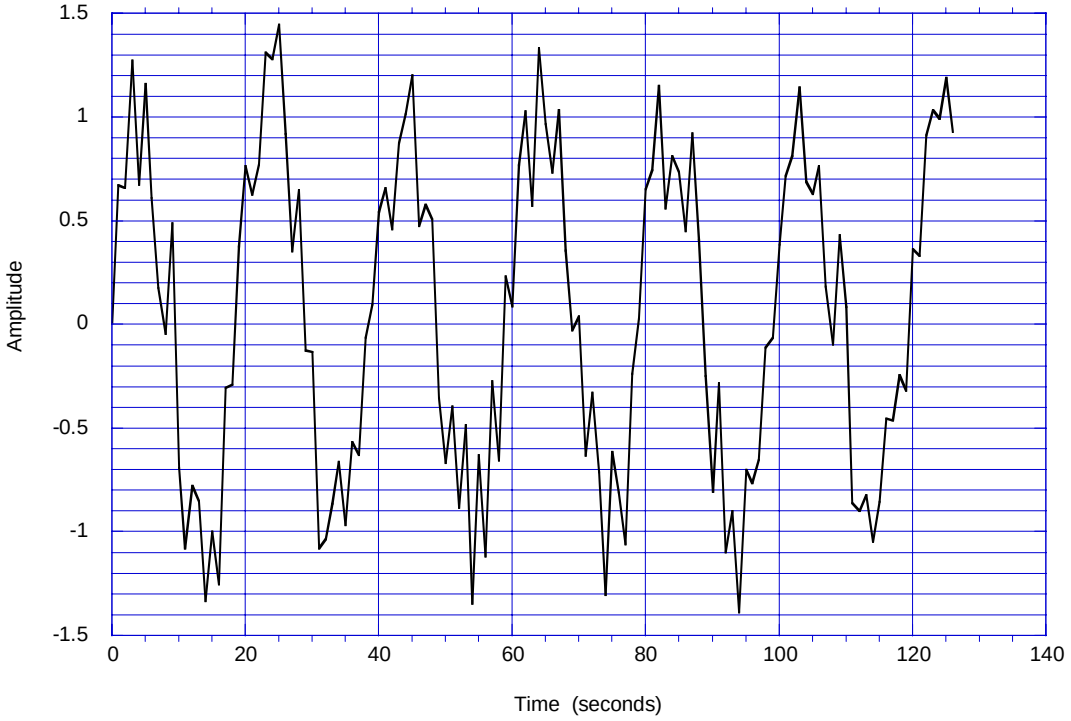

FIGURE C-3. TIME WAVEFORM OF A NOISED SINUSOID

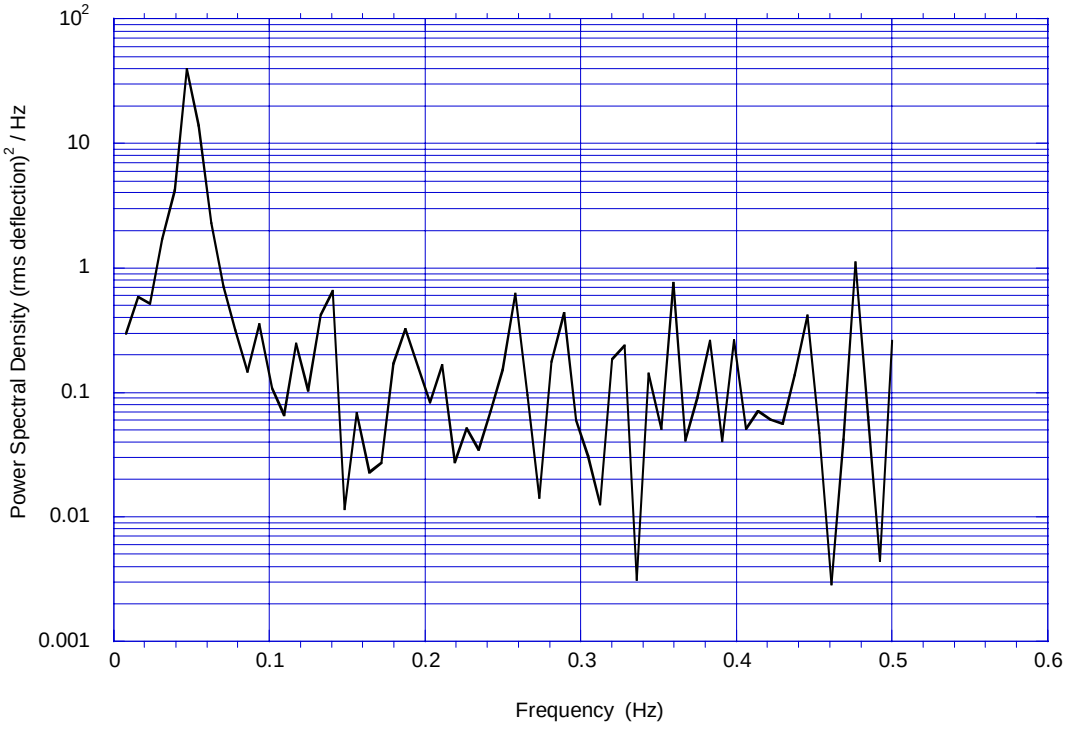

FIGURE C-4. POWER SPECTRAL DENSITY OF A NOISED SINUSOID

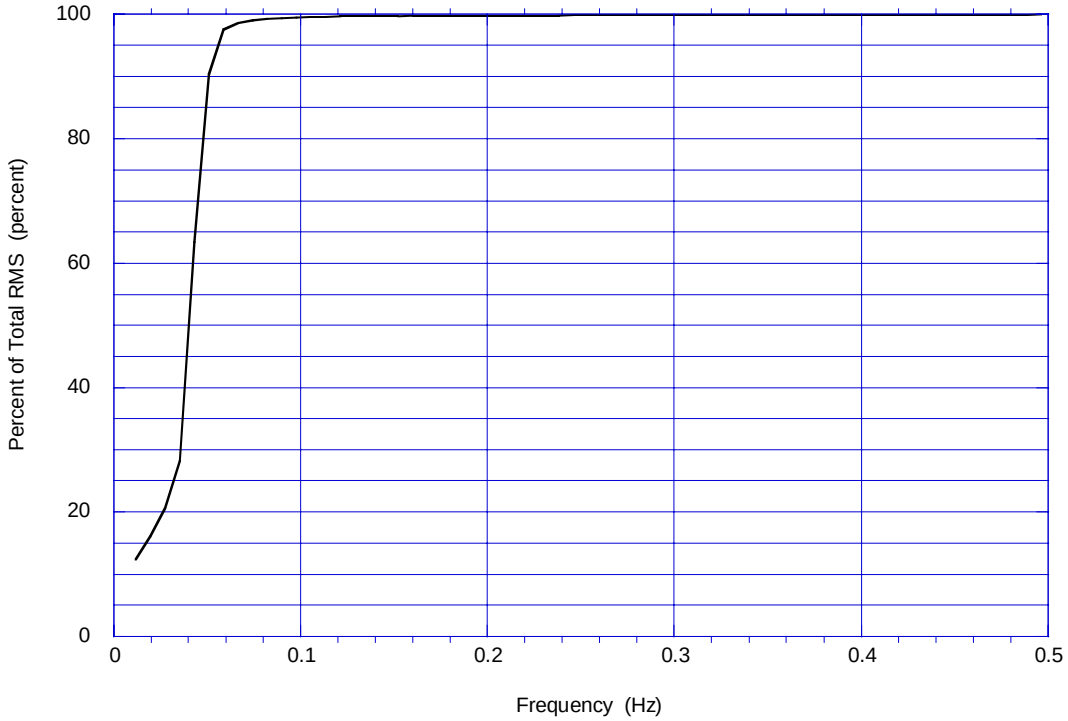

FIGURE C-5. PERCENT OF PURE SINUSOID RMS VS FREQUENCY

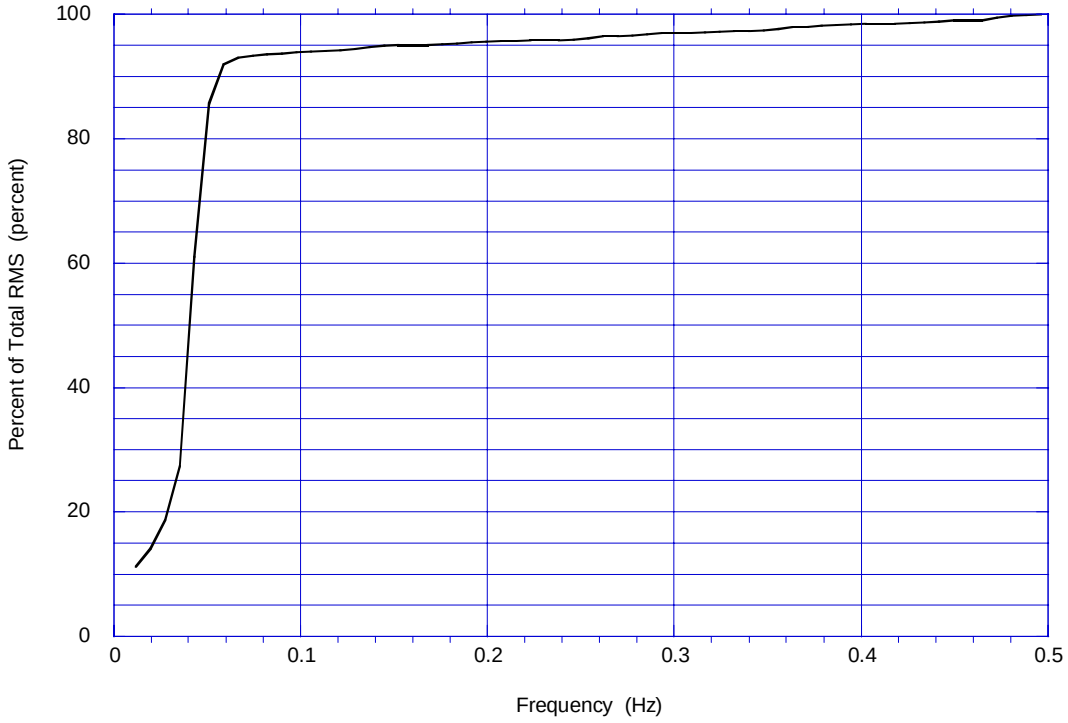

FIGURE C-6. PERCENT OF NOISED SINUSOID RMS VS FREQUENCY

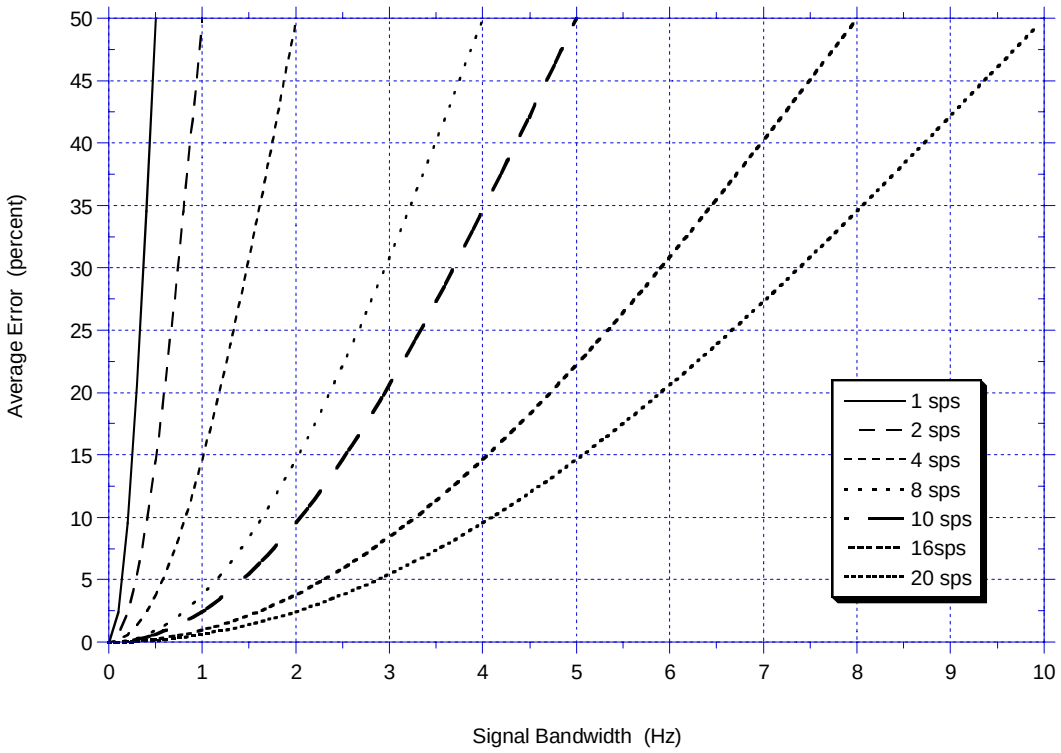

FIGURE C-7. AVERAGE PEAK ERROR VS BANDWIDTH BY SAMPLING RATE

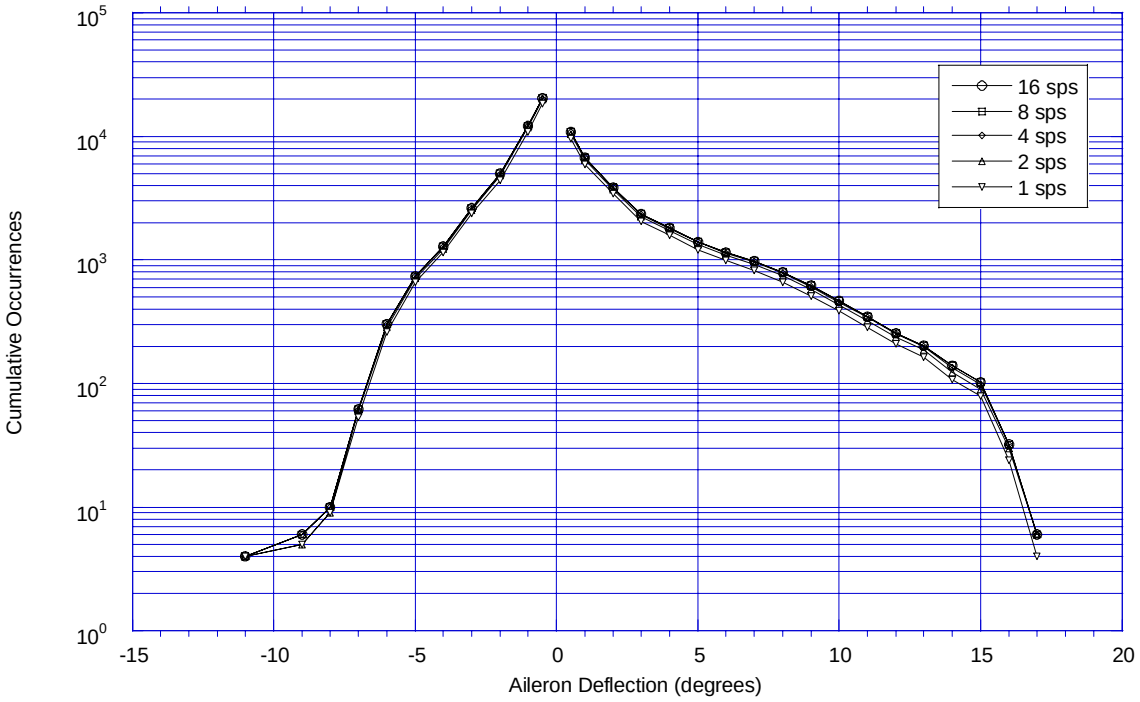

FIGURE C-8. CUMULATIVE OCCURRENCES OF AILERON DEFLECTION

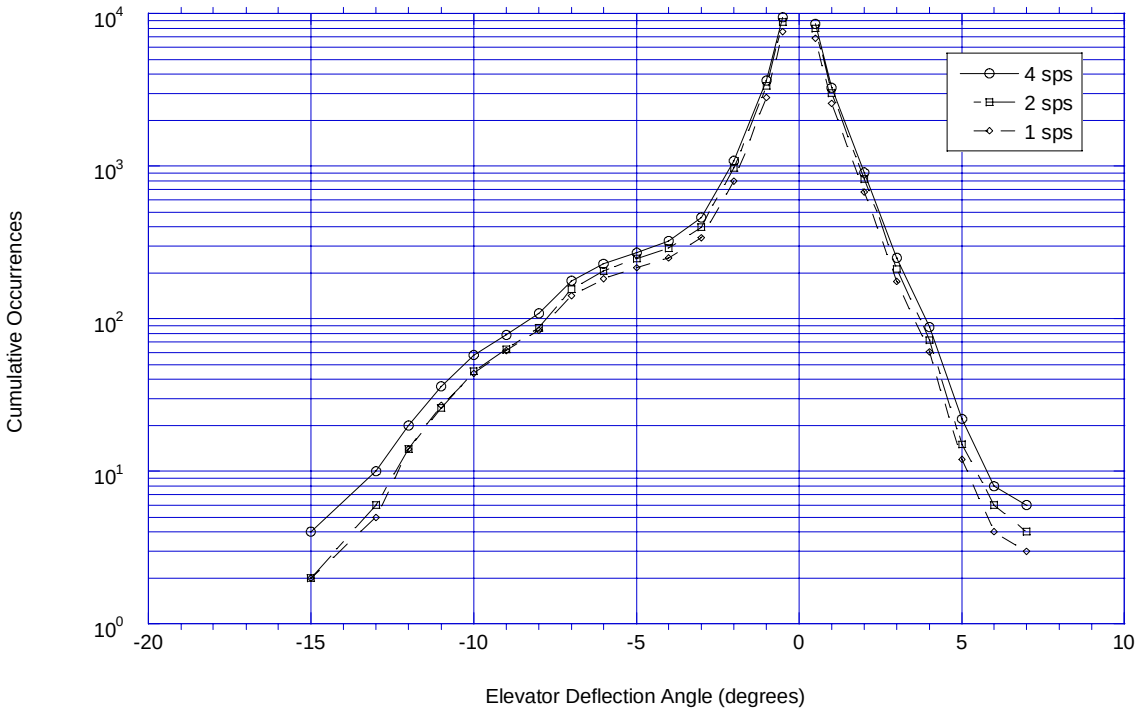

FIGURE C-9. CUMULATIVE OCCURRENCES OF ELEVATOR DEFLECTION

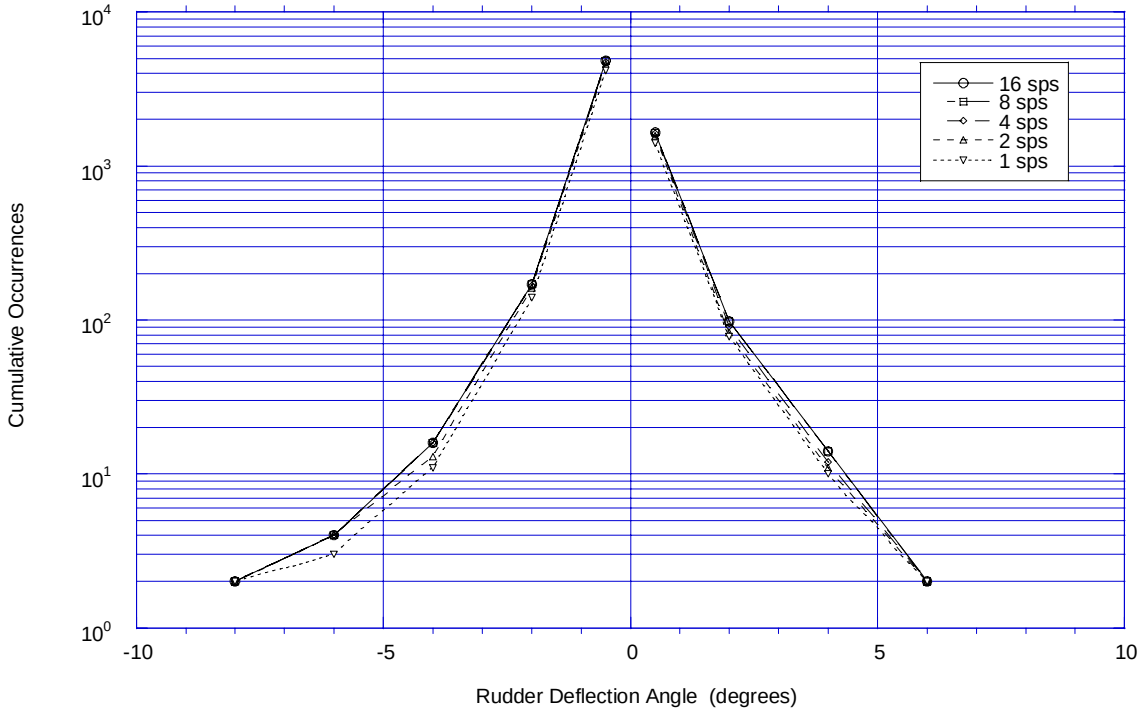

FIGURE C-10. CUMULATIVE OCCURRENCES OF RUDDER DEFLECTION

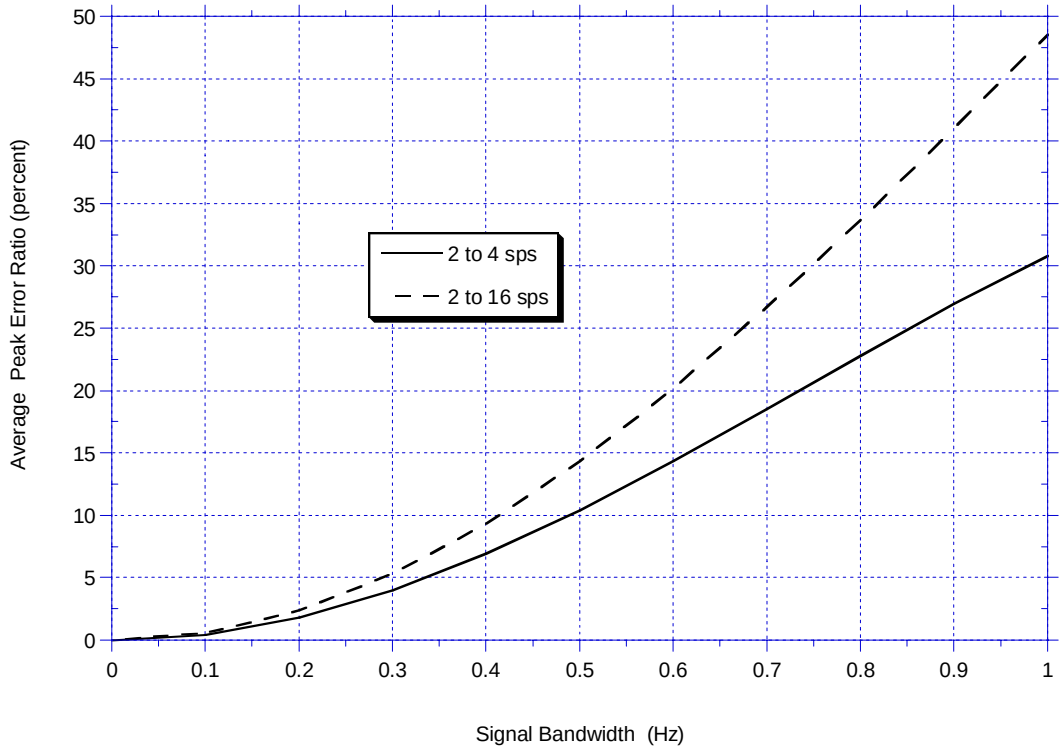

FIGURE C-11. AVERAGE DELTA PEAK ERROR VS SIGNAL BANDWIDTH

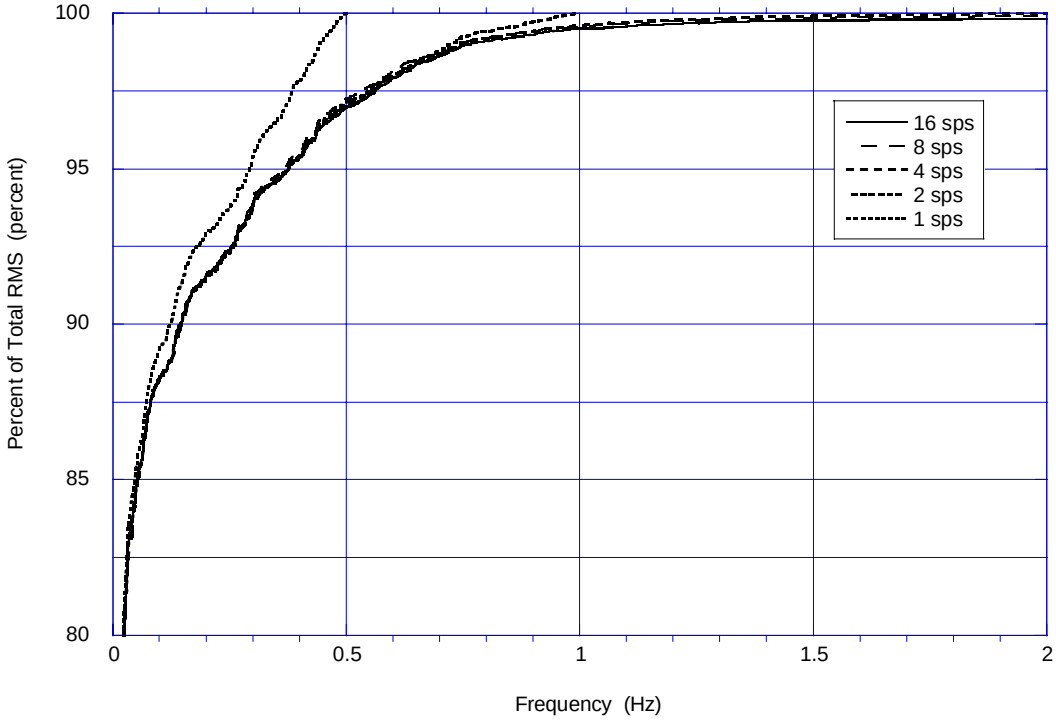

FIGURE C-12. PERCENT OF ALERON RMS VS FREQUENCY FOR DIFFERENT SAMPLING RATES

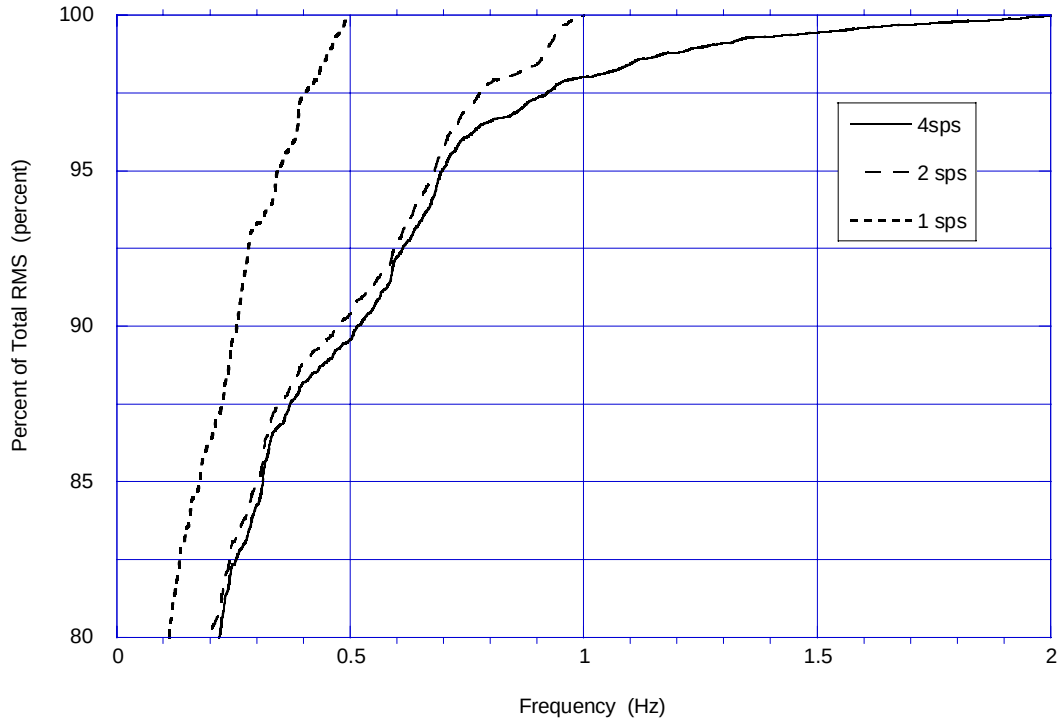

FIGURE C-13. PERCENT OF ELEVATOR RMS VS FREQUENCY FOR DIFFERENT SAMPLING RATES

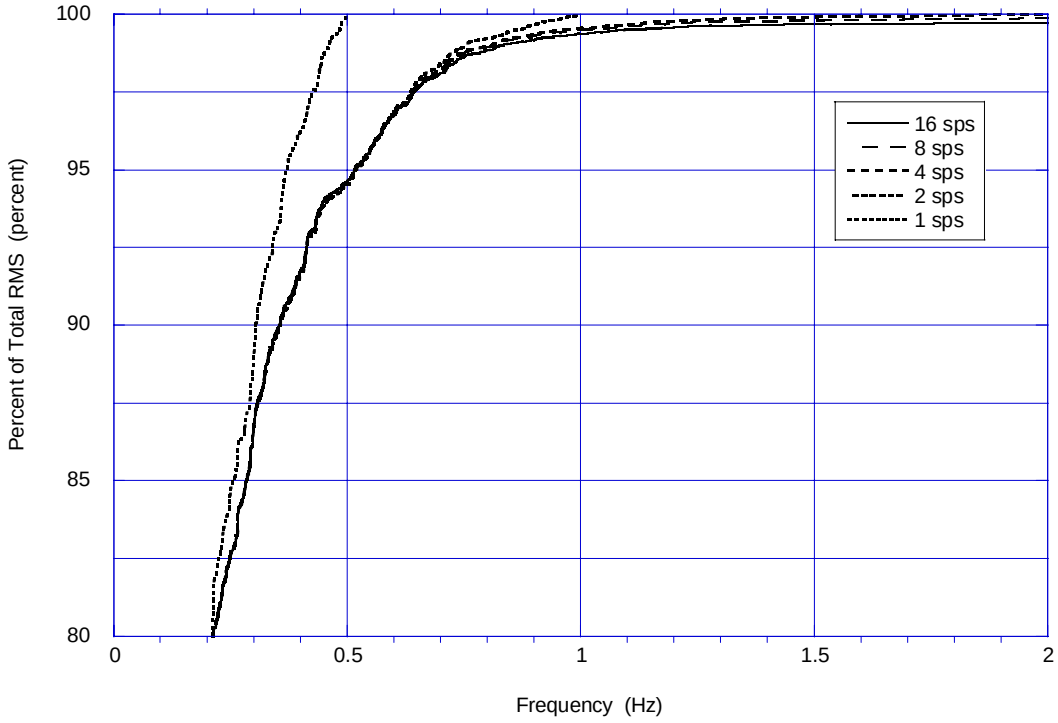

FIGURE C-14. PERCENT OF RUDDER RMS VS FREQUENCY FOR DIFFERENT SAMPLING RATES

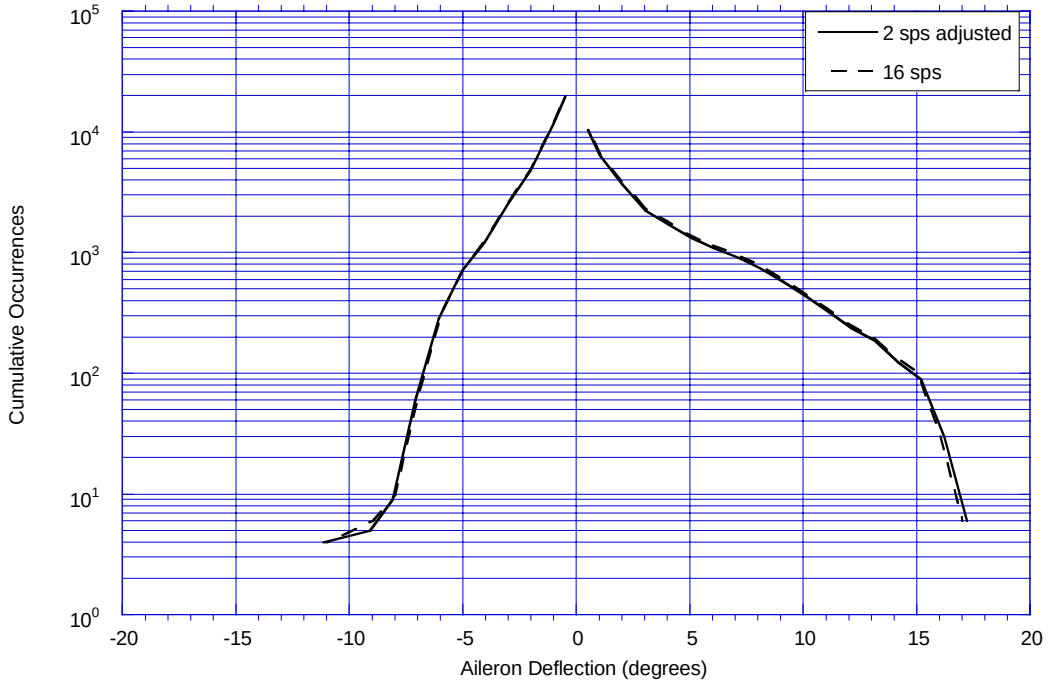

FIGURE C-15. COMPARISON OF ADJUSTED AND MEASURED AILERON CUMULATIVE OCCURRENCES

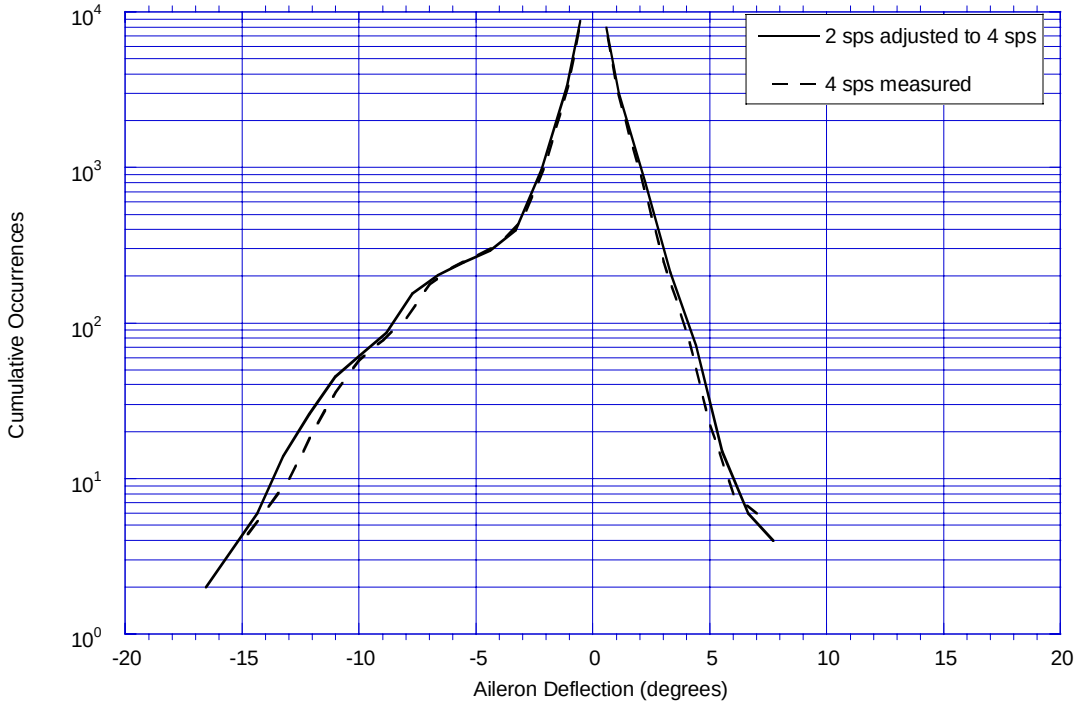

FIGURE C-16. COMPARISON OF ADJUSTED AND MEASURED ELEVATOR CUMULATIVE OCCURRENCES

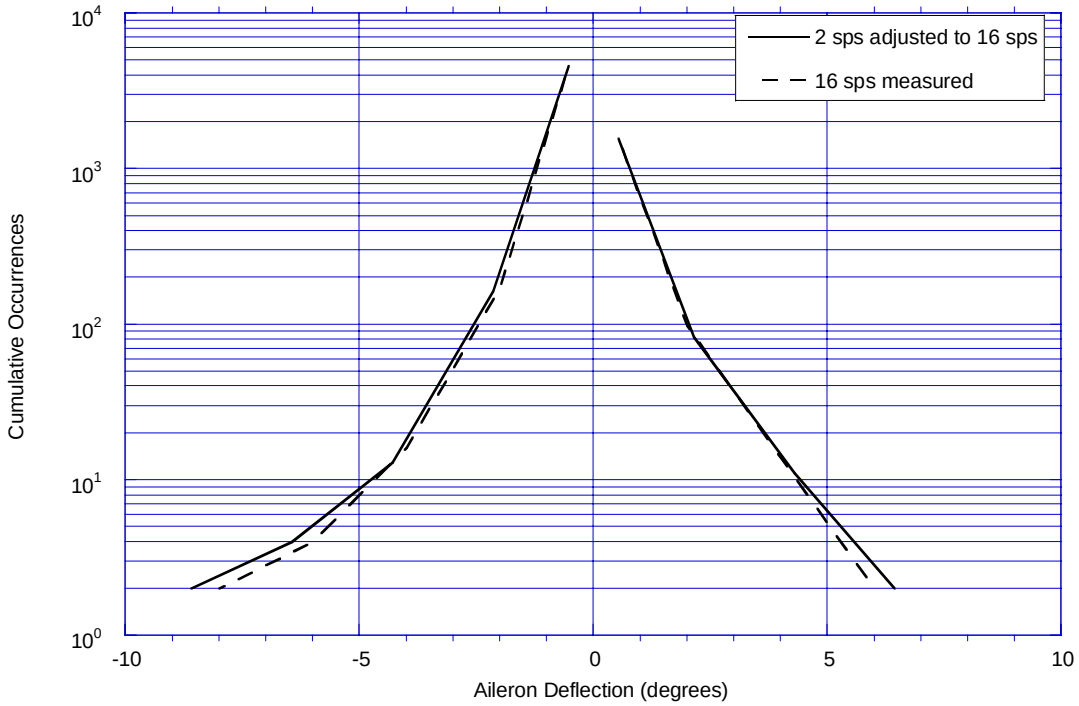

FIGURE C-17. COMPARISON OF ADJUSTED AND MEASURED RUDDER CUMULATIVE OCCURRENCES

TABLE C-1. CUTOFF FREQUENCY AT 95% RMS

Control Surface	Flight Sequence 3	Flight Sequence 35	Flight Sequence 62
Aileron	0.02	0.01	0.15
Elevator	0.5	0.07	0.43
Rudder	0.25	0.15	0.35

APPENDIX D—COMMENTS ON UDR-TR-2004-00146, R. HOWES, CESSNA AIRCRAFT COMPANY

Although this report expresses concern about the aliasing effects in general terms the specific effects of aliasing were not explored in this report. Mr. Robert L. Howes, Manager of Loads, Acoustics and Structural Dynamics at the Cessna Aircraft Company has pointed out that down sampling without proper filtering may result in aliasing and will skew the results and underestimate the final peak exceedances. This addendum contains his note discussing the results from a small test case. The results in the note underscore the conclusions of the report that existing sampling rates are too low and that the minimum sampling rates derived in this study cannot be considered conservative estimates.

.

Comments on UDR-TR-2004-00146, "A Study of Sampling Rate Requirements for Some Load Parameter Statistics."

Introduction

The study (ref 1) under discussion was conducted in support of an FAA Airborne Data Monitoring Systems program. The objective of the work was to determine the impact of sampling rates on flight and ground usage data. Flight data was taken from three flights on a typical commercial transport aircraft. The data was acquired at 16 samples per second. The sampling rate was then successively reduced and the impact on parameter exceedance data was examined. Sampling rates of 8,4,2 and 1 s/s were considered. The original flight data was processed to reflect the reduced sample rates using a downsampling technique. Downsampling refers to the practice of reducing sample rate by simply selecting every nth sample. This technique invites frequencies in the original data that exceed the new Nyquist frequency to alias into the downsampled data. Any aliasing that occurs will skew the exceedance calculations. If the reduced sample rates are generated from the original data by filtering and decimating, the bias introduced by aliasing is eliminated. An example is offered here to demonstrate the possible effects of this bias.

Discussion

Consider a second order system with the transfer function shown in figure 1. This is intended to represent the CG acceleration response to atmospheric turbulence. In fact, the system was chosen to represent a rigid body response around .5 Hz, a structural response at 2.5Hz another at 3.0 Hz and one at 6.0 Hz. These values were chosen as an approximation to the data shown in the referenced study, taken from the spectral data included there.

Figure 2: Impulse response, sample system

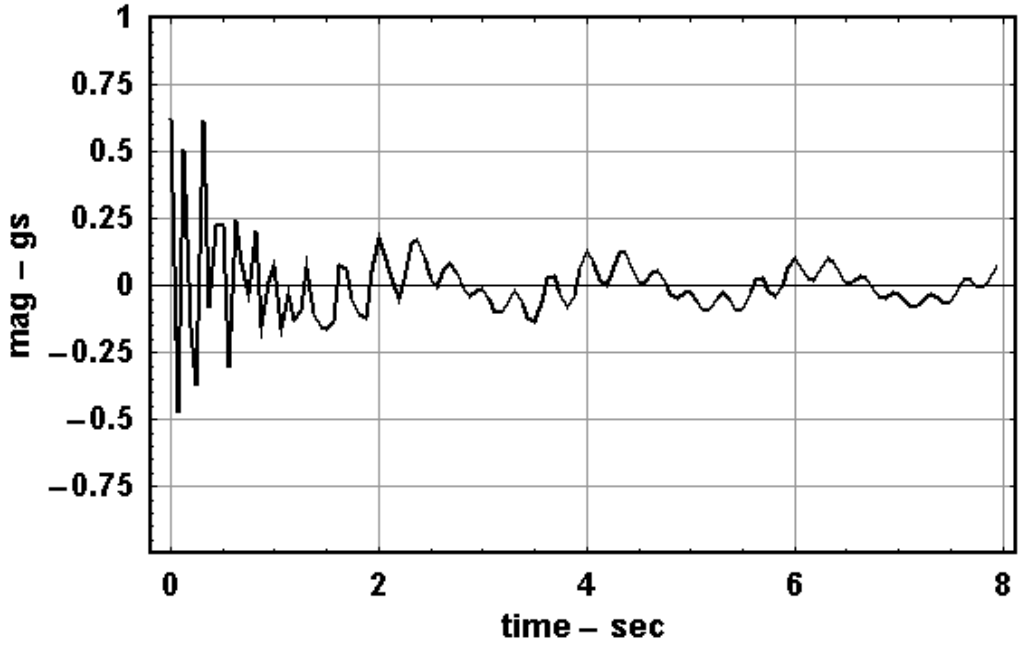

The resulting output was downsampled to 8 samples/second and filtered and decimated to 8 samples/sec[5]. In each case the resulting time histories were processed with a peak counting routine and exceedance data were extracted. Figure 3 shows the resulting exceedance curves.

Figure 3: Exceedance calculations

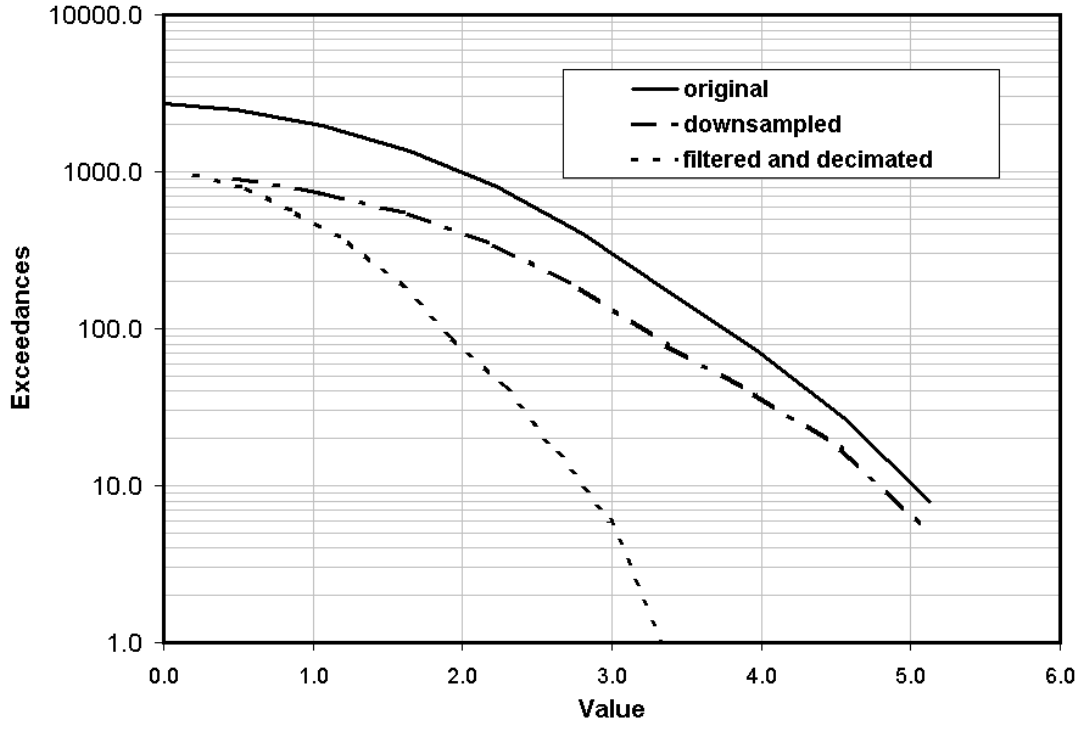

[4] See

[5] See [3] *downsample* and *decimate* functions

Figure 1: $H(f)$ for sample system

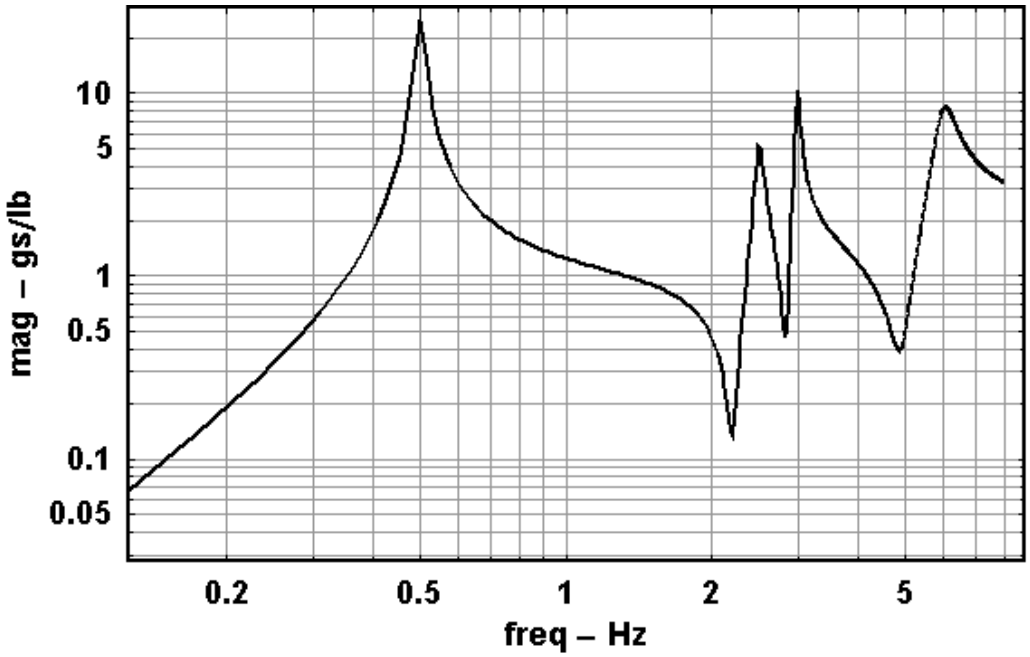

The model in figure 1 was constructed from the following modal parameters[1]:

Table 1: Modal parameters for sample system

Frequency, Hz, f_i	Damping, %, ζ_i	Weighting, h_i
0.5	2.0	1.0
2.5	2.0	0.2
3.0	1.0	0.2
6.0	5.0	0.8

Sampled data for this test case was generated using a random number sequence for the input[2]. The output was generated at 16 samples/second by filtering the random input with a FIR filter[3] derived from the impulse response of the system shown in figure 1[4]. Figure 2 shows the impulse response used to derive the filter.

---

[1] System was synthesized using $H(f) = \sum_i h_i \frac{\beta_i^2}{(1-\beta_i^2) + 2i\beta_i\zeta_i}, \quad \beta_i = \frac{f}{f_i}$

[2] See [3], *randn* function.

3 See [3], *filter* function.

Figures 4a and 4b show PSD estimates calculated from the output for each case. Notice that in the downsampled case there is a significant peak around 2 Hz that is not present in the other two cases. This is aliased data generated by the downsampling done without filtering. It is the 6 Hz content folded around the new Nyquist frequency of 4 Hz. It is this extraneous peak that has skewed the results. Notice that PSD for the data generated at 8 samples/second by filtering and decimating the original data looks like the PSD for the original data minus the 6 Hz peak.

Figure 4a: PSD of 16 s/s data

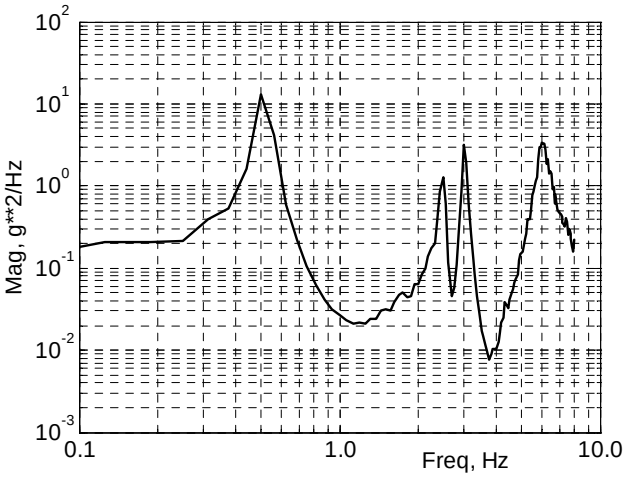

Figure 4b: PSDs of 8 s/s data

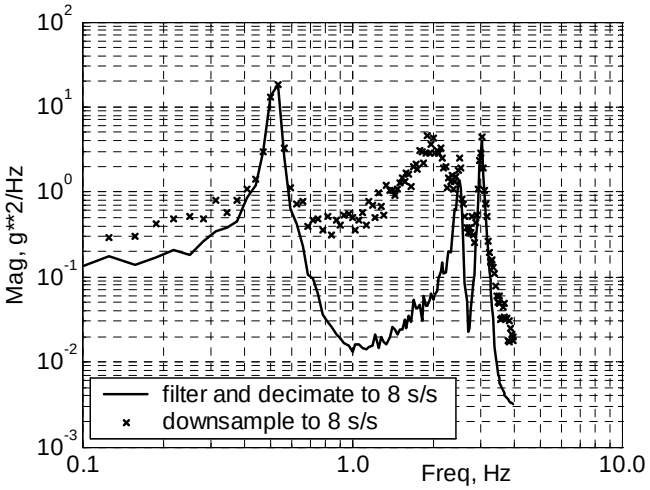

From reference 2, the exceedance curves of figure 3 are given by

$$N = N_0 e^{\left[-\frac{1}{2}\left(\frac{z}{\sigma_z}\right)^2\right]} \tag{1}$$

or

$$\ln N = \ln N_0 - \frac{1}{2\sigma_z^2} z^2 \tag{2}^6$$

where

$$\sigma_z^2 = \int_0^\infty S_{zz}(f)\,df \tag{3}$$

and

$$N_0 = \frac{1}{\sigma_z}\left[\int_0^\infty f^2 S_{zz}(f)\,df\right]^{\frac{1}{2}} \tag{4}$$

---

[6] (2) has the form, $f(x) = ax^2 + b$ where $f(x) = \ln N$, $a = -\frac{1}{2\sigma_z^2}$ and $b = \ln N_0$. Note that

$$\frac{d^2 f(x)}{dx^2} = -\frac{1}{\sigma_z^2}$$

Inspection of (2) and (3) shows that Introducing extraneous peaks in S_{zz} artificially increases the integral in (3). This results in an increase in σ_z and skews the exceedance data at higher values. The effect on N_0 is less dramatic.

Conclusion

The signal processing procedures used in the referenced study to reduce the sample rates of the data under consideration likely skewed the results in some cases. This effect would not change the conclusion, e.g. insufficient sample rates introduce inaccuracies in the resulting exceedance data. Rather it understated the errors that are introduced. A final look at figure 3 shows that when sample rates exclude higher frequencies the exceedance data at higher values is significantly underestimated.

List of References

1. Rustenburg, J.;Tipps, D.O.; Skinn, D.; UDR-TR-2004-00146; "A Study of Sampling Rate Requirements for some Load Parameter Statistics"; Sept 2004.
2. Jones, J.G.; "A Unified Discrete Gust and Power Spectrum Treatment of Atmospheric Turbulence", Royal Aircraft Establishment; Technical Memorandum Aero 1315; April 1971.
3. Signal Processing Toolbox for use with MATLAB, User's Guide, Version 5, The MathWorks, Sep 2000.

Robert L. Howes
Manager, Loads, Acoustics and Structural Dynamics
Cessna Aircraft Company